

THE
LONDON, EDINBURGH, AND DUBLIN
PHILOSOPHICAL MAGAZINE
AND
JOURNAL OF SCIENCE.

[SIXTH SERIES.]

SEPTEMBER 1923.

XXXVII. *On the Energy in the Magnetic Circuit of a Magneto.*
By N. W. McLACHLAN, D.Sc., F.Inst.P., M.I.E.E.*

Introduction.

A PRELIMINARY treatment of this subject has been given in a former paper†. The cardinal points which emerged from the analysis were formulated on the basis of zero loss, and subject to the magnet always being worked at a point situated upon the hysteresis quadrant, *i. e.*, a variation in reluctance caused the working-point to traverse the boundary line of the quadrant, and *not a subsidiary loop as it does in practice.*

It is the purpose of the present paper to treat the problem differently and more crucially, making assumptions which are in closer accord with practice—*e. g.*, no restriction has been placed on the shape of the armature; and to show that the optimum point for a magnet is not on the hysteresis loop at all, but on an auxiliary curve which is associated with the locus of the intersection of subsidiary loops and armature reluctance curves‡. The value of B corresponding to this optimum point is not necessarily equal to that on the main quadrant for which the product BH is a maximum. Owing to the nature of the formulæ for the energy obtainable from the magneto, there is a temptation to show that a physical concept of the electromagnetic energy associated with the

* Communicated by the Author.

† 'Electrician,' July 30th and Aug. 6th, 1920.

‡ See fig. 7.

primary winding can be derived from the hysteresis quadrant by imagining the magnet to be an elastic medium which stores and restores the primary energy—*i. e.*, a magnetic accumulator. It will be demonstrated that, so far as the present analysis goes, there is no substantial reason why the magnet and the primary should be correlated in such a fashion, and that any variations inherent in the magnet are due to changes in reluctance* of the path followed by the magnetic flux which is common to the magnet and its external circuit. The energy concomitant with such variations is associated, through the medium of the armature, with the external source causing rotation.

In Part I. it was shown that the energy of magnetized iron was a subject for experimental investigation before any definite formula giving the value could be established. Pending the production of such data, it will be assumed that the unknown factor Q to which reference was made is numerically equal to $\frac{1}{\mu}$, where μ is the permeability of the pole-shoe and armature iron.

Elementary Analytical Treatment.

HYPOTHESES A.

- (1) There is no loss incurred as the armature rotates, whether the winding is open or closed on itself.
- (2) The flux through the magnet and its external circuit is constant from make to break.
- (3) The magnetic leakage is zero, and the flux density in the magnet limbs is uniform.
- (4) The working-point for the magnet is situated on the main hysteresis loop.
- (5) On open circuit the reluctance does not vary with the position of the armature.
- (6) The armature is never run continuously on short-circuit—*i. e.*, the demagnetizing influences are merely those which accompany normal running where no short-circuit device is employed to suppress sparking at the plug.

Derivation of Energy Equations.

In fig. 4 is shown diagrammatically the hysteresis quadrant of the magnet steel obtained by some approved method when the metal forms a closed magnetic circuit. OA is the reluctance curve of the armature for varying flux densities—*i. e.*, it shows the relation between the

* This may be caused by armature reaction, eddy currents, or variation in the configuration of the magnetic circuit.

flux density and the value of H necessary to impel the flux through the armature, air-gaps, and pole-pieces. The flux density in the magnet is that corresponding to X , and the total flux through the circuit is the product of this ordinate and the cross-sectional area of the magnet. We will now derive an expression for the electromagnetic energy stored in the primary circuit when the armature rotates on closed circuit from the position of fig. 1 to that of fig. 2 or 3.

From the familiar equation to the magnetic circuit, we have at make (refer to fig. 1):

$$H_1 l_m = N_1 \rho_1, \quad . \quad . \quad . \quad . \quad . \quad (1)$$

where

H_1 = external m.m.f. due to demagnetizing force on magnet caused by armature reluctance,

l_m = mean length of magnet which may be taken along neutral axis from centres of pole-pieces,

N_1 = total flux through magnet,

ρ_1 = reluctance of path external to magnet.

For figs. 2 and 3, at break we can write

$$H_1 l_m + 4\pi ni = N_1 \rho_2, \quad . \quad . \quad . \quad . \quad . \quad (2)$$

where

ni = armature ampere turns,

ρ_2 = reluctance of external path traversed by flux.

From hypotheses (2) and (3) the magnet and armature fluxes are constant, and therefore H_1 is the abscissa of the point X in fig. 4 or 8. The path external to the magnet which is traversed by the flux has a greater reluctance in the position of fig. 2 or 3 than in that of fig. 1, and the m.m.f. to overcome the additional reluctance is supplied by the armature in virtue of the current in its winding; in fact, the armature current due to induction during rotation from make to break is concomitant with the alteration in reluctance. As a first approximation, we will assume that the self-inductance in figs. 2 and 3 position is defined symbolically by

$$Li = Nn, \quad . \quad . \quad . \quad . \quad . \quad (3)$$

where

L = self-inductance of armature in position of figs. 2 and 3,

i = armature current (abs. units),

n = „ turns,

N = total flux cut during rotation from make to break.

Transforming (2), we get

$$ni = (N_1\rho_2 - H_1 l_m)/4\pi.$$

Fig. 1.

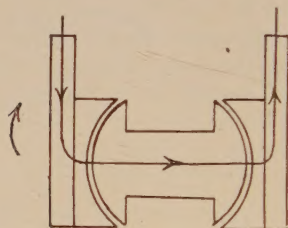


Diagram showing configuration with armature at -90° to mid-position.

Fig. 2.

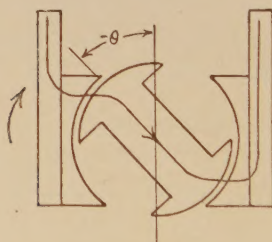


Diagram showing configuration when break occurs *before* mid-position.

Fig. 3.

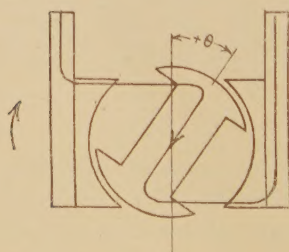
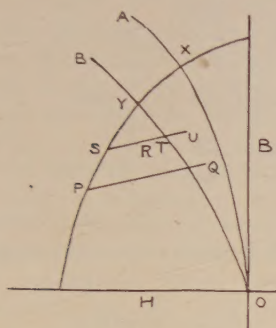


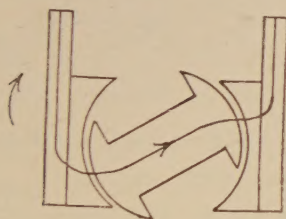
Diagram showing configuration when break occurs *after* mid-position.

Fig. 4.



Hysteresis loop, armature reluctance curves and subsidiary lines.

Fig. 5.



Configuration when make occurs before -90° position.

Substituting from (1),

$$\begin{aligned} ni &= (N_1\rho_2 - N_1\rho_1)/4\pi \\ &= \frac{N_1}{4\pi}(\rho_2 - \rho_1). \end{aligned} \quad (4)$$

Now energy

$$W = \frac{1}{2}Li^2 = Li \cdot i/2,$$

and substituting for Li from (3)

$$W = \frac{Nni}{2}. \quad (5)$$

Substituting the value of ni from (4) in (5), we obtain

$$W = \frac{NN_1}{8\pi}(\rho_2 - \rho_1). \quad (6)$$

If we write $\rho_2 = p\rho_1$, where $p = \text{a constant}$, equation (6) becomes

$$W = \frac{NN_1}{8\pi} \rho_1(p-1),$$

which on substitution from (1) gives

$$W = \frac{NH_1}{8\pi} l_m \cdot (p-1). \quad \dots \dots (7)$$

Now N , the flux cut by the armature during rotation from make to break, depends upon the angular movement θ , and may be written

$$N = N_1\phi(\theta),$$

where $\phi(\theta)$ is a function of θ .

Hence, substituting in (7) for N , we get

$$W = \frac{N_1H_1}{8\pi} l_m \phi(\theta)(p-1),$$

and since $N_1 = B_1A$,

$$W = \frac{B_1H_1}{8\pi} \phi(\theta) \cdot (p-1) \times \text{volume of magnet};$$

or

$$\text{Energy per unit volume of magnet} = \frac{B_1H_1}{8\pi} \cdot Z, \quad \dots (8)$$

where $Z = \phi(\theta)(p-1)$ and B_1H_1 is a point on the hysteresis quadrant.

This expression is similar to (16) obtained in Part I. ('Electrician,' July 30th, 1920).

More detailed Analytical Treatment.

In order to proceed with the analytical treatment, we must modify some and discard others of the old hypotheses. The variation in reluctance of the circuit external to the magnet has been disregarded hitherto, when the armature revolves with the primary open-circuited. In general, the reluctance in the position of fig. 1 is a minimum, and increases until at 90° thereto it reaches a maximum value. The variation is of the order of 25 per cent.

Suppose a magneto to be assembled and the magnet to be energized *in situ*, the armature occupying the position illustrated in fig. 1. The working-point on the hysteresis

quadrant will be X in fig. 8. If the armature is rotated on open circuit to a position 90° ahead of fig. 1, X (in fig. 8) will travel down the quadrant to P, which is the intersection of the quadrant and the armature reluctance curve for the new position. Between X and P we have a series of reluctance curves for the different angular positions of the armature. If rotation is continued until the conjugate position of fig. 1 (180° ahead) is attained, the magnet operates along a subsidiary loop PQ which is represented by a straight line, this being a conveniently close approximation *. Further and continued rotation on open circuit results in a cyclic movement round the subsidiary loop. Concomitant with the variation in reluctance of the external circuit there is a variation of the energy stored in the system. From Q to P work is done in rotating the armature, and energy is stored in the system external to the magnet. It can be shown that at P the energy in the external system per unit volume of magnet, in the absence of armature current, may be written $\frac{B_1 H_1}{8\pi}$ and at Q, $\frac{B_2 H_2}{8\pi}$ †. Hence the work done during rotation from the position of fig. 1 through 90° is $\frac{(B_1 H_1 - B_2 H_2)}{8\pi}$.

In the latter position (mid-position) the armature is in a state of unstable equilibrium; for in the absence of external constraint—*e. g.* friction, eddy current, and hysteresis loss—if it is moved from its initial position either clockwise or anticlockwise, it will fly back to the configuration of fig. 1 or its conjugate. When, however, it reaches either of these positions, it has attained a certain velocity and travels on through 90° in virtue of its momentum. If any energy is added externally when the motion commences, the armature will pass through the latter position and continue to rotate *ad infinitum*. In practice since there are considerable losses due to hysteresis and eddies in the core and surrounding metal masses, the armature executes a damped oscillation about one of the positions indicated in fig. 1, and finally comes to rest there. The number of oscillations is a rough measure of the total damping on open circuit. The damping is of course due to the combined effect of electrical and mechanical losses. This flyback or unstable phenomenon is well known, and the principle is used in certain forms of

* Watson, Journal I. E. E. vol. lix. p. 449 (1921).

† Evershed, Journal I. E. E. vol. lviii. p. 780 (1920).

electromagnetic relay. During the oscillatory motion, the energy relation can be expressed in the following form :

$$\begin{aligned}
 & \text{Work done during rotation from position of fig. 1 (1) to} \\
 & \quad \text{position (2) } 90^\circ \text{ ahead minus loss incurred} \\
 & \quad = \text{Initial potential energy of position (2),} \\
 & \quad = \text{Potential + Kinetic energies in any intermediate} \\
 & \quad \quad \text{position} \\
 & \quad + \text{Total loss from time oscillation started.}
 \end{aligned}$$

We will now deal with the problem when the armature circuit is closed at make and opened at break. Starting from Y (fig. 4) with a machine whose magnet has just been magnetized with the armature in fig. 1 position, let rotation occur until the configuration of fig. 3 is attained. The armature current increases from zero, and in so doing it constrains the flux to pass through the core. The point Y remains fixed until mid-position, *i. e.* 90° ahead, is reached. Beyond this point the field due to the armature current opposes the magnet, and the point Y moves down the quadrant until the point S* is gained, where we will assume that the contact-breaker opens and the spark occurs. The primary current is suddenly reduced to zero and then reversed, due to the oscillation which follows break. As the primary current oscillates after break, the point S moves up and down a subsidiary line SU. The final state of the magnet when the current is zero is at the point R, this being the intersection of the armature reluctance curve for the particular armature position, and the subsidiary line. In this discussion we have tacitly assumed that there is no lag between the current changes in the armature and the flux changes in the magneto. This is not so in practice owing to eddy currents. The current having decayed to zero, and the armature rotation having been continued, the reluctance decreases until the conjugate position of fig. 1 is reached, when the working-point for the magnet is T in fig. 4. The primary closes once more and the cycle of operations is repeated, the magnet operating along the line SU. The point S is attained due to the largest demagnetizing force exerted by the armature, and in a magneto which was never short-circuited, except during the normal "make" period, the location of this point would depend on the position of the timing lever at full retard. If, however, the magnet was subjected to high-speed short-

* It is assumed that S is further down the quadrant than the intersection of the reluctance curve for mid-position.

circuit conditions, the point S would be further down the quadrant and the working-line would be PQ.

With the aid of this explanatory matter we can now apply the foregoing analytical methods, with the essential modifications.

HYPOTHESES B.

- (1) From $\theta = -90^\circ$ to $\theta = 0^\circ$ (mid-position) the magnet flux and the external or demagnetizing m.m.f. exerted on the magnet are constant; from $\theta = 0^\circ$ to the point of break the magnet flux decreases, and the external m.m.f. increases by an amount dependent on the angular movement beyond mid-position.
- (2) There is no loss in either the magnet or the armature.
- (3) There is no magnetic leakage, and the flux density in the magnet limbs is uniform.
- (4) The flux changes in the whole magnetic circuit are simultaneous.

At make we have (fig. 1)

$$H_1 l_m = N_1 \rho_1, \quad (9)$$

and for break *before or at* mid-position

$$H_1 l_m + 4\pi ni = N_1 \rho_2. \quad (10)$$

For a point of break *beyond* mid-position

$$H_2 l_m + 4\pi ni = N_2 \rho_2 + \psi(\theta) \cdot 4\pi ni, \quad . . . (11)$$

where $\psi(\theta)$ is a function of θ , and the other symbols have the same meaning as previously. The term $\psi(\theta)4\pi ni$ represents the demagnetizing effect due to the armature current beyond mid-position.

By hypothesis,

$$(H_2 - H_1) l_m = \psi(\theta) \cdot 4\pi ni. \quad (12)$$

Thus, combining (11) and (12), we obtain

$$H_1 l_m + 4\pi ni = N_2 \rho_2. \quad (13)$$

From (9) and (10) we get

$$ni = \frac{N_1}{4\pi} \cdot (\rho_2 - \rho_1),$$

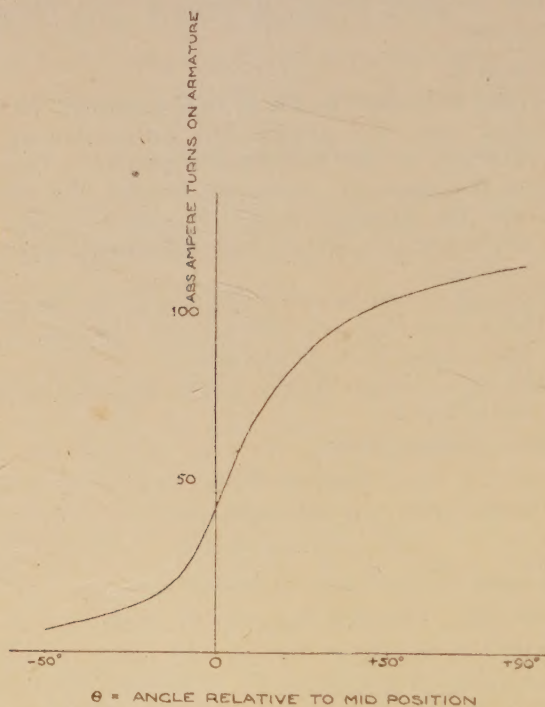
which is identical with (4). Since $Li = Nn$ (see (3)), we find with the same reasoning as that used in obtaining (8), that for a point of break prior to mid-position,

$$\text{Total energy } W = \frac{B_1 H_1}{8\pi} \cdot Z \times \text{volume}, \quad . . . (14)$$

where Z depends on the angular movement of the armature

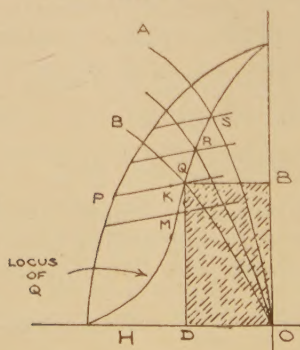
from make to break, and B_1 , H_1 are the coordinates of the point Q in figs. 7 and 8.

Fig. 6.



Curve showing relation between armature ampere-turns and angular position of armature, the total flux being 26,800 lines.

Fig. 7.



Showing locus of intersection of armature reluctance curves and subsidiary lines.

For a point of break *beyond mid-position* :—

From (9) and (13),

$$ni = (N_2\rho_2 - N_1\rho_1)/4\pi.$$

Putting $N_2 = N_1$, as it is approximately in practice, and $\rho_2 = p\rho_1$, we get

$$ni = \frac{N\rho_1}{4\pi} (p-1). \quad . \quad . \quad . \quad . \quad . \quad (15)$$

From (5), $W = \frac{Nni}{2}$, where $N = N_1\phi(\theta)$ as in (8).

Substituting the value of ni from (15) in the last equation,

$$W = \frac{N_1^2}{8\pi} \cdot \rho_1 \cdot (p-1)\phi(\theta). \quad . \quad . \quad . \quad . \quad (16)$$

Since $H_1 l_m = N_1 \rho_1$ and $N_1 = B_1 A$, (16) becomes

$$\begin{aligned} W &= \frac{B_1 H_1}{8\pi} \cdot (p-1) \cdot \phi(\theta) \cdot \text{volume of magnet} \\ &= \frac{B_1 H_1}{8\pi} Z \text{ per unit vol. of magnet,} \end{aligned} \quad (17)$$

where $Z = (p-1)\phi(\theta)$, and depends on the position at break relative to that at make—*i. e.*, on the angular movement of the armature, and B_1, H_1 are the coordinates of the point Q in fig. 8. If the magnet has been subjected to short-circuit conditions, Q will be further down the curve AXO of fig. 8.

In equations (8), (14), and (17) the factor Z appears. Its value cannot be computed mathematically to any degree of accuracy, but fortunately the components embodied therein can be ascertained experimentally for any given type of magneto. Thus if Z is found empirically, the validity of the analysis can be tested by measuring the total spark-energy, allowance being made for loss during transformation, and comparing the result with that computed from (14) or (17) according to the point of break. If make occurs at a point other than that depicted in fig. 1, say fig. 2 or fig. 5, it is sufficiently accurate to take the values of B_1 and H_1 at the position in question. The armature reluctance curve will be different in each case.

The available energy is given by the expression $\frac{Nni}{2}$, and this is equivalent to

$$\frac{4\pi ni}{l_m} \cdot \frac{B_1 A l_m}{8\pi} \cdot \phi(\theta) = \left[\frac{4\pi}{2 \cdot 4\pi} \cdot \frac{l_m}{l_m} \cdot N_1 \phi(\theta) \right].$$

Thus the energy per unit volume of the magnet is $\frac{4\pi ni}{l_m} \cdot \frac{B_1}{8\pi} \phi(\theta)$. This expression could of course have been obtained much earlier in the treatment, but it does not contain the factor H_1 , and would by itself be of no assistance in the final issue when the optimum magnet is derived. Equating the latter expression for W per unit volume of magnet to that found in (17), we obtain

$$\frac{4\pi ni}{l_m} \cdot \frac{B_1 \phi(\theta)}{8\pi} = \frac{B_1 H_1}{8\pi} \cdot (p-1) \phi(\theta)$$

or $(p-1) = \frac{4\pi ni}{H_1 l_m} \quad \dots \dots \dots (18)$

Moreover, in order to determine $(p-1)$ experimentally, the armature is fixed in definite positions, and the current required to maintain the working flux is found for each position. This yields ni , the armature ampere-turns for various angular positions. An actual curve is illustrated in fig. 6. The only point which remains indefinite is that during actual working a variation in flux occurs, due to demagnetization of the magnet when the armature is beyond mid-position; but this is not sufficiently serious to be taken into account for the angular movements which occur in practice. If the curve showing flux for various positions with the armature on open circuit is found (see fig. 9), also the data of fig. 8, the value of Z can be computed from the expression

$$Z = (p-1) \phi(\theta) = \frac{4\pi ni}{H_1 l_m} \cdot \frac{N}{N_1} \quad \dots \dots \dots (19)$$

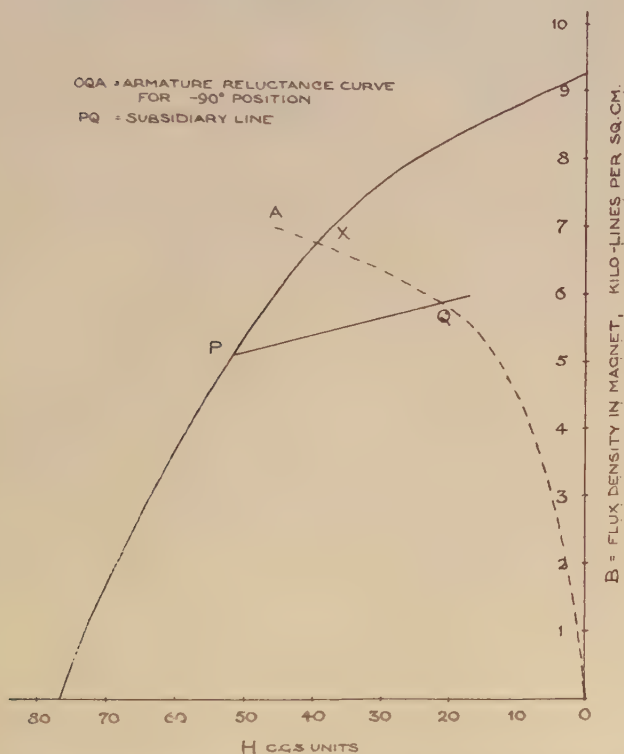
Computation of the Factor Z.

In fig. 6 * is shown what may conveniently be termed an armature reluctance curve, in which the ampere-turns to maintain the working flux in various angular positions are plotted against the angular movement of the armature from mid-position. Fig. 8 shows the hysteresis quadrant, armature

* The author is indebted to Mr. E. A. Watson for figs. 6 and 8, and data connected therewith.

reluctance curve for -90° , and a subsidiary line; whilst fig. 9 gives the *assumed* relationship between flux through the armature on open circuit and the angle from mid-position.

Fig. 8.



Hysteresis loop, armature reluctance curve and subsidiary lines for actual machines.

By aid of these diagrams the results given in the Table were obtained. Z was computed, using equation (19).

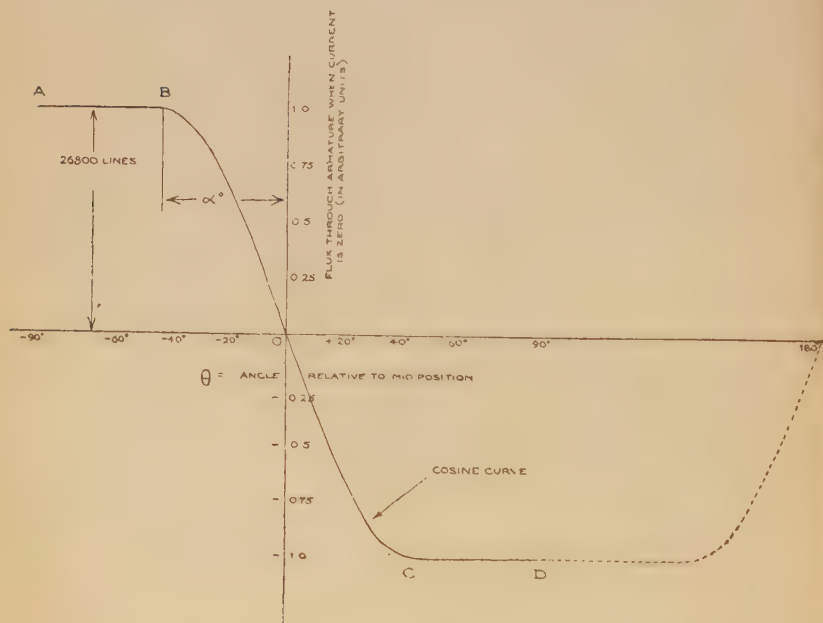
The mean length of the magnet on neutral axis = 25 cm.,

and the

Cross-sectional area of the magnet . . = 4.62 sq. cm.

In fig. 10 is plotted the available energy for various armature positions, this of course being in the present instance directly proportional to Z . Since energy $= \frac{1}{2} I a^2 = kZ$, where $k = \frac{B_1 H_1}{8\pi}$ vol., the armature current, assuming the inductance to be invariable, is proportional to the square root of the energy, and to that of Z . This is illustrated by the curve

Fig. 9.



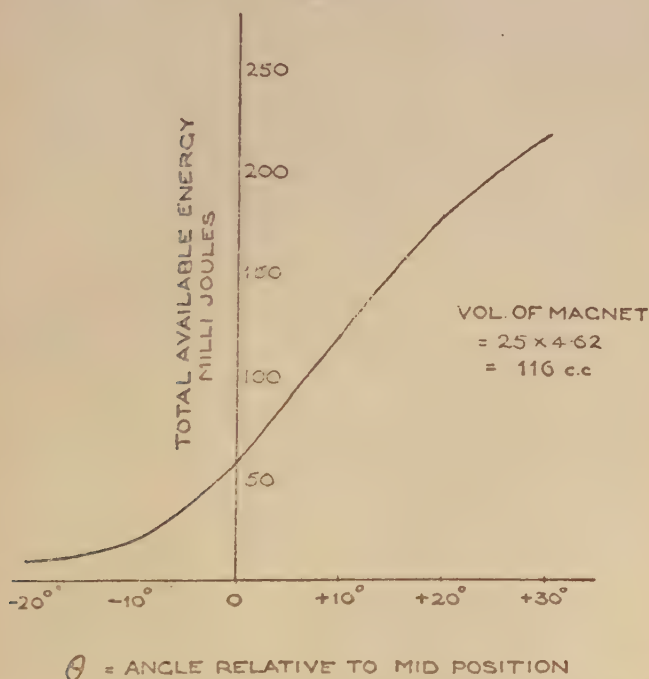
Curve showing relation between flux through armature and angle relative to mid-position.

of fig. 11. In all cases the change of curvature is rather abrupt, like the characteristic of a rectifier, owing to the shape of the flux curve of fig. 9, which we assumed for simplicity to be a cosine curve with straight horizontal pieces extrapolated. In practice the top of the curve is not quite straight, and due to its being rounded off the energy and current curves do not change curvature so abruptly as those shown here.

Determination of Conditions for Maximum Energy with a Magnet of Fixed Dimensions.

Having already obtained an expression for the available energy associated with the primary winding in terms of commensurable coefficients of the magnetic circuit, the next step is to ascertain the condition under which the energy with a magnet of fixed dimensions has its maximum

Fig. 10.



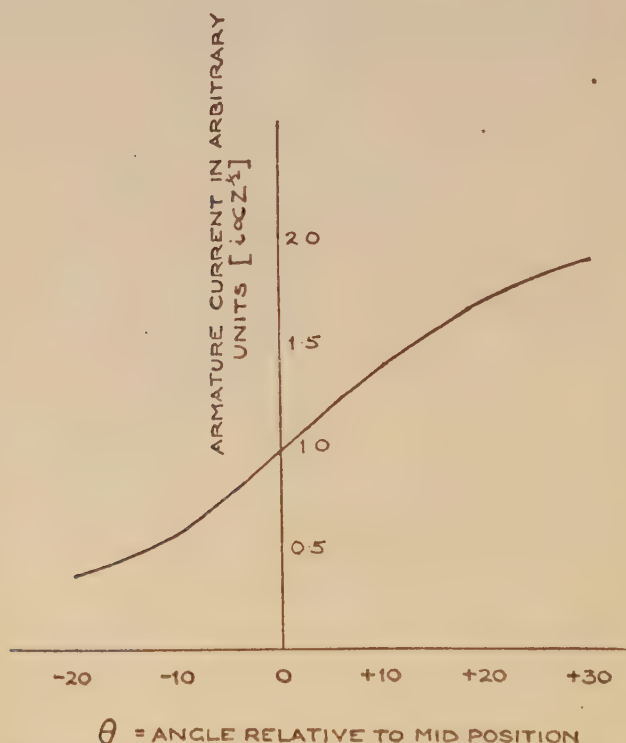
Curve showing total available energy from magneto with a magnet 4.62 sq. cm. in cross-section and 25 cm. mean length, for various points of break, make occurring at -90° , there being zero loss during rotation.

value. The first case to be considered will be one in which the armature diameter and length are fixed.

After the armature has been run on short-circuit at high speed, we get the graphs shown on fig. 7, where PQ is the working or subsidiary line. When the armature is at -90° to mid-position the magnet is worked at Q, and

when operating under short-circuit conditions * the magnet functions from P up and down the subsidiary line. The energy obtainable when the machine is functioning normally (*i. e.* there is no short-circuiting) is equal to

Fig. 11.



Curve showing relation between armature current at break, in arbitrary units, for various angular positions, make occurring at -90° , there being zero loss during rotation.

$\frac{B_1 H_1 Z}{8\pi}$ ergs per c.c. of magnet, where B_1 and H_1 are the coordinates of the point Q. For a certain value of the air-gap the graphs PQ and BQO are obtained. If the air-gap be varied (either increased or decreased) the graphs will also alter, and for a series of air-gaps there will be a corresponding series of graphs, each yielding a different

* In this case the primary is closed for one or more revolutions of the armature. Thus there is no spark at the plug.

TABLE.

The circuit is made at $\theta = -90^\circ$, and broken at the values in column 1.

$\theta =$ Angular position of armature at break relative to mid-position. (Degrees).	H_1 on subsidiary line. (c.g.s. units.)	B_1 on subsidiary line. (Lines per sq. cm.)	$\frac{1}{2}i$, Turns \times absolute amperes.	Total flux change between make & break, $N - N_1 = B_1$	$p - l$.	Z.	W. Available energy for magnet of 116 c.c. volume. (Milli-joules.)
-20	23	5800	15	0.36	0.33	0.15	9.2
-10	"	"	22	0.66	0.48	0.32	20
0	"	"	43	1.0	0.94	0.91	60
+10	"	"	66	1.34	1.44*	1.98*	120
+20	"	"	81	1.64	1.77*	2.9*	180
+30	"	"	91	1.87	1.9*	3.55*	217

* The variation in B_1 is neglected.

working line for the magnet. The energy obtainable in every instance is dependent on the product of the co-ordinates at Q, R, etc. It is necessary, of course, that the magnet should be re-magnetized before securing each individual working line. The locus of the point Q is a curve of the form drawn in fig. 8. This curve is determined empirically for any particular type of magneto.

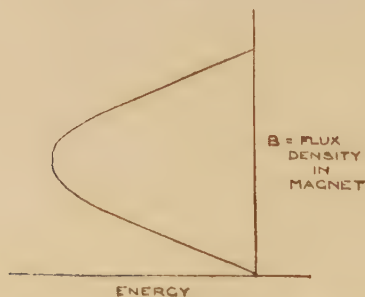
We may write

$$\begin{aligned} Z &= (p-1)\phi(\theta) \\ &\text{as before (see (19))} \\ &= \left(\frac{\rho_2}{\rho_1}-1\right) \frac{N}{N_1}. \end{aligned}$$

There is a possibility that $\frac{\rho_2}{\rho_1}$ and $\frac{N}{N_1}$ will vary with the air-gap, and therefore the best policy is to ascertain the value of Z for the different air-gaps as shown in the section immediately preceding.

Having found the various factors in the expression $B_1 H_1 Z$, it now becomes possible to draw a curve showing the relationship between energy and B_1 for any given point of break. The value of Z depends evidently on the latter, and there is a family of energy curves for various points of break. In every instance the curve will have a maximum

Fig. 12.



Curve showing energy relationship for given magnet and varying flux density in magnet.

energy value (see fig. 12), and the air-gap corresponding to this will be the optimum. Clearly there will be an optimum value of B_1 , and this may vary for different points of break, although the variation might be inappreciable from a practical view-point. It would be a lucky coincidence if BH were a maximum on the main loop for the same value of B as

that on the energy curve at, say, full retard, this timing position being associated with the slowest speeds. From a practical standpoint it is desirable that such a coincidence should occur, and more particularly if all the optimum B 's for various points of break were identical. In general, the shape of the energy curve is similar, excepting for small values of B , to that exhibited in fig. 12.

Determination of Optimum Armature Diameter when Magnet, Air-Gap, and Armature Length are fixed.

It ought to be evident from the preceding section that the optimum B_1 and corresponding energy obtainable from the machine is, with a given magnet, chiefly a question of armature reluctance. Having fixed the gap and the magnet, the procedure is similar to that above, excepting that the armature diameter is varied. In all probability, for any definite point of break or ignition, the values of B for optimum gap or armature diameter will not be very different.

Determination of Optimum Magnet when Armature, Magnetic Section, and Air Gap are fixed: Consideration of a further problem.

Having found the optimum value of B_1 for the particular brand of magnet steel, as set forth above, the length of the magnet is arranged so that the flux density is identical with B_1 where the working subsidiary line intersects the armature reluctance curve. This gives the maximum energy from the magneto per unit volume of magnet steel for the cross-section in question; nevertheless, the amount of energy might be inadequate. In such a case the machine would have to be re-dimensioned, or a larger magnet used—in which latter circumstances the optimum conditions would not hold. The solution of the problem indicated here is approximate, since there may be a variation in Z . A more accurate answer could be obtained by varying the length of the magnet until the required value is obtained.

There is another case which apparently arises, viz.: to find the optimum magnet * so that the magnet can supply a definite amount of energy. From the analysis already given, it will be clear that the energy obtainable from the machine (in the primary winding) does not depend solely on the magnet, and that the energy per unit volume of magnet

* The magnet of minimum volume for which the energy from the machine has a prescribed value.

may vary according to the relative proportion of magnet, air-gap, and armature. At present no definite solution can be offered, but with a large accumulation of practical data it will doubtless be possible to frame a good working rule applicable to a certain class of magneto.

The Pseudo-relationship between the Energy in the Primary and Energy Storage in the Magnet.

In attempting to correlate the variation in energy in the primary circuit with a similar variation in the magnet, the latter is imagined to be an accumulator which is virtually charged and discharged as the primary circuit is opened and closed. As a popular method of explaining the action and function of the magnet this might find favour, but we will endeavour to show that there does not exist any evidence to warrant the scientific accuracy of such a statement. Referring to fig. 7, suppose the working-line is PQ; then the magnet, under normal operation, functions from Q at make to K at break, the latter point not being far from the former. Assuming for simplicity that the points are coincident, the energy per unit volume of magnet is proportional to the shaded area, *provided Z be constant for all points of break*. But the latter condition is not satisfied, as the results in the Table clearly testify. Since there is little movement from Q to K*, the shaded area remains approximately constant during operation (make to break), and therefore, apart from Foucault currents in the metal masses, the magnet enjoys a comparatively undisturbed career until of course the spark occurs or the armature is short-circuited†. With these subsequent actions we are, however, not concerned meanwhile. Moreover, this constancy of condition precludes any accumulation or decumulation of energy within the magnet structure to a degree which can be approximately equal to that liberated from the primary at break. Hence we are compelled to conclude that the electromagnetic energy associated with the primary circuit is derived entirely and continuously from the source causing rotation of the armature, and that the magnet is merely an agent or accessory which enables this energy phenomenon to occur, just as in a Wimshurst machine the frictional effect of the brushes plays a somewhat similar part. So far as motion along the line PQ is concerned, it is easy to apprehend that, apart from eddy-current effects in the magnet, the magnet is perfectly

* Assuming make at -90° and break at mid-position or 0° .

† See previous footnote on p. 352.

elastic. There is, however, prior to break, no potential energy variation in the magnet of a magnitude approaching that of the primary energy at break.

Owing to the mechanical reaction between magnet and armature, there is a potential energy relationship; for were the armature (carrying current) fixed, and the magnet free to move, motion would ensue, thus converting potential energy into kinetic energy. This, however, is an issue of a purely mechanical nature, resulting from electrical action at a distance.

It is of interest to speculate on the energy in the primary if make occurs at -90° and break occurs at $+90^\circ$, this being of course quite beyond the limits which practice demands. In the latter position the demagnetizing force on the magnet is considerably reduced due to leakage, and we may assume that the external m.m.f. is balanced by the armature current, and that the latter is also sufficient to maintain the final flux*. Thus the current is approximately of such a value that its m.m.f. is twice the external m.m.f. of the magnet. Hence, for this terminal position, $4\pi ni = 2H_2l_m$. Substituting in the equation

$$W = \frac{B_2 H_2}{8\pi} \cdot Z = \frac{4\pi ni}{l_m} \cdot \frac{B_2}{8\pi} \frac{N}{N_1},$$

$$\left[\text{since from (19) } H_2 Z = \frac{4\pi ni}{l_m} \cdot \frac{N}{N_1} \right]^\dagger$$

we get, since $N = 2N_1$,

$$W = \frac{2H_2 l_m}{8\pi l_m} \cdot \frac{2N_1}{N_1} \cdot B_2 = \frac{B_2 H_2}{2\pi}$$

per unit volume of magnet,

where $B_2 H_2$ is on the hysteresis quadrant.

In this case we are tempted to correlate the area $B_2 H_2$ with the primary energy, but it is well to remember that the initial conditions were at the point $B_1 H_1$, and if any relationship were formulated, it would have to include the area $B_1 H_1$. This, however, would hardly meet the circumstances, unless the point $B_1 H_1$ were situated upon the axis of B . Such a condition would necessitate zero reluctance for the -90° position at make, and this does not occur in practice. When the expression $B_1 H_1$ is used in conjunction with a permanent magnet as shown herein, the value obtained represents the energy in the system *external to the magnet*.

* This is slightly less than the original flux at -90° , owing to the demagnetizing effect on the magnet.

† It is assumed as at top of p. 347, that $N_2 = N_1$.

The Influence of Armature Resistance.

This phase of the subject is all-important in practice, since the effect of resistance is greatest on full retard at slow speeds, especially when starting in cold weather. If the resistance is zero, as we have assumed hitherto, the available energy is independent of the speed of rotation, provided there are no other losses. It may be well to state, therefore, that the term "effective resistance" includes the effect of all losses from make to break, and that the ohmic resistance of the armature means the d.c. resistance of the winding. For the sake of illustration, assume the current rise from make to break is sinusoidal:

then $i = \frac{E}{(R^2 + \omega^2 L^2)^{\frac{1}{2}}}$. If R , the effective resistance, is small

compared with ωL , then $i = \frac{E}{\omega L}$, this being the value for a

resistanceless coil of inductance L . This condition is satisfied approximately at high speeds, where the current is nearly constant over a wide range of speed. E , the induced e.m.f., varies directly as the speed; so does ω ; hence, if L is assumed constant, i is independent of speed. With the magneto it is well known that the voltage and current waves depart considerably from sinusoidal formation. Thus, in order to deal with the problem mathematically, we must either resolve the voltage wave into its harmonic components, using Fourier's theorem, or adopt a simpler procedure. The *assumed* relationship between the flux through the armature and the angle of rotation from -90° is shown in fig. 9. The configuration from -180° to $+180^\circ$ approaches that of a rectangular flux wave. Assume AB in fig. 9 to be parallel with the θ axis, and BC to be a portion of a cosine curve whose period is smaller than that of the flux alternations. From A to B we have the relationship $N = N_1$, and from B to C $N = N_1 \cos \theta = N_1 \cos \omega t$, where $\omega = 2\pi n \frac{90^\circ}{\alpha}$, n being the r.p.s. of the armature. When the armature moves from $\theta = -90^\circ$ at A to θ at B , there is no change of flux through it, and therefore no current will flow in the primary winding. From B to C , however, there is a variation in flux, and we have the following relation:

$$L \frac{di}{dt} + Ri = E = nN_1 \frac{d \cos \omega t}{dt}$$

$$= -\omega n N_1 \sin \omega t,$$

where R and L are assumed constant. The solution of

this equation is given by

$$i = \frac{\omega n N_1}{(R^2 + \omega^2 L^2)^{\frac{1}{2}}} \cos \left[\omega t - \tan^{-1} \frac{\omega L}{R} \right] - \frac{\omega n N_1 R}{R^2 + \omega^2 L^2} e^{-\frac{Rt}{L}}, \quad (20)$$

where ω = angular velocity corresponding to the rate of flux interlinkage along BOC due to rotation of the armature.

For given values of magnet flux N_1 , armature turns n , effective resistance R , and inductance L , it can be shown from (20) that the current i for a definite value of ωt (θ on the curved portion) increases with ω . Now in moving from B to C, ωt is 180 electrical degrees*; hence, for large current, ω should be large, *i. e.* the slope from B to C should be steep, in order that the rate of flux interlinkage may be correspondingly rapid. It is obviously the energy loss due to the effective resistance that prevents the current attaining its full value. This means that at break the flux through the armature is less than that at make, owing to the lack of constraint caused by reduction in current—or, in other words, the flux is not fully distorted. Thus ωL should be great in comparison with R , so that the $i^2 R$ time integral $\int i^2 R dt = \text{energy lost}$ is small. For low speeds this would necessitate a large value of ω —that is, a steep slope at BC. In the limit when $\omega = \infty$, BC is perpendicular to the θ axis and the flux curve is truly rectangular. If this condition could obtain in practice, the current in an armature of finite effective resistance R would attain its full value at break whatever the speed of rotation, provided it was not zero. Thus, in the actual machine, we conclude that for meritorious performance at low speeds, the effective resistance (chiefly ohmic copper loss) should be small and the flux curve as nearly rectangular as possible. The latter criterion involves a very rapid increase in reluctance of the circuit external to the magneto in the neighbourhood of the ignition point. In practice, where the timing is variable as a rule, it is essential, in order to carry out this suggestion, that the flux curve should be bodily retarded or advanced according to the point of break. In a certain class of magneto the effect is simulated approximately by varying the configuration of the magnetic circuit external to the magnet, thus altering the flux distribution for different angular positions relative to mid-position. The variation generally occurs at the pole tips, these being movable; but from a practical, and certainly from a commercial viewpoint, it is hardly worth the additional complications and

* Or, more concisely, $\theta = \pi/2\omega$.

expense. In the ideal case as cited above, the rate of flux cutting should be equal for all timing positions and should be extremely high. A magneto fitted with variable pole-tips falls short of the hypothetical case, the discrepancy naturally being most marked at slow speeds.

We will now tabulate the preceding argument in symbolic form, using equation (20) :

$$i = \frac{\omega n N_1}{(R^2 + \omega^2 L^2)^{\frac{1}{2}}} \left[\cos(\omega t - \alpha) - \frac{R}{(R^2 + \omega^2 L^2)^{\frac{1}{2}}} \cdot e^{-\frac{Rt}{L}} \right].$$

A. At very low speed, when $R \geq \omega L$, we obtain

$$i \doteq \frac{\omega n N_1}{R} \cos \omega t = \frac{E}{R}, \quad (21)$$

where E = induced e.m.f.

Thus Ohm's law holds, and the current and voltage waves are almost similar in shape simultaneously. Clearly the value of R should be as small as possible, other factors, such as contact breaker sparking at high speeds, being taken into account in fixing its value.

B. At high speed (when the current is independent of speed) $\omega L \geq R$, and we get

$$i = \frac{\omega n N_1}{\omega L} \cos \left(\omega t - \frac{\pi}{2} \right) = \frac{n N_1}{L} \sin \omega t = \frac{n N_1}{L} \sin \theta. \quad (22)$$

C. At break * in case (A), the current at break,

$$I_B = \frac{\omega n N_1}{R} \quad (23)$$

(dependent on speed).

D. At break in case (B), the current at break,

$$I_B = \frac{n N_1}{L} \quad (24)$$

(independent of speed).

E. The "decrease" in current at low speed, due to resistance R , is approximately

$$\frac{n N_1}{L} - \frac{\omega n N_1}{L} = n N_1 \left[\frac{1}{L} - \frac{\omega}{R} \right]. \quad . . . (25)$$

* $\theta = 90^\circ$ in this instance.

As ω increases, the quantity in brackets tends to zero, assuming L and R to remain constant. This equation is only approximate, and if we take the limiting case where the bracket is zero, $\omega L = R$. This does not mean that the full value of the current is attained when $\omega L = R$; the equation can be interpreted by saying that, were $\omega L = R$ for all speeds of rotation, R and the ignition-point being fixed, the current at break would always be the same. In each case terms involving the exponential $e^{-R/L}$ have been neglected, and from an analytical standpoint it is well to remember that these equations are not rigorous, and are merely intended to show in a simple manner the influence of resistance. These remarks apply with equal force to the energy equations about to be given.

F. Energy at break (mid-position) in case (C)

$$W = \frac{1}{2}LI_B^2 = \frac{1}{2}L \frac{\omega^2 n^2 N_1^2}{R^2}. \quad \dots \dots (26)$$

G. Energy at break in case (D)

$$= \frac{1}{2}L \frac{n^2 N_1^2}{L^2} = \frac{n^2 N_1^2}{L}. \quad \dots \dots (27)$$

H. Ratio of (28) to (29)

$$= \frac{\omega^2 L^2}{R^2}. \quad \dots \dots (28)$$

From (28) we again see that the energy is augmented by increase in speed and by decrease in resistance.

From the approximate equations deduced in this section, we are in a position to examine the problem of securing the optimum conditions when there is a loss of energy during rotation. At low speed we get from (26)

$$\text{Energy at break : } W = L\omega^2 n^2 N_1^2 / 2R^2.$$

For a given speed of rotation ($\propto \omega$), armature turns n , and armature effective resistance R (chiefly cupric loss at low speed), if N_1 is increased by reducing the air-gap and keeping the armature diameter constant, or by augmenting it so that the distance between the pole-faces is unaltered, the self-inductance L is increased and also the energy at break. The formula would clearly not apply when the air-gap was so small that L became numerically important compared with R . Thus we can, after a little consideration, see that with a certain magnet for any particular speed of

rotation there is (a) an optimum gap for a given armature, (b) an optimum armature diameter for given gap and armature length. Similarly, at any definite speed there is an optimum magnet *, *i. e.* one for which the magneto energy per unit volume of magnet is a maximum. At high speed, where $\omega L \gtrsim R$, it is clear from (27) that the energy is independent of the speed, and its value does not differ very materially from the theoretical value. In this case the value of B on the auxiliary curve of fig. 7, for which the optimum condition was satisfied would be smaller than that at low speed, since it is desirable in the latter case to increase the flux through the armature, and therefore through the magnet. Moreover, the optimum gap or the optimum armature diameter decreases with reduction in speed, whilst the flux N_1 increases.

An approximate method of determining the optimum magnet at the lowest running speed on full retard would be as follows:—Find the optimum magnet as shown herein when there is no loss, *i. e.* the armature effective resistance is zero and the air-gap is as small as possible mechanically. Then augment the length of the magnet by an amount best determined from experience. In practice it is known that the best procedure to adopt in securing satisfactory performance at low speeds is to make the air-gap as small as is possible mechanically.

Conclusion.

From a practical standpoint it is only the energy at slow speeds that matters, although the question of a highly advanced ignition for racing motors has to be considered also. As a general rule, if the energy at slow speeds is adequate, that at high speeds is adequate too. Resistance effects have not been introduced into the energy analysis associated with the hysteresis quadrant, as the treatment would be very cumbersome and unwieldy. The method just indicated for ascertaining the optimum magnet at slow speeds is probably sufficiently accurate to fulfil most practical requirements. Since the cost of magnet steel is not exorbitant, it is of minor importance if the magnet is slightly oversize. In many cases, if not all, the size of magnet can be determined (the exigencies of the situation sometimes demand that it shall be) empirically, but it is always desirable, if possible, to reduce design to an arithmetical basis.

* Assuming the cross-sectional area to be fixed.

The problem of energy transfer from primary to secondary has not been discussed. The energy transformation and the proportion of the primary energy in the initial capacity spark is, for given numbers of turns and armature diameter, chiefly a question of the coefficient of coupling between the two windings. The smaller the air-gap, the greater this coefficient. In the induction-coil there is an optimum coupling, *i.e.* one which gives the greatest secondary peak voltage for a given current broken in the primary; but in the magneto the optimum is not so marked owing to the large iron loss, although it exists. At low speed the effect of resistance, as we have shown already, demands a small air-gap and therefore a close coupling to obtain sufficient primary current at break. Moreover, in this case, where an appreciable proportion of the energy is dissipated in heat in the armature prior to break, the optimum coupling involves not only the relation between the primary and secondary circuits, but also the value of the primary current at break. The optimum magnet in this case would be one for which the electrostatic energy in the spark ($\frac{1}{2}C_2V_2^2$) per unit volume of magnet was a maximum*. Since C_2 is assumed fixed, it is clear that V_2 should be a maximum. This introduces a problem of much greater magnitude and complexity than we have contemplated hitherto, and it is not proposed to pursue the subject any further at present.

We may close with the following summary of salient deductions:—

- (1) In the absence of loss or at high speeds where the armature current is constant: (a) with an armature and magnet of prescribed dimensions, there is a certain air-gap for which the electromagnetic energy associated with the primary winding at break is a maximum. The optimum point for the magnet is not situated on the main hysteresis loop, but on an auxiliary curve which is the intersection of subsidiary lines and armature reluctance curves: (b) when the dimensions of armature, air-gap, and magnet section are fixed, there is a certain length of magnet for which the energy associated with the primary at break per unit volume of magnet is a maximum.

* Assuming ignition depends entirely on the capacity component of the spark. In cold weather it appears that the inductive component plays an equally important part when the mixture is improperly vaporized.

- (2) In the actual machine (where loss occurs) at low speeds of rotation, conclusions (a) and (b) are valid, but the optima values vary with the speed.
- (3) For meritorious performance at low speeds on retard, the air-gap should be as small as is mechanically possible. Also the primary resistance (ohmic chiefly) should be as small as is compatible with satisfactory operation and freedom from contact-breaker sparking at high speeds.

XXXVIII. *Orbits in the Field of a Doublet, and generally of Two Centres of Force.* By Sir G. GREENHILL*.

THE orbit in the field of a magnetic molecule doublet, discussed by Dr. D. Wrinch in the *Phil. Mag.* May 1922, is a special case of Euler's problem (1760) of the path of a particle in the gravity field of the attraction or repulsion of two fixed spheres. A subsequent discussion is carried out at great length in Legendre's *Fonctions elliptiques*, i. p. 411. to the extent of 150 pages.

1. Resuming the investigation given on the "Stability of Orbits," *Proceedings of the London Math. Society (L.M.S.)* xxi. 1888, the motion is referred to the coordinates ϕ, θ on the Weir Azimuth Chart, defined by the conformal representation

$$x + iy = c \operatorname{ch}(\phi + i\theta), \quad x = c \operatorname{ch} \phi \cos \theta, \quad y = c \operatorname{sh} \phi \sin \theta, \quad . \quad (1)$$

$$\frac{x^2}{c^2 \operatorname{ch}^2 \phi} + \frac{y^2}{c^2 \operatorname{sh}^2 \phi} = 1, \quad \frac{x^2}{c^2 \cos^2 \theta} - \frac{y^2}{c^2 \sin^2 \theta} = 1, \quad . \quad (2)$$

a system of confocals, such that ϕ is constant along the confocal ellipse, θ along the confocal hyperbola, with foci at S, S', $x = \pm c, y = 0$; and with r, s the focal distance SP, S'P of a point P

$$r, s = c(\operatorname{ch} \phi \mp \cos \theta). \quad . \quad . \quad . \quad (3)$$

The potential function (P.F.) of two Newtonian centres of force at S, S' is written

$$U = U_1 + U_2, \quad U_1 = \frac{Ac^3}{r}, \quad U_2 = \frac{Bc^3}{s}; \quad . \quad . \quad . \quad (4)$$

so that if U_1 is the P.F. of a sphere of radius c , density ρ , and centre at S, $A = \frac{1}{2}\pi G\rho = \omega^2$, where ω is the angular velocity of a satellite grazing the surface of the sphere.

* Communicated by the Author.

The kinetic energy (K.E.) of unit particle

$$\begin{aligned}\frac{1}{2}v^2 &= \frac{1}{2}\left(\frac{dx}{dt}\right)^2 + \frac{1}{2}\left(\frac{dy}{dt}\right)^2 = \frac{1}{2}c^2(\text{sh } \phi \cos \theta \phi' - \text{ch } \phi \sin \theta \theta')^2 \\ &\quad + \frac{1}{2}c^2(\text{ch } \phi \sin \theta \phi' + \text{sh } \phi \cos \theta \theta')^2 \\ &= \frac{1}{2}c^2(\text{ch}^2 \phi - \cos^2 \theta)(\phi'^2 + \theta'^2), \quad (5)\end{aligned}$$

and then the Energy Equation may be written

$$\begin{aligned}\frac{1}{2}(\text{ch}^2 \phi - \cos^2 \theta)(\phi'^2 + \theta'^2) \\ = \frac{A}{\text{ch } \phi - \cos \theta} + \frac{B}{\text{ch } \phi + \cos \theta} + H, \quad (6)\end{aligned}$$

and H is negative if the orbit does not stretch to infinity.

2. Euler's second integral can be obtained in a more general form by introducing the stream-function (S.F.) V, orthogonal to a (P.F.) U, defined by

$$\frac{dV}{dx} = y \frac{dU}{dy}, \quad \frac{dV}{dy} = -y \frac{dU}{dx},$$

or

$$\frac{dV}{d\phi} = y \frac{dU}{d\theta}, \quad \frac{dV}{d\theta} = -y \frac{dU}{d\phi}, \quad (1)$$

in the elliptic orthogonal coordinates, ϕ, θ ; or any other orthogonal pair.

Then if h, h' denote the angular momentum (A.M.) of unit particle at P about S, S'; U_1, U_2 a P.F. of a radial field of force from S, S', and V_1, V_2 their S.F.; also χ, ψ, ω denoting the angles SPS', S'SP, SSP, so that

$$h = -r^2 \frac{d\psi}{dt}, \quad h' = s^2 \frac{d\omega}{dt}; \quad \text{then with } \frac{dU}{ds} = \frac{1}{y} \frac{dV}{sd\omega},$$

$\frac{1}{r} \frac{dh}{dt}$ = resolved force of compound field perpendicular to SP

$$= \frac{dU_2}{ds} \sin \chi = \frac{1}{y} \frac{dV_2}{sd\omega} \sin \chi. \quad (2)$$

$$h' \frac{dh}{dt} = \frac{rs \sin \chi}{y} \frac{dV_2}{dt} = 2c \frac{dV_2}{dt}; \quad (3)$$

and similarly

$$h \frac{dh'}{dt} = -2c \frac{dV_1}{dt}, \quad \frac{1}{2} \frac{dhh'}{dt} = -c \frac{dV_1}{dt} + c \frac{dV_2}{dt}, \quad (4)$$

$$\frac{1}{2} h h' = -c V_1 + c V_2 + K', \quad K' = K c^4, \quad (5)$$

the Action equation.

Thus if p, p' is the perpendicular from S, S' on the tangent of the orbit,

$$pp' = \frac{hh'}{v^2} = \frac{-cV_1 + cV_2 + K'}{U_1 + U_2 + H'} \quad \dots \quad (6)$$

the general geometrical relation.

The Energy is constant along a line of constant P.F., and the Action is constant along an orthogonal line of force, S.F. constant.

Or the P.F. gives lines of equal Energy, and the S.F. gives orthogonal lines of force of equal Action (Mauertuis).

3. In Euler's problem of the two Newtonian central fields of force, about S, S' ,

$$U_1 = \frac{Ac^3}{r}, \quad V_1 = Ac^3 \cos \psi, \quad U_2 = \frac{Bc^3}{s}, \quad V_2 = -Bc^3 \cos \omega, \quad (1)$$

$$\frac{1}{2}hh' = -Ac^4 \cos \psi - Bc^4 \cos \omega + Kc^4; \quad \dots \quad (2)$$

and with the elliptic coordinates ϕ, θ ,

$$\cos \psi = \frac{1 - \operatorname{ch} \phi \cos \theta}{\operatorname{ch} \phi - \cos \theta}, \quad \cos \omega = \frac{1 + \operatorname{ch} \phi \cos \theta}{\operatorname{ch} \phi + \cos \theta}, \quad \dots \quad (3)$$

$$\begin{aligned} h &= (x-c)y^* - yx^* = c^2(\operatorname{ch} \phi - \cos \theta)(\operatorname{sh} \phi \theta^* - \sin \theta \phi^*) \\ &= -r^2 \frac{d\psi}{dt}, \quad \dots \quad (4) \end{aligned}$$

$$\begin{aligned} h' &= (x+c)y^* - yx^* = c^2(\operatorname{ch} \phi + \cos \theta)(\operatorname{sh} \phi \theta^* + \sin \theta \phi^*) \\ &= s^2 \frac{d\omega}{dt}, \quad \dots \quad (5) \end{aligned}$$

$$\begin{aligned} \frac{\frac{1}{2}hh'}{c^4} &= \frac{1}{2}(\operatorname{ch}^2 \phi - \cos^2 \theta)(\operatorname{sh}^2 \phi \theta^{*2} - \sin^2 \theta \phi^{*2}) \\ &= -A \frac{1 - \operatorname{ch} \phi \cos \theta}{\operatorname{ch} \phi - \cos \theta} - B \frac{1 + \operatorname{ch} \phi \cos \theta}{\operatorname{ch} \phi + \cos \theta} + K, \quad \dots \quad (6) \end{aligned}$$

and this is Euler's Second Integral, to be translated in Mauertuis' Principle of Action.

By a happy accident Euler found the variables could be separated in his special problem into the equations

$$\frac{1}{2}(\operatorname{ch}^2 \phi - \cos^2 \theta)^2 \phi^{*2} = -H \operatorname{ch}^2 \phi + (A+B) \operatorname{ch} \phi - H - K, \quad (7)$$

$$\frac{1}{2}(\operatorname{ch}^2 \phi - \cos^2 \theta)^2 \theta^{*2} = -H \cos^2 \theta + (A-B) \cos \theta + H + K, \quad (8)$$

$$\begin{aligned} \frac{2dt^2}{(\operatorname{ch}^2 \phi - \cos^2 \theta)^2} &= \frac{d\phi^2}{H \operatorname{ch}^2 \phi + (A+B) \operatorname{ch} \phi - H - K} \\ &= dT^2 = \frac{d\theta^2}{-H \cos^2 \theta + (A-B) \cos \theta + H + K}, \quad (9) \end{aligned}$$

where the variables are seen separated, but this separation is

exceptional for the particular law of two fixed centres of gravitating force; and writing

$$\begin{aligned}\Phi & \text{ for } H \operatorname{ch}^2 \phi + (A+B) \operatorname{ch} \phi - H - K, \\ \Theta & \text{ for } -H \cos^2 \theta + (A-B) \cos \theta + H + K, \quad . \quad (10)\end{aligned}$$

the integrals $\frac{d\phi}{\sqrt{\Phi}}$ and $\frac{d\theta}{\sqrt{\Theta}}$ are seen to be elliptic integrals; and A, B, H, K are of the dimensions of ω^2 , or -2 in time.

4. A centre of attraction varying as the distance may, however, be introduced at O, and the variables can still be separated. For writing its P.F.

$$\frac{1}{2}C(x^2 + y^2) = \frac{1}{2}C(c^2(\operatorname{ch}^2 \phi - \sin^2 \theta),$$

to be added to U, requires the addition to V of

$$-\frac{1}{2}Cc^2 \operatorname{sh}^2 \phi \sin^2 \theta = -\frac{1}{2}Cy^2;$$

and this adds

$$\frac{1}{2}C \operatorname{sh}^2 \phi \operatorname{ch}^2 \phi \text{ to } \Phi \text{ and } \frac{1}{2}C \sin^2 \theta \cos^2 \theta \text{ to } \Theta.$$

But the further integration becomes hyperelliptic and intractable.

And the addition to U of a term $g.c = g.c \operatorname{ch} \phi \cos \theta$, to represent a uniform gravity field in the direction SS', does not lead to a separation of the variables, and further progress is impracticable.

The S.F. $-\frac{1}{2}Cy^2$ corresponds to a P.F. Cx , of a uniform field C; but $\frac{1}{2}C(x^2 + y^2)$ is not to be associated as a P.F.

5. Euler employs new variables u, v , which are found to be our $\tan \frac{1}{2}\theta$, $\operatorname{th} \frac{1}{2}\phi$; and his p, q are our $c \cos \theta, c \operatorname{ch} \phi$ (*Mémoires de Berlin*, 1760).

We shall follow Legendre's notation where p, q are used to denote $\operatorname{th} \frac{1}{2}\phi, \tan \frac{1}{2}\theta$; and then

$$\begin{aligned}\tan \frac{1}{2}\psi &= \cot \frac{1}{2}ASP = \frac{p}{q}, \quad \tan \frac{1}{2}\omega = \tan \frac{1}{2}AS'P = p'q, \\ \operatorname{ch} \phi &= \frac{1+p^2}{1-p^2}, \quad \operatorname{sh} \phi = \frac{2p}{1-p^2}, \quad d\phi = \frac{2dp}{1-p^2}, \\ \cos \theta &= \frac{1-q^2}{1+q^2}, \quad \sin \theta = \frac{2q}{1+q^2}, \quad d\theta = \frac{2dq}{1+q^2}, \quad . \quad (1) \\ \frac{d\phi}{\sqrt{\Phi}} &= \frac{2dp}{\sqrt{P}}, \quad \frac{d\theta}{\sqrt{\Theta}} = \frac{2dq}{\sqrt{Q}},\end{aligned}$$

$$\begin{aligned}P' &= H(1+p^2)^2 + (A+B)(1-p^4) - (H+K)(1-p^2)^2 \\ &= -(K+A+B)p^4 + 2(2H+K)p^2 - K + A + B, \\ Q' &= -H(1-q^2)^2 + (A-B)(1-q^4) + (H+K)(1+q^2)^2 \\ &= (K-A+B)q^4 + 2(2H+K)q^2 + K + A - B, \quad (2)\end{aligned}$$

and thus with time $t=t_1+t_2$, we can write

$$dt = (\text{ch}^2 \phi - \cos^2 \theta) \left(\frac{d\phi}{\sqrt{2\Phi}} \text{ or } \frac{d\theta}{\sqrt{2\Theta}} \right) \\ = \frac{\text{sh}^2 \phi d\phi}{\sqrt{2\Phi}} + \frac{\sin^2 \theta d\theta}{\sqrt{2\Theta}} = dt_1 + dt_2, \quad \dots (3)$$

$$dt_1 = \frac{\text{sh}^2 \phi d\phi}{\sqrt{2\Phi}} = \frac{8p^2}{(1-p^2)^2} \frac{dp}{\sqrt{2P'}}, \\ dt_2 = \frac{\sin^2 \theta d\theta}{\sqrt{2\Theta}} = \frac{8q^2}{(1+q^2)^2} \frac{dq}{\sqrt{2Q'}}, \quad \dots (4)$$

in which again the variables are separated, and t_1, t_2 depend on elliptic integrals of the First, Second, and Third kind (E.I., I, II, III), as well as an algebraical term, where previous experience guides us to a form

$$\frac{2p\sqrt{P'}}{1-p^2} \text{ or } \text{th } \frac{1}{2}\phi\sqrt{\Phi} \text{ in } t_1 \\ \text{and } \frac{2q\sqrt{Q'}}{1+q^2} \text{ or } \tan \frac{1}{2}\theta\sqrt{\Theta} \text{ in } t_2; \quad \dots (5)$$

and when these are removed, we are left with elliptic integrals alone, as in § 17.

Legendre devotes 125 pages more to a discussion and classification of the different cases that can arise of the orbits, and appears to have lighted incidentally on the theory of Transformation.

It would lead too far to attempt to follow Legendre; but a start can be made on the elliptic or hyperbolic orbit, or a portion of it, described under the two centres of force; and in the case where the orbit is unstable, we can follow up the shape of the orbit as it falls away from the unstable path, or approaches it again asymptotically.

An investigation of the Stability of such an orbit was given in Proc. L. M. S. 1888, when the conditions were adjusted so that an ellipse or hyperbola was described, or a portion of the curve, employing the theorem that if the curve can be described under each centre of force separately, the same orbit can be described when both forces act, the squared velocity being then the sum (or difference) of the separate squared velocities.

6. In a complete ellipse, $\phi = \beta$, we find

$$V^2 = \left(\frac{d\phi}{dt} \right)^2 = \Phi = H \text{ch}^2 \phi + (\Lambda + B) \text{ch } \phi - H - K \\ = H(\text{ch } \phi - \text{ch } \beta)^2, \quad \dots (1)$$

with $A + B = -2H \operatorname{ch} \beta$, and H is negative, the motion stable.

In a complete branch of the hyperbola, $\theta = \alpha$,

$$Q^2 = \left(\frac{d\theta}{dt} \right)^2 = \Theta = -H \cos^2 \theta + (A - B) \cos \theta + H + K \\ = -H(\cos \theta - \cos \alpha)^2, \quad . \quad . \quad . \quad (2)$$

with $A - B = 2H \cos \alpha$, and B negative, force at S' repelling; thus H is positive and the motion stable.

Reduce B to zero in the complete ellipse, and the motion is the ordinary planetary orbit; and reducing B still further to negative values, as in the hyperbolic branch, put $B = -D$.

When the forces are equal at aphelion from S of the ellipse, the breaking point is reached; and after that, as D is increased, Θ can vanish, and an arc of the ellipse is described, provided the forces to S and from S' are equal at the breaking point of zero velocity, say $\phi = \beta$, $\theta = \alpha$; so that we can put

$$A = n^2(\operatorname{ch} \beta - \cos \alpha)^2, \quad D = n^2(\operatorname{ch} \beta + \cos \alpha)^2, \\ \Phi = n^2(\operatorname{ch} \phi - \operatorname{ch} \beta)^2, \quad . \quad . \quad . \quad (3)$$

$$\text{with} \quad H + K = -H \operatorname{ch}^2 \beta, \quad A - D = -2H \operatorname{ch} \beta, \\ H = 2n^2 \cos \alpha,$$

and the motion is unstable unless $\cos \alpha$ is negative, and the larger half of the ellipse is described, with little or no play from $\phi = \beta$. Then

$$Q^2 = \left(\frac{d\theta}{dT} \right)^2 = \Theta = 2n^2(\cos \theta - \cos \alpha)(\operatorname{ch}^2 \beta - \cos \alpha \cos \theta), \quad (4)$$

giving θ as an Elliptic Function (E.F.) of T , in the form

$$\tan \frac{1}{2}\theta = \tan \frac{1}{2}\alpha \operatorname{cn} mT. \quad . \quad . \quad . \quad (5)$$

So, too, under two centres of attraction at S, S' , a particle placed at rest where the two forces are equal, at (ϕ, α) , can oscillate on the arc of the hyperbola $\theta = \alpha$, with

$$\Theta = -H(\cos \theta - \cos \alpha)^2,$$

$$H + K = -H \cos^2 \alpha, \quad 2H \cos \alpha = A - B = -4n^2 \operatorname{ch} \beta \cos \alpha, \\ H = -2n^2 \operatorname{ch} \beta, \quad . \quad . \quad . \quad (6)$$

and the motion is unstable. And

$$P^2 = \left(\frac{d\phi}{dT} \right)^2 = \Phi = 2n^2(\operatorname{ch} \beta - \operatorname{ch} \phi)(\operatorname{ch} \beta \operatorname{ch} \phi - \cos^2 \alpha), \\ \operatorname{th} \frac{1}{2}\phi = \operatorname{th} \frac{1}{2}\beta \operatorname{cn} mT. \quad . \quad . \quad . \quad (7)$$

But if repelled from S, S' with the sign of A, B changed,

$$Q^2 = \left(\frac{d\theta}{dT} \right)^2 = \Theta = -2n^2 \operatorname{ch} \beta (\cos \theta - \cos \alpha)^2, \quad (8)$$

and the motion is stable along the hyperbolic arc reaching to infinity; with

$$P^2 = \left(\frac{d\phi}{dT} \right)^2 = \Phi = 2n^2 (\operatorname{ch} \phi - \operatorname{ch} \beta) (\operatorname{ch} \beta \operatorname{ch} \phi - \cos^2 \alpha), \quad (9)$$

$$\coth \frac{1}{2} \phi = \coth \frac{1}{2} \alpha \operatorname{cn} mT.$$

With the stability examined otherwise, from

$$\frac{dQ}{dT} = \frac{d\Theta}{2d\theta},$$

$$\frac{d^2 Q}{Q dT^2} = -2n^2 \operatorname{ch} \beta (\sin^2 \theta - \cos^2 \theta + \cos \alpha \cos \theta)$$

$$= -2n^2 \operatorname{ch} \beta \sin^2 \alpha \quad \dots \quad (10)$$

along $\theta = \alpha$; here Q can fluctuate slightly between close limits, and the motion is stable.

A further discussion will be found in the Proc. London Math. Society, vol. xxii., 1888, "Stability of Orbits."

7. Putting $A + B = 0$ in the general case introduces some simplification into the integrals, making $\Phi = H \operatorname{sh}^2 \phi - K$, and gives the field of force of a bar magnet along SS'.

Thus if a particle is placed at rest anywhere on the line O γ where the forces are equal, it will proceed to oscillate in a semi-ellipse, $\phi = \beta$, with $\Phi = 0$; and then, if

$$A = -B = \frac{1}{2} \omega^2, \quad A - B = \omega^2,$$

$$\frac{1}{2} (\operatorname{ch}^2 \beta - \cos^2 \theta)^2 \left(\frac{d\theta}{dt} \right)^2 = \Theta = \omega^2 \cos \theta, \quad \dots \quad (1)$$

$$\omega t = \int (\operatorname{ch}^2 \beta - \cos^2 \theta) \frac{d\theta}{\sqrt{(2 \cos \theta)}} \quad \dots \quad (2)$$

An algebraical term Z can be set aside, where

$$Z = \frac{1}{3} \sin \theta \sqrt{(2 \cos \theta)}, \quad \frac{dZ}{d\theta} = \frac{\cos^2 \theta}{\sqrt{(2 \cos \theta)}} - \frac{1}{3} \frac{1}{\sqrt{(2 \cos \theta)}}. \quad (3)$$

and then

$$\omega t = (\operatorname{ch}^2 \beta - \frac{1}{3}) \int \frac{d\theta}{\sqrt{(2 \cos \theta)}} - Z, \quad \dots \quad (4)$$

in which

$$\int \frac{d\theta}{\sqrt{(2 \cos \theta)}} = \operatorname{cn}^{-1} \sqrt{(\cos \theta)}, \quad \dots \quad (5)$$

to a lemniscate modular angle 45° .

The analogous case can be considered when the velocity is due to a twin vortex, at S, S' ; and the orbits are circles or Cassinians, as of a cyclone, tornado, habbab, waterspout, air whirl, dust column, will o' the wisp, friar's lanthorn.

8. With $H=0$, so that the velocity is zero at infinity, then as in the restriction of pendulum motion,

I. $A+B>K$.

II. $A+B<K$.

(1) $\Phi=(A+B) \operatorname{ch} \phi-K$.

$$=(A+B+K) \operatorname{sh}^2 \frac{1}{2} \phi$$

$$+(A+B-K) \operatorname{ch}^2 \frac{1}{2} \phi$$

$$=(A+B+K) \frac{\operatorname{dn}^2 u}{\kappa^2 \operatorname{sn}^2 u}.$$

(2) $\operatorname{th} \frac{1}{2} \phi=\operatorname{cn} u$

$$\operatorname{ch} \frac{1}{2} \phi=\frac{1}{\operatorname{sn} u}$$

$$\operatorname{sh} \frac{1}{2} \phi=\frac{\operatorname{cn} u}{\operatorname{sn} u}$$

$$d\phi=-\frac{2 \operatorname{dn} u \operatorname{dn} u}{\operatorname{sn} u}$$

$$\kappa^2=\frac{A+B+K}{2 A+2 B}$$

(3) $dT=\frac{d\phi}{\sqrt{\Phi}}=-\frac{2 \kappa \operatorname{dn} u}{\sqrt{(A+B+K)}}$

$$=(K+A+B) \operatorname{sh}^2 \frac{1}{2} \phi$$

$$-(K-A-B) \operatorname{ch}^2 \frac{1}{2} \phi$$

$$=(K+A+B) \frac{\operatorname{cn}^2 u}{\operatorname{sn}^2 u}.$$

$$=\operatorname{dn} u$$

$$=\frac{1}{\kappa \operatorname{sn} u}$$

$$=\frac{\operatorname{dn} u}{\kappa \operatorname{sn} u}$$

$$=-\frac{2 \operatorname{cn} u \operatorname{dn} u}{\operatorname{sn} u}$$

$$=\frac{2 A+2 B}{K+A+B}.$$

$$=-\frac{2 \operatorname{dn} u}{\sqrt{(K+A+B)}}.$$

And as in pendulum motion,

θ oscillating.

θ circulating.

(4) $\Theta=(A-B) \cos \theta+K$

$$=(A-B+K) \cos ^2 \frac{1}{2} \theta$$

$$-(A-B-K) \sin ^2 \frac{1}{2} \theta$$

$$=(A-B+K) \operatorname{cn}^2 v$$

(5) $\cos \frac{1}{2} \theta=\operatorname{dn} v$

$$\tan \frac{1}{2} \theta=\frac{\kappa}{\kappa'} \operatorname{cn} (K-v)$$

$$d\theta=2 \kappa \operatorname{cn} v \operatorname{dn} v$$

$$\kappa^2=\frac{K+A-B}{2 A-2 B}$$

(6) $dT=\frac{d\theta}{\sqrt{\Theta}}=\frac{2 \kappa \operatorname{dn} v}{\sqrt{(A-B+K)}}$

$$=(K+A-B) \cos ^2 \frac{1}{2} \theta$$

$$+(K-A+B) \sin ^2 \frac{1}{2} \theta$$

$$=(K-A+B) \operatorname{dn}^2 v$$

$$=\operatorname{cn} v$$

$$=\operatorname{tn} v$$

$$=2 \operatorname{dn} v \operatorname{dn} v$$

$$=\frac{2 A-2 B}{K+A-B}$$

$$=\frac{2 \operatorname{dn} v}{\sqrt{(K-A+B)}}.$$

In a further exploration when H is restored in Θ , the effect in the associated pendulum is as if the axle was made

to revolve about a vertical axis on a whirling arm with angular velocity m , where H may be replaced by m^2 , and the reduction of the various cases that arise is given in the Report on Gyroscopic Theory, p. 204 (1914), ranging from $\tan \frac{1}{2}\theta = \tan \frac{1}{2}\alpha \operatorname{cn} (K-v)$ to $\operatorname{th} \frac{1}{2}\beta \operatorname{tn} v$.

A different shape of a compound pendulum can make H negative, and then $H = -m^2$.

This motion can be projected stereographically into free pendulum oscillation. And the ϕ integral is reduced immediately to a preceding θ form by the substitution

$$\operatorname{th} \frac{1}{2}\phi = \tan \frac{1}{2}\theta, \quad \operatorname{ch} \phi = \sec \theta, \quad d\phi = \sec \theta d\theta. \quad (7)$$

9. In the special field of the magnetic molecule at O considered by Dr. Wrinch, Phil. Mag. May 1922, where our c is zero, by the coalescence of S and S' , and the preceding analysis nugatory, replace Euler's results by

$x + iy = c \exp(\phi + i\theta)$, $x, y = ce^\phi (\cos \theta, \sin \theta)$, $r = ce^\phi$, (1)
equivalent to replacing $\operatorname{ch} \phi$, $\operatorname{sh} \phi$ by e^ϕ , and

$$U = c \left(-\frac{d}{dx} \right) \frac{Bc^3}{r} = B \frac{c^4 x}{r^3} = Bc^2 e^{-2\phi} \cos \theta,$$

$$V = Bc^3 \frac{y^2}{r^3} = Bc^3 e^{-\phi} \sin^2 \theta = B \frac{c^4}{r} \sin^2 \theta, \quad (2)$$

$$\frac{dV}{d\phi} = y \frac{dU}{d\theta}, \quad \frac{dV}{d\theta} = -y \frac{dU}{d\phi}. \quad (3)$$

Weir's Azimuth diagram is replaced here by concentric circles, of radius in G.P. for equal increments of ϕ , and radiating lines at equal angular interval of θ .

The work is essentially not more complicated if a centre of gravitation is introduced at O , as if the A sphere was magnetic as well as gravitating, making

$$U = Ac^2 e^{-\phi} + Bc^2 e^{-2\phi} \cos \theta = A \frac{c^3}{r} + B \frac{c^4}{r^2} \cos \theta,$$

$$V = -Ac^3 \cos \theta + Bc^3 e^{-2\phi} \sin^2 \theta = -Ac^3 \cos \theta + B \frac{c^4}{r} \sin^2 \theta. \quad (4)$$

Then in the ordinary polar equations of motion, resolving transversely,

$$\frac{dh}{dt} = \frac{dU}{d\theta} = -Bc^2 e^{-2\phi} \cos \theta, \quad (5)$$

$$h \frac{dh}{dt} = -Bc^4 \sin \theta \frac{d\theta}{dt}, \quad \text{with } h = c^2 e^{2\phi} \frac{d\theta}{dt}. \quad (6)$$

and integrating

$$\frac{1}{2}h^2 = Bc^4 \cos \theta + Kc^4, \quad e^{-4\phi} dt^2 = \frac{d\theta^2}{2B \cos \theta + 2K}.$$

where

$$\frac{1}{2}\theta' = \sqrt{\left(\frac{K}{K+B}\right)} r = \sqrt{(1-\frac{1}{2}\kappa^2)} F(\frac{1}{2}\theta, \kappa), \kappa = \sqrt{\frac{2B}{K+B}}. \quad (2)$$

SA, SA' the perihelion and aphelion distance; and the apsidal angle is raised from π to $2K\sqrt{(1-\frac{1}{2}\kappa^2)}$.

This is somewhat analogous to the case of the Einstein orbit, where the addition of the term $3mh^2u^4$ to μu^2 changes the orbit from

$$\frac{1}{SP} = \frac{\cos^2 \frac{1}{2}\theta}{SA} + \frac{\sin^2 \frac{1}{2}\theta}{SA'} \text{ into } \frac{\operatorname{cn}^2 \frac{1}{2}p\theta}{SA} + \frac{\operatorname{sn}^2 \frac{1}{2}p\theta}{SA'} \quad (3)$$

(Phil. Mag. Jan. 1921).

11. The investigation of some possible orbits is carried out by Dr. Wrinch in the Phil. Mag., May 1922; also in August 1910, p. 380, by J. H. Jeans.

The curvilinear coordinates of the confocals on Weir's Azimuth Diagram can be employed in Perigal's manner of the construction of Lissajous figures of vibration, for the general case of two centres of force, tacking from one corner to the opposite of small curvilinear rectangles, taking the step in ϕ and θ in the ratio of $d\phi$ or $\sqrt{\Phi}$ and $d\theta$ or $\sqrt{\Theta}$.

A standard orbit of this nature would be worth investigation as a useful Research, to add to those attempted by Legendre, utilising Elliptic Function Theory to obtain a closed figure.

A specimen orbit winding about inside a finite curvilinear rectangle would have the appearance of an analogous Lissajous figure of simple vibration contained in a plane rectangle of straight sides. These curves could be shown by a spot of light reflected from a pair of mirrors in vibration, with surfaces of appropriate curvature.

Putting $B=0$ should reduce our orbit to a plane elliptic or hyperbolic orbit about the focus S. And if the conditions are adjusted to make S' the other focus, so that the orbit is given by ϕ or θ a constant, we notice that while the Time is given by the sector area round S, the Action is represented by the sector area round S'.

With $B=0$, Φ changes into $-\Theta$ by the change of $\operatorname{ch} \phi$ into $-\cos \theta$, or P' into $-Q'$ by a change of p^2 into $-q^2$.

Thence the modulus κ is the same in the two elliptic integrals, and the orbit is given by the Algebraical Addition Theorem, in the form

$$r = Ax + By + C, \dots \dots \dots (1)$$

$$\text{or} \quad A \operatorname{ch} \phi \cos \theta + B \operatorname{sh} \phi \sin \theta + C - \operatorname{ch} \phi + \cos \theta = 0. \dots (2)$$

12. If the body has a velocity communicated perpendicular to the plane SPS' , it will describe an orbit in three-fold space; and referred to the plane SPS' revolving with angular velocity $\frac{d\rho}{dt}$, a first integral is $y^2 \frac{d\rho}{dt} = \text{a constant}$, which Legendre denotes by H . We replace his H^2 by Dc^4 , so that D is of the dimensions ω^2 , the same as our H, K, A, B .

No difference is made in the resolution of the motion parallel to SS' : but the effect of the rotation $\frac{d\rho}{dt}$ is to diminish $\frac{d^2y}{dt^2}$ by $y\left(\frac{d\rho}{dt}\right)^2$ or $D\frac{c^4}{y^3}$ in the resolution along MP , and so to add $D\frac{c^4}{y^3}(x-c, x+c)$ to $\frac{dh}{dt}, \frac{dh'}{dt}$ in (3), (4), § 2.

Thus $\frac{dhh'}{dt}$ in (4) is increased by

$$\begin{aligned} & D\frac{c^4}{y^3}(x-c)\left[(x+c)\frac{dy}{dt}-y\frac{dx}{dt}\right] \\ & + D\frac{c^4}{y^3}(x+c)\left[(x-c)\frac{dy}{dt}-y\frac{dx}{dt}\right] \\ & = 2\frac{Dc^4}{y^3}\left[(x^2-c^2)\frac{dy}{dt}-xy\frac{dx}{dt}\right] \\ & = -Dc^4\frac{d}{dt}\frac{x^2-c^2}{y^2} = Dc^4\frac{d}{dt}\cot\psi\cot\omega, \quad (1) \end{aligned}$$

making the total in (4), § 2,

$$\frac{1}{2}hh' = -cV_1 + cV_2 + Kc^4 - Dc^4\frac{c^2-c'^2}{y^2}. \quad (2)$$

At the same time a term $\frac{1}{2}y^2\left(\frac{d\rho}{dt}\right)^2 = \frac{Dc^4}{2y^2}$ must be added to the Energy in (5) § 1; and this changes (6) § 5, (6) § 6 into

$$\begin{aligned} & \frac{1}{2}(\text{ch}^2\phi - \cos^2\theta)(\theta'^2 + \phi'^2) \\ & = H + \frac{A}{\text{ch}\phi - \cos\theta} + \frac{B}{\text{ch}\phi + \cos\theta} - 2\frac{D}{\text{sh}^2\phi \sin^2\theta}, \quad (3) \end{aligned}$$

$$\begin{aligned} & \frac{1}{2}(\text{ch}^2\phi - \cos^2\theta)(\text{sh}^2\phi\theta'^2 - \sin^2\theta\phi'^2) = \\ & K - A\frac{1 - \text{ch}\phi \cos\theta}{\text{ch}\phi - \cos\theta} - B\frac{1 + \text{ch}\phi \cos\theta}{\text{ch}\phi + \cos\theta} \\ & - D\frac{\text{ch}^2\phi \cos^2\theta - 1}{\text{sh}^2\phi \sin^2\theta}; \quad (4) \end{aligned}$$

thence (7), (8) § 3 change to

$$\frac{1}{2}(\text{ch}^2 \phi - \cos^2 \theta)^2 \phi'^2 =$$

$$H \text{ch}^2 \phi + (A + B) \text{ch} \phi - H - K - \frac{1}{2}D \coth^2 \phi = \Phi, \quad (5)$$

$$\frac{1}{2}(\text{ch}^2 \phi - \cos^2 \theta)^2 \theta'^2 =$$

$$-H \cos^2 \theta + (A - B) \cos \theta + H + K - \frac{1}{2}D \cot^2 \theta = \Theta, \quad (6)$$

so that $\frac{1}{2}D \coth^2 \phi$, $\frac{1}{2}D \cot^2 \theta$ are to be subtracted from the former values of Φ , Θ , and the variables can still be separated.

Legendre then puts $\text{ch} \phi = u$, $\cos \theta = z$, and

$$\frac{dy}{\sqrt{\Phi}} = \frac{du}{\sqrt{U}},$$

$$U = H(u^2 - 1)^2 + (A + B)u(u^2 - 1) - K(u^2 - 1) - \frac{1}{2}Du^2, \quad (7)$$

$$\frac{d\theta}{\sqrt{\Theta}} = \frac{dz}{\sqrt{Z}},$$

$$Z = H(z^2 - 1)^2 - (A - B)z(z^2 - 1) - K(z^2 - 1) - \frac{1}{2}Dz^2, \quad (8)$$

and so the integrals are elliptic still. And

$$dt = (\text{ch}^2 \phi - \cos^2 \theta) \left(\frac{d\phi}{\sqrt{2\Phi}} \text{ or } \frac{d\theta}{\sqrt{2\Theta}} \right) = \frac{u^2 du}{\sqrt{2U}} + \frac{z^2 dZ}{\sqrt{2Z}}, \quad (9)$$

$$\begin{aligned} d\rho &= \sqrt{D} \frac{e^2}{y^2} dt = \sqrt{D} \frac{\text{sh}^2 \phi + \sin^2 \theta}{\text{sh}^2 \phi \sin^2 \theta} \left(\frac{d\phi}{\sqrt{2\Phi}} \text{ or } \frac{d\theta}{\sqrt{2\Theta}} \right) \\ &= \frac{\sqrt{D} d\phi}{\text{sh}^2 \phi \sqrt{2\Phi}} + \frac{\sqrt{D} d\theta}{\sin^2 \theta \sqrt{2\Theta}} = \frac{\sqrt{D} du}{(u^2 - 1) \sqrt{2U}} + \frac{\sqrt{D} dz}{(z^2 - 1) \sqrt{2Z}}, \end{aligned} \quad (10)$$

introducing the Elliptic Integral of the Third Kind.

A C term in the P.F. U. in § 4 due to a central force at 0 varying as the distance will add $\frac{1}{4}C(u^2 - 1)(2u^2 - 1)^2$ and $\frac{1}{4}C(z^2 - 1)(2z^2 - 1)^2$ to U and Z, and the integrals are seen to become hyperelliptic.

13. In the extension to three-fold space of this compound field of gravity and magnetism, proceeding as before in § 9, resolving transversely

$$\frac{dh}{dt} = -Bc^2 e^{-2\phi} \sin \theta + D \frac{c^4 \cos \theta}{r^2 \sin^3 \theta}, \quad \dots \quad (1)$$

$$h \frac{dh}{dt} = -Bc^4 \sin \theta \frac{d\theta}{dt} + Dc^4 \frac{\cos \theta}{\sin^3 \theta} \frac{d\theta}{dt}, \quad \dots \quad (2)$$

$$\frac{1}{2}h^2 = Bc^4 \cos \theta + Kc^4 - \frac{1}{2}D \frac{c^4}{\sin^2 \theta}, \quad \dots \quad (3)$$

and in the Energy relation

$$\frac{1}{2}v^2 = \frac{1}{2}\left(\frac{dr}{dt}\right)^2 + \frac{h^2}{2r^2} + D\frac{c^4}{2y^2} = Hc^2 + A\frac{c^3}{r} + B\frac{c^4}{r^2}\cos\theta, \quad (4)$$

$$\frac{1}{2}\left(\frac{dr}{dt}\right)^2 = Hc^2 + A\frac{c^3}{r} - K\frac{c^4}{r^2}, \quad . \quad . \quad . \quad (5)$$

the terms in B and D cancelling; or with $\frac{c}{r} = u$,

$$\frac{du}{\sqrt{(2H + 2Au - Ku^2)}} = u^2 dt = \frac{c^2 d\theta}{h}, \quad . \quad . \quad (6)$$

while from (8), with $\cos\theta = z$,

$$\frac{r^3}{c^4}\left(\frac{dz}{dt}\right)^2 = 2(Bz + K)(1 - z^2) - D. \quad . \quad . \quad (7)$$

In the planetary orbit, $B=0$, h is constant, and D may be ignored.

Moving on the surface of a sphere, of radius

$$r=a, \quad \frac{dr}{dt}=0, \quad \text{when} \quad Ha^2 + Aac - Kc^2 = 0,$$

and with $\frac{dr}{dt} = R$,

$$\frac{1}{2}R^2 = Ha^2 + A\frac{c^3}{r} - K\frac{c^4}{r^2}, \quad \frac{dR}{dt} = -A\frac{c^3}{r^2} + 2K\frac{c^4}{r^3}. \quad (8)$$

$$\frac{1}{R}\frac{d^2R}{dt^2} = 2A\frac{c^3}{r^3} - 6K\frac{c^4}{r^4}, \quad . \quad . \quad . \quad (9)$$

so that this motion is unstable unless $2A\left(\frac{c}{a}\right)^3 - 6K\left(\frac{c}{a}\right)^4$ is negative, or $Kc > \frac{1}{3}Aa$, and then over the sphere

$$\left(\frac{a}{r}\right)^4\left(\frac{dz}{dt}\right)^2 = 2(Bz + K)(1 - z^2) - D, \quad . \quad . \quad (10)$$

representing a Spherical Pendulum motion, and as a conical pendulum it will give a circular orbit to the body.

14. The extreme case may be mentioned where S' recedes to an infinite distance from S (L.M.S. 1888) and then changing to an origin at S , we write

$$x + iy = \frac{1}{2}a(\phi + i\theta)^2,$$

$$x = \frac{1}{2}a(\phi^2 - \theta^2), \quad y = a\phi\theta, \quad r = \frac{1}{2}a(\phi^2 + \theta^2). \quad . \quad (1)$$

The gravity field of B away at S' is practically uniform near S, and

$$U = \frac{Aa^3}{r} - 2Bax = \frac{2Aa^2}{\phi^2 + \theta^2} - Ba^2(\phi^2 - \theta^2),$$

$$V = -Aa^3 \frac{\phi^2 - \theta^2}{\phi^2 + \theta^2} + Ba^3 \phi^2 \theta^2, \quad . \quad . \quad . \quad (2)$$

$$\frac{1}{2}(\phi^2 + \theta^2)(\phi'^2 + \theta'^2) = \frac{2A}{\phi^2 + \theta^2} - B(\phi^2 - \theta^2) + H, \quad . \quad (3)$$

$$\frac{1}{2}(\phi^2 + \theta^2)(\phi'^2 \theta'^2 - \phi'^2 \theta'^2) = -A \frac{\phi^2 - \theta^2}{\phi^2 + \theta^2} - B\phi^2 \theta^2 + K, \quad . \quad (4)$$

$$\frac{1}{2}(\phi^2 + \theta^2)^2 \phi'^2 = -B\phi^4 + H\phi^2 + A + K = \Phi, \quad (5)$$

$$\frac{1}{2}(\phi^2 + \theta^2)^2 \theta'^2 = +B\theta^4 + H\theta^2 + A - K = \Theta, \quad (6)$$

and so the variables are separated;

$$\frac{d\phi}{\sqrt{\Phi}} \pm \frac{d\theta}{\sqrt{\Theta}} = 0,$$

$$dt = dt_1 + dt_2 = \frac{\phi^2 d\phi}{\sqrt{2\Phi}} + \frac{\theta^2 d\theta}{\sqrt{2\Theta}} = \frac{u du}{2\sqrt{U}} + \frac{z dz}{2\sqrt{Z}}, \quad (7)$$

with $u = \phi^2 = \frac{r+x}{a}$, $z = \theta^2 = \frac{r-x}{a}$, $r \pm y = \frac{1}{2}a(\phi \pm \theta)^2$;

confocal parabolas along ϕ, θ constant; thus leading to elliptic integrals of the Legendre-Jacobi-Weierstrass form, to be identified with the integrals in § 5, with p replaced by ϕ , and q by θ .

The diagram here is covered with confocal parabolas, and an orbit can be constructed by tacking from one corner to the next of the curvilinear rectangles, ruled by parabolas of appropriate spacing. Thus with $B=0$, $H=0$, the orbit is an oblique trajectory parabola.

15. A complete parabola, $\phi = \beta$, can be described, with

$$\Phi = -B(\phi^2 - \beta^2)^2, \quad H = 2B\beta^2, \quad A + K = -B\beta^4, \quad . \quad (1)$$

and the motion is stable if B is positive.

Described freely under each force separately, the $\frac{1}{2}(\text{vel})^2$ is $A \frac{a^3}{r}$ and $2Bar$, and their difference is then the actual $\frac{1}{2}(\text{vel})^2$ of the orbit.

The parabola breaks at the vertex, $\theta = 0$, if $A = K = -\frac{1}{2}B\beta^4$, where the two forces are then equal and

opposite ; so that A and B are of opposite sign, and taking A negative, the orbit is stable in each half parabola.

If this orbit breaks at $\theta = \alpha$, where the forces are equal,

$$\Theta = B(\theta^2 - \alpha^2)(\theta^2 + \alpha^2 + 2\beta^2), \quad t = \int (\theta^2 + \alpha^2) \frac{d\theta}{\sqrt{2\Theta}},$$

introducing the E.I., I and II.

If B is positive, $\alpha < \theta < \infty$, along a parabolic arc, stretching to infinity, and in stable motion.

But $\alpha > \theta > -\alpha$ if B is negative, and the oscillatory motion of ϕ is unstable ; and with $\phi = \beta \operatorname{th} pu$, $\theta = \alpha \operatorname{cn} qu$.

16. In general, with $A - K = 0$ in a further exploration

$$\frac{d\theta}{\sqrt{\Theta}} = \frac{d\theta}{\theta \sqrt{B\theta^2 + H}},$$

$$\begin{aligned} \int \frac{d\theta}{\sqrt{\Theta}} &= \frac{1}{\sqrt{H}} \operatorname{sh}^{-1} \sqrt{\frac{H}{B\theta^2}}, \text{ or } \sqrt{\frac{1}{-H}} \sin^{-1} \sqrt{\frac{-H}{B\theta^2}} \\ &= \left(\frac{1}{\sqrt{H}} \text{ or } \frac{1}{\sqrt{-H}} \right) \frac{\operatorname{ch}^{-1}}{\cos^{-1}} \sqrt{\frac{B\theta^2 + H}{B\theta^2}}; \quad (1) \end{aligned}$$

or with $A - K$ not too large, and positive or negative,

$$A \sim K = Ba^2b^2,$$

$$\begin{aligned} \Theta &= (A - K) \left(1 + \frac{\theta^2}{a^2}\right) \left(1 + \frac{\theta^2}{b^2}\right), \text{ or } (K - A) \left(1 - \frac{\theta^2}{a^2}\right) \left(\frac{\theta^2}{b^2} - 1\right), \\ &= (A - K) \frac{\operatorname{dn}^2 u}{\operatorname{cn}^4 u}, \quad \text{ or } (K - A) \frac{\kappa^4}{\kappa'^2} \operatorname{sn}^2 u \operatorname{cn}^2 u, \quad (2) \end{aligned}$$

$$\theta = a \operatorname{tn} u, \quad a = b\kappa', \quad \text{ or } \quad \theta = a \operatorname{dn} u, \quad b = a\kappa', \quad (3)$$

$$\int \frac{d\theta}{\sqrt{\Theta}} = \frac{u \sqrt{\kappa'}}{4 \sqrt{(B \cdot A - K)}}, \text{ or } \frac{u}{4 \sqrt{(B \cdot K - A)}}, \quad (4)$$

$$\begin{aligned} \Phi &= (A + K) \left(1 - \frac{\phi^2}{c^2}\right) \left(1 - \frac{\phi^2}{d^2}\right), \quad A + K = Bc^2d^2, \\ &= (A + K) \frac{\operatorname{sn}^2 v \operatorname{dn}^2 v}{\kappa'^2} = cd \sqrt{(B \cdot A + K)} \frac{\operatorname{sn}^2 v \operatorname{dn}^2 v}{\kappa'^2}, \quad (5) \end{aligned}$$

$$\int \frac{d\phi}{\sqrt{\Phi}} = \frac{v \sqrt{\kappa\kappa'}}{4 \sqrt{(B \cdot A + K)}} \quad (6)$$

So also with $A + K$ zero or small.

17. In a further determination of a time integral in § 5, for t_1 and t_2 , and first for t_2 , with $\cos \theta = x$,

$$\sqrt{(2H)} dt_2 = \sqrt{\left(\frac{1-x^2}{-x^2 + \frac{A-B}{H}x + 1 + \frac{K}{H}} \right)} dx = \frac{dx}{\sqrt{y}}. \quad (1)$$

putting, in a Quadric Transformation,

$$y = \frac{-x^2 + \frac{A-B}{H}x + 1 + \frac{K}{H}}{1-x^2}, \quad y-1 = \frac{\frac{A-B}{H}x + \frac{K}{H}}{1-x^2}. \quad (2)$$

Solving this as a quadratic for x ,

$$(y-1)x^2 + \frac{A-B}{H}x - y + 1 + \frac{K}{H} = 0, \quad (3)$$

$$x = \frac{-\frac{A-B}{2H} + \sqrt{(y-y_1 \cdot y-y_2)}}{y-1}. \quad (4)$$

Here y_1, y_2 are the turning points of y , corresponding to x_1, x_2 of x ;

$$y_1 - y \cdot y_2 - y = (y-1) \left(y-1 - \frac{K}{H} \right) + \left(\frac{A-B}{2H} \right)^2, \\ y_1 - 1 \cdot y_2 - 1 = \left(\frac{A-B}{2H} \right)^2, \quad (5)$$

$$\frac{y-y_1}{1-y_1} = \frac{(x-x_1)^2}{1-x^2}, \quad \frac{y-y_2}{1-y_2} = \frac{(x-x_2)^2}{1-x^2}, \quad (6)$$

$$\frac{dx}{dy} = \frac{\sqrt{(y_1-1 \cdot y_2-1)}}{(y-1)^2} + \frac{2y-y_1-y_2}{(y-1) \sqrt{(4 \cdot y-y_1 \cdot y-y_2)}} \\ - \frac{\sqrt{(y-y_1 \cdot y-y_2)}}{(y-1)^2}. \quad (7)$$

Guided by § 5 we can infer an algebraical term Z to set aside in t_2 , where with $Y = 4 \cdot y - y_1 \cdot y - y_2 \cdot y - y_3$, and $y_3 = 0$,

$$Z = \frac{\frac{1}{2}\sqrt{Y}}{y-1}, \quad \frac{dZ}{dy} = \frac{-\frac{1}{2}\sqrt{Y}}{(y-1)^2} + \frac{3y^2 - 2(y_1 + y_2)y + y_1y_2}{(y-1)\sqrt{Y}}, \quad (8)$$

$$\sqrt{(2H)} \frac{dt_2}{dy} - \frac{dZ}{dy} = \frac{y_1-1 \cdot y_2-1}{(y-1)\sqrt{Y}} - \frac{y-1}{\sqrt{Y}} + \frac{\sqrt{(y_1-1 \cdot y_2-1)}}{(y-1)^2\sqrt{y}}. \quad (9)$$

$$\frac{2H}{A-B} [\sqrt{(2H)t_2 - Z}] = \int \frac{\sqrt{(y_1-1) \cdot y_2-1}}{y-1} \frac{dy}{\sqrt{Y}} - \int \frac{y-1}{\sqrt{(y_1-1) \cdot y_2-1}} \frac{dy}{\sqrt{Y}} + \int \frac{dy}{(y-1)^2 \sqrt{Y}}, \quad (10)$$

Here the second integral depends on the E.I., I and II, and in the region $\infty > y > y_1 > 1 > y_2$,

$$\int_{y, y_1}^{\infty} \frac{\sqrt{(y_1-y_3)} dy}{\sqrt{Y}} = u \text{ or } eK, K, \\ \int_{y_2}^1 \frac{\sqrt{(y_1-y_3)} dy}{\sqrt{Y}} = v \text{ or } fK, \quad . \quad . \quad . \quad (11)$$

to modulus $\kappa^2 = \frac{y_2-y_3}{y_1-y_3} = \frac{y_2}{y_3}$, and we take

$$y_1 = \frac{1}{\kappa^2 \operatorname{sn}^2 v}, \quad y = \frac{y_1}{\operatorname{sn}^2 u} = \frac{1}{\kappa^2 \operatorname{sn}^2 u \operatorname{sn}^2 v}, \quad y_2 = \frac{1}{\operatorname{sn}^2 v}, \\ y-y_1 = \frac{\operatorname{cn}^2 u}{\kappa^2 \operatorname{sn}^2 u \operatorname{sn}^2 v}, \quad y-y_2 = \frac{\operatorname{dn}^2 u}{\kappa^2 \operatorname{sn}^2 u \operatorname{sn}^2 v}, \\ \frac{y-y_1}{y-y_3} = \operatorname{cn}^2 u, \quad \frac{y-y_2}{y-y_3} = \operatorname{dn}^2 u, \quad . \quad . \quad . \quad . \quad (12)$$

and then the second integral in (10)

$$\int \frac{y-1}{\sqrt{(y_1-1) \cdot y_2-1}} \frac{dy}{\sqrt{Y}} = \frac{\kappa^2 \operatorname{sn}^3 v}{\operatorname{cn} v \operatorname{dn} v} \int \left(\frac{1}{\kappa^2 \operatorname{sn}^2 u \operatorname{sn}^2 v} - 1 \right) du \\ = \frac{\operatorname{sn} v}{\operatorname{cn} v \operatorname{dn} v} \int \frac{du}{\operatorname{sn}^2 u} - \frac{u \kappa^2 \operatorname{sn}^3 v}{\operatorname{cn} v \operatorname{dn} v}. \quad (13)$$

$$\text{And with } \frac{d^2}{du^2} \log \operatorname{sn} u = \frac{d}{du} \frac{\operatorname{cn} u \operatorname{dn} u}{\operatorname{sn} u} = 1 - \operatorname{dn}^2 u - \frac{1}{\operatorname{sn}^2 u},$$

$$\int \frac{du}{\operatorname{sn}^2 u} = u - \operatorname{E} \operatorname{am} u - \frac{\operatorname{sn} u \operatorname{dn} u}{\operatorname{sn} u}; \quad . \quad . \quad . \quad (14)$$

where, in the Jacobi notation,

$$\operatorname{E} \operatorname{am} u = \frac{E}{K} u + \operatorname{zn} u, \quad \operatorname{zn} u = \frac{d}{du} \log \Theta u$$

is Jacobi's zeta function, Zu ; and further

$$\operatorname{zs} u = \frac{d}{du} \log Hu = \operatorname{zn} u + \frac{\operatorname{cn} u \operatorname{dn} u}{\operatorname{sn} u}, \\ \operatorname{zs}(K-v) = \operatorname{zn}(K-v) + \frac{\operatorname{cn}(K-v) \operatorname{dn}(K-v)}{\operatorname{sn}(K-v)} \\ = -\operatorname{zn} v + \frac{\operatorname{sn} v \operatorname{dn} v}{\operatorname{cn} v}. \quad . \quad . \quad . \quad . \quad (15)$$

The second integral in (10) thus adds up to

$$u \left(\frac{\text{sn } v}{\text{cn } v \text{ dn } v} - \frac{\kappa^2 \text{sn}^3 v}{\text{cn } v \text{ dn } v} \right) - \frac{\text{sn } v}{\text{cn } v \text{ dn } v} \left(\frac{\text{E}}{\text{K}} u + \text{zn } u + \frac{\text{cn } u \text{ dn } u}{\text{sn } u} \right) \\ = u \frac{\text{sn } v \text{ dn } v}{\text{cn } v} - \frac{\text{sn } v}{\text{cn } v \text{ dn } v} \left(\frac{\text{E}}{\text{K}} u + \text{zs } u \right). \quad (16)$$

The first integral in (10) is already in the standard form of Π , Jacobi's E.I. III,

$$\Pi = \int_0^u \frac{\kappa^2 \text{sn } v \text{ cn } v \text{ dn } v \text{ sn}^2 u \text{ du}}{1 - \kappa^2 \text{sn}^2 u \text{ sn}^2 v} = u \text{zn } v + \frac{1}{2} \log \frac{\Theta(v-u)}{\Theta(v+u)}, \quad (17)$$

and then the first and second integral in (10) make up

$$\frac{1}{2} \log \frac{\Theta(v-u)}{\Theta(v+u)} - u \text{zs } (K-v) + \frac{\text{sn } v}{\text{cn } v \text{ dn } v} \left(\frac{\text{E}}{\text{K}} u + \text{zs } u \right). \quad (18)$$

Finally the third integral is elementary

$$\int_0^{\infty} \frac{dy}{(y-1)^2 \sqrt{y}} = \frac{1}{2} \log \frac{\sqrt{y+1}}{\sqrt{y-1}} - \frac{\sqrt{y}}{y-1} \quad \dots \quad (19)$$

and the term in (10)

$$\frac{2\text{HZ}}{\text{A}-\text{B}} = \sqrt{\left(\frac{y-y_1}{y_1-1} \cdot \frac{y-y_2}{y_2-1} \right)} \frac{\sqrt{y}}{y-1}, \quad \dots \quad (20)$$

so that, in all,

$$\frac{2\text{H}}{\text{A}-\text{B}} \sqrt{(2\text{H})t_2} = \log \frac{\Theta v \Theta u + \text{H} v \text{H} u}{\Theta 0 \Theta(v+u)} \\ - u \text{zs } (K-v) + \frac{\text{sn } v}{\text{cn } v \text{ dn } v} \left(\frac{\text{E}}{\text{K}} u + \text{zs } u \right) \\ + \left(\frac{\text{cn } u \text{ dn } u}{\kappa^2 \text{sn}^2 u \text{ cn } v \text{ dn } v} - 1 \right) \frac{\kappa \text{sn } u \text{ sn } v}{1 - \kappa^2 \text{sn}^2 u \text{ sn}^2 v}. \quad (21)$$

18. In the degenerate case of $\text{A}=\text{B}$,

$$y-1 = \frac{\text{K}}{1-\kappa^2}, \quad y_2 = 1, \quad y_1 = 1 + \frac{\text{K}}{\text{H}}, \quad \frac{\text{K}}{\text{H}} = y_1 - y_2 = \frac{\kappa'^2}{\kappa^2}, \quad \dots \quad (1)$$

$$x = \sqrt{\frac{y-y_1}{y-y_2}} = \frac{\text{cn } u}{\text{dn } u} = \text{sn}(K-u),$$

$$\frac{dx}{dy} = \frac{y_1 - y_2}{(y-y_2) \sqrt{(4-y-y_1)(y-y_2)}}, \quad \dots \quad (2)$$

$$\sqrt{(2H)}dt_2 = \frac{dx}{\sqrt{y}} = \frac{y_1 - y_2}{y - y_2} \frac{dx}{\sqrt{Y}}, \quad . \quad . \quad . \quad (3)$$

with

$$r = K, \quad y = \frac{1}{\kappa^2 \operatorname{sn}^2 u}, \quad y - y_2 = \frac{\operatorname{dn}^2 u}{\kappa^2 \operatorname{sn}^2 u},$$

$$\begin{aligned} \kappa(2H)t_2 &= \int \kappa^2 \operatorname{cn}^2 (K - u) du = \int_0^{\cdot} [\operatorname{dn}^2 (K - u) - \kappa'^2] du \\ &= \left(\frac{E}{K} - \kappa'^2 \right) u - \operatorname{zn} (K - u). \quad . \quad . \quad . \quad (4) \end{aligned}$$

19. In the Quadric Transformation (Q.T.) for the expression of x by the E.F. to modulus (γ , G), in a sequence

$$\infty > a > b > x > c > d > -\infty,$$

as we have taken H positive and the orbit circling round the line SS' , in the expression

$$y = \frac{a - x \cdot x - d}{b - x \cdot x - c}, \quad b, c = \pm 1, \quad . \quad . \quad . \quad (1)$$

$$\frac{b - x}{a - x} = \frac{b - c}{a - c} \operatorname{sn}^2 \frac{1}{2} eG,$$

$$\frac{x - c}{a - x} = \frac{b - c}{a - b} \operatorname{cn}^2 \frac{1}{2} eG,$$

$$\frac{x - d}{a - x} = \frac{b - d}{a - b} \operatorname{dn}^2 \frac{1}{2} eG, \quad . \quad . \quad . \quad (2)$$

$$\gamma^2 = \frac{b - c \cdot a - d}{a - c \cdot b - d}, \quad \gamma'^2 = \frac{a - b \cdot c - d}{a - c \cdot b - d},$$

A.R.'s of a, b, c, d . And at $x = \infty, y = 1$,

$$\gamma^2 \operatorname{sn}^2 \frac{1}{2} fG = \frac{b - c}{a - c}, \quad \operatorname{sn}^2 \frac{1}{2} fG = \frac{b - d}{a - d},$$

$$\operatorname{cn}^2 \frac{1}{2} fG = \frac{a - b}{a - d}, \quad \operatorname{dn}^2 \frac{1}{2} fG = \frac{a - b}{a - c}, \quad . \quad . \quad (3)$$

$$\frac{b - x}{a - x} = \gamma^2 \operatorname{sn}^2 \frac{1}{2} eG \operatorname{sn}^2 \frac{1}{2} fG,$$

$$\frac{x - c}{a - x} = \frac{\gamma^2 \operatorname{cn}^2 \frac{1}{2} eG \operatorname{sn}^2 \frac{1}{2} fG}{\operatorname{dn}^2 \frac{1}{2} fG},$$

$$\frac{x - d}{a - x} = \frac{\operatorname{dn}^2 \frac{1}{2} eG \operatorname{sn}^2 \frac{1}{2} fG}{\operatorname{cn}^2 \frac{1}{2} fG}, \quad . \quad . \quad . \quad (4)$$

$$\begin{aligned}
 y &= \frac{\operatorname{dn}^2 \frac{1}{2} e G}{\gamma^2 \operatorname{sn}^2 \frac{1}{2} e G \operatorname{cn}^2 \frac{1}{2} e G} \cdot \frac{\operatorname{dn}^2 \frac{1}{2} f G}{\gamma^2 \operatorname{sn}^2 \frac{1}{2} f G \operatorname{cn}^2 \frac{1}{2} f G} \\
 &= \frac{1 + \operatorname{dn} e G}{1 - \operatorname{dn} e G} \cdot \frac{1 + \operatorname{dn} f G}{1 - \operatorname{dn} f G} \\
 &= \frac{1}{\kappa^2 \operatorname{sn}^2 e K \operatorname{sn}^2 f K} = \frac{1}{\kappa^2 \operatorname{sn}^2 u \operatorname{sn}^2 v}, \quad (5)
 \end{aligned}$$

in accordance with the Q.T. in (1) above.

Other Q.T. formulas are

$$\sqrt{\kappa \operatorname{sn} e K} = \gamma \operatorname{sn} \frac{1}{2} e G \operatorname{sn} (1 - \frac{1}{2} e) G, \quad . \quad . \quad (6)$$

so that, when $e=0$,

$$\begin{aligned}
 \sqrt{\kappa K} &= \frac{1}{2} \gamma G \quad \text{and} \quad \sqrt{\kappa K'} = \gamma G', \\
 \frac{K'}{K} &= \frac{2G'}{G}, \quad \kappa = \frac{1 - \gamma'}{1 + \gamma'}, \quad . \quad . \quad (7)
 \end{aligned}$$

$$\frac{1}{2} e G = \int_x^b \frac{\frac{1}{2} \sqrt{(a-c) \cdot (b-d)} dx}{\sqrt{(a-x) \cdot (b-x) \cdot (x-c) \cdot (x-d)}}, \quad . \quad . \quad (8)$$

$$e K, K = \int_{y, y_1}^{\infty} \frac{\sqrt{(y_1 - y_3)} dy}{\sqrt{(4 \cdot y - y_1 \cdot y - y_2 \cdot y - y_3)}}, \quad . \quad . \quad (9)$$

Then, also,

$$\begin{aligned}
 \frac{1 - \operatorname{cn} f G}{1 + \operatorname{cn} f G} &= \frac{\operatorname{sn}^2 \frac{1}{2} f G \operatorname{dn}^2 \frac{1}{2} f G}{\operatorname{cn}^2 \frac{1}{2} f G} = \frac{b-d}{a-c}, \quad \frac{1 - \operatorname{dn} f G}{1 + \operatorname{dn} f G} = \frac{b-c}{a-d}, \\
 \operatorname{cn} f G &= \frac{a-b-c+d}{a+b-c-d}, \quad \operatorname{dn} f G = \frac{a-b+c-d}{a+b-c-d}, \\
 \operatorname{sn} f G &= \frac{2\sqrt{(a-c) \cdot (b-d)}}{a+b-c-d}, \quad \gamma \operatorname{sn} f G = \frac{2\sqrt{(a-d) \cdot (b-c)}}{a+b-c-d}, \\
 \gamma' \operatorname{sn} f G &= \frac{2\sqrt{(a-b) \cdot (c-d)}}{a+b-c-d} \quad . \quad . \quad . \quad (10)
 \end{aligned}$$

A modification will be required with b, c conjugate imaginary, and $a, d = \pm 1$, with the sequence

$$\infty > x > a > d > x > -\infty,$$

and

$$y = \frac{x-b \cdot x-c}{x-a \cdot x-d} = \frac{(x-m)^2 + n^2}{x^2 - 1} = \frac{x^2 - \frac{A-B}{H} x - 1 - \frac{K}{H}}{x^2 - 1}.$$

Then with $(a-m)^2 + n^2 = H^2$, $(d-m)^2 + n^2 = K^2$,

$$\kappa^2 = \frac{(H+K)^2 - (a-d)^2}{4HK}, \quad \kappa'^2 = \frac{(a-d)^2 - (H-K)^2}{4HK}.$$

$$2eG, 2fG = \int_1^{x, \infty} \frac{\sqrt{(HK)} dx}{\sqrt{X}},$$

$$\frac{x-1}{x+1} = \frac{H}{K} \cdot \frac{1 - \operatorname{cn} 2eG}{1 + \operatorname{cn} 2eG} = \frac{1 + \operatorname{cn} 2f}{1 - \operatorname{cn} 2f} \cdot \frac{1 - \operatorname{cn} 2e}{1 + \operatorname{cn} 2e},$$

$$x = \frac{1 - \operatorname{cn} 2e \operatorname{cn} 2f}{\operatorname{cn} 2e - \operatorname{cn} 2f},$$

$$= \frac{1}{2} \frac{\operatorname{sn}(f+e) \operatorname{dn}(f-e)}{\operatorname{dn}(f+e) \operatorname{sn}(f-e)} + \frac{1}{2} \frac{\operatorname{dn}(f+e) \operatorname{sn}(f-e)}{\operatorname{sn}(f+e) \operatorname{dn}(f-e)}$$

$$= \frac{1}{2} \frac{\operatorname{cn}(1-f-e)}{\operatorname{cn}(1-f+e)} + \frac{1}{2} \frac{\operatorname{cn}(1-f+e)}{\operatorname{cn}(1-f-e)},$$

$$y = 4HK \frac{\operatorname{dn}^2 2eG}{\operatorname{sn}^2 2eG} = \frac{\operatorname{cn}^2(1-2f)G}{\operatorname{cn}^2(1-2e)G},$$

$$2eG, 2fG = \int_{y, y_1}^{\infty} \frac{\sqrt{(y_1 - y_3)} dy}{\sqrt{(4 \cdot y - y_1 \cdot y - y_2 \cdot y - y_3)}},$$

with $y_2 = 0$, and there is no Quadric Transformation in

$$y - y_1 = (1 - y_1) \frac{(x - x_1)^2}{x^2 - 1}, \quad y - y_3 = (1 - y_3) \frac{(x - x_3)^2}{x^2 - 1},$$

$$\frac{dy}{dx} = \frac{2m(x - x_1)(x - x_3)}{(x^2 - 1)^2}, \quad \frac{(y_1 - y_3) dy}{y - y_1 \cdot y - y_3} = \frac{2(x_1 - x_3) dx}{x - x_1 \cdot x - x_3},$$

$$y_1 - y_3 = HK = m(x_1 - x_3).$$

20. For the time t_1 , change the sign of B, and write x for $\operatorname{ch} \phi$; a similar reduction will hold, but in a new sequence

$$\infty > x > a > b > c > d,$$

$$\infty > y_1 > y_2 > 1 > y > y_3 = 0.$$

And when H is negative, the form of t_2 will serve for t_1 , with a sequence

$$\infty > a > x > d > b > c.$$

A Pseudo-Elliptic Case may be attempted, by taking $f=1, \frac{1}{2}, \frac{2}{3}, \frac{1}{3}, \dots$; and then the Theta functions can be replaced by algebraical expressions.

XXXIX. *Energy Relations in the High-Tension Magneto.* By
ELWYN JONES, M.Sc., *University Research Student, Uni-
versity College of North Wales, Bangor**.

THE problem of determining the energy of the induced primary current in a high-tension magneto from the various constants of the machine and the speed of rotation is of importance not only in connexion with the practical design of magnetos, but also on the theoretical side, especially in view of the well-known fact that the "permanent" magnet, between the poles of which the armature rotates, undergoes periodic fluctuations in strength during the rotation. The magnetic properties of the steel magnet are thus brought into play, and the question arises whether the changes of energy of magnetization of the magnet contribute in any appreciable degree to the useful energy produced by the machine.

The experiments described in the present paper were made with the object of determining in a particular case the values of the more important terms which appear in the energy equation of a magneto.

The Energy Equation.

This equation may be expressed as follows:—

Mechanical work done in rotating the armature from a certain zero position, in which the contact pieces of the interrupter are brought together, to any position θ° from zero

$$\begin{aligned} &= \text{increase of magnetic energy of the system} \\ &+ \text{heat generated in the primary wire between} \\ &\quad \text{zero and } \theta^\circ \\ &+ \text{thermal effects in the iron and steel portions of} \\ &\quad \text{the machine} \quad \dots \dots \dots (1) \end{aligned}$$

The magnetic energy of the system includes the following parts:—

(1) The electrokinetic energy of the induced current in the primary coil, represented in the usual notation by the integral $\frac{1}{8\pi} \int B H \, dr$, taken throughout the whole of the system and the surrounding space.—This part includes the

* Communicated by Prof. E. Taylor Jones.

energy, $\frac{1}{2}Li^2$, due to the self-inductance of the primary coil and the current i induced in it, and the mutual energy of the primary coil due to its presence in the field of the magnet. The electrokinetic energy may also be expressed in the form $\frac{1}{2}iN$, where N is the total flux through the windings of the primary coil. The electrokinetic energy is zero in the zero position, in which $i=0$.

It should be explained that we are not here concerned with the conversion of the energy of the primary current into the energy of the secondary circuit, which is the immediate source of the energy of the spark. The manner of conversion of the primary energy is essentially the same in the magneto as in the induction coil, and has been fully discussed by Professor Taylor Jones in his 'Theory of the Induction Coil'*. Our present problem is limited to the estimation of the amount of energy in the primary circuit which is available for such conversion, and this energy is represented by the term $\frac{1}{2}Li^2$.

(2) The intrinsic energy of magnetization.—According to the theory of Larmor†, the energy of magnetization is equal to the integral $\frac{1}{2}\int BIdv$ taken throughout the volume of the iron and steel portions of the system. It is believed that at least a part of the change of energy of magnetization is compensated by thermal effects occurring within the magnetic material, but it does not appear to have been definitely ascertained whether the whole of the energy of magnetization is to be accounted for in this way.

Although the measurements described in the present paper allow of a determination of the change of energy of magnetization, we shall not include it as a separate term in the equation, but rather assume that it is partly compensated by the thermal effects forming the third term on the right-hand side of equation (1).

(3) The mutual energy of the magnetized material and the field in which it is placed.—The change of this part of the energy includes the integral $v\int_0^\theta IdH$ or approximately $v\int_0^\theta BdH$ for each portion of the magnetized material, which gives in a closed cycle the usual hysteresis loss. The change of mutual energy may be estimated from the magnetization curves of the iron and steel. In the case of the iron it is comparatively small, owing to the small value of H in

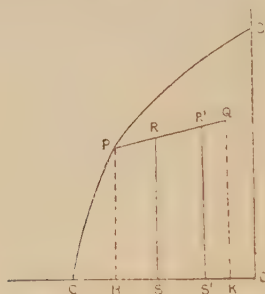
* 'Theory of the Induction Coil' (Pitman & Sons, 1921).

† Proc. Roy. Soc. vol. lxxi. p. 229 (1902-3).

this material. In the case of the steel magnet, let BC in fig. 1 represent the "curve of demagnetization" of the magnet after its original magnetization, and let P, Q be the limits of the small cycle corresponding to any point P on the curve. The point P represents the greatest degree of demagnetization to which the magnet has been subjected. The point Q corresponds to the zero position of the armature.

Then the integral $\int_0^\theta B dH$ for the magnet is represented approximately by the area RQKS, the point R corresponding to position θ .

Fig. 1.



The change of mutual energy also includes a term $r \int H dI$, which we shall assume (as in the case of the energy of magnetization) to be in part compensated thermally.

The second term on the right-hand side of equation (1), the copper loss, is represented by the expression $\int_0^\theta i^2 R \frac{d\theta}{\omega}$, where R is the resistance of the primary wire and ω is the speed of rotation.

In the third term on the right-hand side of (1), in addition to the thermal effects which are assumed to compensate the change of energy of magnetization, are also included losses due to eddy currents in the core and pole-pieces. Although the eddy current losses during the rapid oscillations which succeed the interruption of the primary current may be very considerable, it is not probable that they are serious in the comparatively slow changes of magnetization accompanying the rotation, more especially as the armature core is composed of thin insulated stallo sheets.

With these modifications the energy equation becomes :

$$\text{Mechanical work } W = \frac{1}{2}Li^2 + \frac{1}{2}iN' + \frac{v_i}{4\pi} \int B_i dH_i + \frac{v_s}{4\pi} \int B_s dH_s + \int_0^\theta i^2 R \frac{d\theta}{\omega} + X_1, \quad (2)$$

where N' is the flux through the primary coil in the position θ due to the magnet, and X_1 represents any uncompensated magnetic energy of an intrinsic nature.

If the armature is rotated from 0 to θ with the primary circuit open, the 1st, 2nd, and 5th terms on the right-hand side of (2) are zero, and the remaining terms are much smaller. The equation now becomes :

$$W' = \frac{v_i}{4\pi} \int_{i=0} B_i dH_i + \frac{v_s}{4\pi} \int_{i=0} B_s dH_s + X_2. \quad (3)$$

Subtracting (3) from (2), we find :

$$W - W' = \frac{1}{2}Li^2 + \frac{1}{2}iN' + \int i^2 R \frac{d\theta}{\omega} + \frac{v_s}{4\pi} [\text{area } RR'S'S] + \frac{v_i}{4\pi} \left[\int B_i dH_i - \int_{i=0} B_i dH_i \right] + X, \quad (4)$$

X being written for $X_1 - X_2$.

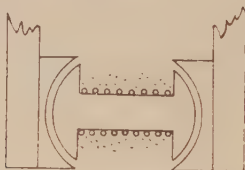
In a recent paper E. A. Watson * has advanced theoretical reasons for the view that the quantity $\frac{v_s}{4\pi} \int B_s dH_s$ representing the diminution of energy of the steel magnet is equal to the energy $\frac{1}{2}Li^2$ in the armature coil available for conversion. In one case at any rate, viz. when the armature is rotated through 180° from zero, it might be expected that some relation must exist between the induced primary current and the demagnetization, since the demagnetization is in this case entirely due to the induced current. It is unlikely, however, that any such simple relation can exist in general: in some positions of the armature, for instance, the effect of the induced current is to increase rather than diminish the degree of magnetization of the magnet.

The experiments described below were arranged for the measurement of the terms in equation (4) for a certain speed of rotation. The measurements were made on a Thomson-Bennett Type A.D. 4 magneto.

* Journ. Inst. Elect. Eng. vol. lix. no. 301 (May 1921).

In the present paper we shall take as the zero position of the armature that in which the axis of its coils is parallel to the field due to the magnet, as shown in fig. 2. The induced current therefore begins to grow from zero in this position.

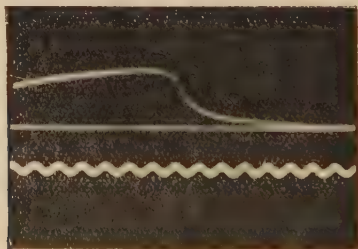
Fig. 2.



1. *Measurement of the induced current in any position of the armature.*

The induced current was determined by means of a current oscillograph designed by Professor Taylor Jones. By using an extra interrupter directly coupled with the armature and rotating with it, this instrument was connected in series with the primary coil. The photograph in fig. 3

Fig. 3.

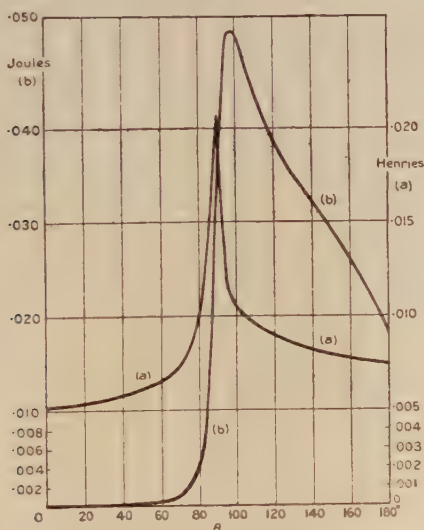


shows a typical curve obtained when the interrupter was so adjusted that contact was made when the armature was in the position shown in fig. 2, and broken when the armature was displaced through 180° from this position. The lower curve is the trace of a ray reflected from a 768 tuning-fork placed near the oscillograph. The curve in fig. 3 gives the value of the induced current at any position of the armature between 0° and 180° . The curve selected for measurement was taken when the armature was rotating at 1505 revolutions per minute. The maximum current at this speed was 3.12 amperes, and it occurred in the position of 102° from zero. The ordinate of the curve was measured in any position required (*i. e.* at any value of θ) by means of a travelling microscope.

2. Measurement of the primary self-inductance.

The current oscillograph was also used to determine the primary self-inductance in any position of the armature. The primary coil was connected in series with the oscillograph, and an A.C. voltmeter in parallel with both. The armature was locked in a position θ° and an alternating current, the R.M.S. value of which was the same as the induced primary current in that position, and whose frequency was approximately that of the rotating armature, was sent through the circuit. The curves obtained with the oscillograph gave the current wave-form, from which the R.M.S. value, i_s , was obtained in the usual way by dividing the maximum value by $\sqrt{2}$. The voltmeter (an instrument of the electro-dynamometer type) gave the R.M.S. voltage, V_s ,

Fig. 4.



at the terminals of the primary coil and oscillograph. The photographs also gave the frequency of the alternations of the current. The self-inductance was calculated from the relation $V_s = i_s \sqrt{R^2 + 4\pi^2 n^2 L^2}$, in which R represents the resistance of the primary coil and that of the oscillograph. The curve giving the self-inductance of the primary coil in different positions of the armature is shown in fig. 4 (a).

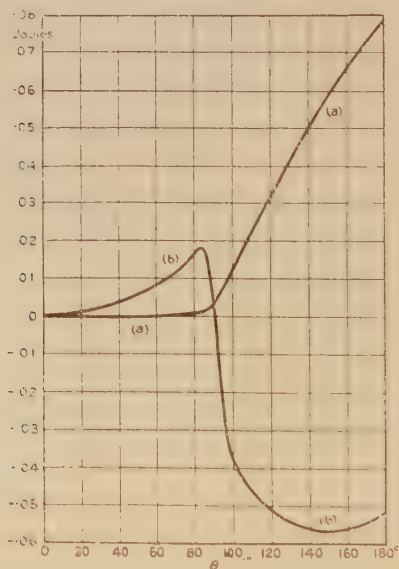
Owing to the low frequency at which the self-inductance was measured, the correction due to the presence of the secondary coil was found to be negligible.

The available energy ($\frac{1}{2}Li^2$) in any position θ° was obtained from the foregoing results, and its variation with θ is shown in fig. 4 (b).

3. *Determination of the heat loss in the primary wire.*

The heat generated in the primary circuit between zero and θ° was obtained from the area of the i^2R curve between zero and θ° . The resistance R , being the total resistance of the circuit traversed by the current i , included the resistance of the oscillograph and connecting wires. The curve (a) in fig. 5 gives the value of the copper loss, $\int i^2 R \frac{d\theta}{\omega}$, in different positions of the armature.

Fig. 5.



4. *Measurement of the change of induction in the magnet.*

A number of small coils were wound on the magnet in different places, and the change of flux through these coils due to rotating the armature from zero to θ° was measured by connecting them in turn to a ballistic galvanometer. The contact pieces of the interrupter were kept apart during the rotation. Dividing these flux changes by the area of cross-section of the magnet and taking the mean, we find the

change of magnetic induction in the magnet due to rotating the armature.

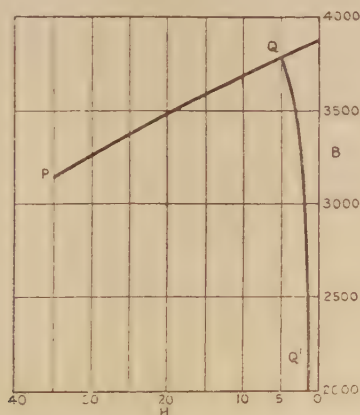
The armature was then clamped in the position θ° , and the current corresponding to that position was sent through the primary coil, one of the magnet coils being connected to the galvanometer. The change of flux in the magnet due to switching on this current in the armature was measured as before.

Combining the two results, we have the total change of magnetic induction in the magnet for the position θ° of the armature. It was found that the maximum demagnetization of the magnet occurred at 125° .

5. Determination of the BH curve for the magnet.

The primary coil was connected to a ballistic galvanometer, and the change of flux through the coil due to rotating the armature from zero to 180° was determined. This gave twice the actual flux passing through the armature in the zero position. Dividing the latter by the area of cross-section of the magnet and adding a correcting term due to

Fig. 6.



leakage flux, we obtain the ordinate of the point Q in figs. 1 and 6. The leakage-flux was obtained by means of an exploring coil, connected to a ballistic galvanometer and placed above and below the armature. The abscissa of the point Q was obtained from the relation

$$H_Q = \frac{N}{L} \left(\frac{2d}{A} + \frac{l}{\mu s} \right),$$

which represents the fact that the magnetomotive force in

the armature and air-gaps is equal to the M.M.F. demagnetizing the magnet*. In this equation

N =flux through the armature in the zero position,

L =length of the steel magnet,

d =thickness of the air-gap between the armature and pole-shoes,

A =area of the curved end of the armature core,

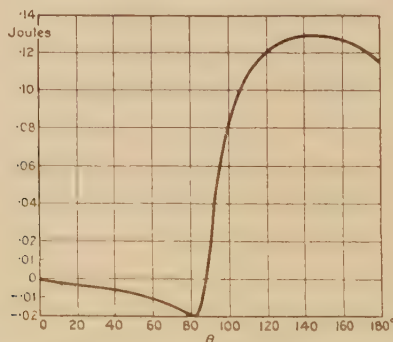
s =area of cross-section of the armature core,

μ =permeability of stalloy corresponding to a flux density $\frac{N}{s}$,

l =length of the armature core along the axis.

The point Q in fig. 6 lies upon the magnetization curve for the armature and air-gaps represented by QQ', various points on which were determined in the same way for other values of the flux density. The magnet was subjected to a demagnetizing force by means of a current passing through a coil wound over the whole length of the magnet, the change of induction in the magnet being measured as before. The demagnetizing force was varied by varying the current, and was gradually increased until the magnetic induction reached the minimum obtained in the experiments described in the previous section. The demagnetization curve obtained for the magnet is the line QP in fig. 6.

Fig. 7.



From these and the results of the measurements described in section 4, the term $\frac{r_s}{4\pi}$ [area RR'S'S] (fig. 1) in equation (4) was calculated for different values of θ , and the curve is shown in fig. 7.

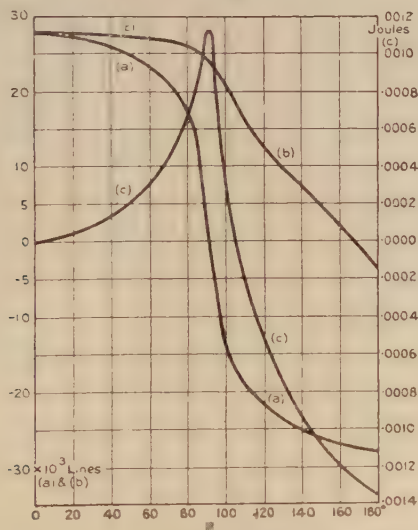
* The magnetic reluctance of the wide cheeks of the armature and of the pole-pieces is neglected.

6. Measurement of the mutual energy of the iron and the field.

The flux due to the magnet through the armature in the position θ° was obtained by connecting the primary coil to a ballistic galvanometer and determining the change of flux produced by rotating the armature from zero to θ° . Subtracting this from the original flux passing through the armature in the zero position, we find the flux in position θ° . The open-circuit flux wave is shown in fig. 8 (a). This value for the flux has to be divided by the area of cross-section of the armature core, in order to reduce it to flux density in the iron.

The flux through the armature due to the current in the position θ° was obtained by locking the armature in this

Fig. 8.



position, connecting the secondary to a ballistic galvanometer and sending the current corresponding to this position through the primary coil. A correction had to be applied to the flux thus obtained, owing to the change in the magnet flux through the armature due to the demagnetizing effect of the current, on the magnet. The amount of demagnetization of the magnet due to the current in the position θ° had been determined in a previous experiment (see section 4, above).

Fig. 8 (b) shows the total flux through the armature in any position during one half-revolution.

Reducing these to flux densities in the armature core and from measurements of the areas in the BH curve for a typical specimen of silicon steel, the term

$$\frac{v_i}{4\pi} \left[\int B_i dH_i - \int_{i=0} B_i dH_i \right]$$

was calculated for different values of θ , and is shown in fig. 8 (c). Since this term is small in comparison with the other terms of equation (4), it was thought sufficient to obtain its value from a typical specimen of silicon steel instead of determining the BH curve for the actual material of the core.

7. The term $\frac{1}{2}iN'$ was obtained from the open-circuit flux wave, a correction being applied due to the reduction of the magnet flux through the armature caused by the induced current. The manner in which this correction was obtained is described in section 6. The values of the term $\frac{1}{2}iN'$ are shown in fig. 5 (b).

8. *Measurement of the work done.*

The couple acting on the armature in the position θ° was measured when the current corresponding to that position was flowing through the primary wire. For this purpose a lever was attached to one end of the armature axle, and a cord, passing from one end of the lever and over a pulley, supported a scale-pan. The position of the pulley was so adjusted that in each position of the armature the cord was at right angles to the lever. In this way the couple was measured which was necessary to hold the armature in the position θ° with the appropriate current flowing in its primary coil. This experiment was then repeated with the primary circuit open, and in this case the couple measured is that required to hold the iron core in the position θ° .

These couples were plotted against θ , and the area of the curve from zero to θ° gives the work done, W or W' .

The difference $W - W'$ is shown in fig. 9 (a)*.

The results of all the above measurements are collected in the Table, in which the first column gives the position θ° of the armature, the second column the work done W in turning the armature from 0 to θ in joules, the third the work done W' on open circuit, the fourth the values of the useful energy $\frac{1}{2}Li^2$, the fifth the mutual energy $\frac{1}{2}iN'$ of the primary

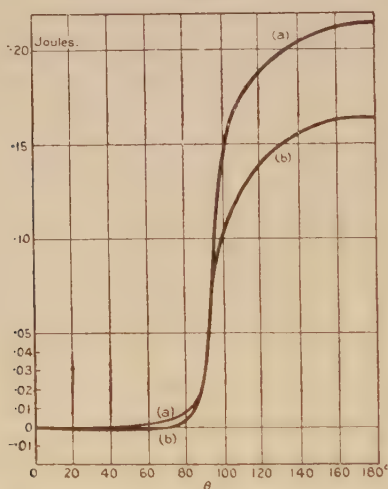
* Frictional work is neglected, being practically eliminated by the process of taking the difference between W and W' : its value is in any case small.

TABLE.

(1) θ .	(2) W .	(3) W' .	(4) $\frac{1}{2}L'^2$.	(5) $\frac{1}{2}N'$.	(6) $\int_0^{\frac{1}{2}\pi} R \frac{d\theta}{\omega}$.	(7) $\frac{v}{4\pi} \int B_s dH_s$.	(8) $\frac{v}{4\pi} \int B_s dH_s$.	(9) Σ .	(10) $W - W'$.
0	0	0	0	0	0	0	0	0	0
20	·00128	·00118	·000018	·00207	·00001	·00314	·00004	·00108	·000103
40	·00496	·00453	·000114	·00184	·000039	·00325	·00012	·00137	·000429
60	·0117	·00996	·000498	·00860	·000233	·0105	·00033	·00152	·00176
70	·0171	·0137	·00121	·0117	·000471	·0135	·000436	·00055	·00338
80	·0271	·0190	·00461	·0164	·000112	·0180	·00065	·00345	·00813
85	·0376	·0229	·0141	·0171	·00183	·0188	·00081	·00135	·0148
90	·0643	·0241	·0350	·00294	·00369	·00258	·0011	·0405	·0402
95	·120	·0255	·0500	·0130	·00758	·0454	·00087	·0831	·0949
100	·168	·0224	·0499	·0376	·0127	·0806	·000354	·105	·146
110	·193	·0175	·0438	·0465	·0230	·106	·000235	·127	·175
120	·204	·0141	·0384	·0510	·0326	·120	·000507	·140	·190
130	·215	·00909	·0318	·0560	·0502	·129	·000970	·156	·206
140	·219	·00607	·0256	·0559	·0659	·128	·00117	·164	·213
160	·220	·00507	·0180	·0512	·0784	·116	·00136	·163	·215

coil at θ° , the sixth the copper loss during the rotation 0 to θ° , the seventh and eighth the loss of mutual energy of the magnet and of the iron core. The ninth column gives the sum of the terms in columns (4) to (8). The last column shows the value of the mechanical work $W - W'$ in the various positions of the armature. The values given in the last two columns are also shown graphically in fig. 9, in which curve (a) represents the mechanical work $W - W'$, and (b) the values given in column (9)—*i. e.*, the total change of magnetic energy (excluding unbalanced intrinsic effects) and the heat loss in the primary wire.

Fig. 9.



It will be seen from fig. 9 that in the neighbourhood of the position 90° the two curves agree closely: at smaller values of θ , $W - W'$ slightly exceeds the magnetic and thermal effects represented in column (9): at larger angles the difference increases, and at 180° about 25 per cent. of the mechanical work done in rotating the armature is unaccounted for by the quantities represented in Table I.

The conclusion to which these experiments point is that the energy developed in the primary coil by its rotation in the field of the magnet is at and near the 90° position (which is the position at which the secondary spark is usually obtained) entirely accounted for by the mechanical, magnetic, and thermal energy in the manner explained above. For positions representing larger angles of rotation of the armature (100° to 180°) there appears to be a loss of energy

from the forms considered in this paper. Possibly this difference appears as heat in the iron and steel of the machine.

With regard to Watson's conclusion that the loss of magnetic energy of the magnet (column (7), Table) is equal to the useful electrokinetic energy generated in the primary coil, together with the heat loss in the primary wire (columns (4) and (6), Table), it will be seen that, according to the measurements described in the present paper, at 180° the loss of energy of the magnet is about 20 per cent. greater than the sum of the electrokinetic energy and the copper loss. The difference is much greater at 120° , and sinks to zero at 97° . At still smaller angles the magnet term is much smaller than the sum of the electrokinetic energy and the copper loss, and is in fact negative at angles less than 90° .

It does not appear therefore that there is any simple relation between the loss of energy of the magnet, as represented by the area $RR'S'S$ in fig. 1, and the useful electrokinetic energy generated in the primary coil.

The efficiency with which useful energy is developed is represented by the ratio of the numbers in the fourth and second columns. The efficiency has a maximum value of about 54 per cent. at 90° .

The experiments described above were carried out in the Physical Laboratories of the University College of North Wales, Bangor. In conclusion, I wish to thank Professor E. Taylor Jones for his most valuable assistance in everything connected with this paper.

XL. Linear, Exponential, and Combined Dampings exhibited by Pendulum Vibrations. By Prof. E. H. BARTON, F.R.S., and H. M. BROWNING, M.Sc., Ph.D., University College, Nottingham.*

[Plates VI. & VII.]

IT is well known that under resistances proportional to the speed, a vibration is exponentially damped. It is consequently never extinguished. Yet we are not aware that all vibrations once started are still in operation. It would therefore appear that vibrations, whether mechanical or electrical, are really subject to other resistances than that single type proportional to the speed which is conventionally

* Communicated by the Authors.

postulated. In July 1922* H. S. Rowell considered theoretically the case of a vibration under a constant resistance, and showed that it resulted in linear damping.

It seemed of interest to the present writers to obtain experimental illustrations of such vibrations in the simplest mechanical manner. This has now been done for vibrations with linear dampings only, exponential only, and for a combination of both. The theory developed for these cases is in satisfactory agreement with the experiments. The vibration records consist of photographs of salt traces left by a pendulum. The damping of this pendulum was produced by (1) solid friction on its lath, or by (2) fluid friction due to air resistance increased by a card, or by (3) both together.

THEORY.

General Equation for Combined Damping.—We may write the equation of motion for combined damping as follows:—

$$m \frac{d^2 y}{dt^2} + r \frac{dy}{dt} + sy \pm F = 0, \quad . \quad . \quad . \quad (1)$$

$$\text{or} \quad \frac{d^2 y}{dt^2} + 2k \frac{dy}{dt} + p^2(y \pm S) = 0, \quad . \quad . \quad . \quad (2)$$

where y is the displacement and m is the mass of the vibrating particle, s is the restoring force per unit displacement, r is the fluid resistance per unit speed, F is the solid resistance of constant numerical value, but of sign opposite to that of the velocity; also

$$2k = \frac{r}{m}, \quad p^2 = \frac{s}{m}, \quad S = \frac{F}{s}. \quad . \quad . \quad . \quad (3)$$

Thus (1) and (2) only hold, with a certain sign of F , for a single half period from one maximum elongation to the next of opposite sign.

Consider first the half period from rest at a positive elongation. Then we may write for this *start* of the motion,

$$\text{for} \quad t = 0, \quad \frac{dy}{dt} = 0, \quad y = S + A. \quad . \quad . \quad . \quad (4)$$

Then the solution of (1) and (2) for the half period defined by (4) requires the negative sign for F and S , and may be written:

$$y - S = Ae^{-kt} \left(\cos qt + \frac{k}{q} \sin qt \right), \quad . \quad . \quad . \quad (5)$$

where

$$q^2 = p^2 - k^2. \quad . \quad . \quad . \quad . \quad . \quad (6)$$

* See Phil. Mag. xlv. pp. 284-285.

It will be seen that this solution satisfies the conditions expressed in equations (4).

The negative elongation y_1 , at the end of this first half period, is found by putting in (5) $t = \pi/q$. We thus obtain

$$y_1 - S = -Ae^{-k\pi/q} = -A\rho, \quad . \quad . \quad . \quad (7)$$

where

$$\rho = e^{-k\pi/q}. \quad . \quad . \quad . \quad . \quad . \quad . \quad (8)$$

For the second half period F and S change sign so that the axis of our exponentially damped vibration is $-S$. And the initial state for this second half period is that given at the end of the first. So for the second half period, if we again let t start from zero, the solution may be written

$$y + S = -(A\rho - 2S)e^{-kt} \left(\cos qt + \frac{k}{q} \sin qt \right). \quad . \quad (9)$$

Proceeding thus we find at the end of the second half period the elongation y_2 given by

$$y_2 + S = (A\rho - 2S)\rho = A\rho^2 - 2S\rho. \quad . \quad . \quad (10)$$

And by continuing in this way we find that after n half periods the original amplitude of $S + A$ becomes reduced to y_n where

$$y_n \pm S = \pm A\rho^n \mp 2S(\rho^{n-1} + \rho^{n-2} + \dots + \rho), \quad . \quad (11)$$

the upper signs being used for n even and the lower signs for n odd.

To make comparisons of recorded dampings which are (1) exponential only, (2) linear only, and (3) a combination of the two, we need some simple way of gauging the damping in each case. It seems desirable for this purpose to fix upon the number of half periods in which the elongation is reduced to one-half. The half is chosen rather than zero because in the latter case for purely exponential damping the number would be infinite.

Thus, if in n half periods the original elongation ($S + A$) becomes reduced to one-half by combined damping, we have, from (11),

$$\begin{aligned} y_n &= \mp S \pm A\rho^n \mp 2S(\rho^{n-1} + \rho^{n-2} + \dots + \rho) \\ &= \frac{S + A}{2}, \end{aligned}$$

$$\text{or} \quad n = \log \left\{ \frac{A(1-\rho) + S(3+\rho)}{2A(1-\rho) + 4S} \right\} \div \log \rho. \quad . \quad (12)$$

Linear Damping.—For $k=0$ in (2) the exponential damping disappears, and the result is a linear damping. In other words, the elongations form an arithmetical progression whose common difference is $-2S$, as seen from equations (4), (7), (10), and (11) for $\rho=1$. Hence, if in a half periods the original elongation $S+A$ is halved, we have

$$S+A-(2S)a = \frac{S+A}{2},$$

whence
$$S = \frac{A}{4a-1} \quad \text{and} \quad a = \frac{S+A}{4S} \quad \dots \quad (13)$$

Exponential Damping.—For $F=0$ in (1) we have $S=0$ in (2) and the subsequent equations; thus the damping is exponential only, or the successive elongations are in geometric progression. Hence, if in b half periods the original amplitude ($S+A$) is halved, we have

$$e^{-k\pi b/q} = 1/2. \quad \dots \quad (14)$$

Comparison of Pure and Combined Dampings.—By equations (8) and (14) we see that

$$\rho^b = 1/2 \quad \text{or} \quad \rho = 2^{-1/b}. \quad \dots \quad (15)$$

Therefore, putting (13) in (12), we find

$$n = \log \frac{2a(1-\rho) + (1+\rho)}{4a(1-\rho) + (1+\rho)} \div \log \rho, \quad \dots \quad (16)$$

which gives n in terms of a and ρ ; and since, as shown in (15), ρ is the b th root of one-half, this may be regarded as giving n in terms of a and b .

Approximation.—When ρ is nearly unity, we may write $(1+\rho)=2$ and $(1-\rho)=\sigma$; then (16) becomes

$$n = \log \frac{1+a\sigma}{1+2a\sigma} \div \log \rho = \left[\log \frac{1+a\sigma}{1+2a\sigma} \right] \div (-\sigma). \quad (17)$$

Experimental Arrangements.—As shown in the photograph of the apparatus (Pl. VI.), the pendulum suspension was a wood lath. On this a card could be attached to increase the fluid friction, and also rubbers made by means of an inverted clip stand could be pressed upon the upper part of the lath to introduce the solid friction. The bob was usually a ring of iron containing a funnel of Cerebos Salt to leave a vibration trace on the board which ran on rails and was drawn along by hand, constancy of speed being assured by the aid

of a metronome. This method was readily adaptable to any desired conditions, and seemed preferable to the use of a motor.

Results.—About fifty photographs of traces were taken, of which twenty-five are reproduced on Pl. VII., and the conditions under which they were obtained are summarized as follows:—

Conditions under which Vibrations occurred.

No. of Figure.	RUBBER.	CARD.	BOB.
1	Wash-leather	None ..	Iron.
2			
3			
4			
5			
6	Cork and Graphite...	None	Iron.
7			
8			
9			
10			
11	Cork, Graphite, and Vaseline	None	Iron.
12			
13			
14			
15			
16	No rubber	Card 10 inches by 5 inches	{ No Iron, but only glass fun- nel supported by wire, to con- tain Salt.
17	Rubber of Cork, Graphite, and Vaseline.....		
18			
19			
20			
21	Cork, Graphite, and Vaseline	Card 10 in. × 5 in.)	Iron.
22		„ 16 in. × 14 in.)	
23		„ 16 in. × 14 in.)	
24		None	
25	No rubber	Card 16 in. × 14 in.)	

The records fall into five sets of five each, and throughout each of the first four sets the damping increases as we proceed in that set. In the last set, which is very special, this is not so.

In the first set (figs. 1-5)* the rubbers were of wash-leather, and evidently for light pressures these did not, on reversal, give the discontinuity of force characteristic of solid friction. This is seen by the damping which at first (fig. 1) approaches exponential and is finally (fig. 5) almost linear.

* The references in the text are to the *Arabic* numerals on the figures. The Roman numerals indicate simply the order of taking the records.

The second set (figs. 6-10), with cork rubbers lubricated with fine graphite powder (as used in the carriages of lace machines), show for the higher pressures the linear dampings characteristic of solid friction. Probably for the very light pressures the contact was not quite continuous, and therefore the damping was not pure.

The third set (figs. 11-15), with vaseline added on the rubbers, seemed to ensure continuous contact, and gave throughout dampings almost linear.

The limits $y = \pm S$ are experimentally shown on figs. 9, 13, and 15. These were obtained by giving the pendulum the maximum displacement which failed to elicit any return motion, since the restoring force was balanced by the opposing frictional force. Figs. 10 and 14 have the centre line, $y = 0$, shown.

It is to be noticed that when first a state of rest is reached anywhere between the limits $y = \pm S$, then the vibration ceases, as may be noticed in the above-mentioned figures. The quick-period quivers shown on figs. 9, 10, 13, 14, and 15 are due to a slight flexibility of the lath not contemplated in the theory.

Figs. 13 and 15 give interesting confirmations of theory as to the relation of the damping to these limits. For from equation (13) we may write

$$\text{Number of half periods to extinction} = \frac{\text{Initial Amplitude}}{\text{Distance between limits}}$$

In the two cases under notice we have

$$\frac{2.7}{0.35} = 7\frac{5}{7}, \text{ or, say, } 8 \text{ half periods,}$$

$$\frac{2.7}{0.9} = 3 \text{ half periods.}$$

The fourth set (figs. 16-20) consists of vibrations of the pendulum without any iron in the bob, but only the glass funnel and salt. A card 10 inches by 5 inches was fastened at the bottom of the lath to effect by air resistance considerable damping of this light pendulum. For fig. 16 no rubbers were in use, and the damping due to fluid friction is seen to be sensibly exponential. For figs. 17-20 the rubbers were used, and with successively greater pressures. The dampings are seen to approach linearity as the solid friction becomes paramount. Fig. 20 has the limits $y = \pm S$ shown, and therefore reveals the effect of the card in contrast with figs. 13 and 15, for which no card was in use,



Photograph of Apparatus.

half amplitude is independent of the initial amplitude, and depends solely upon the damping in use according to the well-known expression (see equation (5)).

Conclusion.—It would seem from the remarks of Mr. H. S. Rowell (*Phil. Mag.* xliv. p. 951, Nov. 1922), and in the light of the above experiments, that vibrational methods might prove useful in the investigation of the type of resisting force introduced by various lubricants.

Also it may be noted that in the case of many electrical vibrations it is quite possible that spark gaps or other phenomena play the part of solid friction in mechanical vibrations, and so ensure the extinction of these electrical vibrations. But hitherto the cause of any such resistance in the electrical case does not appear to have received the attention it deserves.

Nottingham,
May 3rd, 1923.

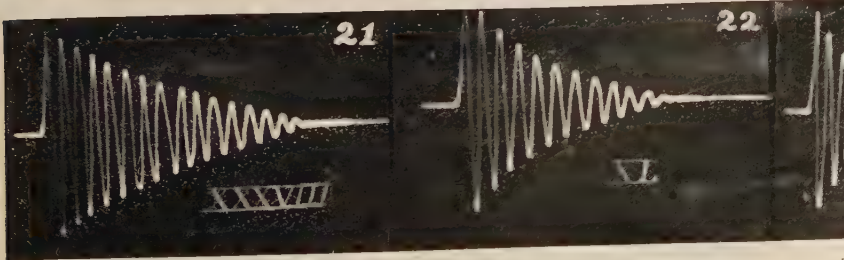
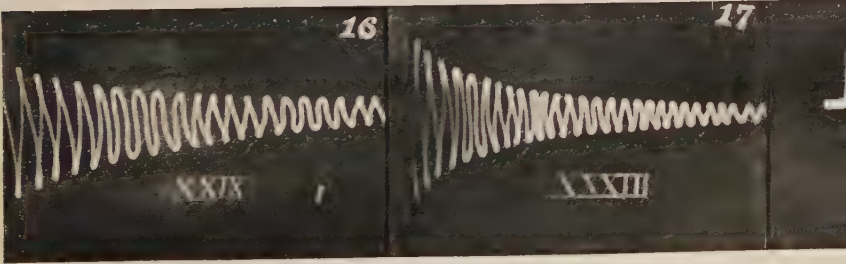
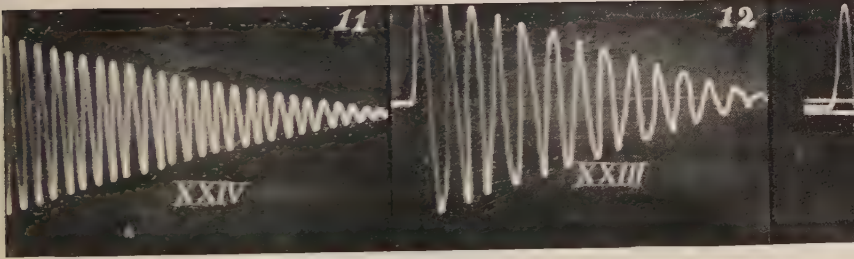
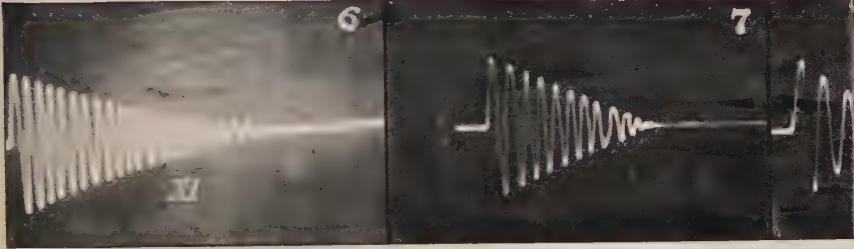
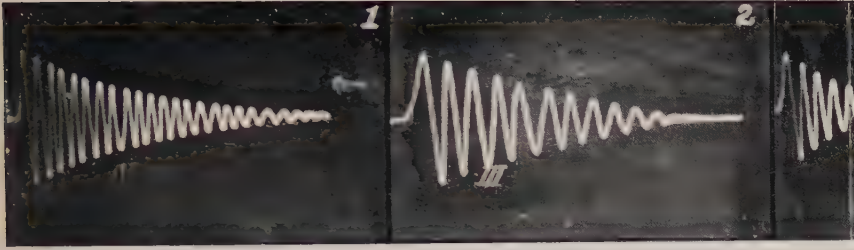
XLI. *On Sub-Continental Temperatures.* *By H. H. POOLE, Sc.D.**

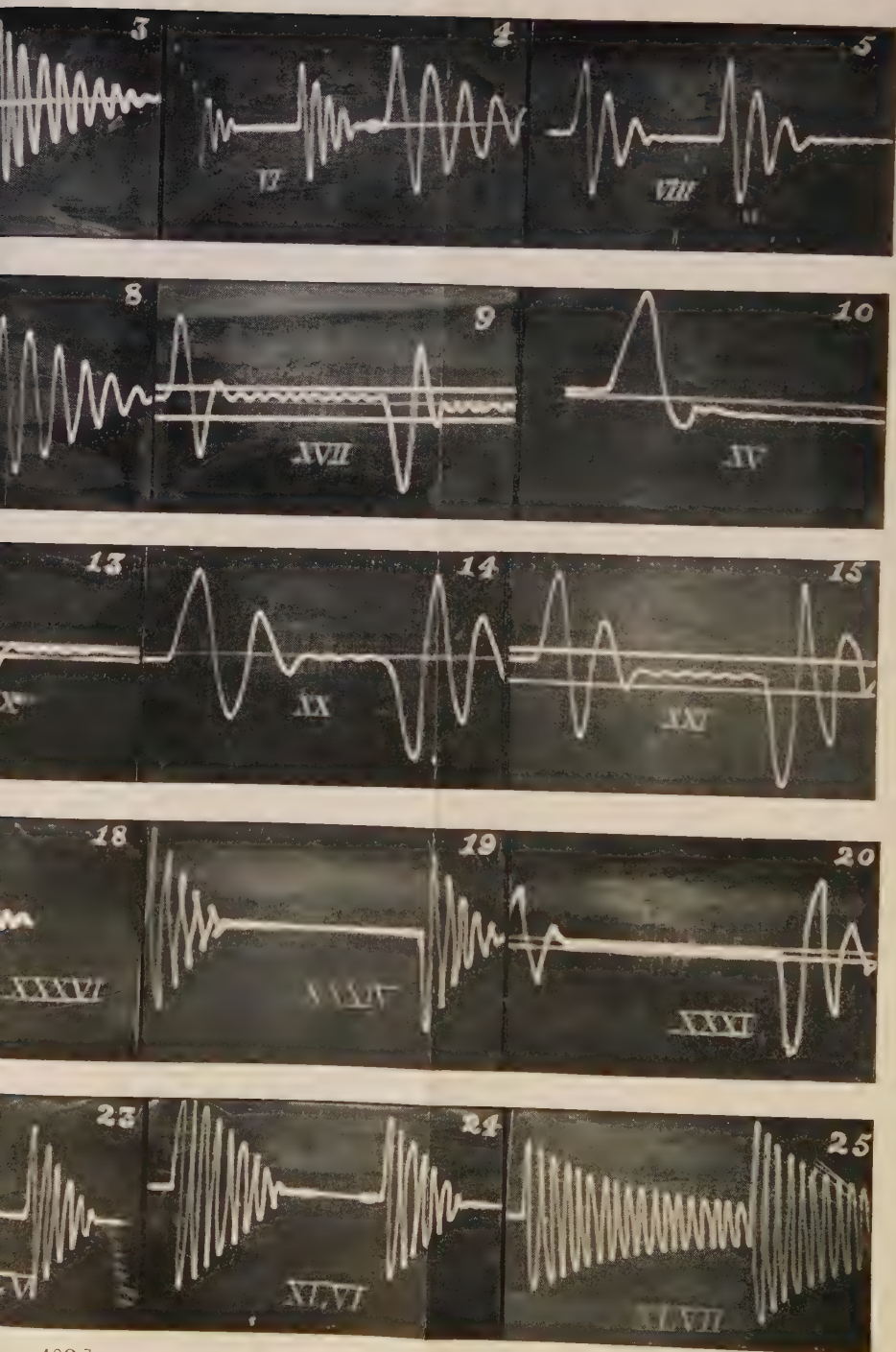
Introduction.

THE theory of radioactive revolutions, recently put forward by Dr. Joly, is based on the apparently justifiable assumption that the radioactivity of the basaltic magma, on which the continental rocks are thought to float, is approximately the same as that of basalt extruded at the surface. It seems to be natural to make the same assumption with regard to the continental rocks. This, however, is contrary to the view previously held that the smallness of the temperature gradient underground involved a very definite limit to the extent in depth of rocks of the relatively high radioactivity met with at the surface †. It may be of interest to reconsider this question, in order to ascertain whether the assumption of uniform radioactivity to the bottom of the continental crust would really involve any serious discrepancy with known facts.

* Communicated by the Author.

† Joly, *Phil. Mag.* October 1912, p. 701. The present paper was almost completed when Joly's most recent paper (*Phil. Mag.* June 1923) appeared.





Distribution of Temperature in a Uniform Layer.

Let us in the first place assume that throughout a layer of the crust, of thickness h , the thermal conductivity, K , and the rate of generation of heat per unit volume, q , are both constant. Let us further assume that, as the continental rocks are not considered to undergo extensive fusion during periods of revolution, the loss of heat from them during these periods is not greatly above the average, so that their temperatures during normal periods are approximately constant, the surface being at a temperature θ_1 and the base of the layer at a temperature θ_2 , which, as will be seen later, should probably be about the melting-point of basalt.

It is easily seen, then, that the temperature, θ , at a depth x is given by the equation

$$\theta = \theta_1 + ax - \frac{qx^2}{2K},$$

where a , the temperature gradient just below the surface, equals

$$\frac{\theta_2 - \theta_1}{h} + \frac{qh}{2K}.$$

It is evident that a would be a minimum if

$$h = \sqrt{\frac{2K(\theta_2 - \theta_1)}{q}}.$$

If the thickness of the layer exceeds this value, a maximum temperature, $\theta_1 + \frac{Ka^2}{2q}$, will occur at a depth $\frac{Ka}{q}$, i. e.

$$\frac{K(\theta_2 - \theta_1)}{qh} + \frac{h}{2}.$$

Below this the flow of heat must take place in a downward direction. What would actually become of this heat is considered later.

If we assume that the average continental rocks are of an "intermediate" character*, we may take as their average Radium content 2×10^{-12} g. per g. †, and as their Thorium content 1.5×10^{-5} g. per g. ‡. Taking the rock density to be 2.7, we find $q = 6.4 \times 10^{-13}$ calory per second per c.c. If we assume that $K = 4 \times 10^{-3}$ c.g.s. units, $\theta_1 = 15^\circ \text{C.}$, and

* Clarke, 'Data of Geochemistry,' 2nd Edition, p. 26 (1911).

† Joly, *loc. cit.*

‡ J. H. J. Poole, Phil. Mag. April 1915, p. 489.

$\theta_2 = 1215^\circ \text{C.}$, we find that a has the minimum value 6.2×10^{-4} degree per centimetre if $h = 38.7$ kilometres. The thickness to be ascribed to the continental mass varies with the height of the land, and also with the level assumed for the upper surface of the basaltic magma in the oceanic areas. The values of a and the maximum temperature θ_m for various values of h are as follows:—

$h \dots$	20	30	40	50	60	70	80	90	100 kilometres.
$a \dots$	7.6	6.4	6.2	6.4	6.8	7.3	7.9	8.5	9.2×10^{-4} degrees per cm.
$\theta_m \dots$	—	—	1215°	1295°	1460°	1680°	1960°	2270°	2660°C.

It is obvious that for the thicker layers, fusion of the acid rocks might be expected to occur. It is possible that these conditions might be realized at the bases of mountain chains, especially during mountain-building epochs.

Discrepancy between the Estimated and the Actual Temperature Gradients.

We see that the temperature gradient just below the surface to be expected on these hypotheses is at least 6×10^{-4} degrees per cm., whereas the actual gradient only averages about 3×10^{-4} . The discrepancy at first sight appears to be rather serious, but there would seem to be several causes tending to reduce the gradient in the neighbourhood of the surface, where alone it is capable of measurement.

Effect of Temperature on the Thermal Conductivity of Rocks.

We have assumed above that K is constant and has the value 4×10^{-3} . Now Debye has shown that we should theoretically expect the conductivity of a crystal to vary inversely as its absolute temperature; and this has been experimentally verified by Eucken*, who found also that the conductivity of crystalline substances, such as marble, fell with rise of temperature, though not so rapidly as that of pure crystals, while the conductivity of amorphous bodies rose with rise of temperature. This is in complete agreement with some determinations by the writer on the thermal conductivities of rocks, although the results in this case were complicated by permanent changes†. It was found that the conductivity of a typical specimen of granite fell from 5.7×10^{-3} at 105°C. to 3.8×10^{-3} at 516°C. A considerable part of this fall was of a permanent nature and was attributed to minute cracking,

* *Ann. der Phys.* xxxiv. p. 185 (1911).

† *Phil. Mag.* July 1912 and January 1914.

but there was also evidence of a considerable recovery of conductivity when the temperature was again reduced. Results of a similar nature were obtained with limestone. Basalt, on the other hand, which was largely glassy, had a conductivity close to 4×10^{-3} almost independent of temperature up to 600° C.

We thus see that there is considerable reason, both theoretical and experimental, for assuming a fall in conductivity with rise in temperature in crystalline rocks. If the writer's figures may be taken as a guide, we would not be very far from the truth in taking $K = 6 \times 10^{-3}$ for granite and limestone close to the surface. No results were obtained for slate, owing to splitting of the rock. A mean of the figures given by other experimenters gives 5.1×10^{-3} for the average of various sedimentary rocks, including slates, limestones, flagstones, and sandstones. As the great majority of gradient determinations have been made in sedimentary rocks, it would seem that we should, in estimating the flow of heat, use a value of K between 5×10^{-3} and 6×10^{-3} , and probably not greater than 5.5×10^{-3} . This would, with the actual gradient, yield a heat-flow of 16.5×10^{-7} calory per second per square centimetre. The heat-flow for a layer 40 kilometres thick, as calculated above, is 25×10^{-7} . For thicker or thinner layers the flow would be greater. Thus a flow of at least 8.5×10^{-7} calory per second remains to be accounted for. It seems probable that, owing to the fall of conductivity with increase in temperature, the value, 4×10^{-3} , previously assumed for the conductivity of the layer is fairly close to the mean value; but the change of conductivity with temperature would of course render the gradients less steep in the upper parts, and steeper in the lower parts, than those which would be obtained from the formula given above.

Effect of Underground Water.

The most obvious suggestion is that the effective conductivity of the surface layers may be augmented by underground water. The great majority of underground temperature observations have been made in bore-holes for wells, or in mines, which generally are to be found in more or less pervious strata. The quantity of water usually occurring in the latter may be judged by the fact that in England about 12 tons of water have to be pumped out for every ton of coal mined*.

The true thermal conductivity of water being very small,

* Sherlock, 'Man as a Geological Agent,' p. 285.

upward transference of heat in it will occur chiefly either by convection currents in "stagnant" water in pores, pockets, and fissures in the rock, or by flowing water, which sinks into the ground to reappear elsewhere as a deep-seated spring with an elevated temperature.

Experiments on the magnitude of the effect to be expected from convection are at present in progress, and will be described in a subsequent paper. The effect, especially in single water columns, is evidently extremely complex, the distribution of the convection currents apparently being very susceptible to accidental disturbances. A summary of the results so far obtained follows.

For gradients of about 0.3° per cm. the "Convectivity" (*i.e.* the vertical heat-flow per sq. cm. divided by the gradient) varies with the diameter and also with the length of the water column used, the extreme values recorded being about 0.3 for a tube 10.25 cm. long by 1.08 cm. diameter, and 2.3 for a tube 23.0 cm. long by 2.03 cm. diameter. Thus for columns of such sizes the convectivity at this gradient is of the same order as the conductivity of copper.

For smaller gradients the convectivity decreases rapidly, being roughly proportional to the 6th power of the gradient for each of two tubes 1.08 cm. diameter, to the gradient for the tube 2.03-cm. diameter, and to the square root of the gradient for two tubes 2.8 cm. diameter. Thus for the smaller isolated cavities and pores in rocks we should expect the convectivity to be negligible for the gradient existing in the earth. A cylindrical column of water 25 cm. deep by 3 cm. diameter should have a convectivity about 0.1, if we may extrapolate the results obtained down to such a small gradient. Larger cavities might be expected to act as better conductors of heat.

There was some evidence that in single columns the convectivity obtained a maximum at about 17°C . This is rather surprising, as, owing to the increased coefficient of expansion and decreased viscosity, we should expect a large increase in convectivity with rise in temperature. This increase was amply verified in the case of a double tube forming a circulating system, in which the ascending and descending currents were prevented from mixing. It is probable that the fall in convectivity observed with a single tube at temperatures over 17°C . is to be ascribed to increased mixing of the currents. As the effect of temperature in single columns is somewhat uncertain, and does not appear to be very great over the range (10° – 20°C .) covered by the experiments with various gradients, no allowance has been made for it in

arriving at the conclusions given above, which may be taken as referring to about 14°C. , the mean temperature of the water in the various tests.

With a double column consisting of two vertical tubes, each about 23 cm. by 1.08 cm., forming a closed water circuit, the results were much more consistent. The convectivity for a given gradient was, over the range covered, approximately proportional to the excess of the mean temperature above 5°C. (as was to be expected from a consideration of the variation of the coefficient of expansion, and viscosity, with temperature): and so the various results with different gradients could all be reduced to the mean temperature 14°C. The reduced convectivity varied from 8.31 for a gradient of 0.30° per cm. to 0.435 for a gradient of 0.0124° per cm., being approximately proportional to the 0.87th power of the gradient. Extrapolating the results down to earth gradient, we find 0.02 for the convectivity. Tests remain to be made with double tubes of other dimensions, but there can be little doubt but that larger tubes will show greatly increased convectivities, and smaller tubes negligible convectivities at earth gradients.

It would seem probable, then, that wherever water occurs in fissures more than a few square centimetres in area, or especially in fissures forming circulating systems, the upward transference of heat by it would be very appreciable, but that we would hardly expect that water in minute pores would appreciably increase the effective conductivity of the rock for the gradient obtaining underground.

As regards flowing water, it would seem that, in certain cases, very considerable quantities of heat may thus be brought to the surface. An examination of the figures for 147 deep wells in the United States*, varying from 400 to 3350 feet deep, with flows ranging from 0.1 to 5500 American gallons per minute, shows that the average flow per well was 311 gallons per minute at about 16°F. above air temperature, the average depth being 1023 feet. This means that the average well was bringing to the surface about 1.75×10^5 calories per second, which would represent a flow of 8.5×10^{-7} calory per sq. cm. per second over an area of about 20 square kilometres per well. It is hard to say how this heat-flow will fall with time, but in the case of natural springs very large quantities of heat are continuously brought to the surface over long periods of time. For example, the hot springs at Bath represent a heat-flow

* United States Geological Survey Water Supply Paper, No. 57.

of about 8.5×10^5 calories per second, *i. e.* enough to provide the flux-density required over an area of 100 square kilometres, and do not appear to have varied much for many years. It is possible that some of this heat may be due to a local concentration of radioactive matter, as the Bath water, like many deep-seated springs, shows considerable radioactivity.

If, of the total rainfall in any locality, a quantity equivalent to one inch per annum sank into the ground to such a depth that it emerged with its temperature raised by 1°C. , the corresponding heat carried off would be about 0.8×10^{-7} calory per second per square centimetre. It would thus seem to be probable that part of the discrepancy might be attributed to flowing water.

Effect of Secular Variations in Climate.

It seems to be worth while to consider what the effect of possible slow climatic changes would be. The retreat of glaciers, which at present appears to be occurring in most parts of the world, would apparently indicate a slow increase in the average temperature. In Europe and North America, where the majority of earth-temperature measurements have been made, this change is generally considered to have progressed more or less continuously since the last ice age.

Let us assume that the surface temperature is undergoing a secular harmonic variation of amplitude α and periodic time T . Then, if there were no subterranean source of heat, the temperature θ at a depth x and a time t would be given by the well-known equation

$$\theta = \theta_0 + \alpha e^{-\frac{2\pi x}{\lambda}} \sin 2\pi \left(\frac{t}{T} - \frac{x}{\lambda} + \frac{\gamma}{2\pi} \right).$$

Here θ_0 is the average surface temperature; λ , the wavelength of the temperature waves, is equal to $\sqrt{4\pi kT}$, where k is the diffusivity; and γ is a phase angle. Since $e^{-2\pi}$ is approximately equal to 1.9×10^{-3} , it is evident that at a depth λ the variations of temperature would be negligible, and the temperature always approximately equal to θ_0 .

During the last glacial epoch the southern edge of the ice field apparently passed through the South of England, where the summer temperature is now about 15°C. When under ice the ground temperature can never have exceeded 0°C. , so possibly 15°C. is a fair figure to assume for the rise which has occurred.

If we assume that at present the surface temperature is equal to the secular mean, θ_0 , we see that we must put

$$\alpha = 15^\circ \text{C. and } \frac{t}{T} + \frac{\gamma}{2\pi} = 0.$$

Thus $\theta = \theta_0 + \alpha e^{-\frac{2\pi x}{\lambda}} \sin \frac{2\pi x}{\lambda}$

and $\frac{\partial \theta}{\partial x} = \frac{2\pi \alpha}{\lambda} e^{-\frac{2\pi x}{\lambda}} \left[\sin \frac{2\pi x}{\lambda} - \cos \frac{2\pi x}{\lambda} \right].$

There would thus be a temperature minimum at a depth $\frac{\lambda}{8}$ below the surface, the temperature being $\frac{\alpha e^{-\frac{\pi}{4}}}{\sqrt{2}}$, i. e. 0.323α below that at the surface. Taking the thermal conductivity as 5.5×10^{-3} , the density as 2.7, and the specific heat as 0.19, we find that $k = 1.07 \times 10^{-2}$, and hence $\lambda = 0.37 \sqrt{T}$. The value to be assigned to T will vary with the date assumed for the middle of the last glacial epoch, about which there appears to be very great uncertainty. If we place this 20,000 years ago, we must put $T = 80,000$ years or 2.52×10^{12} seconds, which makes λ nearly equal to 6 kilometres. The temperature gradient would be -1.6×10^{-4} degree per centimetre at the surface, falling to zero at a depth of 750 metres, below which there would be a very small positive gradient. The excess of temperature, $\delta\theta$, at the surface over that at a depth x metres would be as follows:—

$x \dots$	100	200	300	400	500	600	700	800	900	1000
$\delta\theta \dots$	1.4	2.5	3.4	4.0	4.4	4.7	4.8	4.8	4.7	4.6^\circ \text{C.}

The actual temperature variation with depth would of course be obtained by superposing the above figures on the uniform positive gradient due to the escape of heat from the interior.

Thus the effect of the secular variation assumed above would be to reduce the actual gradient for the first few hundred metres by a quantity of the order of 1° per hundred metres, which would go far towards reducing the discrepancy in the heat-flux. An increase in gradient with depth appears to have been clearly established in deep borings*. We may note that the depth at which any given value of $\delta\theta$ occurs is proportional to \sqrt{T} , so that if we were

* Daly, Am. Journ. Sc., May 1923, p. 354.

to make $T=320,000$ years, the corresponding depths would all be doubled, and the effect on the temperature gradient would be halved.

If, however, we assume that during the last few hundred thousand years the mean temperature θ_0 has been $7\frac{1}{2}^\circ \text{C.}$ below the present average, and that the harmonic variations giving rise to successive glacial periods were of amplitude $7\frac{1}{2}^\circ \text{C.}$, so that at present we are enjoying a temperature maximum, or, at least, have reached a temperature equal to the previous maxima, we must evidently, for the present

day, put
$$\frac{t}{T} + \frac{\gamma}{2\pi} = \frac{1}{4}, \quad \text{and} \quad \alpha = 7\frac{1}{2}^\circ \text{C.}$$

Then
$$\theta = \theta_0 + \alpha e^{-\frac{2\pi x}{\lambda}} \cos \frac{2\pi x}{\lambda},$$

and
$$\frac{\partial \theta}{\partial x} = -\frac{2\pi \alpha}{\lambda} e^{-\frac{2\pi x}{\lambda}} \left[\sin \frac{2\pi x}{\lambda} + \cos \frac{2\pi x}{\lambda} \right].$$

Thus the minimum temperature would now occur at a depth

$\frac{3\lambda}{8}$, the temperature being $\alpha \left[1 + \frac{e^{-\frac{3\pi}{4}}}{\sqrt{2}} \right]$, i. e. 1.067α below

that at the surface. If, as before, we make $T=80,000$ years, and consequently $\lambda=6$ kilometres, we must date the middle of the last glacial period 40,000 years ago. The minimum would now occur at a depth of 2250 metres, the temperature being 8°C. below that at the surface. The distribution of temperature with depth would now be as follows:—

$x \dots$	200	400	600	800	1000	1200	1400	1600	1800	2000	2200	2400
$\partial \theta \dots$	1.6	3.0	4.3	5.3	6.2	6.8	7.3	7.7	7.9	8.0	8.0	8.0

The effect would thus be to reduce the actual gradient by about 0.6° per 100 metres for the first 1000 metres, with smaller reductions for greater depths. The variation of gradient with depth to be expected on this hypothesis would be less noticeable than on the previous one; while the estimate of the heat-flow from the lower parts of the crust would have to be increased by some 20 per cent. to allow for the effects of climatic changes, the excess being used up in raising the temperature of the upper layers in conformity with the general increase of surface temperature.

Heat Evolved during Volcanic Eruptions.

Immense quantities of heat are brought to the surface during violent eruptions, but these are so uncommon both in time and locality that their effect on the average loss of heat is probably small. It could hardly, however, be classed as absolutely negligible. The volume of the lava poured out during the eruption of Skapta Jokul in 1783 has been estimated at 25 cubic kilometres. This would mean the liberation of about 2×10^{19} calories—as much heat as would be generated in a century by a layer of rock of the assumed radioactivity 10 kilometres thick and covering an area of a million square kilometres. It is difficult to say to what extent this heat is to be ascribed to the continental rocks, and to what extent to the underlying magma.

During revolutionary periods immensely greater quantities of lava are extruded, mostly derived from the underlying magma. As the equilibrium temperature of the central parts of the thicker layers of continental rocks would be expected to be considerably above the melting-point of basalt, we would expect these great flows to reduce the temperature of these layers very considerably, so that during the intervening stable periods the temperature of the continental masses would be slowly rising again. Thus our assumption of constant temperature would have to be modified, and the heat-flux to be expected at the surface correspondingly reduced.

Conclusions as to the Reality of the Gradient Discrepancy.

It has been pointed out above that there are several factors affecting the gradient near the surface, and that every factor would be expected to produce an appreciable lowering of the gradient. We do not possess sufficient data to enable us to calculate the actual magnitude of the effects to be expected, so that it does not seem to be possible to quantitatively explain away the discrepancy. As, however, all the factors act in the same direction, it is not surprising that the actual gradient is considerably smaller than we would expect to find it, if their effects were absent.

We are thus led to the conclusion that the smallness of the gradient just below the surface cannot be regarded as any evidence against the occurrence of radioactivity, similar to that of surface rocks, throughout the whole depth of the continental masses.

Accumulation of Heat below the Continental Masses.

We have seen above that we should expect a downward flow of heat at the base of any continental mass exceeding 40 kilometres thick. Even with somewhat thinner layers there would be very little upward flow from the underlying magma, which would accordingly accumulate heat energy faster than similar magma at an equal depth below the ocean. We should thus expect fusion of the magma to occur much sooner beneath the continents than elsewhere. This comparatively light liquid magma would tend to find its way towards the surface, by flowing upwards along the sloping lower surface of the continental mass towards its thin edges. This may have some connexion with the prevalence of volcanoes along continental margins.

By the time that a sufficiently world-wide accumulation of heat had occurred to usher in a revolution, we should expect to find the continents floating on vast masses of liquid magma, probably at a temperature above the average. Even if the ocean floor remained sufficiently rigid during a revolution to prevent the relative motions of the continents suggested by Wegener, we should still expect tidal forces to produce an east to west motion of the crust as a whole relative to the core during these periods. The continents would thus drift away from the magma which previously underlay them.

It seems almost certain that the subsequent resolidification of the magma would take place from below upwards. The crustal motion would thus ultimately be arrested by the "grounding" of the deeper continental masses on solidified magma. It is conceivable that large localized tangential stresses might thus be set up which might cause the intense horizontal compression often evident in mountainous areas*.

At the close of the cycle, then, we should find the contents resting on solidified magma, whose latent heat of fusion would form a sink for the heat flowing downwards from the overlying continent for ages to come.

Summary.

A consideration is given of the temperature distribution in a uniform layer of solid rock of radioactivity equal to that of the Earth's surface materials, and whose lower surface is at the melting-point of basalt. Figures are given for the

* This is only another way of looking at an idea already suggested by Dr. Joly.

maximum temperature to be expected, on certain assumptions, for layers of different thicknesses. The following factors, which affect the temperature gradient near the surface, are considered :—

- (1) Variation of thermal conductivity with temperature.
- (2) Effect of underground water. Some results of experiments on convection in vertical water-columns show that we might expect large effects with water in fissures of moderate size, but only very slight effects with pores.
- (3) Secular variation of climate.
- (4) Heat evolved during volcanic eruptions.

As it is shown that all these effects conspire to reduce the temperature gradient, it is contended that the smallness of the latter is no evidence against the uniform distribution of radioactivity throughout the continental layer.

It is suggested that owing to tidal stresses and consequent crustal motions the continents towards the end of revolutionary periods become "stranded" on solidified magma, and that during inter-revolutionary periods the heat evolved in their lower layers is largely used in re-melting this magma.

Royal Dublin Society
June 8, 1923.

XLII. *Grouping of the Lines of the Secondary Spectrum of Hydrogen.* By K. BASU*.

THE problem of the secondary spectrum of hydrogen continues to be as interesting as ever, as can be easily seen from the large number of experimental and theoretical papers appearing on the subject. It seems now to be fairly well established that the secondary spectrum is due to the molecule of hydrogen. But we are still in the dark about the mechanism underlying the combination of two Bohr-hydrogen atoms to form the molecule and the genesis of radiation in the process. In considering the process of combination of two atoms which, according to Langmuir, is attended with the evolution of 82,000 calories of heat per gm.-molecule, it is often assumed that a molecular spectrum is emitted, the limiting frequency of which is given by the Bohr relation

$$h\nu = W \quad (\text{heat evolved}).$$

* Communicated by Prof. Megh Nad Saha.

The assumption is based upon the analogy of the origin of the atomic spectrum. We know that when one electron combines with an ionized atom, the atomic spectrum is produced. If W is the heat of ionization, the limiting frequency of the atomic spectrum is given by the relation

$$h\nu = W \quad (\text{heat of ionization}).$$

But a little consideration will show that this law cannot hold in the case of molecular dissociation. For then the limiting frequency of the molecular spectrum of hydrogen would lie at $\lambda = 3600 \text{ \AA.U.}$ But the fact that ordinary H_2 -gas is quite transparent to radiation of this wave-length shows that Bohr's rule cannot be applied to any case of molecular dissociation. The secondary spectrum extends to about $\lambda = 3300$, which is also against Bohr's rule, provided this spectrum is regarded as the molecular spectrum.

It is also evident that in view of the enormous number of lines in this spectrum, any attempt at grouping will meet with a certain amount of success, which, after all, may turn out to be quite fortuitous.

The laws are expected to be more complicated than in the case of line spectra, since the distance between the nuclei must, as a matter of course, occur in the formula. An attempt was made to see if any of the lines may be regarded as due to H_2^+ , *i.e.* two hydrogen nuclei at a definite distance l cm. from each other with an electron revolving about them. The case has been already treated by F. Tank (*Ann. d. Phys.* Bd. lix.) and L. Silberstein, because the dynamics can be handled by the Hamilton-Jacobian method, but it has not been applied to the case of the secondary spectrum. Using Bohr's rule, the frequency comes out in the form

$$\nu = 4N \left[\frac{1}{(n_1 + n_2 + \Delta n_2)^2} - \frac{1}{(n_1' + n_2' + \Delta n_2')^2} \right],$$

where N = Rydberg number, n_1, n_1' are azimuthal quantum numbers, n_2, n_2' are radial quantum numbers, and

$$\Delta n_2 = 16\pi^4 l^2 m^2 e^4 / h^4 n_2^3.$$

Thus Δn_2 involves the distance between the nuclei. The value of l can only be guessed. Let us assume $l = 1 \times 10^{-8} \text{ cm.}$, which is slightly less than $2a$, a = radius of the Bohr H-atom.

Then

$$\nu = A - \frac{4N}{\left(n_1 + n_2 + \frac{3 \cdot 55}{n_2^3} \right)^2}.$$

Let us classify the lines under the following heads :—

- (i.) For $n_2 = 1$, $\nu = A_{1x} - \frac{438710.76}{(n_1 + 4.55)^2}$;
 (ii.) For $n_2 = 2$, $\nu = A_{2\infty} - \frac{438710.76}{(n_1 + 2.44)^2}$;
 (iii.) For $n_2 = 3$, $\nu = A_{3\infty} - \frac{438710.76}{(n_1 + 3.13)^2}$;
 (iv.) For $n_2 = 4$, $\nu = A_{4\infty} - \frac{438710.76}{(n_1 + 4.055)^2}$;
 (v.) For $n_1 = 0$, $\nu = B_{0\infty} - \frac{438710.76}{\left(n_2 + \frac{3.55}{n_2^3}\right)}$;

where $A_{1x} = 21191.16$, obtained by putting $n_1 = 0$ in the second term of the right-hand member of (i.) ; in the same way $(A_{2x}, A_{3x}, A_{4x}, B_{0x}) = (22254.17, 25720.5, 26680.6, 21191.91)$, when we put respectively $n_1 = 2, 1, 0, 0$ in the corresponding second terms of the right-hand members of (ii.), (iii.), (iv.) and (v.).

For the First Series :

$A_{1\infty}$	n_1	$\nu_{\text{cal.}}$	$\nu_{\text{obs.}}$
21188.91	10	19116.86	19116.92
"	11	19374.86	19372.41
"	12	19587.41	19584.89

For the Second Series :

$A_{2\infty}$	n_1	$\nu_{\text{cal.}}$	$\nu_{\text{obs.}}$
22254.17	10	19419.27	19411.74
"	11	19825.47	19829.35
"	12	20060.00	20061.11

For the Third Series :

$A_{3\infty}$	n_1	$\nu_{\text{cal.}}$	$\nu_{\text{obs.}}$
25720.5	10	23175.75	23179.81
"	11	23523.15	...
"	12	23804.04	23804.13

For the Fourth Series :

$A_{4\infty}$	n_1	$\nu_{\text{cal.}}$	$\nu_{\text{obs.}}$
26680.6	10	24459.77	24456.46
"	11	24243.78	...
"	12	24978.6	24976.76

For the Fifth Series :

$B_{0\infty}$	n_2	$\nu_{\text{cal.}}$	$\nu_{\text{obs.}}$
21186.81	10	16802.44	16802.38
"	11	17562.11	17562.35
"	12	18141.33	18140.19

But the above coincidences, though interesting, can hardly be claimed to have solved the problem of the molecular spectrum, because the distance between the nuclei has been taken

arbitrarily. If some other value were assumed, we should probably get some other coincidences.

In view of the fact that we are yet far removed from the satisfactory solution of the coupling of two Bohr H-atoms to form an H_2 -molecule, which is by far the simplest problem of this class we can think of, is it not a bit too premature to attempt the general solution of the problems of chemical combination of more complicated atoms like Na and Cl, as has been done in the theories of Lewis and Langmuir? To the same category must belong the large number of radiation theories of monomolecular reaction, which are all based upon the Bohr rule $h\nu = \text{heat of dissociation}$.

University College of Science and Technology,
Calcutta, India.

XLIII. The Absorption of Light by Sodium Vapour. By
F. H. NEWMAN, D.Sc., A.R.C.S., *Professor of Physics,*
University College, Exeter.*

[Plate VIII.]

1. INTRODUCTION.

THE normal operation of an arc below ionization results in the excitation of the first line of the principal series, providing that the energy of the electrons is equal to, or greater than, the resonance potential. As the accelerating potential in the arc is increased, the intensity of this line increases, approximately proportional to the total number of electrons, until the ionization potential is reached. At this point there should be, according to the Bohr theory of the atom, a pronounced decrease in the intensity of the line, and this decrease takes place at the voltage at which the complete line spectrum is produced. The line $1.5S-2p$ is the result of inelastic collision with electrons having energy equal to the resonance potential, but as this voltage is exceeded, electrons which at a slightly lower value would give rise to this line, now produce the complete spectrum. Any line of the series $1.5S-m_p$, where m is greater than 2, is necessarily excited at the sacrifice of the line $1.5S-2p$. After a certain voltage has been reached, however, the intensity of any line per unit number of electrons present per c.c. attains a saturation value, in agreement with the quantum theory, for the number of quanta radiated is proportional to the number of

* Communicated by the Author.

collisions, and hence, approximately, to the number of electrons present.

In a previous communication by the author * it has been shown that under certain physical conditions in the sodium vapour are, the D lines of sodium are relatively much brighter than the lines of the subordinate series, although of course these latter lines are always much fainter than the D lines. In this work the applied potential difference was so large that the saturation value of the intensity of any line must have been attained, and the effect was explained by the self-reversal of the subordinate series lines. The atoms of sodium vapour in this case must be in an abnormal state, by which is meant that the valency electron, instead of being in the 1.5 S stable orbit, must be displaced to the first p ring. This condition can be brought about by an electrical stimulus, the density of the electrons being very great. Then the energy necessary for the displacement of the electron to the first p ring may be obtained either by direct impact with electrons possessing the requisite resonance potential, or it may be absorbed as radiation emitted by neighbouring atoms in which the electron is temporarily in the first p ring. At high vapour-pressure and considerable current density, it is probable that most of the energy in the abnormal atom is derived from the second of these sources. Under ordinary conditions nearly all the atoms of a vapour exist in the normal state, and the value of the energy is a minimum. Light corresponding to a given line in the spectrum will be absorbed when the atoms pass from this state to a state in which the electron revolves in one of the p rings. Unexcited sodium vapour shows, therefore, absorption corresponding to the principal series lines only. If, however, the atoms can be brought to the condition that a considerable proportion have the electron in the $2p$ ring, then the radiation absorbed when white light is passed through the vapour will be the lines which in the emission spectrum arise when the electron is displaced from the $2p$ ring to outer stationary orbits, *i. e.* the subordinate series lines.

It appears probable that this abnormal state of the vapour can be produced not only by electrical stimulation, but also by high temperature, for King † observed absorption in the subordinate series lines of the alkalis with his electric furnace. Using a special plug at the centre of the tube, by which temperatures above 3200° C. could be obtained, and excluding oxygen, these absorption lines in the subordinate

* Phil. Mag. vol. xlv. (1923).

† Phys. Rev. vol. xviii. (1921).

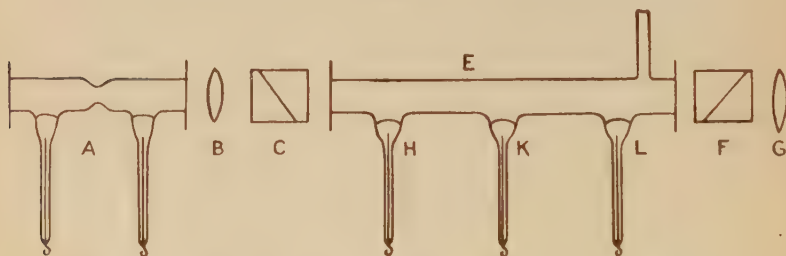
series exhibited sharpness and freedom from dissymmetry, so that their wave-lengths could be accurately measured. The temperature required is very high, much higher than that used when the absorption of the principal series lines is observed; and it is possible that the atoms will only begin to absorb the subordinate series lines when they are nearly hot enough to emit the lines of the principal series. A thermal or electrical stimulus can cause the electron to assume one of the stationary orbits, and as Sala* has pointed out, the temperature necessary to ionize atoms is probably approximately proportional to the ionization potential. This would explain the absence of certain elements in the sun. The temperature in the latter is so high that the atoms of these missing elements are completely ionized, and so the lines due to the ionized atom only would be present, and in the majority of cases these lie in the ultra-violet region.

The present work forms a continuation of that described in the previous paper.

2. EXPERIMENTS.

In the previous work a sodium-potassium alloy vapour arc lamp had been used, and the light from a constriction in it had been viewed after passing along a wider portion of the lamp. By this means the bright radiation had passed through

Fig. 1.



a column of feebly luminous sodium vapour, and a marked decrease in the brightness of the subordinate series lines, relative to that of the D lines, was noted. The apparatus used in the present experiments is shown in fig. 1.

The sodium-potassium alloy vapour arc lamp A was arranged so that the constriction was horizontal and endways on. The radiation, made parallel by a lens B, passed through a nicol prism C, and then through the quartz tube E acting as a sodium vapour arc lamp. Emerging, the light was

* Phil. Mag. vol. xlv. (1922).

transmitted through another nicol prism F, and it was then brought to a focus at the slit of the collimator by means of the lens G. The ends of the quartz tube E were closed by quartz plates, and three electrodes were arranged so that the arc could be struck between H and K, or it could be lengthened so as to pass between H and L. The distance between H and K and between K and L was about 10 cm. E was placed within an electric heater, the ends of the tube projecting beyond the heater to keep the wax from melting, and, as an extra precaution, the wax was water-cooled. The temperature was measured with a mercury thermometer placed within the electric heater. Pieces of sodium had been placed at H, K, L, and the lamp E was kept highly exhausted.

The electric arc is much more difficult to maintain with sodium than it is with the alloy of sodium and potassium, and it requires a much greater applied potential difference before it will strike. Whereas the lamp containing the alloy would work with as small a potential difference as 40 volts, 100 volts was required for the sodium lamp, and it had to be maintained highly exhausted before it would work successfully. If the vapour-pressure of the sodium became too great the lamp would not work. The arc when struck did not fill the tube completely, but confined itself to the lower part of the tube, so that the upper portion was filled with sodium radiation much less intense in brightness than in the actual arc. This was very convenient, as it enabled the radiation from A to be passed through E without being masked by the intense sodium arc.

When the nicol prisms were crossed, the radiation from E alone entered the spectroscope, and by rotating C the intensity of the light entering the spectroscope could be varied.

The lamp A was of quartz with a constriction at the centre, the distance between the two electrodes being about 10 cm. The arc was struck by heating the alloy with a bunsen burner, and then passing a weak discharge from a small induction coil through the vapour. The spectrum from this type of lamp showed the potassium lines much brighter than they were in the lamp previously described by the author*. The older form was much smaller, and, as a result, when once the arc was struck, the temperature increased rapidly and the vapour-pressure became fairly large. When an electric discharge, or any electric current, is passed through a mixture of sodium and potassium vapours, the sodium lines

* Phil. Mag. vol. xliv. (1922).

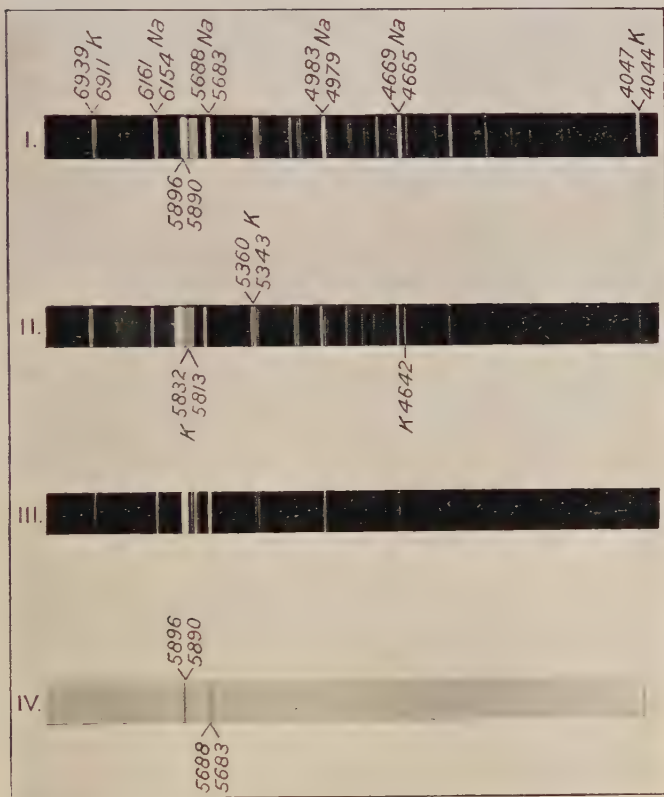
always predominate unless the partial pressure of the potassium is many times greater than that of the sodium. So in the present case, when the arc was first struck, the potassium lines were very strong, particularly at the ends of the lamp where the temperature, and so the sodium vapour-pressure, were low. At the constriction the potassium lines were faint. The pair $\lambda 4642$ was very prominent although it has the series notation $1.5S-2d$. This line appears bright with heavy currents—5 amps. per sq. cm.—and is shown in Pl. VIII. (II.).

With high current density a continuous spectrum was emitted, beginning at $\lambda 7000$ and ending at $\lambda 5480$, and also extending from $\lambda 4980$ to the ultra-violet region, the first portion being by far the strongest. As the current density was decreased, the line spectrum became more prominent and the continuous spectrum less so. Another interesting feature of the lamp was the production of an emission fluting spectrum. These bands appeared at all current densities, but were particularly bright when the current density was small. They could be divided into four groups, and although they were equally spaced in a group, this spacing varied in the different groups. The heads of the bands were situated between the limits $\lambda 6700$ and $\lambda 5500$.

When light from the lamp A was passed through the unexcited sodium vapour in E there was considerable reversal of $\lambda 5890$, $\lambda 5896$, but no apparent effect on any other line in the spectrum. Striking the arc in E and passing the radiation from A through the feebly luminous sodium vapour in E, the subordinate series lines of sodium decreased very much in brightness, although there was, as far as could be judged visually, no change in the intensity of the potassium lines. This is shown in Pl. VIII. (I. & II.), the exposures being the same in each spectrogram. The effect was most marked when the temperature of the lamp E, as measured by the thermometer, was 150°C . It is certain, however, that the actual temperature in the lamp itself must have been greater than this, owing to the passage of the arc. At higher temperatures the vapour-pressure of the sodium within E became too large, and prevented the arc from being struck. This decrease in intensity was most marked when the arc in E passed between the electrodes H and L.

When the radiation from A was sent through the intense light within E no definite result was obtained, as the luminosity within E was brighter than that from A.

A carbon arc was now substituted for the lamp A, and an



- I. Spectrum from alloy vapour lamp.
- II. Radiation from lamp passed through feebly luminous sodium vapour.
- III. Radiation from lamp passed through feebly luminous sodium and potassium vapours.
- IV. White light passed through feebly luminous sodium vapour.

attempt made to reverse the subordinate series lines of sodium on a continuous spectrum. There was no apparent reversal when the white light was passed through the intense radiation in E, but when it was sent along the top part of the tube so that it was transmitted through the feebly luminescent sodium vapour, marked absorption of $\lambda 5688$, $\lambda 5683$, and feeble absorption of $\lambda 6161$, $\lambda 6154$ was noted. In addition, there was considerable absorption of $\lambda 5896$, $\lambda 5890$, showing that in the feebly luminous vapour there were many atoms in the normal condition. This is shown in Pl. VIII. (IV.). The temperature of the sodium vapour in E as measured by the thermometer was 150°C. , and the arc passed between H and L.

The alloy of sodium and potassium was now substituted for the sodium in E, and the arc passed between H and L. Examining the radiation from A after it had been transmitted through the feebly luminous portion of E, showed that all the lines of sodium and potassium except $\lambda 5896$, $\lambda 5890$ became much fainter, Pl. VIII. (III.)

From these experiments it is concluded that electrically luminescent sodium and potassium vapours show different absorption of light effects from those exhibited by the normal vapours, and these effects are produced by atoms in an abnormal state, the valency electron being in the first p ring instead of the 1.5S orbit.

3. SUMMARY.

1. The radiation from a sodium-potassium alloy vapour arc lamp was sent through feebly luminous sodium vapour. The subordinate series lines of sodium decreased in intensity.

2. White light from an electric arc passed through this feebly luminous sodium vapour showed absorption of $\lambda 6161$, $\lambda 6154$, $\lambda 5688$, $\lambda 5683$ lines belonging to the subordinate series.

3. These effects are explained by the presence of atoms in an abnormal state, this state being brought about by an electrical stimulus. The valency electron of these atoms is in the first p ring.

XLIV. *On the Polarization of the Light scattered by Gases and Vapours.* By C. V. RAMAN, M.A., D.Sc. (Hon.), Palit Professor of Physics in the Calcutta University, and K. SESHAGIRI RAO, M.A., University of Madras Research Scholar*.

1. Introduction.

THE work of Lord Rayleigh† and others has shown conclusively that the light scattered transversely by gases is not in general perfectly polarized, but shows a defect of polarization which at the ordinary temperature and pressure is characteristic of each gas. This result is of great interest, and has been interpreted as due to the optical anisotropy of the scattering molecules, which is different for different gases. Observation shows that with monatomic gases such as argon the scattered light is almost completely polarized, while more complex molecules show a very marked imperfection of polarization. The exact measurement of the state of polarization of the scattered light for different gases, and of its variations with temperature, pressure, and the frequency of the incident light, is an experimental problem of the first importance. Preliminary measurements were published by Rayleigh, Cabannes, and Gans. These disagreed considerably among themselves; the most reliable data that have so far appeared are those obtained in Rayleigh's own later work, in which some very careful measurements were made with special precautions to secure accuracy. The table given below collects the data referred to, the last column showing Rayleigh's definitive measurements. The figures give the ratio of the weak to the strong component of polarization as a percentage.

	Rayleigh. I.	Cabannes.	Gans.	Rayleigh. II.
Argon	0·8	...	0·46
Hydrogen	1·7	1 to 2	...	3·83
Nitrogen	3·0	2·5 to 2·8	3·0	4·06
Air	4·2	3·7 to 4·0	...	5·0
Oxygen	6·0	5·1 to 5·4	6·7	9·4
Carbon dioxide	8·0	9·5 to 9·9	7·3	11·7
Nitrous oxide	14·0	...	12·0	15·4

* Communicated by the Authors.

† Rayleigh, Proc. Roy. Soc. vol. xcv. p. 155; vol. xcvii. p. 435; vol. xcvi. p. 57. Cabannes, *Ann. der Physique*, tome xv. pp. 1-150. Gans, *Ann. der Physik*, lxxv. p. 97 (1921).

Rayleigh in his experiments used a photographic method. Each measurement required several exposures, each of several hours' duration. Direct *visual* measurements of the state of polarization, if they were possible, would obviously be much more expeditious, and would enable a large number of gases and vapours to be examined. It was with the object of determining whether accurate measurements were possible by visual methods and to find the influence of the frequency of incident radiation that the present work was undertaken, and the paper describes the results so far obtained.

While dealing with this subject, it should be mentioned, as has been already remarked by one of us elsewhere, that in the case of dense gases and vapours *not* obeying Boyle's law, the state of polarization of the scattered light should not be independent of the temperature and pressure. In fact, when the scattering is greater than in proportion to the density, the scattered light should be more perfectly polarized. Observations with carbon dioxide under pressure, ether, benzene, and pentane vapours entirely confirm this indication of theory.

2. Experimental Arrangements.

In order that visual measurements might be possible, very intense illumination is obviously required. This was obtained with the aid of a powerful optical combination of an astronomical telescope of 18 cm. aperture and 200 cm. focal length and a converging lens placed beyond its focus. A beam of sunlight which fills the object-glass of the telescope and passes through the combination is converged by it into an extremely intense beam of a few millimetres diameter but of small angle. With such intense illumination, the scattering of light by gases and vapours becomes a very conspicuous phenomenon, and is of a brilliant sky-blue colour. With the help of a double-image prism it is easy to observe visually that the transversely scattered light is not completely polarized.

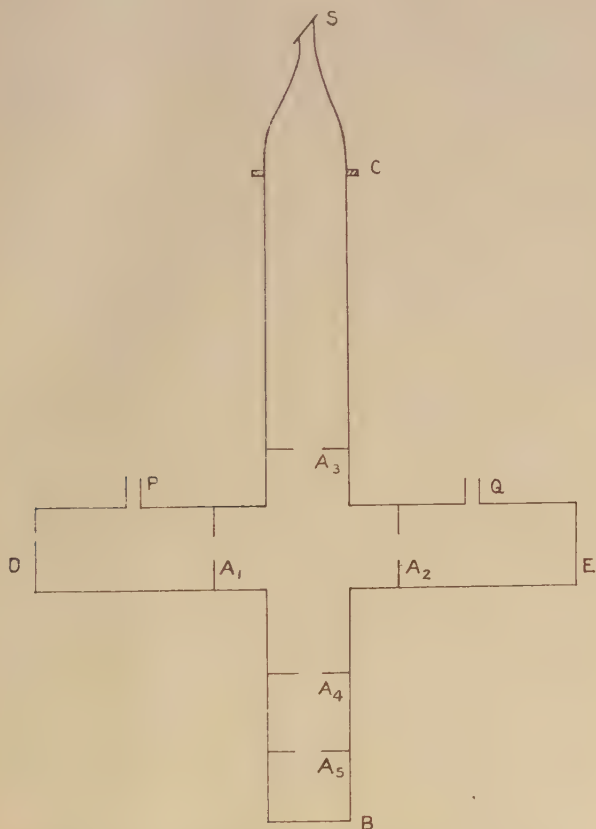
As in Rayleigh's experiments, the gas is contained in a vessel in the form of a cross-tube, the primary beam passing along one arm and the scattered beam being observed in the perpendicular direction. For accurate work the most important thing is of course the adequate blackness of the background, against which the faint light under investigation is to be observed. It is essential that special attention should be given to the way in which the far end of the vessel against which the observations are made is constructed.

It must be so arranged as to send back exceedingly little or, better still, no light at all. For, if the back of the tube returns any light, serious error will be introduced, for the visibility of the fainter track of the two seen through the double-image prism would be greatly diminished. In fact, preliminary experiments with a cross in which the background was not perfect gave invariably values for the intensity of the weaker component of polarization which were much too small. In his final experiments Rayleigh used a curved horn blown out of dark green glass and fitted to the far end of the observation tube. Any light which fell into the mouth of the horn was reflected internally from side to side towards the end away from the observing side. As such a horn was not available to us, other expedients had to be tried. The final arrangement adopted was to use a dark green conical glass bottle with its bottom cut out. The neck was ground down obliquely at an angle of 45° , and to this was cemented a dark glass plate. It was found that this gave quite a good background, and the use of sunlight, which gives beams of relatively small divergence, is specially favourable for avoiding stray illumination.

The cross-tube was made of zinc, and was 7 cm. in diameter. The arm to which the conical bottle was attached was about 36 cm. in length, and the other three arms were 25 cm. in length. The metal parts were all soldered together. The primary beam entered through the plate-glass window D, and passing through the circular diaphragms A_1 and A_2 of diameter 2 cm., fell on the window E. The laterally scattered light was observed through the window B. A diaphragm was placed at A_3 so as to cut off any stray light getting inside. Apertures A_1 and A_5 served to cut off from view any stray light that fell on the edges of A_3 and which tended to make these edges luminous as seen from the window. C is the glass bottle fixed to the observation arm. S is the dark glass plate cemented to the bottle at an inclination of 45° . The glass bottle was painted dead black outside and wrapped in black cloth as an additional precaution. The inside of the cross was completely painted dead black. The glass windows were fixed in position by screwing brass caps on to the ends of the tube. Thick rubber washers were placed between the metal and the glass so as to distribute the pressure and to make the whole air-tight. The ends of the cap were further coated with a cement made of a mixture of rosin and wax so as to prevent any leakage. The air-tightness of the whole apparatus was tested, and it was found that there was a leakage of about

10 cm. of mercury in one hour. It was, however, thought not advisable to spend time in making it more perfectly air-tight, as the gas could be passed for a sufficiently long time to ensure that all air was driven out, and also as the observations were all made visually in a short time. P and Q are the ends for the entrance and exit of the stream of gas.

Fig. 1.



As mentioned above, brilliant sunlight concentrated by an 18-cm. aperture object-glass combined with a short focus lens was used. By suitable diaphragms stray light can be entirely cut off and prevented from entering the cross-tube. In order to make quantitative observations and to determine the ratio of the two components of polarization of scattered light, it is very essential that the eye should be

properly screened from all outside light and must be able to see only the two patches of light. For this purpose a small dark room made of thick canvas stretched on wooden supports was built up in front of the observation window of the cross-tube. A hole of just the size of the diameter of the cross-tube admitted a little of the observation arm of the cross into the room and the photometric apparatus—that is, the double-image prism and the nicol—were mounted within it. The room could be made perfectly dark, and when the eye had been for some time accustomed to the darkness, the two patches of light seen through the double-image prism could be easily made out. Even in the case of hydrogen, which scatters only about a fourth as much as air, there was no great difficulty experienced in seeing the two tracks.

The method employed to measure the imperfection of polarization was to use the double-image prism and a square-ended nicol. The double-image prism when properly oriented gave the two images, which had intensities in the same ratio as the polarized components of the scattered light. These two intensities were then equalized by the nicol. This method is very convenient, as continuous adjustments can be made. In working with the prisms, there are, as pointed out by Rayleigh, two possible sources of error. One is, that it might be possible that, starting with the unpolarized light, the double-image prism would not produce two images of equal intensity within the desired limits of accuracy, and hence the ratio of the intensities with partially polarized light could not be taken as a true measure of the constitution of the light; and the second is, that it might be possible that the $\tan^2\theta$ law does not hold. For accurate determination it is therefore very essential to know that these sources of error do not conspire to produce errors beyond the desired limit of accuracy.

The following method was therefore adopted to test the

Fig. 2.



behaviour of the prisms. A ground-glass screen was illuminated by an electric lamp, and a black screen with a rectangular aperture was placed in front of it. The aperture gave perfectly unpolarized light, and could be viewed through

the double-image prism and nicol to be tested. In front of the double-image prism another nicol was mounted to polarize the light in any desired orientation, and the test was carried out by determining the ratio of the vertical and horizontal components of polarization of the beam transmitted through it in different orientations. Both nicols were mounted at the centres of accurately divided circles so that their orientations could be read off very accurately. Preliminary tests with the unpolarized light showed that the double-image prism produced images of practically equal intensity. The double-image prism was then adjusted so that the two images were just touching each other and were in a line. This secured that the direction of vibrations in the images were approximately horizontal and vertical. The polarizing nicol was then mounted in front of the double-image prism, and the orientations in which one of the two images vanished were noted. They differed by 90° , as was to be expected. The nicol was then set at a definite orientation ϕ with the vertical, the double-image prism remaining fixed, and the ratio of the intensities of the vertical and the horizontal components in the beam passed by it was determined by rotating the second nicol and equalizing the brightness of the two images. The ratio was found to be $\tan^2\phi$ without appreciable error.

Measurements were also made with a few vapours of organic liquids such as benzene, ether, and pentane. These have a large vapour-pressure at ordinary temperatures, and consequently also a large scattering power, and were also found to have no tendency to form fogs or decompose under the action of light. As these vapours either act on or are absorbed by the paint used inside the cross-tube, another cross-tube of the same dimensions was used. The inside was not painted with any substance, but was merely chemically blackened. The background in this case was not of course as perfect as in the cross-tube used for the gases; but as the vapours have relatively a very large scattering power, it was thought that the background could not have introduced any appreciable error.

3. Preparation and Supply of Gases and Vapours.

The gases experimented upon were oxygen, hydrogen, carbon dioxide, nitrous oxide, and air. Of these, oxygen and carbon dioxide were bought in compressed cylinders, and were nearly quite pure. As hydrogen and nitrous oxide could not be had in cylinders at Calcutta, they were prepared

in the laboratory in the usual way. Hydrogen was prepared from pure H_2SO_4 and pure zinc in a Kipp's apparatus. The gas was passed in succession through potassium hydroxide and strong sulphuric acid. Nitrous oxide was prepared by heating ammonium nitrate, with the usual precautions. The gas was passed in succession through potassium hydroxide and strong sulphuric acid. During the whole time of observation the gases were passed at a slow rate so as to get always fresh gas under observation and thus avoid the formation of any fog, though there was no evidence of such formation. The cross was first exhausted, and the gas was then allowed to stream. In each case, before any observations were taken the gas was allowed to pass for a sufficiently long time to ensure that all air had been driven out. The gases were dried over phosphorus pentoxide before they entered the cross.

As the dark glass plate cemented to the bottle was not meant to stand any outward pressure, precautions had to be taken in filling the cross with the gas to see that at no time did the pressure inside exceed one atmosphere. To do this the entrance-tube was connected to a glass T-tube. Through one arm the gas was allowed to stream, and the other arm was connected to a long narrow tube dipping in mercury. Thus the pressure in the cross-tube could be registered, and at the same time, if the pressure inside exceeded one atmosphere, the gas could escape freely. As soon as the pressure was one atmosphere the manometer-tube was closed and the exit-tube opened.

In the case of vapours the cross-tube was connected to a small quantity of pure liquid and exhausted. The tube was filled with the vapour by the evaporation of the liquid.

4. *Adjustments and Results.*

The cross was mounted in position and the two lenses arranged to give a beam of light parallel to the axis of the cross-tube. The adjustments could be made by observing the patches of light at the two windows. The double-image prism and the nicol were mounted in front of the observation window so as to be in the direction of the axis of the tube. The double-image prism was so adjusted that the duplicate images were just touching and in continuation of each other. The patch of light under observation was nearly rectangular, and was of fair width. As before stated, a slight error in setting the double-image prism involves only a negligible error in the measurements. To set the double-image prism accurately in position, measurements of the ratio of the intensities

were made near and on either side of the correct position of the double-image prism by altering its position slightly, and by trial the position which gave the minimum ratio was determined. This gave the correct position for the double-image prism.

Before starting the measurements, the blackness of the background was tested when the light was on by pumping out all the gas. Further, of the gases chosen, hydrogen scattered least, and showed an imperfection of polarization of less than 4 per cent. The weaker component due to hydrogen should thus be excessively feeble. It was found that even this faint track could be easily seen as a bright patch against a perfectly dark background, provided of course the eye was sufficiently accustomed to darkness. There was thus no reason to suspect that the background was defective in any way. Measurements were accordingly made with confidence. In the case of vapours, the scattered light was many times brighter than in gases, and the observations were distinctly more easy.

A large number of readings (not less than fifty) were taken for each gas, and the mean of all these was taken to calculate the ratio. The following table gives the final results.

Ratio of Weak to Strong Component in percentages.

	Authors.	Rayleigh's later results.	Rayleigh's earlier results.
H ₂	3.6 *	3.83	...
O ₂	8.4	9.4	...
CO ₂	10.6	11.7	...
Air.....	4.37	5.0	...
N ₂ O	14.3	15.4	...
Benzene.....	6.8	...	6.0
Pentane.....	2.8	...	1.2
Ether.....	5.0	...	1.7

It will be seen from the above figures that the values obtained for the imperfection of polarization of gases are much higher than any of those of previous investigations except those obtained in Rayleigh's final work, and that in the case of the five gases studied, Rayleigh's final

* It may be remarked that the imperfect polarization determined visually for H₂ agrees very closely with the value deduced by Havelock from dispersion theory (*Proc. Roy. Soc.*, May, 1922, p. 164).

values are distinctly higher than ours. The cause of the discrepancy is not entirely clear. It will be noticed that Rayleigh worked with an arc lamp and by photographic photometry, whereas we used the visual region of the spectrum and direct eye observation. To determine whether a difference in the effective wave-length has an effect on the state of polarization, a series of observations were made with colour filters. The effect was carefully looked for in carbon dioxide, oxygen, and air. For getting different wave-lengths, Wratten colour filters were interposed in the path of the light, and, as before, a large number of readings were taken for each colour. It was found that throughout the visible region the polarization was practically constant, and it would seem therefore that the difference cannot be attributed to this cause. We are of opinion that the visual method is particularly direct and simple, and that the results given by it are entitled to considerable weight. In regard to the three vapours studied, Rayleigh's results obtained in his earlier work are, we think, decidedly too low.

210 Bowbazaar Street,
Calcutta,
March 22nd, 1923.

*XLV. The Reaction of the Air to a Circular Disk Vibrating about a Diameter. By E. T. HANSON, B.A.**

THE following short paper was initially suggested to the author by a study of the oscillations of projectiles. It is, however, of more importance as the discussion of a hydrodynamical problem which admits of solution.

It is submitted partly as an example which bears interesting comparison with the corresponding problem solved by Lord Rayleigh in his 'Theory of Sound,' vol. ii. p. 302; partly also as an illustration of the use of Bessel's functions and the associated functions.

If a rigid body be executing small oscillations in air, it experiences two reactions. One is manifested as an increase in the inertia of the body. The other as a damping force tending to decrease the amplitude of the oscillations.

So far as I know the problem has been completely solved in two cases.

These are :—

- (1) The infinite plane wall bounded on one side by the fluid and oscillating normally to itself.
- (2) The spherical pendulum.

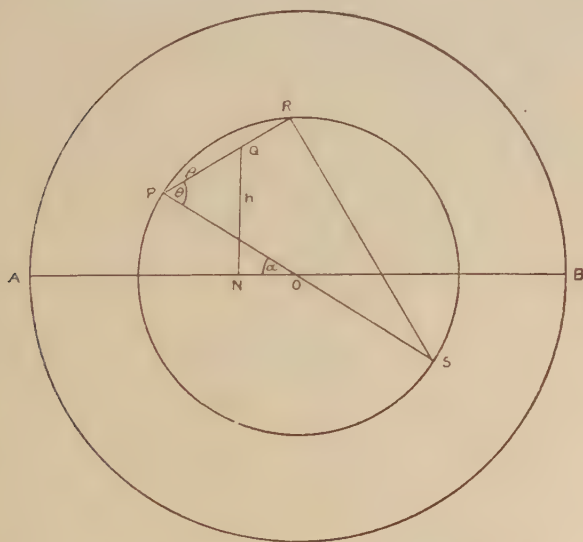
* Communicated by the Superintendent of the Admiralty Research Laboratory. The author is indebted to the Admiralty for permission to publish this paper.

In both of these cases the forced motion at every point of the fluid can be determined.

The only other problem that has been solved is that of a circular disk vibrating normally to itself in a circular hole in an infinite plane wall. This is the problem already referred to as having been solved by Lord Rayleigh. Its solution consists of expressions for the increase in inertia and the damping force due to the reaction of the air, but no account is taken of the effect of the edge of the disk upon the motion.

In all these cases the motion is symmetrical about an axis. No solution has hitherto been given for the case of a rigid body vibrating about a fixed axis, and for this reason as well the problem is worth consideration. In this paper expressions are found for the reaction of the air to a circular disk vibrating about a diameter in a circular hole in an infinite plane wall. In this case also no account is taken of the effect of the edge of the disk, but, since this limitation is common to both problems, it is probable that the comparison is only slightly vitiated.

Fig. 1.



In fig. 1, AB is the fixed diameter about which the disk is executing small oscillations. Let dS_Q be an infinitesimal area at Q distant ρ from P. Let $\frac{\partial}{\partial n}$ denote differentiation normally to the disk. Let ϕ be the velocity potential at P

due to the sources brought into play by the vibration of the disk. Then

$$\phi = -\frac{1}{2\pi} \iint \frac{\partial \phi}{\partial n} \cdot \frac{e^{-ik\rho}}{\rho} dS_Q, \quad . \quad . \quad . \quad (1)$$

where $\frac{2\pi}{k} = \lambda$ is the wave-length in air corresponding to the period of vibration of the disk.

We assume a time factor $e^{i\sigma t}$ for the vibration of the disk. If δp denote the change of pressure at P,

$$\left. \begin{aligned} \delta p &= -\rho_0 \dot{\phi} \\ &= -i\rho_0 \sigma \phi, \end{aligned} \right\} \quad . \quad . \quad . \quad . \quad (2)$$

where ρ_0 is the undisturbed density of the air. The change of pressure on an element of the plate at P is, therefore,

$$-i\rho_0 \sigma \phi dS_P.$$

Let the angular oscillation about AB be given by

$$\Omega = \omega e^{i\sigma t}.$$

If h be the perpendicular distance of Q from AB

$$\frac{\partial \phi}{\partial n} = h\Omega.$$

Hence

$$\phi = -\frac{1}{2\pi} \iint h\Omega \frac{e^{-ik\rho}}{\rho} dS_Q, \quad . \quad . \quad . \quad (3)$$

For the total turning moment reacting upon the disk we have

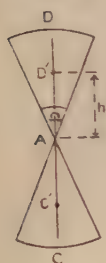
$$M = -\frac{i\rho_0 \sigma}{\Omega} \iint h\Omega \phi dS_P, \quad . \quad . \quad . \quad (4)$$

In order to effect the integration of (3) it is convenient to take an analogy from the theory of the ordinary potential, a method first suggested by Maxwell. Looking at the disk edgewise (fig. 2), construct a very narrow double wedge on each side of the diameter of oscillation which is perpendicular, through A, to the plane of the paper. Let Ω be the small angle of this wedge.

Divide the face of the disk into small equal areas dS . Let h be the perpendicular distance of one of these small areas from the diameter of oscillation.

Considering the wedge as a solid body let its density be taken as unity. Then the mass of a small cylinder, whose generating lines pass through the boundary of dS and are perpendicular to CD , is $h\Omega dS$.

Fig. 2.



If we assume the law of attraction between two small masses to be such that their potential is proportional to $e^{-ik\rho}/\rho$, where ρ is the distance between them, then ϕ may be said to represent the potential at any point due to the wedge.

Consider now the work that would require to be done to disintegrate the wedge and carry the fragments to infinity. Suppose that this is done ring by ring and that the portion $DD'CC'$ has already been dissociated.

Let P be a point on the circumference of the remaining portion of the wedge, then the work expended in taking a small element to infinity is

$$\phi_P h\Omega dS,$$

where ϕ_P is the potential at P due to the remaining portion of the wedge.

Hence the whole work done in disintegrating the wedge is

$$\iint \phi_P h\Omega dS. \quad \dots \quad (5)$$

If the centre portion $C'D'$ had been first removed and if ϕ'_P were the potential at P due to the remaining outer portion $CC'DD'$, then the whole work expended could be expressed by

$$\iint \phi'_P h\Omega dS. \quad \dots \quad (6)$$

It is evident that

$$\phi_P + \phi'_P = \phi$$

and that (5) and (6) must be equal.

Hence

$$\iint h\Omega \phi dS = 2 \iint h\Omega \phi_P dS.$$

If ϕ be now written for ϕ_P , (3) becomes

$$\phi = -\frac{\Omega}{\pi} \iint h \frac{e^{-ik\rho}}{\rho} dS_Q. \quad \dots \quad (7)$$

After integration of (7) ϕ must be substituted in (4).

We have now to evaluate the double integral in (7). From fig. 1 we have

$$h = \rho \sin(\theta - \alpha) + c \sin \alpha. \quad \dots \quad (8)$$

Hence

$$\phi = -\frac{\Omega}{\pi} \iint \{ \rho \sin(\theta - \alpha) + c \sin \alpha \} e^{-ik\rho} d\theta d\rho, \quad (9)$$

where the integration has to be taken over the portion PRS of the disk.

Let $z = 2kc$
and let

$$\begin{aligned} \int_{-\frac{1}{2}\pi}^{+\frac{1}{2}\pi} e^{-iz \cos \theta} d\theta &= 2 \int_0^{\frac{1}{2}\pi} e^{-iz \cos \theta} d\theta \\ &= 2P. \end{aligned}$$

We shall require the following results:—

$$\text{and } \left. \begin{aligned} \int_{-\frac{1}{2}\pi}^{+\frac{1}{2}\pi} \sin \theta \cos \theta e^{-iz \cos \theta} d\theta &= 0 \\ \int_{-\frac{1}{2}\pi}^{+\frac{1}{2}\pi} \sin \theta e^{-iz \cos \theta} d\theta &= 0. \end{aligned} \right\} \quad \dots \quad (10)$$

If we first integrate (9) with respect to ρ from 0 to $2c \cos \theta$, and use (10) we obtain

$$\begin{aligned} \phi = -\frac{\Omega}{\pi} \int_{-\frac{1}{2}\pi}^{+\frac{1}{2}\pi} \left[-\sin \alpha \left\{ \left(\frac{i}{k^2} z \cos^2 \theta + \frac{1}{k^2} \cos \theta \right) e^{-iz \cos \theta} - \frac{1}{k^2} \cos \theta \right\} \right. \\ \left. + \sin \alpha \left\{ \frac{i}{2k^2} z e^{-iz \cos \theta} - \frac{iz}{2k^2} \right\} \right] d\theta. \quad \dots \quad (11) \end{aligned}$$

Now P satisfies the differential equation

$$\frac{\partial^2 P}{\partial z^2} + \frac{1}{z} \frac{\partial P}{\partial z} + P = -\frac{i}{z}. \quad \dots \quad (12)$$

Using (11), (12), and (4) it is not difficult to show that

$$M = -i\rho_0\sigma \iint \frac{h\Omega}{\pi} \left[4i + zP + 4 \frac{\partial P}{\partial z} + z \cdot \frac{\pi}{2} \right] \frac{i \sin \alpha}{k^2} dS_P, \quad (13)$$

the integration to be taken over the whole disk.

The right hand side of (13) can be integrated with respect to α , using

$$h = c \sin \alpha$$

and

$$dS_P = c d\alpha dc.$$

We then get

$$M = \frac{\rho_0 \sigma \Omega H}{8k^5}, \dots \dots \dots (14)$$

where

$$H = \int_0^{2kR} z^2 \left\{ 4i + zP + 4 \frac{\partial P}{\partial z} + z \frac{\pi}{2} \right\} dz,$$

and R is the radius of the disk.

Then with the help of (12) we can show that

$$H = \left[-z^3 \frac{\partial P}{\partial z} + 6Pz^2 - 12 \int zP \partial z + \frac{\pi z^4}{8} + iz^3 \right]_0^{2kR}. \quad (15)$$

Now

$$\left. \begin{aligned} \text{where} \quad P &= \frac{\pi}{2} [J_0(z) - iK_0(z)], \\ K_0(z) &= \frac{2}{\pi} \int_0^{\frac{1}{2}\pi} \sin(z \sin \theta) \partial \theta. \\ \text{Also} \quad \frac{\partial J_0}{\partial z} &= -J_1, \\ \frac{\partial K_0}{\partial z} &= \frac{2}{\pi} - \frac{K_1}{z}, \\ \int z J_0 \partial z &= z J_1, \\ \int z K_0 \partial z &= K_1. \end{aligned} \right\} \dots \dots (16)$$

J_0 and J_1 are the Bessel functions of order zero and first respectively.

Substituting from (16) in (15) the latter can be reduced to

$$\begin{aligned} -H &= \left[z J_1 \left\{ 6\pi - \frac{\pi}{2} z^2 \right\} - 3\pi z^2 J_0 - \frac{\pi z^4}{8} \right] \\ &\quad - i \left[K_1 \left\{ 6\pi - \frac{\pi}{2} z^2 \right\} - 3\pi z^2 K_0 + 2z^3 \right] \\ &= A + iB, \quad \text{say,} \dots \dots \dots (17) \end{aligned}$$

in which the variable z now stands for $2kR$.

Whence

$$-M = \frac{\rho_0 \sigma \Omega}{8k^5} (A + iB). \dots \dots \dots (18)$$

$$= -A_1 \Omega - iB_1 \sigma \Omega, \quad \text{say.} \dots \dots (19)$$

Let I be the moment of inertia of the disk about its axis of oscillation. Let K be the oscillatory couple, of period $2\pi/\sigma$, applied to the disk.

Then the equation of motion of the disk is expressed by

$$(I + B_1) \frac{\partial \Omega}{\partial t} + A_1 \Omega = K. \quad (20)$$

B_1 therefore represents an addition to the inertia of the disk and A_1 is a damping coefficient due to the expending of energy in the production of waves. Two cases are of interest, namely, when R is small compared to the wave-length and when R is correspondingly great.

The expansions of K_0 and K_1 are

$$\begin{aligned} \frac{\pi}{2} K_0 &= z - \frac{z^3}{1^2 \cdot 3^2} + \frac{z^5}{1^2 \cdot 3^2 \cdot 5^2} - \dots, \\ \frac{\pi}{2} K_1 &= \frac{z^3}{1^2 \cdot 3} - \frac{z^5}{1^2 \cdot 3^2 \cdot 5} + \frac{z^7}{1^2 \cdot 3^2 \cdot 5^2 \cdot 7} - \dots \end{aligned}$$

When z is small,

$$\left. \begin{aligned} A &= -\frac{\pi z^8}{2 \cdot 2 \cdot 4 \cdot 4 \cdot 6 \cdot 8}, \\ B &= -\frac{z^5}{1 \cdot 3 \cdot 5}. \end{aligned} \right\} \dots \quad (21)$$

(Considering first the addition to the inertia, we have

$$B_1 = \frac{4\rho_0 R^5}{1 \cdot 3 \cdot 5},$$

so that B_1 is independent of the period and the wave-length.

Imagine a hemisphere of air to become rigid on one side of the disk, and to oscillate with the disk.

The moment of inertia of this hemisphere about the diameter of oscillation is πB_1 .

Hence the increase of inertia is represented by $1/\pi$ times the inertia of such a hemisphere.

The damping term is observed to be extremely small, a result which is to be expected in the absence of viscosity, but its magnitude has not been hitherto determined.

In the case of the disk oscillating normally to itself the damping term is proportional to R^4 .

When z is large we require the asymptotic expansions of $J_0 J_1 K_0 K_1$.

The first terms in the expansions are

$$J_0 = \left(\frac{2}{\pi z}\right)^{\frac{1}{2}} \cos\left(z - \frac{\pi}{4}\right), \quad J_1 = -\left(\frac{2}{\pi z}\right)^{\frac{1}{2}} \sin\left(z - \frac{\pi}{4}\right),$$

$$K_0 = \left(\frac{2}{\pi z}\right)^{\frac{1}{2}} \sin\left(z - \frac{\pi}{4}\right), \quad K_1 = \frac{2z}{\pi}.$$

Hence when z is large

$$\left. \begin{aligned} A &= -\frac{\pi z^{\frac{1}{2}}}{8}, \\ B &= -z^{\frac{3}{2}}. \end{aligned} \right\} \dots \dots \dots (22)$$

The above solution is interesting as compared with that for the disk oscillating normally to itself. The great difference between the two solutions is due to the fact that, in the problem just solved, the air on opposite sides of the diameter of oscillation is in opposite phases of its motion.

For small values of z the series K_0 and K_1 are both rapidly convergent. Even when $z=2$ only four terms of each series are required to obtain values correct to three decimal places.

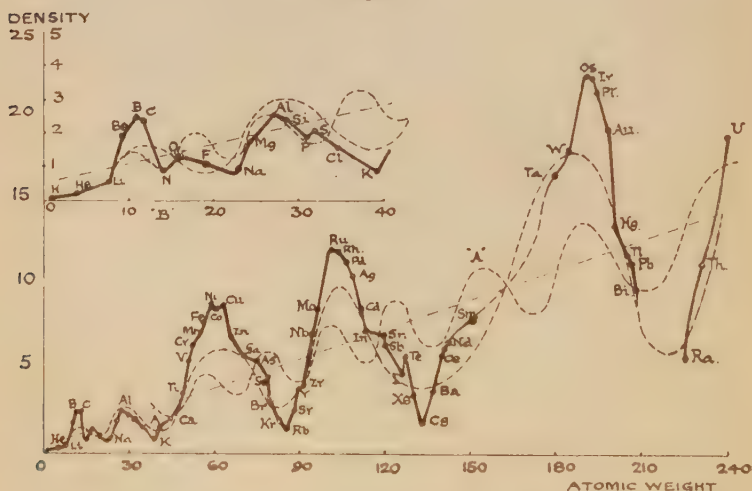
The following short table may be found useful :—

z .	$\frac{\pi}{2} K_0$.	$\frac{\pi}{2} K_1$.
0	0	0
·2	·119	·003
·4	·393	·021
·6	·576	·072
·8	·745	·164
1	·893	·311
1·2	1·019	·523
1·4	1·125	·782
1·6	1·189	1·149
1·8	1·230	1·561
2	1·243	2·031

XLVI. *The Curves of the Periodic Law.*—II. By W. M. THORNTON, *Professor of Electrical Engineering in Armstrong College, Newcastle-on-Tyne* *.

1. **T**HE rise and fall of the densities of the elements shown in fig. 1 resembles the side elevation of a somewhat irregular spiral drawn upon a transparent cone. The end elevation of such a curve of uniform angular pitch is a logarithmic spiral. This possibly suggested the scheme of representation of the elements on such a spiral given by Dr. Johnstone Stoney, in which the densities of the argon group were forecast†. Sir William Crookes, in his Presidential Address to the Chemical Section of the British Association in 1886, arranged the elements symmetrically about a line through those of maximum density, and obtained a zigzag curve dividing the elements in a remarkable manner. The present note deals with the minor fluctuations of the density curve.

Fig. 1.



The periods of the oscillations in fig. 1 increase with distance from the origin, but not so uniformly as they do on the cone spiral, where they are strictly proportional to it. Any regular periodic curve of this kind can be represented by a combination of harmonic curves chosen by inspection or analysis. The larger dotted curve in fig. 1 is that which

* Communicated by the Author.

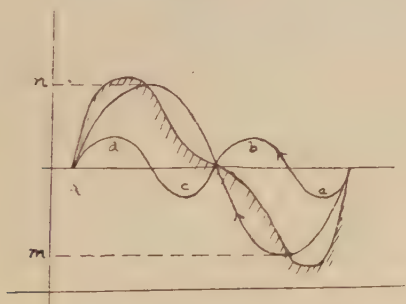
† Phil. Mag. [6] iv. pp. 411, 504 (1902).

appears to fit the observed curve of densities best as a fundamental, amplitude and period varying. It is the representation of that great periodic change in the configuration of the outer electrons in an atom under their own forces which a successful theory of atomic formation must explain. It is not the graph of the central force of the nucleus, for this, being proportional to the nuclear mass, changes by uniform steps, and is represented by the dotted straight centre line.

On the fundamental curve there is superposed one of double frequency, the amplitude and phase of which in fig. 1 are chosen by inspection. This curve can be regarded by analogy as representing some form of retardation in the change of atomic volume of the nature of hysteresis*—that is, a change of arrangement caused by the resultant force to which the fundamental is due, always occurring so as to produce the same deviation from the mean position in successive half periods.

In fig. 2, moving from right to left, the effect of the

Fig. 2.



double period at *a* is to make the resultant density less than normal, taking the fundamental curve to represent the normal type of change. At *b* it is greater, at *c* less, and at *d* greater.

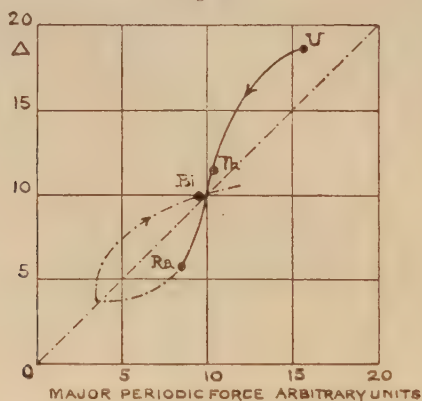
2. The physical and chemical properties of the elements appear to depend as much upon the minor periodic change as upon the fundamental. In order to bring out the differences between them, curves are given below in which the ordinates are densities, and abscissæ the projections of the major harmonic curve on the vertical axis. Thus in fig. 5, to take a clear example, the horizontal range from 3 to 11.5 arbitrary units corresponds to *mn* on the vertical axis of fig. 2, where

* Phil. Mag. xxxiv. pp. 70-75 (July 1917).

this represents the oscillations of the fundamental in that part of the curve of densities. The abscisse being drawn to the same scale as the densities, the centre line of the loops is inclined at 45 degrees. If the density rose and fell in every case proportionally to the fundamental alone the loops would close on to the centre line.

The first curve (fig. 3) contains uranium, thorium, and radium. Of these, the first two have densities greater than normal, as shown by the position of the minor periodic curve drawn above the mean line in fig. 1. Radium is somewhat below it. Densities greater than normal in reference to the major periodic curve may be called over-saturated; radium is, on this view, under-saturated.

Fig. 3.



The second group (fig. 4) begins with bismuth and ends with caesium, passing through the region of rare earths. This loop differs from the rest in having double flexure on the descending side. The elements there are alternately over- and under-saturated twice in falling from the maximum to the minimum. This appears to have had a marked influence on the densities of the rare elements. Those whose densities are known—erbium 4.7, lanthanum 6.1, praseodymium 6.47, cerium 6.68, neodymium 6.95, samarium 7.75—all lie on a small part of the curve in the neighbourhood of cerium. It would seem that, after tantalum, the elements which should lie immediately below it in fig. 4 are unable to form in the usual manner, and precipitate into a group having normal atomic weights, so that they take their places in the descending scale of elements, but abnormally small densities.

3. For the electric degradation theory of matter to be consistent, the increasing radioactivity from uranium to radium should be capable of explanation as a consequence of

Fig. 4.

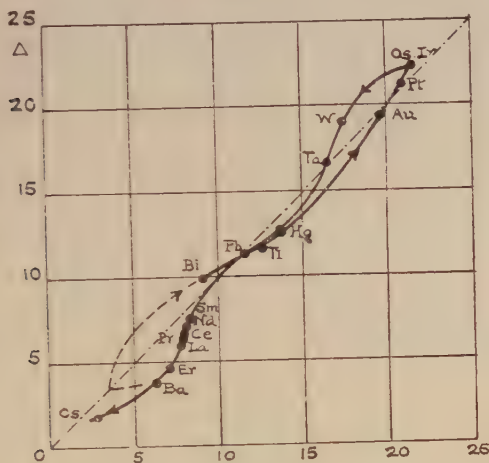
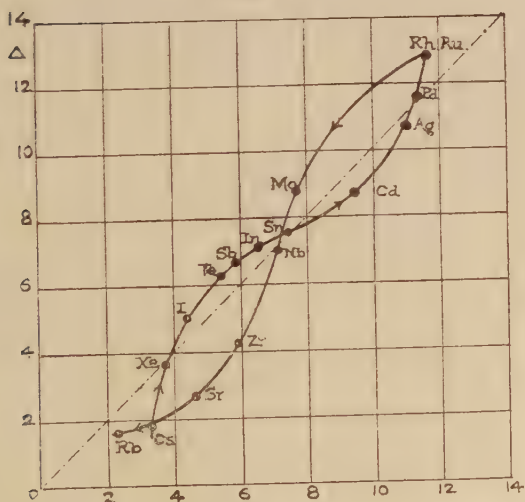


Fig. 5.

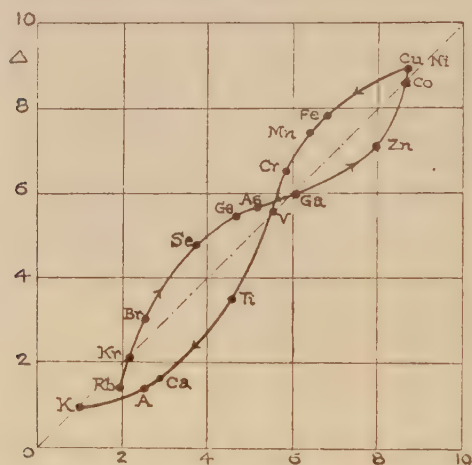


feebler control or of stronger force of expulsion. If the rate of change of density with atomic weight were such that the loss of the smallest possible unit of mass produced very

great expansion of the remaining electric structure, the atom would be on the point of explosion, and any increase in the rate would make it impossible for an atom to cohere.

When an atom is already relatively light, a rapid fall of the curves of figs. 3 to 8 usually means instability, as in radium, or perhaps scarcity, as in the rare earths. In figs. 7 and 8 there are no elements in that part of the curve. When, on the other hand, the atoms are contracting and their density increasing, the first steady atom to be formed, that is bismuth, implies the cessation of instability, and it is not normally radioactive.

Fig. 6.

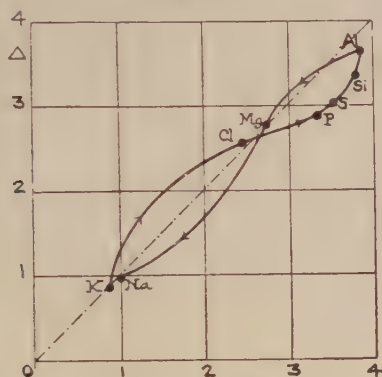


The increase of density from bismuth to osmium in fig. 1 is extremely rapid, and the maximum is reached more to the right of the main period maximum than in the other cases. In falling from this maximum, the force is aided by the falling minor period, and is constrained to pass to the right rather than to the left of the crest at A. One possible cause of the rare earths may be contained in the reason for the very rapid shrinkage of the atomic structure from bismuth to osmium, and any theory of atomic formation by grouping of electrons should account for strong forces of contraction in this region.

There are more elements on the side of the curve in which the density is rising as the atomic weight falls, than on the descending side—that is, atoms shrink slowly and expand quickly with fall of atomic weight.

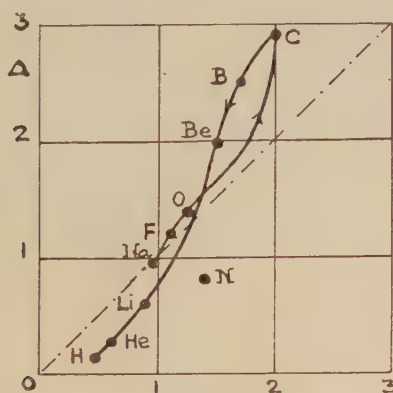
In general, elements on the rising side of the upper loop, such as gold or silver, are relatively under-saturated and ductile, while those on the falling side are harder. The same characteristic properties are in figs. 6 and 7.

Fig. 7.



As might be expected, the positions on the curves indicate with few exceptions their corresponding places in the tables of the periodic law. The density of liquid nitrogen, however, follows not the main period, but the minor, as seen in fig. 1 at $\frac{1}{2}B$, and it is half as dense as it would have been had it

Fig. 8.



followed the curve of fig. 8 after oxygen. It will be noted that there are no elements even in fig. 6 at the tops of the curves on the over-saturated, *i. e.* falling side, and there are none in fig. 7 above the centre line of mean density.

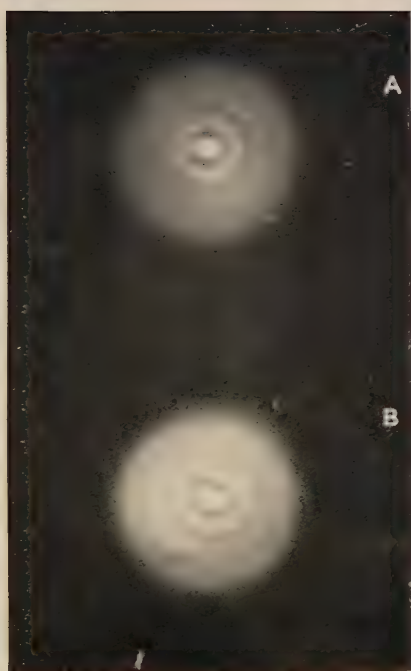
4. This mode of representing densities in reference to a smooth harmonic curve of the same period as the observed curve of fig. 1 is not speculative, for, after the cause of spectra and valency, the existence of a periodic centripetal force or resultant pressure is the most evident fact an electric theory of atomic formation has yet fully to explain. It can hardly be doubted that the double period oscillation of the density curve indicates the presence of an important factor in atomic formation. This can only arise in the adjustments of the positions of the outer electrons with each loss of a proton from the nucleus. It is premature to speculate on its nature, but since the main rise and fall of density indicate successive storage and release of potential energy in the atom, the double period curve indicates where this is retarded or increased. The effect is common to hysteresis in any cyclic operation, magnetization of iron for example, in which change is at first retarded and later accelerated by intermolecular forces. In the present case it is possibly a consequence of the limitations of position entailed by the restricted number of electrons. The existence of elements with widely different properties seems to depend upon having comparatively few electrons in the rings. If there were many more the number of positions of stability would be increased and characteristic differences lessened.

XLVII. *Note on the Illumination of the Spectroscope with End-on Vacuum Tubes.* By T. R. MERTON, F.R.S., and R. C. JOHNSON, B.A., B.Sc.*

[Plate IX.]

ONE of the essential conditions in the accurate determination of wave-lengths by micrometric measurements of spectra which are photographed in juxtaposition, consists in securing that the prism or grating shall be uniformly and completely illuminated both in the case of the comparison spectrum and the spectrum under investigation. The difficulty of securing this is greatly aggravated when vacuum tubes are used as a source of light in an end-on position; and it can at once be seen that it is, in fact, impossible to illuminate the prism or grating quite uniformly under these conditions unless the aperture of the spectroscope is very small, since the pencil of rays which emerge axially from the capillary subtend a very small angle, and result in the formation of a bright spot on the collimating lens. Prof. Fowler has informed us that this fact may be largely

* Communicated by the Authors.



responsible for the difficulty which is always experienced in getting reliable wave-length measurements from end-on tubes. It has been found that a considerable advantage can be gained both as regards the evenness of illumination and the total intensity by silvering, by the usual chemical methods, the outer walls of the capillary. It is obvious that this must be the case, but the exact theoretical investigation is rather complicated and tedious. To test the question experimentally a vacuum tube of the usual H form with a capillary about 2 mm. internal bore and 25 cm. long was prepared, the capillary being bent in the centre through about a right angle. The tube contained air at a few millimetres pressure, and one half of the capillary was silvered externally. A qualitative comparison of the intensity from the two ends was then made as follows.

The tube was excited by means of an alternating current transformer, and photographs with the same time of exposure were taken of each end of the capillary in an end-on position, using an ordinary photographic camera arranged to bring the end of the capillary to a focus about halfway between the camera lens and the photographic plate. The pattern on the plate was thus similar to that which would be formed on the collimating lens of a spectroscope with a condensing lens between the vacuum tube and the slit. The patterns from the two ends of the capillary were photographed in adjacent positions on the same plate, and a typical result is shown in Pl. IX., where A is the extra-focal image from the unsilvered, and B that of the silvered capillary.

The gain in intensity and uniformity in B is plainly seen, as also the rings surrounding the bright spot due to the axial pencil of rays. This peculiar system of rings is due to reflexions from the inner walls of the capillary, and can be seen, for example, when light from an extended source is viewed through a polished cylindrical tube. It is seen that with end-on tubes certain zones of the dispersing system are more effectively illuminated; and these only receive a small fraction of the light in comparison with the central spot due to the axial pencil. With a silvered capillary this effect is greatly mitigated, but it is clear that with the unsilvered tube there is not only a serious source of error if the tube is not very carefully adjusted but a very appreciable reduction in the resolving power of the spectroscope.

The Clarendon Laboratory,
Oxford,
March 7th, 1923.

XLVIII. *Unit Magnification Surfaces of a Glass Ball.*
 By ALICE EVERETT, M.A., *National Physical Laboratory* *.

THE theory of the unit surfaces of lenses may be regarded as the generalization of the theory of the unit or principal planes which play so large a part in elementary lens design. The unit surfaces are the loci traced by pairs of conjugate points for unit magnification on rays bound by some condition, such as passing through a fixed point O. There are two separate problems to consider according as the conjugate points are the primary or secondary foci of each other. In either case it has been found that the positions and forms of the loci change with the position of the fixed point. For a symmetric system the unit surfaces, both primary and secondary, for any position of O on the optic axis all touch the Gaussian unit or principal planes at their points of intersection with the axis, the equations of the principal planes being merely a first approximation to the equations of the unit surfaces, on the assumption that the inclinations and incident heights of the rays are so small that their squares are negligible.

The case of rays from a fixed point O incident upon a solid glass sphere in air will serve as a simple illustration.

Magnification at a point is generally different in different directions. In the present case, unit magnification is taken to signify equality of conjugate line elements drawn perpendicular to the ray, and lying in the meridional plane, or in the sagittal planes through the ray, according as we are dealing with the primary or secondary foci, respectively.

First it will be shown that for a single ray refracted through a sphere, the secondary unit points coincide at the point of intersection of the incident and emergent paths, and the primary unit points are the feet of the perpendiculars from the centre upon the incident and emergent paths.

Let C be the centre of the sphere (fig. 1): O the fixed point; A and B the points of incidence and emergence; M the middle point of AB; S the point of intersection of the incident and emergent rays AS, SB; and P and P' the feet of the perpendiculars from C upon these rays. S obviously lies on CM. The whole path of the ray lies in the diametral plane ACB, and is symmetrical with respect to the diameter CM.

Hence the images of M formed at the two faces of the

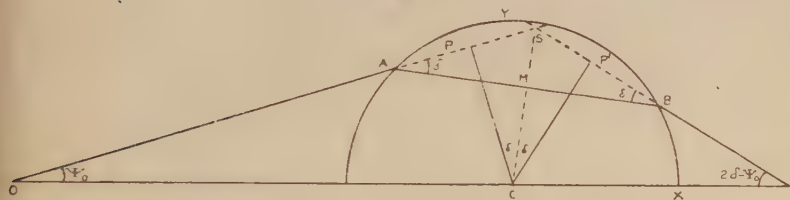
* Communicated by the Author.

sphere by thin pencils proceeding outwards from M along MA , MB will be equal, and therefore the points conjugate to M with respect to the two faces will be a pair of unit points with respect to the whole sphere.

It is known that for a single refraction the secondary foci lie on a straight line through the centre. Thus the point S is the secondary focus of M for either face of the sphere, and therefore the secondary unit points for the whole sphere coincide at S , which is a self-conjugate point.

As regards the primary foci, it is known that in the case of a single surface the feet of the perpendiculars from the centre of curvature on the incident and refracted rays are conjugate points. Therefore P is the primary focus of M

Fig. 1.



Refraction through a Glass Ball (Solid Sphere).

for refraction at the first face, and P' is the primary focus of M for refraction at the second face. Hence P , P' are primary unit points.

The positions of the unit points may be verified by putting the magnification equal to unity in the known formulæ connecting focal distance and magnification.

The above reasoning may evidently be extended to the case of symmetrical refraction through n concentric spheres bounding homogeneous media, or ($n=\infty$) a single sphere with density a function of distance from the centre.

The next step is to find the loci of the unit points for rays through O in a plane through OC . The unit surfaces are evidently the surfaces of revolution generated by rotating these plane loci about OC .

The Gaussian unit planes coincide in the plane through C at right angles to OC . The plane loci of P and P' are evidently the pedal curves of the caustics, or envelopes, of the incident and emergent rays respectively.

The plane locus of P , the object primary unit point, is obviously a portion of a semicircle on OC as diameter. The

loci of P' and S are curves of higher degree, though the graphic construction is so simple and evident that description is needless.

Let ϕ, ϕ' be the angles of incidence and refraction at the first face of the sphere; ψ the inclination of the incident ray to OC; $\delta = \phi - \phi'$; r = radius; and $c = OC$.

Then $\sin \phi = \mu \sin \phi'$, and $r \sin \phi = c \sin \psi$.

Taking C, the centre of the sphere, as origin of coordinates, and OC as axis of x , the following are the polar coordinates of the points named:—

$$\begin{array}{ll} \text{S} & \rho = r \sin \phi \sec \delta, \quad \theta = 90^\circ - (\delta - \psi), \\ \text{P}' & \rho = r \sin \phi, \quad \theta = 90^\circ - (2\delta - \psi), \\ \text{M} & \rho = r \sin \phi', \quad \theta = 90^\circ - (\delta - \psi). \end{array}$$

The Cartesian coordinates are:—

$$\begin{array}{ll} \text{S} & x = r \sin \phi \sec \delta \sin (\delta - \psi), \quad y = r \sin \phi \sec \delta \cos (\delta - \psi), \\ \text{P}' & x = r \sin \phi \sin (2\delta - \psi), \quad y = r \sin \phi \cos (2\delta - \psi), \\ \text{M} & x = r \sin \phi' \sin (\delta - \psi), \quad y = r \sin \phi' \cos (\delta - \psi). \end{array}$$

It can easily be seen from the above that all the loci touch the axis of y at the centre of the sphere. Also, by finding dy/dx , it can be shown that for $\phi = 90^\circ$, or grazing incidence (which by symmetry involves grazing emergence), the locus of S touches the incident path at its point of intersection with a circle concentric with the given circle, and of radius μr (the outer circle in Young's well-known construction); the locus of P' touches the refracting circle and the emergent ray at their point of contact; and the locus of M touches the path in the sphere at its point of intersection with a concentric circle of radius $r \mu$ (Young's inner circle).

In the case where O lies at infinity and the incident rays are parallel to OC, the following comparatively simple polar equations are found for the plane unit loci, the axis of y being taken as initial line, and χ being the angle swept out by the radius vector in the clockwise direction:—

$$\text{Locus of S} \quad \rho = \frac{\mu r \tan \chi}{\sqrt{\mu^2 + 1 - 2\mu \cos \chi}}.$$

$$\text{Locus of P}' \quad \rho = \frac{\mu r \sin \frac{\chi}{2}}{\sqrt{\mu^2 + 1 - 2\mu \cos \frac{\chi}{2}}}.$$

$$\text{Locus of M} \quad \rho = \frac{r \sin \chi}{\sqrt{\mu^2 + 1 - 2\mu \cos \chi}}.$$

The case where the incident rays are parallel, and $\mu = \sec 45^\circ = 1.4142$, may be cited as an example.

The loci are of a stable nature. Curves drawn for other values of OC between ∞ and 1.5 show the same general character as those in fig. 2. When O lies at infinity, the locus of P coincides with the radius along the axis of y —*i. e.*, with the trace of the coincident Gaussian unit planes—and the point of grazing emergence or terminal point of the locus of P' lies below the axis of x , so that the emergent ray is deviated through more than a right angle, and the sphere acts like a reflector. As O moves in from infinity along the axis of x towards the refracting circle, the terminal point of the P' curve moves upwards anti-clockwise along the circumference.

For a value of OC about 1.5 , the P' curve begins to cross the axis of y and show a point of inflexion, and as O draws still nearer to the circumference of the circle, the curve encroaches more and more on the second quadrant. When O lies inside the circle, grazing incidence of course cannot occur.

XLIX. *On the Propagation of certain Types of Electromagnetic Waves.* By D. R. HARTREE, B.A., St. John's College, Cambridge*.

§ 1. *Introduction.*

THE investigation which led to the solutions of Maxwell's equations given in the present paper was suggested originally by the properties of the disturbance in the less dense medium in the case of total reflexion at the surface of separation of two transparent media.

This disturbance of course satisfies Maxwell's equations. It is propagated without change of form as a plane wave, but its properties differ from those of the simplest type of plane wave in three respects, *viz.*:—

- (a) The amplitude is not constant over a wave front (defined as a continuous surface joining points of equal phase);
- (b) the wave is not purely transverse;
- (c) the wave does not travel with the normal velocity of light in the medium.

In a discussion, the question arose as to how far the

* Communicated by Dr. T. J. La. Bromwich, F.R.S., Prælector in Mathematics at St. John's College, Cambridge.

existence in free æther of waves with properties (a) and (b) depended on the existence of a material boundary (which of course exists in the total reflexion case), which might be considered as a kind of support to the wave; and specially whether it was possible for a plane wave, concentrated, so to speak, in a small part of the wave front, to travel in free æther without spreading or changing its form.

§ 2. Equations of the Electromagnetic Field.

For the purposes of the present paper we need only consider the divergence equation and the wave equation for the electric intensity \mathbf{E} in free æther, viz.,

$$\text{div } \mathbf{E} = 0, \quad . \quad . \quad . \quad (2.1)$$

$$\left(\nabla^2 - \frac{1}{c^2} \frac{\partial^2}{\partial t^2} \right) \mathbf{E} = 0. \quad . \quad . \quad . \quad (2.2)$$

Only plane waves will be considered, and the axis of z will be taken perpendicular to the wave front.

In Cartesians, (2.1) gives

$$\frac{\partial E_x}{\partial x} + \frac{\partial E_y}{\partial y} + \frac{\partial E_z}{\partial z} = 0, \quad . \quad . \quad . \quad (2.3)$$

from which it appears that unless the amplitude varies over the wave front in such a way that

$$\frac{\partial E_x}{\partial x} + \frac{\partial E_y}{\partial y} = 0$$

a longitudinal component of \mathbf{E} must be present. When such a component is present, "plane-polarized waves" will be taken to mean waves in which the component of \mathbf{E} in the plane of the wave front has a fixed direction.

If a solution of the wave equation has the form

$$\phi(x, y) \cdot \psi(z, t),$$

then

$$\frac{1}{\phi} \left[\frac{\partial^2 \phi}{\partial x^2} + \frac{\partial^2 \phi}{\partial y^2} \right] = - \frac{1}{\psi} \left[\frac{\partial^2 \psi}{\partial z^2} - \frac{1}{c^2} \frac{\partial^2 \psi}{\partial t^2} \right]. \quad . \quad (2.4)$$

The left- and right-hand sides of this equation are respectively functions of (x, y) and (z, t) , and must therefore both be constant. The simplest group of solutions is that for which this constant is zero; one solution of this group has been treated by Lord Rayleigh* in connexion with the

* Phil. Mag. [5] vol. xliv. p. 199 (1897); 'Scientific Papers,' vol. iv. p. 327.

propagation of electric waves along parallel cylinders. If this constant is not taken as zero, then another group of solutions is obtained. Special solutions of these two types are considered in §§ 3 and 4.

The boundary conditions for the solutions in which we are interested are $E=0$, $H=0$ at infinity in the plane of the wave front.

§ 3. Plane-polarized waves propagated with velocity c .

There is no restriction in taking the axis of x in the direction of the transverse component of E .

For waves propagated with velocity c

$$\frac{\partial^2 \psi}{\partial z^2} - \frac{1}{c^2} \frac{\partial^2 \psi}{\partial t^2} = 0,$$

so from (2.4) the following expressions,

$$\left. \begin{aligned} E_x &= \xi(x, y) \cdot \cos \kappa(z-ct), \\ E_y &= 0, \\ E_z &= \zeta(x, y) \cdot [a \cos \kappa(z-ct) + \sin \kappa(z-ct)], \end{aligned} \right\} \quad (3.1)$$

satisfy the wave equation if

$$\frac{\partial^2 \xi}{\partial x^2} + \frac{\partial^2 \xi}{\partial y^2} = 0, \quad \text{and} \quad \frac{\partial^2 \zeta}{\partial x^2} + \frac{\partial^2 \zeta}{\partial y^2} = 0. \quad (3.2)$$

This solution represents a wave, of wave-length $2\pi/\kappa$, with amplitudes varying over the wave front in the manner defined by ξ and ζ respectively, travelling with velocity c along the axis of z without change of form.

On substituting (3.1) in the divergence equation and equating coefficients of the sine and cosine terms separately (since the divergence equation must hold for all values of z and t), we find

$$a = 0: \quad \frac{\partial \xi}{\partial x} + \kappa \zeta = 0. \quad (3.3)$$

Obviously if ξ satisfies (3.2), then ζ determined from (3.4) satisfies (3.2) automatically, so the divergence equation can be considered as defining ζ when a function ξ is found satisfying the wave equation. This is also the case with the more elaborate solution considered in the next section. It will also be noticed that the condition $a=0$ means that the

longitudinal component is in quadrature with the transverse component.

From (3.2) it follows that if ξ, ζ are zero at infinity in all directions in the plane of the wave front, or at any boundary, then they are zero all over the wave front. Hence it is not possible for a simple plane wave with amplitude varying over the wave front to travel with the normal velocity of light unless supported in a way which makes it possible for ξ to be non-zero over some boundary, which may be internal or external to the region occupied by the wave.

§ 4. *Plane-polarized waves propagated with velocity other than c .*

The character of the wave in the less dense medium in total reflexion suggests the trial of a solution of the form

$$\left. \begin{aligned} E_x &= \xi(x, y) \cdot \cos \kappa_1(z - c_1t), \\ E_y &= 0, \\ E_z &= \zeta(x, y) \cdot [a \cos \kappa_1(z - c_1t) + \sin \kappa_1(z - c_1t)], \end{aligned} \right\} \quad (4.1)$$

where

$$\kappa_1 = 2\pi\mu/\lambda = \kappa\mu, \quad \mu = c/c_1,$$

c_1 being the velocity of the waves considered, and λ/μ their wave-length. μ may be considered as the refractive index of the æther for the waves; for the total reflexion case it is greater than 1, and varies with the angle of incidence of the light in the denser medium. [The argument of the periodic term has been written $\kappa_1(z - c_1t)$ and not $\kappa(z - c_1t)$, so that in the total reflexion case λ is the *normal* wave-length in *vacuo*.]

In these formulæ the function $\psi(z, t)$ of (2.4) has the form

$$\psi = A \cos \kappa_1(z - c_1t + \alpha),$$

so that

$$\frac{\partial^2 \psi}{\partial z^2} - \frac{1}{c^2} \frac{\partial^2 \psi}{\partial t^2} = -\kappa_1^2 [1 - (c_1/c)^2] \psi = -\kappa^2 (\mu^2 - 1) \psi.$$

Hence in accordance with (2.4)

$$\frac{\partial^2 \phi}{\partial x^2} + \frac{\partial^2 \phi}{\partial y^2} - \kappa^2 (\mu^2 - 1) \phi = 0, \quad . \quad . \quad . \quad (4.2)$$

where ϕ is either of the two functions ξ and ζ . The divergence equation gives

$$a = 0; \quad \frac{\partial \xi}{\partial x} + \kappa_1 \zeta = 0, \quad . \quad . \quad . \quad . \quad (4.3)$$

which corresponds to (3.3).

In order that ξ, ζ shall tend to zero as x, y tend to infinity, it must be possible for a maximum value of ϕ to occur when ϕ has a positive value. But for ϕ to be a maximum,

$$\frac{\partial^2 \phi}{\partial x^2} + \frac{\partial^2 \phi}{\partial y^2} < 0.$$

Hence from (4.2)

$$\kappa^2(\mu^2 - 1)\phi < 0,$$

so for this maximum to occur for $\phi > 0$, μ must be less than 1.

Hence if it is possible to have waves of the type required, they will be propagated with a velocity greater than the normal velocity of light.

In the case of the wave in the less dense medium in total reflexion the variation of amplitude in a direction perpendicular to the bounding surface is exponential, and its velocity is less than the normal for that medium. From this it might be expected that it would not be possible for a wave travelling with velocity less than c in free aether to satisfy the boundary conditions of zero amplitude at infinity in the plane of the wave front.

Transforming (4.2) to polars in the plane of the wave front gives

$$\left[\frac{\partial^2}{\partial r'^2} + \frac{1}{r'} \frac{\partial}{\partial r'} + \frac{1}{r'^2} \frac{\partial^2}{\partial \theta'^2} + \kappa^2(1 - \mu^2) \right] \phi = 0. \quad (4.4)$$

Consider the solution in which the distribution of values of ξ is such that ξ is independent of θ . Then (4.4) reduces to

$$\left[\frac{\partial^2}{\partial r'^2} + \frac{1}{r'} \frac{\partial}{\partial r'} + \kappa^2(1 - \mu^2) \right] \xi = 0,$$

of which the solution remaining finite at $r=0$ is

$$\xi = A J_0[\kappa r(1 - \mu^2)^{\frac{1}{2}}]. \quad (4.5)$$

(Negative values must of course be interpreted as indicating a change of phase of π .) This solution satisfies the condition $\xi \rightarrow 0$ as $r \rightarrow \infty$.

It appears then that the plane wave with amplitude varying over the wave front in accordance with (4.5) will be propagated without change of form with velocity $c_1 = c/\mu$. Since the principal maximum of J_0 is more than three times as large as any other, this wave can reasonably be said to be concentrated over a small part of the wave front as compared with a simple plane wave. But since for large values of r J_0 is of order $r^{-\frac{1}{2}}$, the energy density is of order r^{-1} , and so the energy of that part of the wave contained between two

planes $z - c_1 t = \text{constant}$ is of the order of r and so does not converge, though of course it does not diverge so rapidly as for a wave with constant amplitude over the wave front, for which the energy is of the order of r^2 .

If the scale of the variation of amplitude is fixed (say by fixing the value of r for which the first zero of ξ occurs), then we must have

$$(1 - \mu^2)/\lambda^2 = \text{const.};$$

whence it follows that μ varies with λ : that is to say, dispersion of light occurs *in vacuo*. It is to be emphasized that this dispersion by free æther occurs in the case of a *plane wave travelling without change of form*, and does not appear to be comparable either with the dispersion which may occur in the neighbourhood of the focus of a spherical wave*, or with the lateral dispersion of light on which a variation of amplitude over the wave front has been impressed by a diffraction grating, for in this case there is change of form and loss of energy laterally.

The value of ξ can be found from (4.3), and the complete expression for E found to be

$$\left. \begin{aligned} E_x &= A J_0[\kappa r(1 - \mu^2)^{\frac{1}{2}}] \cdot \cos \kappa_1(z - c_1 t), \\ E_y &= 0, \\ E_z &= A[(1 - \mu^2)/\mu^2]^{\frac{1}{2}} \cdot \cos \theta \cdot J_1[\kappa r(1 - \mu^2)^{\frac{1}{2}}] \cdot \sin \kappa_1(z - c_1 t) \cdot \end{aligned} \right\} \quad (4.6)$$

The presence of the factor $\cos \theta$ in E_z shows that the values of the longitudinal component are not symmetrical about the axis of z .

The formulæ for the components of H are rather heavy and not particularly interesting in themselves; if they are obtained and the Poynting energy vector calculated, it is found that the instantaneous value of this vector has a component in the plane of the wave front, but the value at a point integrated over a period is perpendicular to the wave front.

The solutions of (4.4), in which ξ varies with θ as well as with r , introduce Bessel functions of order greater than zero, and are zero on the axis of z instead of having a maximum there. For large values of r , the energy integrated over the wave front is of order r as in the solution already considered.

* See Gouy, "Sur la Propagation Anomale des Ondes," *Annales de Chimie et de Physique*, 6th ser. vol. xxiv. p. 145 (1891).

These results show that the propagation of electromagnetic waves concentrated, to a certain extent, in a small region of the wave front, without loss of energy laterally, is not inconsistent with Maxwell's equations. The possible bearing of this on the quantum theory, and particularly on the photoelectric effect, was kept in mind, and in fact partly suggested the work, but in view of the fact that the energy integrated over a wave front does not converge, it does not seem likely that the present results have any bearing on these questions.

§ 5. *Possible experimental verification of the solution.*

It might be interesting to obtain experimental verification of the solution obtained in the last section. The properties of the waves suggest two possible experiments.

Suppose an instrument, similar to a zone plate, were constructed so as to give the variation of amplitude over the transmitted wave front required by (4.5). Then

- (1) since the waves travel unchanged once they are produced, this plate should throw a sharp shadow if placed in parallel light, without any light being diffracted, however small its scale,
- (2) the abnormal wave velocity might be detected by an interference method.

§ 6. *Summary.*

Some solutions of Maxwell's equations are found which represent plane waves, with amplitude varying over the wave front, travelling without change of form. In general, the electric intensity in such waves will have a longitudinal component. If the waves travel with the normal velocity of light, they must be supported by some material boundary: but it is possible to find solutions representing such waves, travelling in free æther with a velocity greater than the normal velocity of light, for which the amplitude over a wave front infinite in extent is always finite. For one such solution there is a region of the wave front in which the amplitude takes considerably larger values than elsewhere, but it does not appear probable that this has any direct bearing on the mechanism of the photoelectric effect, as appears possible at first sight.

I wish to thank Dr. Bromwich for his criticism and advice in connexion with this paper.

L. *The Motion of Electrons in Gases under Crossed Electric and Magnetic Fields.* By RABINDRA N. CHAUDHURI, M.Sc., Ph.D., King's College, London*.

IT has been shown in a previous paper by Richardson and Chaudhuri† that a certain magnetic field acting perpendicular to the electric intensity large enough to stop the electron current (in vacuum) between a hot wire and a concentric anode, is insufficient when there is a trace of gas present. This effect occurs even below the ionization potential of the surrounding gas. It was shown, at least in air and in nitrogen, that the residual current could be accounted for as largely due to the collisions between electrons and gas molecules. It might, however, be also due to the formation of heavy ions by the slow-velocity electrons combining with gas molecules, and the magnetic field being insufficient for the heavy ions, the latter find their way to the anode. So that in any case the magnitude of the residual current should be some characteristic of the gas. In the following, two important gases, A and CO, have been studied.

As before, the source of electrons was a tungsten filament (radius a) stretched along the axis of a cylindrical anode (radius b). The electric field (potential difference V) was applied between the hot wire and the anode, and the magnetic field H was parallel to the filament, so that the electric and magnetic fields were perpendicular to each other. Under these conditions, the electrons will describe a cycloidal spiral about the filament, and the maximum distance attained by the electron will be given by

$$H^2 = \frac{8V \cdot \log r/a}{e/m \cdot r^2 \cdot \log b/a} + \frac{8V_1^2}{e/m \cdot r^2}, \quad \dots (1)$$

where V_1 = the voltage equivalent to the initial velocity of the electrons.

Substituting the values of e/m , and a ($=.005$ cm.), and b ($=1.0$ cm.), we get

$$H^2 = \frac{8.4V \cdot \log r/a}{r^2} + 45.0 \frac{V_1^2}{r^2}, \quad \dots (2)$$

where V and V_1 are in volts.

* Communicated by Prof. O. W. Richardson, F.R.S.

† Phil. Mag. Feb. 1923, p. 337.

‡ This number was erroneously given in the last paper as 89.

The accelerating potential applied between the filament and the anode in these experiments was 4.2 volts, and taking the maximum initial velocity possessed by a measurable number of electrons as 1.5 volts, we get

$$H^2 = \frac{35.28 \log r/0.005}{r^2} + \frac{67.5}{r^2} (3)$$

Thus we see, if there is no gas present, when a magnetic field of 160 units is used, then the maximum velocity electrons will be confined within a distance of 0.096 cm., and zero velocity ones will be within 0.06 cm., from the axis of the hot wire.

But if, however, any traces of gas are present, the electrons might combine with gas molecules and will find their way to the anode as heavy ions, the magnetic field necessary to stop the electrons being now insufficient (more than 4000 would be required); or, it might be that the electrons on their way have their velocity altered by a collision so as to cause them to move in new spiral paths about an axis parallel to the magnetic field. In this way by a repeated number of collisions, they might ultimately reach the anode. If, however, the latter supposition is true, we should be able to find out the length of the mean free path of the electrons in this particular gas.

Description of the Apparatus.

The thermionic tubes used in these experiments are the same as before, and the filament and cylindrical anode are of the same material and dimensions. The tube was connected with the gas-generating part by means of glass tubing, so that it might not be contaminated while being transferred (see previous paper, page 342). The inlet *i* of the apparatus was connected through a liquid-air trap *L* to a quartz tube containing two porcelain boats in which some small bits of calcium are kept to prepare Argon from air. There is a glass tube containing a copper spiral which can be heated electrically to absorb oxygen. This in turn is joined to a set of apparatus to obtain carbon monoxide, etc. It is essential in these experiments to have the gas as pure as possible, and that is why the thermionic tube was connected with the gas-generating part by means of glass tubing. Care was taken as much as possible to avoid any greased taps. The electrical connexions and the rest of other details were the same as before.

Experiments in Argon.

Argon was obtained by two different ways: one sample was supplied by the British Oxygen Company, and the other was prepared from air in the Laboratory. The first sample was let in through the inlet *i*, and was allowed to wash the whole apparatus for several minutes. Afterwards closing the inlet, the gas was pumped out to a fraction of a mm. pressure: the filament was then heated and the anode bombarded in the usual way. The calcium tube was next heated gradually, by which impurities in argon like O, N, CO₂, etc., are absorbed. The calcium tube should not be heated continuously, as it is found that hydrogen diffuses through it when it is very hot. The difficulty of preparing argon free from traces of hydrogen or nitrogen is very great—when the argon lines only are seen in the spectrum tube, the gas is experimented upon, otherwise the process is repeated till pure gas is obtained. Argon was also prepared from air in the laboratory, by introducing air through *i* and then pumping down to a few mm. pressure. The calcium tube is then heated to absorb other constituents of air. In both cases, the same sort of result was obtained when the gas used was very pure.

The following results were obtained, when only the argon lines were visible. Liquid air was kept in the traps LL.

TABLE I.

Accelerating Potential = 4.25 volts.

Heating Current on the filament = 1.25 amp.

Pressure inside the tube.	Saturation Current without magnetic field.	Residual Current with magnetic field.	Magnetic Field.	Percentage of Residual to Saturation Current.
230×10^{-4} mm.	$4200 \times 3 \times 10^{-10}$ amp.	$8.5 \times 3 \times 10^{-10}$ amp.	160	0.20
150 "	4200 "	6.5 "	"	0.15
85 "	4680 "	5.0 "	"	0.11
48 "	4440 "	0.5 "	"	0.01
28 "	4560 "	0.0 "	"	0.00

These results are plotted in fig. 1 (A), and it will be seen that the percentage is very little indeed. But the

results like the above are very difficult to get; usually, however, the following sort of values of the percentage are found.

Fig. 1.

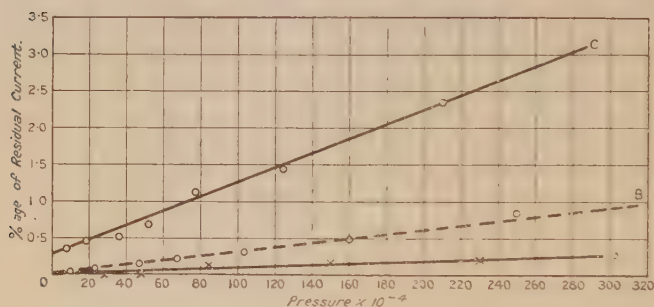


TABLE II.

Accelerating Potential = 4.2 volts.

Heating Current = 1.20 amp.

Pressure inside the tube.	Saturation Current without magnetic field.	Residual Current with magnetic field.	Magnetic Field.	Per-centage.
389×10^{-4} mm.	$1932 \times 3 \times 10^{-10}$ amp.	$28.0 \times 3 \times 10^{-10}$ amp.	160	1.4
250 "	1890 "	15.5 "	162	0.82
160 "	1896 "	9.0 "	160	0.47
103 "	1899 "	6.8 "	160	0.31
67 "	1920 "	4.0 "	164	0.20
47 "	1920 "	3.0 "	164	0.15
23 "	1920 "	1.6 "	164	0.08
10 "	1920 "	0.7 "	164	0.04

These values are plotted in fig. 1 as the dotted line (B), which gives a higher percentage than before. However, both these are exceptionally small in comparison with air or nitrogen (*e. g.* for air 15.0, and nitrogen 12.9, at 100×10^{-4} mm.).

It is also interesting to see what happens if there is some vapour present, such as that of water, grease, or mercury, as is sometimes found if the liquid air is not kept in the traps. The following results were obtained when liquid air was not kept in the traps, and the argon was not very pure.

TABLE III.

Accelerating Potential = 4.25 volts.

Heating Current = 1.3 amp.

Pressure inside the tube.	Saturation Current without magnetic field.	Residual Current with magnetic field.	Magnetic Field.	Percentage.
330×10^{-4} mm.	$1500 \times 3 \times 10^{-10}$ amp.	$70.0 \times 3 \times 10^{-10}$ amp.	164	4.66
210 "	1530 "	36.0 "	166	2.35
124 "	1530 "	22.0 "	166	1.44
77 "	1660 "	17.0 "	164	1.09
51 "	1620 "	11.5 "	164	0.71
35 "	1680 "	8.5 "	166	0.52
18 "	1680 "	7.5 "	164	0.44
8 "	1680 "	6.0 "	164	0.35

These points are plotted in fig. 1 on the top (C). It will be seen here that there is a perceptible amount of residual current even when the recorded pressure is zero.

Thus we see when the argon used is very pure and not contaminated with any vapour, the amount of residual current in a crossed electric and magnetic field is very little indeed in comparison with other gases. We shall, however, discuss this later on.

Experiments in Carbon Monoxide.

In order to study the effect in some other gas, carbon monoxide was chosen, because of its similarity with some of the properties of nitrogen. The gas was prepared in the same apparatus as that used for nitrogen (previous paper). Fresh P_2O_5 and KOH bulbs were joined, and the portions of the glass apparatus to prepare the gas were washed very carefully with distilled water so that traces of the other gases might not be left there. The carbon monoxide was obtained by the action of pure sulphuric acid on formic acid. Care was taken in collecting the gas that no air-bubbles remained on the top of the liquids, and several portions of the gas collected were pumped out. Afterwards, some gas was kept over the drying P_2O_5 and KOH bulbs for a few days before passing into the experimental tube. By this, water, sulphuric, sulphurous, or carbonic acid vapour will be absorbed by the KOH bulb, and the pentoxide will also help to keep the gas dry. Now, a little of the gas is introduced and pumped down to 300×10^{-4} mm. pressure, and the copper spiral is heated to absorb any oxygen that might contaminate the CO. After heating the filament the wire and the tube are ready for the experiment. The following

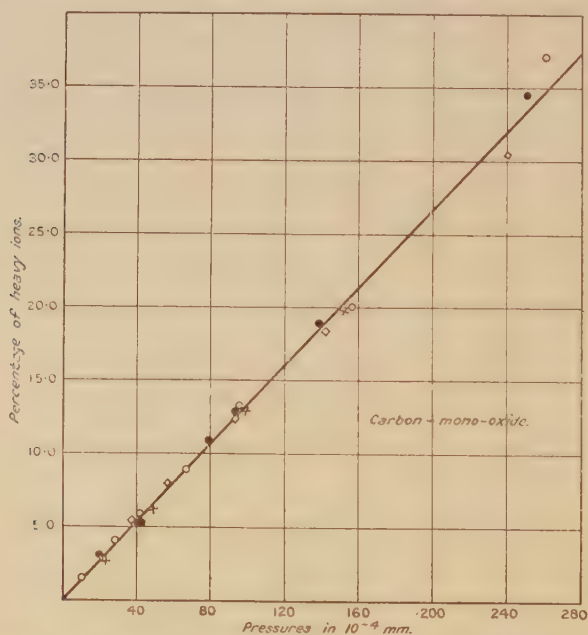
results were obtained with carbon monoxide when liquid air was kept in the traps and they were found to repeat invariably.

TABLE IV.

Accelerating Potential = 4.1 volts.
Filament Current = 0.95 amp.

Pressure inside the apparatus.	Saturation Current without magnetic field.	Residual Current with magnetic field.	Magnetic Field.	Per-centage.
260×10^{-4} mm.	$470.4 \times 3 \times 10^{-10}$ amp.	$175 \times 3 \times 10^{-10}$ amp.	164	37.2
156 "	537.6 "	107 "	165	20.0
98 "	556.8 "	74 "	164	8.9
67 "	528.0 "	47 "	162	5.9
42 "	508.0 "	30 "	162	5.9
28 "	518.4 "	21.5 "	160	4.1
10 "	528.0 "	8 "	160	1.5

Fig. 2.



These results are plotted in fig. 2. It will be seen here that the percentage of the residual current is very nearly the same as that in nitrogen (see Phil. Mag. Feb. 1923, p. 349). It might be supposed that the CO is contaminated by nitrogen, but as there was hardly any diminution of pressure when the copper spiral was heated, it shows the absence of air and so of nitrogen. Hence there is no doubt about the

purity of the carbon monoxide. The points marked as ○ are for the data given above, and the other points are given by subsequent experiments.

For comparative purposes it might be of some interest to tabulate the values of the residual currents with different gases, when the conditions are more or less the same.

TABLE V.

Gas.	Percentage at 2.0×10^{-4} mm.	Percentage at 60×10^{-4} .	Percentage at 100×10^{-4} .	Percentage at 200×10^{-4} .
Air	0.4	9.0	15.0	29.8
Nitrogen	0.3	7.9	13.0	26.0
Carbon monoxide..	0.3	8.0	13.3	26.8
Argon	0.00	0.0	0.1	0.2

Residual Current and the Velocity of the Impinging Electron.

It must have been noticed that we have always used the same accelerating potential for the electrons, as well as the same magnetic field to curl them up. This was done to compare the percentage (of residual current to the initial saturation current) in different gases, when the velocity of the impinging electron and its length of path in the gas (so that it meets with the same number of molecules) are the same. The next point of importance would be to see how far the percentage depends on the velocity of the electron. This was studied in carbon monoxide and the results are given below.

In our thermionic tube we had the magnetic field parallel to the hot wire, so that the electrons were curling round it. But, as the electrons are emitted with all velocities, the zero-velocity ones will be nearest and the highest-velocity ones producing a detectable current farthest away from the hot wire, under the action of the fields. We can adjust the values of H and V in such a way that, when the velocity of the impinging electron is increased, the maximum distance r from the wire, along its axis, is kept the same.

Thus we had, from (1)

$$H^2 = \frac{8V \log r/a}{e/m \cdot r^2 \log b/a} + \frac{8V_i}{e/m \cdot r^2}.$$

Taking $H = 160$, $V = 4.2$ volts, and average initial energy corresponding to 1.5 volts, we had $r = 0.95$ cm. Now, if we keep r the same, we can find out what value of H will correspond to any other potential. It is found that

$$H^2 = 2735.9V + 14770,$$

where V is in volts.

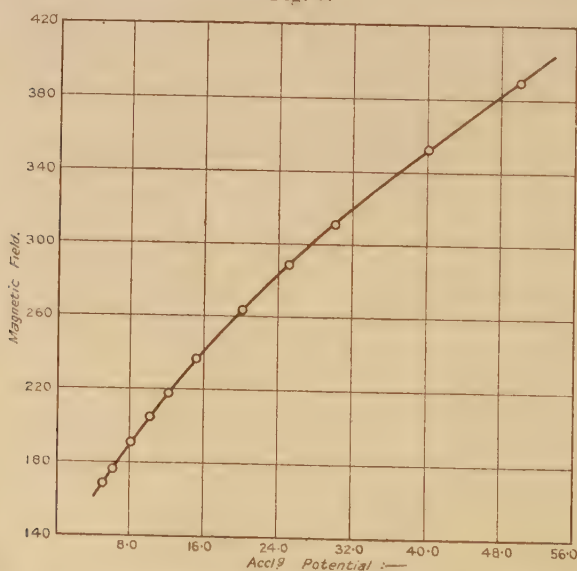
In the following table are given the values of H corresponding to different accelerating potentials, so that the electrons are always kept at the same distance, .095 cm., from the hot wire, and consequently the length of the path of the electrons in the gas is the same.

TABLE VI.

Accelerating Potential.	Magnetic Field.
5	168.7
6	176.6
8	191.5
10	205.2
12	218.2
15	236.3
20	263.6
25	288.4
30	311.2
40	352.7
50	389.3

These values are plotted in fig. 3, which can be used as a sort of calibration curve.

Fig. 3.



The following are the results of experiments in carbon monoxide. The gas was prepared in the usual way, and all precautions were taken to keep the pressure constant while the gas was examined. Liquid air was kept in the traps to stop the advance of any vapour into the thermionic tube.

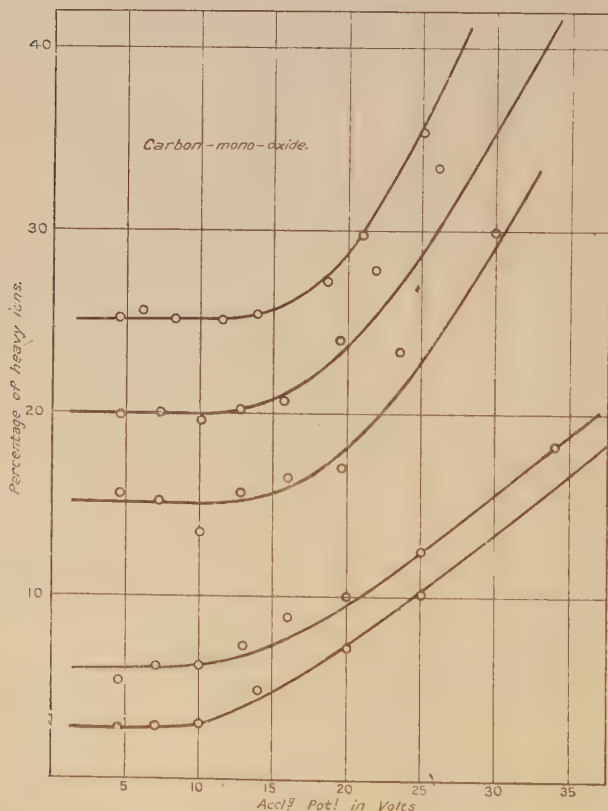
TABLE VII.

Heating current = 0.95.

Accelerating Potential.	Saturation Current without magnetic field.	Residual Current with magnetic field.	Magnetic Field.	Per-centage.
Pressure = 168×10^{-4} mm.				
4.5 volts	$444 \times 3 \times 10^{-10}$ amp.	$112 \times 3 \times 10^{-10}$ amp.	166	25.2
7.0 "	444 "	114 "	184	25.6
8.3 "	432.9 "	108 "	194	25.0
9.0 "	455.1 "	114 "	198	25.1
11.5 "	457.3 "	115 "	214	25.1
13.8 "	456.6 "	116 "	228	25.4
18.5 "	460.3 "	126 "	255	27.3
21.0 "	466.2 "	139 "	272	29.8
25.0 "	481.0 "	170 "	295	35.3
Pressure = 124×10^{-4} mm.				
4.5 volts	$427 \times 3 \times 10^{-10}$ amp.	$85 \times 3 \times 10^{-10}$ amp.	166	19.9
7.0 "	458 "	92 "	184	20.0
10.0 "	406 "	79 "	205	19.4
12.8 "	406 "	83 "	224	20.4
15.5 "	420 "	87 "	240	20.7
19.5 "	420 "	101 "	264	24.0
21.7 "	406 "	113 "	276	27.8
29.0 "	409.5 "	138 "	310	33.7
Pressure = 82×10^{-4} mm.				
4.5 volts	$510.3 \times 3 \times 10^{-10}$ amp.	$60 \times 3 \times 10^{-10}$ amp.	166	13.4
7.2 "	542.7 "	72 "	186	15.1
10.0 "	530.6 "	62 "	205	13.3
12.7 "	534.6 "	73 "	225	15.5
16.0 "	502.2 "	73 "	242	16.5
19.7 "	534.6 "	80 "	265	17.0
23.5 "	550.8 "	113 "	284	23.4
30.0 "	567.0 "	147 "	315	29.9
Pressure = 34×10^{-4} mm.				
4.5 volts	$481.3 \times 3 \times 10^{-10}$ amp.	$28 \times 3 \times 10^{-10}$ amp.	166	5.3
7.0 "	508.2 "	31 "	184	6.1
10.0 "	496.7 "	31 "	205	6.2
13.0 "	215.9 "	38 "	225	7.3
15.9 "	492.9 "	44 "	242	8.9
20.0 "	512.1 "	51 "	266	9.9
25.0 "	519.8 "	65 "	290	12.5
34.0 "	575.9 "	94 "	335	18.2
Pressure = 14×10^{-4} mm.				
4.5 volts	$406 \times 3 \times 10^{-10}$ amp.	$11 \times 3 \times 10^{-10}$ amp.	166	2.7
7.0 "	413 "	12 "	184	2.9
10.0 "	399 "	12 "	205	3.0
14.0 "	413 "	20 "	230	4.8
20.0 "	402.5 "	29 "	265	7.2
25.0 "	434 "	44 "	290	10.1
34.0 "	476 "	87 "	336	18.3

All these results are plotted in fig. 4. It will be seen from these curves that the percentage tends to keep fairly constant up to a certain voltage, about 10 in our case, after which the residual current begins to increase. The ionization potential of CO is also 10 volts. What happens, I believe, is, when the velocity reaches the ionization potential,

Fig. 4.



some more electrons are produced which in turn might form some fresh heavy ions, or these electrons, being knocked off near the electrode, find their way to the anode.

Thus we see that the percentage of residual current does not depend on the velocity of the impinging electron up to a certain limit, viz., the ionization potential, after which the result becomes complicated by other phenomena.

Discussion.

The most interesting results of these investigations are the comparatively small magnitude of the residual current in argon under the same conditions as in other gases, and approximately the same amount in carbon monoxide as in nitrogen. It was suggested in the previous paper (*loc. cit.*) that the formation of heavy ions is relatively unimportant in comparison with the collision of electrons with gas molecules. Under the conditions of the experiment, it is found that when a collision has once taken place, the electrons cannot go back to the hot wire, nor can they accumulate in the field, and the only place to go to would be the anode after a repeated number of collisions. However, if this view is correct, we should be able to get an approximate idea of the mean free path of an electron in the gas concerned.

To do this, we require to know the length of the path (s) of an electron in the magnetic field when no collision occurs. We can take, approximately, this to be equal to an arc of a circle whose radius is equal to the maximum distance r which the electron travels from the axis. Then

$$s = r(\pi - 2 \sin^{-2} a/r),$$

where a is the radius of the hot wire.

If we suppose the length of the mean free path of an electron is the same under the action of the fields as that when they are absent, then the proportion ξ which collide in path s is

$$\xi = \int_0^s e^{-\frac{x}{\lambda}} \frac{dx}{\lambda} = 1 - e^{-\frac{s}{\lambda}}.$$

$$\therefore \lambda = -s/\log_e(1-\xi).$$

When $H=160$, $r=0.8$ as the mean of the distances of the electrons from the wire, we get

$$s = 0.08 \times 3.015 = 0.24120 \text{ cm.}$$

Now at $100 \cdot 10^{-4}$ mm. pressure, ξ for argon is 0.01, and for CO is 0.867. Then we get

$$\lambda_{\text{argon}} = 24.12 \text{ cm.}$$

$$\text{and } \lambda_{\text{CO}} = 1.69 \text{ ,,}$$

$$\text{i. e., } \lambda_{\text{argon at 760 mm.}} = 32.0 \times 10^{-5} \text{ cm.,}$$

$$\lambda_{\text{CO}} \text{ ,, ,, } = 2.2 \times 10^{-5} \text{ ,,}$$

From the Kinetic Theory, taking the diameters of molecules, we get $\lambda_{\text{argon}} = 3.6 \cdot 10^{-5}$ and $\lambda_{\text{CO}} = 3.25 \cdot 10^{-5}$, and it will be seen that the mean free path of an electron in argon is about 10 times that deduced from the Kinetic Theory

from molecular data. Also, the mean free path in carbon monoxide is of the same order of magnitude as that obtained from Kinetic Theory.

In some experiments on the motion of electrons in hydrogen (shortly to be communicated) it was found that the mean free path in molecular hydrogen is about 1.24×10^{-5} cm. Thus the mean free path in argon is more than 20 times that in hydrogen. An abnormally large value of the free path in argon has also been observed by Townsend and Bailey*. They found, after making corrections for the velocity of agitation of electrons in the electric field, that the mean free path in argon is about 60 times larger than that in hydrogen.

However, this apparent disagreement of the mean free path of an electron in argon from that given by the Kinetic Theory cannot be explained, even if we take into consideration the temperature of the gas in which the electrons are moving.

Summary.

In this paper we have seen that when electrons are moving through any gas, the current between the emitting source and the anode is not stopped by a magnetic field (large enough to stop the current in vacuum) acting perpendicular to the electric intensity.

In argon the residual current is very small, whereas in carbon monoxide the fraction is fairly large: *e. g.*, at 100.10^{-4} mm. pressure the percentage in argon is 0.1, whereas in carbon monoxide it is 13.3.

It has been also found, when the velocity of the impinging electron is increased, that the percentage of the residual current does not increase, at least up to the ionization potential of the gas (CO). After that potential, the percentage of residual current increases.

Assuming the residual current is due to the electrons colliding several times with gas molecules, it is possible to find an expression for the mean free path of the electron; and the value found in CO agrees fairly with that deduced from Kinetic Theory.

An abnormally large free path is obtained in argon, and the value obtained is about 10 times more than that obtained from the Kinetic Theory.

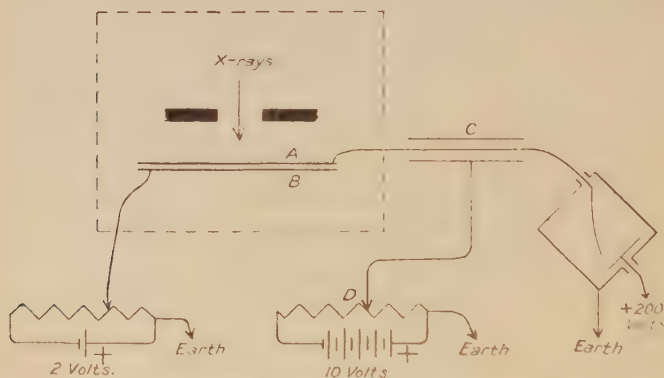
In conclusion, I wish to express my gratitude to Prof. Richardson for his suggestions and advice during the course of this work.

* Phil. Mag. vol. xliii. p. 1127.

component of the velocity of thermions emitted from a comparatively small surface of hot platinum towards an extensive plane opposite. In the corresponding X-ray experiment the electronic currents measured were necessarily much smaller, and, moreover, no variation of the opposing electrostatic field, caused, for example, by the charging of an electrometer, could be allowed during a run. A "null" method of employing a tilted electroscopie was therefore devised and other precautions employed that are given below.

3. In fig. 1, A and B represent two sheets of filter-paper, each about 16 sq. cm. in area, insulated from each other and about 1 mm. apart. The side of A remote from B was made conducting by rubbing with pure graphite. The side towards B was coated with one sheet of ordinary gold-leaf.

Fig. 1.



Both faces of B were rubbed with graphite; whilst this makes the surface a good conductor, I have never been able to detect any electronic emission from it. The gold-leaf of the screen A was connected directly to a Wilson's tilted electroscopie by a short lead sheathed for 10 cm. of its length with an insulated metal tube 2 cm. in diameter, the potential of which could be varied continuously from 0 to -10 volts by turning a handle on the continuous rheostat D. The potential of B could be maintained steady at any desired value. It was not varied beyond the range ± 2 volts.

4. The method of experimenting was as follows:—After the gold-leaf system with A attached had been earthed and insulated, C earthed, and B at, say, -1 volt, the X-ray beam was started. The system A would normally begin to

All lead parts were given a thin film of paraffin-wax and earthed. F, F are sheets of graphited filter-paper, about 1 mm. from A and B respectively, placed there for the double purpose of limiting the volume in the neighbourhood of A and of screening it from stray electrostatic fields. That the whole arrangement was quite successful for the purpose for which it was intended was determined by replacing A by an exactly similar sheet, but without the gold-leaf upon it. On now making a run in a manner described above, even under the most favourable conditions with B charged positively, no readable deflexion could be obtained. The readings could therefore be plotted without any corrections or adjustments. To approach ideal conditions, the area radiating electrons must be small in comparison with the whole area of the parallel plates used for testing their speeds. The effect of increasing the area of these plates is to diminish the currents measured. To obtain measurable currents the full radiation from a tungsten target "radiator" pattern Coolidge tube was employed, the tube being excited by means of a transformer.

6. Two characteristic curves are shown in fig. 3, the ordinates representing the charge acquired in 1 minute by the system A, maintained at zero potential, the abscissæ give the potential of B in volts. Curve I is for a current of 2 milliamperes through the tube, curve II for 3.5 milliamperes. The points on the two curves were taken alternately and after equal intervals of time, the heating current of the cathode of the Coolidge tube being maintained during the whole experiment and varied slightly for alternate points to give the above outputs. The smoothness of the two curves indicates the accuracy of the observational points.

7. Both curves show that 85 per cent. of the electrons emitted have velocities less than that given by a fall through 2 volts, and the argument against their being true dependent photo-electrons described in paragraph 1 is as follows:—The results are complicated by the incident radiation being heterogeneous, but M. and L. de Broglie have shown from considerations of the absorption law of Bragg and Peirce * that selective absorption of frequency ν will occur when $\nu = \frac{1}{2}\nu_0$, where ν_0 is a natural frequency existing in an absorbing element. Taking this to be the L_{a_1} frequency for gold (w.l. = 1.27×10^{-8} cm.), the major velocity of the dependent electrons emitted in these experiments should be

* *Comptes Rendus*, Sept. 1921, p. 527.

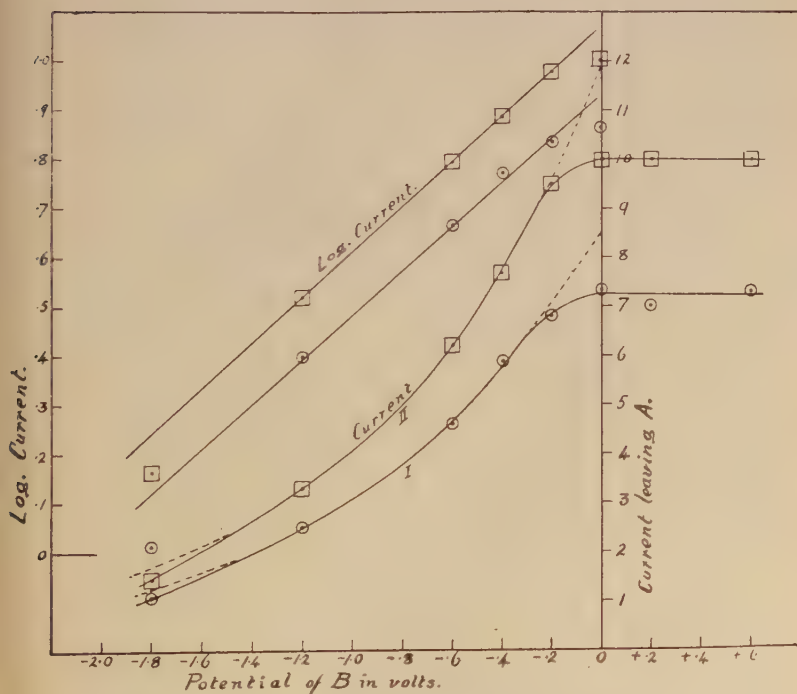
given by

$$Ve = h(\nu - \nu_0) = h\nu_0/3 \quad \dots \quad (iii)$$

$$\therefore V = 3.35 \times 10^3 \text{ volts.}$$

The curves show that this cannot be the case. Considering now that the energy-distribution curve for the radiation from the Coolidge tube is continuous, it follows that residues such as (iii) will also form a continuous series, but, as the

Fig. 3.



major number of electrons emitted have comparatively zero speed, if these were the true photo-electrons, then the emission spectrum from the Coolidge tube should correspond exactly to that from gold. Again, interesting results on these low-speed electrons have recently been obtained by Shearer*, though the design and method of using of his

* Phil. Mag. xlv. p. 806 (1922).

apparatus differ from that described herein in many important respects, the present design, described above, being especially adapted to the measurement of the normal component of the velocities of the slowest rays. His general conclusions are that these electrons may be called independent, that their properties are similar to those of the δ -rays produced by α -rays, and that they are produced by the intermediary rapid β -rays. Two other factors that might enter must be considered. The first is the effect of the secondary X-rays from the gold. In a previous paper* the writer has shown that this must be too small to produce a major effect, and the most frequent normal component of the speed, being in the neighbourhood of 0.48 volt, corresponds to ionization by rays in the visible region of the spectrum if we use the value 3×0.48 volts to calculate the mean resultant energy of these slow rays. The second effect is due to the thermal reaction accompanying the recoil of an atom emitting a rapid β -ray. Interest in this subject has been renewed recently by P. L. Kapitza†, who has shown that the slow electronic δ -radiation arising from the impact of α -particles is due to thermal effects arising from localized points of impact, the intermediary being high-speed electrons. Richardson's thermionic equations are applied to the resultant distribution of δ -radiation, and temperatures of the order $20,000^\circ$ abs. are assigned to the centres yielding the observed most probable speed.

8. If the distribution of speeds is Maxwellian, the current received by the plate opposite the radiator, and therefore that leaving the radiator designed as described in paragraph 3, is governed by the equation‡

$$\log_e i/i_0 = - \frac{ne}{RT} V_1, \quad . \quad . \quad . \quad . \quad (iv)$$

where n is the number of molecules in 1 c.c. of a perfect gas at 0° C. and 760 mm. pressure, R is the gas constant for this quantity of gas, V_1 is the retarding potential reducing the current from i_0 to i , $ne = .43$ e.m. unit, $R = 3.7 \times 10^3$ erg/deg. C. The curves show how far the distribution in speeds differs from the logarithmic distribution represented by the dotted lines in fig. 3. It should be pointed out here

* Phil. Mag. xli. p. 130 (1921).

† Phil. Mag. xlv. p. 989 (1923).

‡ O. W. Richardson, 'The Emission of Electricity from Hot Bodies,' 1916, p. 144.

that no special preparation of the surface to ensure cleanliness was possible, and the vacuum maintained was of the order $\cdot 01$ cm. of mercury. These two factors would probably account for the loss of a fraction of the very slowest electrons, indicated by a bending over of the curves to the current axis. Assuming that the curves are logarithmic over the major part of their length and that the process of emission can be compared with the thermionic process, we have from both curves using formula (iv) $T = 1.1 \times 10^4$ deg. abs.

9. That atomic recoil can scarcely account for this high temperature is shown as follows:—The velocity of recoil of a stationary atom of mass M yielding an electron of energy eV will be $(2meV)^{\frac{1}{2}}/M$. In the present case $M = 197 \times 1.66 \times 10^{-24}$ gm. for a gold atom, $V = 4.4 \times 10^4$ volts, being the peak potential supplied to the Coolidge tube, and hence the velocity of recoil $= 3.4 \times 10^4$ cm./sec. as compared with an average velocity of 1.89×10^4 cm./sec. due to the thermal motion of gold atoms at 15° C. A simple calculation shows that under the most favourable circumstances of recoil, *i. e.*, when the direction of motion of the ejected electron is opposite to that of thermal motion of the atom, and therefore the above velocities will be added, the resulting energy of the atom cannot be greater than that corresponding to 2300° abs. The approximate average velocity corresponding to a temperature of 1.1×10^4 deg. abs. is 11.6×10^4 cm./sec., and consequently an atom would need a thermal velocity of $(11.6 - 3.4) \times 10^4$ cm./sec. at least before recoil in order to acquire this temperature. Taking this velocity, *viz.* 8.2×10^4 cm./sec. and the average velocity at normal temperature as 1.89×10^4 cm./sec., the ratio is 4.3. The ratio of the number of atoms whose velocities lie between $4.3u$ and $4.3u + du$ to those that lie between u and $u + du$, where u is the root mean square of the velocity of the atoms, from Maxwell's distribution law is then only of the order 10^{-10} to 1. This, together with the fact that very few of all the atoms present are influenced by the radiation, rules out the possibility of centres acquiring the extremely high temperature of 1.1×10^4 deg. abs. by recoil alone.

10. We are therefore left to account for the experimental observations in some such manner as follows. The original form of the energy is that of the fast-moving β -rays, the final form is energy of the same type but degraded. The primary β -ray of large energy yields a large number of slow β -rays all of similar origin—or δ -rays, as they have been

called,—energy corresponding to that of the ionization potential being taken from the parent store at each inelastic impact. Only the most loosely bound electrons are affected. The mechanism of the interchange of energy is difficult to conceive, but colour is lent to this view by the fact that C. T. R. Wilson's tracks of β -particles are unforked, *i. e.* a rapid β -ray only produces by impact with atoms other β -rays or ions whose energy is very small in comparison with that of the parent particle. Very rarely does a large change of energy by direct impact occur. The logarithmic distribution of the particles will be the subject of further investigation.

Abstract.

It is shown that the normal component of the velocity of over 85 per cent. of the electrons emitted from a gold film under the influence of a heterogeneous beam of X-rays is less than 2 volts. The distribution with velocity bears a relationship to that of the thermions from a hot body. It is argued that the mode of production of these slow electrons can scarcely be due to atomic recoil consequent on the ejection of a rapid β -ray nor to the action of the transformed X-ray energy into energy of longer wave-length. The analogy with the thermionic process probably arises from the fact that in both cases only the outermost system of electrons take part in the action, though the mechanism of the two processes must differ considerably, in the present case the intermediary being the rapid primary β -ray.

The distribution with velocity of the electron atmosphere, from the point of view of thermionics in the case investigated, corresponds to a temperature of 11,000° abs. It becomes important, therefore, to investigate under all conditions the correspondence between the two processes.

A "null" method of using an electroscopes is described.

My best thanks are due to Professor A. Griffiths for giving me the facilities of his laboratory, and to the Governors of Birkbeck College for a grant for the purposes of this research.

Birkbeck College (University of London),
E.C. 4.

LII. *Two Solutions of the Stress Equations, under Tensions only, expressed in general Orthogonal Coordinates, with two deductions therefrom.* By R. F. GWYTHER, M.A.*

THIS paper is in continuation with a portion of one entitled "An Analytical Discrimination of Elastic Stresses in an Isotropic Body" †, and I employ the same notation {P, Q, R, S, T, U} for stress and {e, f, g, a, b, c} for strain. There are two solutions, one giving the elements of stress in terms of three functions θ , and one in terms of three functions ψ , each of them being general solutions. As there will be no transformation of coordinate axes, the two solutions will be considered separately. I now find that I should have attributed the θ -solution in Cartesians to Maxwell, and the ψ -solution to Morera.

Ultimately I combine the two solutions to derive the six equations of identity connecting the differential coefficients of the elements of strain in an orthogonal coordinate system.

1. I propose to find the solution, step by step, of the stress-equations, under tensions only, which I shall consider in the form

$$\begin{aligned} \frac{\partial}{\partial \xi} \left(\frac{P}{h_2 h_3} \right) + h_1 \frac{\partial}{\partial \eta} \left(\frac{U}{h_3 h_1^2} \right) + h_1 \frac{\partial}{\partial \xi} \left(\frac{T}{h_1^2 h_2} \right) \\ + \frac{1}{h_2^2 h_3} \frac{\partial h_2}{\partial \xi} Q + \frac{1}{h_2 h_3^2} \frac{\partial h_3}{\partial \xi} R = 0, \\ h_2 \frac{\partial}{\partial \xi} \left(\frac{U}{h_2^2 h_3} \right) + \frac{\partial}{\partial \eta} \left(\frac{Q}{h_3 h_1} \right) + h_2 \frac{\partial}{\partial \xi} \left(\frac{S}{h_1 h_2^2} \right) \\ + \frac{1}{h_3^2 h_1} \frac{\partial h_3}{\partial \eta} R + \frac{1}{h_3 h_1^2} \frac{\partial h_1}{\partial \eta} P = 0, \\ h_3 \frac{\partial}{\partial \xi} \left(\frac{T}{h_2 h_3^2} \right) + h_3 \frac{\partial}{\partial \eta} \left(\frac{S}{h_3^2 h_1} \right) + \frac{\partial}{\partial \xi} \left(\frac{R}{h_1 h_2} \right) \\ + \frac{1}{h_1^2 h_2} \frac{\partial h_1}{\partial \xi} P + \frac{1}{h_1 h_2^2} \frac{\partial h_2}{\partial \xi} Q = 0, \end{aligned} \quad (1)$$

and I shall retain this notation throughout.

The solutions present themselves in two triads.

* Communicated by the Author.

† Phil. Mag. July 1922, p. 274.

Taking as the starting-point

$$\begin{aligned} P &= \dots, & Q &= -h_3^2 \frac{\partial^2 \theta_1}{\partial \zeta^2} \dots, & R &= -h_2^2 \frac{\partial^2 \theta_1}{\partial \eta^2} \dots, \\ S &= h_2 h_3 \frac{\partial^2 \theta_1}{\partial \eta \partial \zeta} \dots, & T &= \dots, & U &= \dots, \end{aligned}$$

which satisfy the equations in third differential coefficients of θ_1 , and proceeding to satisfy the equations in the next lower degrees of differential coefficients, we find the expressions terminate. At this stage and in other stages throughout the paper we make use of the two triads of identities between the second differential coefficients of h 's and squares and products of first differential coefficients, which I shall cite as Lamé's Identities. I quote one identity from each triad:—

$$\begin{aligned} h_2 h_3 \frac{\partial^2 h_1}{\partial \eta \partial \zeta} &= 2 \frac{h_2 h_3}{h_1} \frac{\partial h_1}{\partial \eta} \frac{\partial h_1}{\partial \zeta} - h_3 \frac{\partial h_1}{\partial \eta} \frac{\partial h_2}{\partial \zeta} - h_2 \frac{\partial h_1}{\partial \zeta} \frac{\partial h_3}{\partial \eta}; \\ \frac{h_2^2}{h_3} \frac{\partial^2 h_3}{\partial \eta^2} + \frac{h_3^2}{h_2} \frac{\partial^2 h_2}{\partial \zeta^2} &= 2 \frac{h_2^2}{h_3^2} \left(\frac{\partial h_3}{\partial \eta} \right)^2 + 2 \frac{h_3^2}{h_2^2} \left(\frac{\partial h_2}{\partial \zeta} \right)^2 + \frac{h_1^2}{h_2 h_3} \frac{\partial h_2}{\partial \xi} \frac{\partial h_3}{\partial \xi} \\ &\quad - \frac{h_2}{h_3} \frac{\partial h_2}{\partial \eta} \frac{\partial h_3}{\partial \eta} - \frac{h_3}{h_2} \frac{\partial h_2}{\partial \zeta} \frac{\partial h_3}{\partial \zeta}. \end{aligned}$$

The final values for the elements of stress are:—

$$\begin{aligned} P &= 2 \frac{h_1^2}{h_2 h_3} \frac{\partial h_2}{\partial \xi} \frac{\partial h_3}{\partial \xi} \theta_1, \\ Q &= -h_3^2 \frac{\partial^2 \theta_1}{\partial \zeta^2} - \frac{h_1^2}{h_3} \frac{\partial h_3}{\partial \xi} \frac{\partial \theta_1}{\partial \xi} + \frac{h_2^2}{h_3} \frac{\partial h_3}{\partial \eta} \frac{\partial \theta_1}{\partial \eta} \\ &\quad + \left(2 \frac{h_3^2}{h_1} \frac{\partial h_1}{\partial \zeta} - h_3 \frac{\partial h_3}{\partial \zeta} \right) \frac{\partial \theta_1}{\partial \zeta} \\ &\quad + 2 \left\{ \frac{h_3^2}{h_1} \frac{\partial^2 h_1}{\partial \zeta^2} - \left(2 \frac{h_3^2}{h_1^2} \frac{\partial h_1}{\partial \zeta} - h_3 \frac{\partial h_3}{\partial \zeta} \right) \frac{\partial h_1}{\partial \zeta} - \frac{h_2^2}{h_1 h_3} \frac{\partial h_1}{\partial \eta} \frac{\partial h_3}{\partial \eta} \right\} \theta_1, \\ R &= -h_2^2 \frac{\partial^2 \theta_1}{\partial \eta^2} - \frac{h_1^2}{h_2} \frac{\partial h_2}{\partial \xi} \frac{\partial \theta_1}{\partial \xi} + \left(2 \frac{h_2^2}{h_1} \frac{\partial h_1}{\partial \eta} - h_2 \frac{\partial h_2}{\partial \eta} \right) \frac{\partial \theta_1}{\partial \eta} \\ &\quad + \frac{h_3^2}{h_2} \frac{\partial h_2}{\partial \zeta} \frac{\partial \theta_1}{\partial \zeta} \\ &\quad + 2 \left\{ \frac{h_2^2}{h_1} \frac{\partial^2 h_1}{\partial \eta^2} - \left(2 \frac{h_2^2}{h_1^2} \frac{\partial h_1}{\partial \eta} - h_2 \frac{\partial h_2}{\partial \eta} \right) \frac{\partial h_1}{\partial \eta} - \frac{h_3^2}{h_1 h_2} \frac{\partial h_1}{\partial \zeta} \frac{\partial h_2}{\partial \zeta} \right\} \theta_1, \end{aligned}$$

$$\begin{aligned}
 S &= h_2 h_3 \frac{\partial^2 \theta_1}{\partial \eta \partial \zeta} + h_1 h_3 \frac{\partial}{\partial \zeta} \left(\frac{h_2}{h_1} \right) \frac{\partial \theta_1}{\partial \eta} + h_1 h_2 \frac{\partial}{\partial \eta} \left(\frac{h_3}{h_1} \right) \frac{\partial \theta_1}{\partial \zeta}, \\
 T &= \frac{h_1 h_3}{h_3} \frac{\partial h_2}{\partial \xi} \frac{\partial \theta_1}{\partial \zeta}, \\
 U &= \frac{h_1 h_2}{h_3} \frac{\partial h_3}{\partial \xi} \frac{\partial \theta_1}{\partial \eta}. \quad \dots \dots \dots (2)
 \end{aligned}$$

By a concurrent cyclic interchange of the subscripts 1, 2, 3; of ξ, η, ζ ; of P, Q, R; and of S, T, U and addition we complete the θ -solution. To complete, for example, the value of P, we take one cyclic step forward from the value of R, and one such step retrograde from the value of Q.

To find a solution from the ψ -triad, we start from

$$\begin{aligned}
 P &= 2h_2 h_3 \frac{\partial^2 \psi_1}{\partial \eta \partial \zeta} \dots, \quad Q = \dots, \quad R = \dots, \\
 S &= h_1^2 \frac{\partial^2 \psi_1}{\partial \xi^2} \dots, \quad T = -h_1 h_2 \frac{\partial^2 \psi_1}{\partial \xi \partial \eta} \dots, \\
 U &= -h_1 h_3 \frac{\partial^2 \psi_1}{\partial \xi \partial \zeta} \dots,
 \end{aligned}$$

and repeat the process as before.

The final values in this case are:—

$$\begin{aligned}
 P &= 2h_2 h_3 \frac{\partial^2 \psi_1}{\partial \eta \partial \zeta} - 2h_3 \frac{\partial h_2}{\partial \zeta} \frac{\partial \psi_1}{\partial \eta} - 2h_2 \frac{\partial h_3}{\partial \eta} \frac{\partial \psi_1}{\partial \zeta} \\
 &\quad - 2 \left\{ h_3 \frac{\partial^2 h_2}{\partial \eta \partial \zeta} + h_2 \frac{\partial^2 h_3}{\partial \eta \partial \zeta} - \frac{h_3}{h_2} \frac{\partial h_2}{\partial \eta} \frac{\partial h_2}{\partial \zeta} - \frac{h_2}{h_3} \frac{\partial h_3}{\partial \eta} \frac{\partial h_3}{\partial \zeta} \right\} \psi_1, \\
 Q &= -2 \frac{h_2 h_3}{h_1} \frac{\partial h_1}{\partial \eta} \frac{\partial \psi_1}{\partial \zeta} + 2 \left\{ \frac{h_3}{h_1} \frac{\partial h_1}{\partial \eta} \frac{\partial h_2}{\partial \zeta} + \frac{h_2}{h_1} \frac{\partial h_1}{\partial \zeta} \frac{\partial h_3}{\partial \eta} \right\} \psi_1, \\
 R &= -2 \frac{h_2 h_3}{h_1} \frac{\partial h_1}{\partial \zeta} \frac{\partial \psi_1}{\partial \eta} + 2 \left\{ \frac{h_3}{h_1} \frac{\partial h_1}{\partial \eta} \frac{\partial h_2}{\partial \zeta} + \frac{h_2}{h_1} \frac{\partial h_1}{\partial \zeta} \frac{\partial h_3}{\partial \eta} \right\} \psi_1, \\
 S &= h_1 h_2 h_3 \frac{\partial}{\partial \xi} \left(\frac{h_1}{h_2 h_3} \frac{\partial \psi_1}{\partial \xi} \right) \\
 &\quad + \left\{ \frac{h_2^2}{h_1} \frac{\partial^2 h_1}{\partial \eta^2} + \frac{h_3^2}{h_1} \frac{\partial^2 h_1}{\partial \zeta^2} - h_2^2 \left(\frac{\partial h_2}{\partial \xi} \right)^2 \right. \\
 &\quad \left. + \frac{2h_1^2}{h_2 h_3} \frac{\partial h_2}{\partial \xi} \frac{\partial h_3}{\partial \xi} - h_3^2 \left(\frac{\partial h_3}{\partial \xi} \right)^2 \right. \\
 &\quad \left. + \frac{h_2}{h_1} \left(\frac{\partial h_2}{\partial \eta} + \frac{h_2}{h_1} \frac{\partial h_3}{\partial \eta} - 2 \frac{h_2}{h_1} \frac{\partial h_1}{\partial \eta} \right) \frac{\partial h_1}{\partial \eta} \right. \\
 &\quad \left. + \frac{h_3}{h_1} \left(\frac{\partial h_3}{\partial \zeta} - 2 \frac{h_3}{h_1} \frac{\partial h_1}{\partial \zeta} + \frac{h_3}{h_2} \frac{\partial h_2}{\partial \zeta} \right) \frac{\partial h_1}{\partial \zeta} \right\} \psi_1.
 \end{aligned}$$

$$\begin{aligned}
T = & -h_1 h_2 \frac{\partial^2 \psi}{\partial \xi \partial \eta} - h_2 \left(\frac{\partial h_1}{\partial \eta} - 2 \frac{h_1}{h_3} \frac{\partial h_3}{\partial \eta} \right) \frac{\partial \psi_1}{\partial \xi} \\
& + h_1 \left(\frac{\partial h_2}{\partial \xi} - \frac{h_2}{h_3} \frac{\partial h_3}{\partial \xi} \right) \frac{\partial \psi_1}{\partial \eta} \\
& + h_1 \left\{ \frac{\partial^2 h_2}{\partial \xi \partial \eta} + \left(\frac{1}{h_1} \frac{\partial h_1}{\partial \eta} - \frac{1}{h_2} \frac{\partial h_2}{\partial \eta} - \frac{1}{h_3} \frac{\partial h_3}{\partial \eta} \right) \frac{\partial h_2}{\partial \xi} \right. \\
& \quad \left. + \frac{h_2}{h_3^2} \frac{\partial h_3}{\partial \eta} \frac{\partial h_3}{\partial \xi} \right\} \psi_1, \\
U = & -h_1 h_3 \frac{\partial^2 \psi_1}{\partial \xi \partial \zeta} - h_3 \left(\frac{\partial h_1}{\partial \zeta} - 2 \frac{h_1}{h_2} \frac{\partial h_2}{\partial \zeta} \right) \frac{\partial \psi_1}{\partial \xi} \\
& + h_1 \left(\frac{\partial h_3}{\partial \xi} - \frac{h_3}{h_2} \frac{\partial h_2}{\partial \xi} \right) \frac{\partial \psi_1}{\partial \zeta} \\
& + h_1 \left\{ \frac{\partial^2 h_3}{\partial \xi \partial \zeta} + \left(\frac{1}{h_1} \frac{\partial h_1}{\partial \zeta} - \frac{1}{h_2} \frac{\partial h_2}{\partial \zeta} - \frac{1}{h_3} \frac{\partial h_3}{\partial \zeta} \right) \frac{\partial h_3}{\partial \xi} \right. \\
& \quad \left. + \frac{h_3}{h_2^2} \frac{\partial h_2}{\partial \zeta} \frac{\partial h_2}{\partial \xi} \right\} \psi_1, \quad (3)
\end{aligned}$$

where again the triad may be completed by cyclic interchange.

Each of these solutions is a complete general solution of the stress-equations.

First deduction.

2. If we express the elements of any stress whatever according to the θ -solution, and the elements of the reverse of that stress according to the ψ -solution, and add the two solutions, the sum of the expressions on the right in each of the six cases will be null.

Stating this result otherwise. If we add the θ -solutions and ψ -solutions in full for each of the six elements of stress, there will be certain related values of $\theta_1, \theta_2, \theta_3, \psi_1, \psi_2, \psi_3$ which will make the value of each element of stress zero.

Both by analogy with the results for Cartesians, and from general considerations, it will appear that the relations between $\theta_1, \theta_2, \theta_3, \psi_1, \psi_2, \psi_3$ in this case are the same as those between $e, f, g, a/2, b/2, c/2$.

We therefore obtain the six identical relations between the

elements of strain, by writing the sum of the θ -solutions, and the ψ -solutions in full, for each element of stress, and then replacing θ_1 by e , θ_2 by f , θ_3 by g , ψ_1 by $a/2$, ψ_2 by $b/2$, ψ_3 by $c/2$, and replacing each element of stress by zero.

The leading terms of the first and fourth of the set have the form

$$0 = -h_2^2 \frac{\partial^2 g}{\partial \eta^2} - h_3^2 \frac{\partial^2 f}{\partial \xi^2} + h_2 h_3 \frac{\partial^2 a}{\partial \eta \partial \xi} + \text{etc.},$$

$$0 = h_2 h_3 \frac{\partial^2 e}{\partial \eta \partial \xi} + \frac{1}{2} h_1^2 \frac{\partial^2 a}{\partial \xi^2} - \frac{1}{2} h_1 h_2 \frac{\partial^2 b}{\partial \xi \partial \eta} - \frac{1}{2} h_1 h_3 \frac{\partial^2 c}{\partial \xi \partial \eta} + \text{etc.}$$

The complete expressions are lengthy, and require the expenditure of a little labour to obtain.

That the expressions on the right, expressed in terms of u , v , w , vanish identically may be verified to any desired extent, but the verification is really only of the accuracy of the work. It is certain that there is one set, and only one set, of identical relations between the differential coefficients of the elements of strain not exceeding the second degree.

An illustration, *ab initio*, in polar cylindrical coordinates is simple. The case of polar spherical coordinates is not much simpler than the general case.

Second deduction.

3. To illustrate these six equations of identity, I proceed to find the six Elastic Stress Relations for this coordinate system.

In the first place, we must replace the elements of strain in these equations by their equivalents in terms of stress.

To explain the further processes, I shall suppose that, for the moment, the *inertia terms* are included in the stress-equations in the form $\rho \ddot{u}$, $\rho \ddot{v}$, $\rho \ddot{w}$. Then we must proceed to obtain from those equations the values of $\rho \ddot{e}$, etc., $\rho \ddot{a}$, etc., after which these inertia terms may be omitted.

Then double the expression for $\rho \ddot{e}$ and subtract the sum of the second and third of the six equations of identity. The details of the simplification are laborious and of little interest. There is again a triad of analogous relations from which we may verify that

$$\nabla^2(P + Q + R) = 0.$$

The final result for the first relation of the first triad is

$$\begin{aligned}
 & \nabla^2 P \\
 & + \frac{2m}{3m-n} \left\{ h_1 h_2 h_3 \frac{\partial}{\partial \xi} \left(\frac{h_1}{h_2 h_3} \frac{\partial}{\partial \xi} \right) + \frac{h_1^2}{h_2} \frac{\partial h_2}{\partial \xi} \frac{\partial}{\partial \xi} - \frac{h_2^2}{h_1} \frac{\partial h_1}{\partial \eta} \frac{\partial}{\partial \eta} \right. \\
 & \quad \left. + \frac{h_1^2}{h_3} \frac{\partial h_3}{\partial \xi} \frac{\partial}{\partial \xi} - \frac{h_3^2}{h_1} \frac{\partial h_1}{\partial \xi} \frac{\partial}{\partial \xi} \right\} (P+Q+R) \\
 & - 2 \left\{ \frac{h_1^2}{h_2^2} \left(\frac{\partial h_2}{\partial \xi} \right)^2 + \frac{h_2^2}{h_1^2} \left(\frac{\partial h_1}{\partial \eta} \right)^2 \right\} (P-Q) \\
 & \quad + 2 \left\{ \frac{h_1^2}{h_3^2} \left(\frac{\partial h_3}{\partial \xi} \right)^2 + \frac{h_3^2}{h_1^2} \left(\frac{\partial h_1}{\partial \xi} \right)^2 \right\} (R-P) \\
 & + 2 \left\{ \frac{h_2 h_3}{h_1^2} \frac{\partial h_1}{\partial \eta} \frac{\partial h_1}{\partial \xi} - \frac{h_2}{h_1} \frac{\partial h_1}{\partial \xi} \frac{\partial h_3}{\partial \eta} - \frac{h_3}{h_1} \frac{\partial h_1}{\partial \eta} \frac{\partial h_2}{\partial \xi} \right\} S \\
 & - 2 \left\{ 2h_3 \frac{\partial h_1}{\partial \xi} \frac{\partial}{\partial \xi} - 2h_1 \frac{\partial h_3}{\partial \xi} \frac{\partial}{\partial \xi} + \frac{h_1 h_3}{h_2^2} \frac{\partial h_2}{\partial \xi} \frac{\partial h_2}{\partial \xi} \right. \\
 & \quad + h_3 \frac{\partial^2 h_1}{\partial \xi \partial \xi} - h_1 \frac{\partial^2 h_3}{\partial \xi \partial \xi} + \frac{h_1}{h_2} \frac{\partial h_2}{\partial \xi} \frac{\partial h_3}{\partial \xi} - \frac{h_3}{h_2} \frac{\partial h_1}{\partial \xi} \frac{\partial h_2}{\partial \xi} \\
 & \quad \left. + \frac{h_1}{h_3} \frac{\partial h_3}{\partial \xi} \frac{\partial h_3}{\partial \xi} - \frac{h_3}{h_1} \frac{\partial h_1}{\partial \xi} \frac{\partial h_1}{\partial \xi} \right\} T \\
 & - 2 \left\{ 2h_2 \frac{\partial h_1}{\partial \eta} \frac{\partial}{\partial \xi} - 2h_1 \frac{\partial h_2}{\partial \xi} \frac{\partial}{\partial \eta} + \frac{h_1 h_2}{h_3^2} \frac{\partial h_3}{\partial \xi} \frac{\partial h_3}{\partial \eta} \right. \\
 & \quad + h_2 \frac{\partial^2 h_1}{\partial \xi \partial \eta} - h_1 \frac{\partial^2 h_2}{\partial \xi \partial \eta} + \frac{h_1}{h_3} \frac{\partial h_2}{\partial \xi} \frac{\partial h_3}{\partial \eta} - \frac{h_2}{h_3} \frac{\partial h_1}{\partial \eta} \frac{\partial h_3}{\partial \xi} \\
 & \quad \left. + \frac{h_1}{h_2} \frac{\partial h_2}{\partial \xi} \frac{\partial h_2}{\partial \eta} - \frac{h_2}{h_1} \frac{\partial h_1}{\partial \xi} \frac{\partial h_1}{\partial \eta} \right\} U = 0. \quad \dots (4)
 \end{aligned}$$

To form the first relation of the second triad, we add to the expression for $\rho \ddot{a}$ the fourth of the six equations of identity, and find

$$\begin{aligned}
 & \nabla^2 S \\
 & + \frac{2m}{3m-n} \left\{ h_2 h_3 \frac{\partial^2}{\partial \eta \partial \xi} + h_3 \frac{\partial h_2}{\partial \xi} \frac{\partial}{\partial \eta} + h_2 \frac{\partial h_3}{\partial \eta} \frac{\partial}{\partial \xi} \right\} (P+Q+R) \\
 & \quad + \frac{h_2 h_3}{h_1^2} \frac{\partial h_1}{\partial \eta} \frac{\partial h_1}{\partial \xi} (2P-Q-R)
 \end{aligned}$$

$$\begin{aligned}
 & + \left\{ 2h_3 \frac{\partial h_2}{\partial \xi} \frac{\partial}{\partial \eta} - 2h_2 \frac{\partial h_3}{\partial \eta} \frac{\partial}{\partial \xi} + h_3 \frac{\partial^2 h_2}{\partial \eta \partial \xi} - h_2 \frac{\partial^2 h_3}{\partial \eta \partial \xi} \right. \\
 & \quad + \frac{h_2}{h_3} \frac{\partial h_3}{\partial \eta} \frac{\partial h_3}{\partial \xi} - \frac{h_3}{h_2} \frac{\partial h_2}{\partial \eta} \frac{\partial h_2}{\partial \xi} \\
 & \quad \left. + \frac{h_2}{h_1} \frac{\partial h_1}{\partial \xi} \frac{\partial h_3}{\partial \eta} - \frac{h_3}{h_1} \frac{\partial h_1}{\partial \eta} \frac{\partial h_2}{\partial \xi} \right\} (Q - R) \\
 & + \left\{ \pm \left\{ \frac{h_2^2}{h_3^2} \left(\frac{\partial h_3}{\partial \eta} \right)^2 + \frac{h_3^2}{h_2^2} \left(\frac{\partial h_2}{\partial \xi} \right)^2 \right\} \right. \\
 & \quad \left. - \left\{ \frac{h_1^2}{h_2^2} \left(\frac{\partial h_2}{\partial \xi} \right)^2 + \frac{h_2^2}{h_1^2} \left(\frac{\partial h_1}{\partial \eta} \right)^2 + \frac{h_1^2}{h_3^2} \left(\frac{\partial h_3}{\partial \xi} \right)^2 + \frac{h_3^2}{h_1^2} \left(\frac{\partial h_1}{\partial \eta} \right)^2 \right\} \right\} S \\
 & + \left\{ 2h_2 \frac{\partial h_1}{\partial \eta} \frac{\partial}{\partial \xi} - 2h_1 \frac{\partial h_2}{\partial \xi} \frac{\partial}{\partial \eta} - 3 \frac{h_1 h_2}{h_3^3} \frac{\partial h_3}{\partial \xi} \frac{\partial h_3}{\partial \eta} \right. \\
 & \quad + h_2 \frac{\partial^2 h_1}{\partial \xi \partial \eta} - h_1 \frac{\partial^2 h_2}{\partial \xi \partial \eta} + \frac{h_1}{h_3} \frac{\partial h_2}{\partial \xi} \frac{\partial h_3}{\partial \eta} - \frac{h_2}{h_3} \frac{\partial h_1}{\partial \eta} \frac{\partial h_3}{\partial \xi} \\
 & \quad \left. + \frac{h_1}{h_2} \frac{\partial h_2}{\partial \xi} \frac{\partial h_2}{\partial \eta} - \frac{h_2}{h_1} \frac{\partial h_1}{\partial \xi} \frac{\partial h_1}{\partial \eta} \right\} T \\
 & + \left\{ 2h_3 \frac{\partial h_1}{\partial \xi} \frac{\partial}{\partial \xi} - 2h_1 \frac{\partial h_3}{\partial \xi} \frac{\partial}{\partial \xi} - 3 \frac{h_1 h_3}{h_2^2} \frac{\partial h_2}{\partial \xi} \frac{\partial h_2}{\partial \xi} \right. \\
 & \quad + h_3 \frac{\partial^2 h_1}{\partial \xi \partial \xi} - h_1 \frac{\partial^2 h_3}{\partial \xi \partial \xi} + \frac{h_1}{h_2} \frac{\partial h_2}{\partial \xi} \frac{\partial h_3}{\partial \xi} - \frac{h_3}{h_2} \frac{\partial h_1}{\partial \xi} \frac{\partial h_2}{\partial \xi} \\
 & \quad \left. + \frac{h_1}{h_3} \frac{\partial h_3}{\partial \xi} \frac{\partial h_3}{\partial \xi} - \frac{h_3}{h_1} \frac{\partial h_1}{\partial \xi} \frac{\partial h_1}{\partial \xi} \right\} U = 0.
 \end{aligned}$$

LIII. The Crystalline Structures of Silver Iodide.

By R. B. WILSEY*.

IN a previous communication† giving the results of X-ray analyses of the crystal structures of the silver halides, the writer reported that silver iodide gave the diffraction pattern (powdered crystal) of the diamond cubic or "zinc-sulphide type" of structure. As stated then, crystals showing evidence of the hexagonal structure had not

* Communication No. 184 from the Research Laboratory of the Eastman Kodak Company.

† R. B. Wilsey, *Phil. Mag.* xlii. p. 262 (1921).

been studied by the X-ray method. Refinements giving greater precision have been introduced in the experimental procedure, and the lattice constants of the silver halides have been re-measured; this time the hexagonal modification of silver iodide was included.

In examining the silver halides by the powder method, Davey * also found the diamond type cubic structure for silver iodide. The diamond cubic structure of silver iodide has recently been questioned by Aminoff †, who states that within the usual experimental error the same lines of the powdered crystal diffraction pattern are given by either the hexagonal or diamond type cubic arrangement, and that the decision between these two structures must be made by other methods. With the aid of Laue diagrams and various crystallographic considerations, Aminoff concludes that the hexagonal structure is the correct structure for silver iodide, and reports the values $a=4.59 \text{ \AA}$, $c=7.73 \text{ \AA}$ for the edge and vertical axis respectively of the elementary hexagonal prism; these figures give the value 1.64 for the axial ratio.

In his "Survey of Existing Crystal Structure Data," Wyckoff ‡ accepts Aminoff's conclusion, stating that incomplete observations of his own "had confirmed the truly hexagonal character of the salt." He points to the deduction of the cubic structure for silver iodide as "a very clear example of the dangers of trying to deduce crystal structures with unaided powder data," and he includes this case in his list of "well established examples" of "known failures to assign correct crystal structures" §.

There is much similarity between the two structures: in either one each atom of one kind is surrounded by four atoms of the other kind at the corners of a tetrahedron; and the atoms of each kind, taken alone, have a close-packed arrangement—in one case that of cubic close packing, and in the other that of hexagonal close packing. Either structure may be derived from the other by parallel shifts in the (111) planes of the cubic structure, or (0001) planes of the hexagonal structure.

A calculation of all the lines of a powdered crystal diffraction pattern to be expected from each structure shows

* W. P. Davey, *Phys. Rev.* xix. p. 248 (1922).

† G. Aminoff, *Geol. För. Förh.* xlv. p. 444 (1922); abstracted in *Physik. Ber.* p. 827 (1922).

‡ R. W. G. Wyckoff, *J. Frank. Inst.* cxcv. p. 349 (1923).

§ R. W. G. Wyckoff, *J. Frank. Inst.* cxcv. p. 531 (1923).

that while the two structures have many lines in common, each has lines not possessed by the other, the hexagonal structure having much the greater number of lines characteristic of its own arrangement. Therefore the powdered crystal method should be able to distinguish between the two structures, provided satisfactory photographs can be obtained.

In the present experiments the samples of silver iodide were prepared from silver nitrate and potassium iodide, both of "reagent purity"; the possible impurities in the samples were small compared with the quantity of foreign substance required to show any effect upon the photograph.

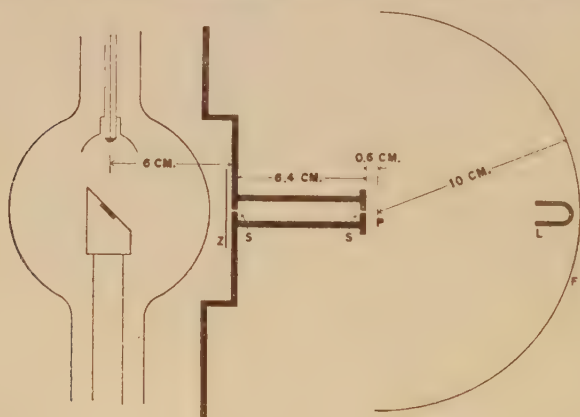
Considerable variation was found in the powder photographs of various samples of silver iodide, all of which were fully exposed under the same conditions. A few samples, including the one originally reported, showed only the lines of the diamond cubic structure, which includes two lines which cannot be accounted for by the hexagonal structure. The other samples varied from those showing one or two faint lines characteristic of the hexagonal structure to samples giving as many as ten such lines in addition to the seven lines common to both structures. All the photographs showing predominantly hexagonal structures contained one line which was most accurately accounted for by the cubic structure, differing from the nearest theoretical hexagonal line by an amount greater than experimental error. The conclusion is that both crystal forms exist, most of the samples showing a mixture of the two in which the hexagonal form predominates. The discrepancies in the results reported by different observers appear to be due to differences in the samples examined rather than in the methods of analysis used.

The accompanying diagram illustrates the experimental arrangement, and gives the essential dimensions of the apparatus. The Coolidge tube with molybdenum target was operated at 30 kv. (effective), and the $K\alpha$ line was isolated with the aid of the zirconium oxide filter Z. The slits S were each 0.4 millimetre wide. A U-shaped piece of lead, L, protected the film from the primary X-ray beam during most of the exposure, and thereby avoided the fogging action of the secondary radiation which would be produced where the primary beam meets the film and cassette. The crystal powder was made into a thin paste with a cellulose varnish and coated upon a thin ribbon of celluloid; when

dry the powdered layer was approximately 0.2 millimetre thick and 2 millimetres wide. The sample was centered in the axis of the spectrometer with the aid of a telescope and crosshair. An exposure of 120 to 150 milliamperere hours was usually sufficient to give a well-exposed film.

The error due to shrinkage of the film during the development process was avoided in the following way:—

Equally spaced notches were cut in the semicircular cassette at approximately 10 degrees apart, and during the exposure these notches were printed on the film by the general scattered radiation. The distances apart of the lines of the diffraction pattern were referred to the spacing of the images of the notches. The final calibration of the spacing of the notches was carried out by a series of powder



photographs of sodium chloride, so that the lattice constants here reported are based on the accepted value of 2.814×10^{-8} cm. for the spacing of the (100) planes of sodium chloride. As a rule the lattice constant determined from a single film did not differ by more than $1/8$ per cent. from the mean value of several films; hence the ratio of any lattice constant to that of sodium chloride should be correct to within $1/4$ per cent.

Duane's* values for the wave-length of the $K\alpha$ doublet of molybdenum are 0.70783×10^{-8} cm. and 0.71212×10^{-8} cm. for α_1 and α_2 respectively, α_1 having double the intensity of α_2 . The weighted mean value 0.7093×10^{-8} cm. was taken as the wave-length of the $K\alpha$ radiation in the present experiments.

* W. Duane, Bull. Nat. Res. Council, vol. i. No. 6, p. 383 (1920).

The angular deviation of each line was determined from the distance apart of its two reflexions on either side of the primary beam, and this value was checked by a measurement of the distances of the lines from the undeviated image of the slit.

A set of data showing the cubic form (zinc-sulphide arrangement) of silver iodide is given in Table I. The first five columns refer to the theoretically computed lines for this structure, and the last four columns refer to the observed data.

TABLE I.

Indices of Form.	No. of Co-operating Planes N.	Phase Factor F.	$N \times F$.	Relative Spacing of Planes, Theoretical d/a .	Observed Angular Deviation 2θ .	Observed Spacing of Planes d in Ångströms.	Side of Elementary Cube in Ångströms.	Estimated Intensity of Line.
111	4	0.5	2	.5774	10 51'	3.749	6.493	10
220	6	1.0	6	.3536	{ *15 49 17 48	2.294	6.487	1
						2.292	6.480	8
311	12	0.5	6	.3014	20 53	1.957	6.493	7
400	3	1.0	3	.2500	25 15	1.623	6.492	1
331	12	0.5	6	.2294	27 35	1.488	6.486	3
422	12	1.0	12	.2041	31 5	1.324	6.485	3
511	12	0.5	6 } 8	.1924	33 1	1.248	6.485	2
333	4	0.5						
440	6	1.0	6	.1768	36 1	1.147	6.490	1
531	24	0.5	12	.1690	37 43	1.097	6.492	1.5
Mean ...							6.488	

* Reflexion of β line, $\lambda = 0.6311 \times 10^{-8}$ cm.

The phase factor, F , of each set of planes, given in column 3, is defined by Hull† as the “ratio of the square of the sum of the amplitudes of reflexion from all the planes added as vectors to the square of their algebraic sum.” In computing phase factors, the amplitude of reflexion was taken proportional to atomic number. In the cases where reflexions from planes of silver atoms differ in phase by 180° from reflexions from planes of iodine atoms, the phase factor is negligible and is not recorded: no lines corresponding to such reflexions were found. The product $N \times F$ gives the relative intensity to be expected of neighbouring lines, provided allowance is made for the decrease of scattering

† A. W. Hull, Phys. Rev. xvii. p. 571 (1921).

power with increasing angle of deviation. Since this function is not known for silver iodide, only a rough correspondence is to be expected between the values of $N \times F$ and the estimated intensities of the lines.

Column 5 gives the theoretical ratio of d (the spacing of the planes) to a (the side of the elementary cube). The observed spacing of the planes is computed from the observed angular deviation by the Bragg relation $n\lambda = 2d \sin \theta$. The value of the side of the elementary cube is computed for each reflexion by dividing the observed spacing by the theoretical value of $\frac{d}{a}$. The substantial agreement of the various cube side values shows how closely each reflexion fits the assumed structure.

Within the range of angles where lines are observable, all the lines required for the diamond cubic structure and none others are present. Two of the lines, the (400) and the (331) reflexions, cannot be accounted for by the hexagonal structure; the (400) line is not near any line of the hexagonal pattern; the theoretical (331) spacing differs from the nearest hexagonal spacing (21 $\bar{3}$ 0) by 0.9 per cent. In the above table the observed (331) line gives a cube side value differing by less than 0.1 per cent. from the mean, thus showing its preference for the cubic lattice. In six powder photographs of various samples of cubic silver iodide, the maximum observed deviation of the (331) cube side value from the mean for the given film was 1/4 per cent., and the average deviation 1/8 per cent. The average cube side for the six exposures was 6.493×10^{-8} cm. Two of these films showed no other lines than those of the diamond cubic structure; the other four each had one faint line (10 $\bar{1}$ 0) belonging only to the hexagonal structure, showing that these samples contained a small proportion of the hexagonal form.

Most of the samples of silver iodide examined showed predominantly the hexagonal structure. Table II. gives a representative set of data obtained from such a sample. If the tetrahedra of the hexagonal structure are equilateral, as are those of the cubic structure, the axial ratio should be 1.633, that of the hexagonal close packing of equal spheres; this value is assumed in the calculations. The positions of the atoms in this structure are:—

Silver	$\begin{cases} m \\ m + 1/3 \end{cases}$	$\begin{cases} n \\ n + 2/3 \end{cases}$	$\begin{cases} pc, \\ (p + 1/2)c, \end{cases}$
Iodine	$\begin{cases} m + 1/3 \\ m \end{cases}$	$\begin{cases} n + 2/3 \\ n \end{cases}$	$\begin{cases} (p + 1/8)c, \\ (p + 5/8)c, \end{cases}$

where m , n , and p have all possible integral values.

This pattern shows one line which fits the cubic (331) spacing much more closely than it does the nearest hexagonal spacing (21 $\bar{3}$ 0) indicating the presence of the cubic crystal form. The data on this line will be considered more fully in a later paragraph.

TABLE II.

Indices of Form.	No. of Co-operating Planes N.	Phase Factor N X F.	Relative Spacing of Planes, Theoretical d/a .	Observed Angular Deviation 2θ .	Observed Spacing of Planes d in Ångströms.	Side of Elementary Hexagon in Ångströms.	Estimated Intensity of Line.	
10 $\bar{1}$ 0	3	.25	.75	.8662	10 12	3.991	4.607	7
0002	1	.50	.50	.8165	10 53	3.742	4.583	7
10 $\bar{1}$ 1	6	.112	.67	.7651	11 35	3.512	4.591	3
10 $\bar{1}$ 2	6	.126	.76	.5941	14 54	2.736	4.606	2
1120	3	1.00	3.00	.5000	{ 15 50 17 46	2.291 2.296	4.582 4.592	1 10
10 $\bar{1}$ 3	6	.184	1.10	.4608	19 18	2.115	4.590	6
20 $\bar{2}$ 0	3	.25	.75	.4331				
11 $\bar{2}$ 2	6	.50	3.00	.4264	20 49	1.963	4.604	8
20 $\bar{2}$ 1	6	.112	.67	.4185				
20 $\bar{2}$ 2	6	.141	.85	.3826				
20 $\bar{2}$ 3	6	.641	3.85	.3389	26 19	1.558	4.598	2
21 $\bar{3}$ 0	6	.250	1.50	.3272				
331	12	(cubic)	27 31	1.492	...	1
21 $\bar{3}$ 1	12	.026	.31	.3209				
10 $\bar{1}$ 5	6	.641	3.85	.3056	29 13	1.406	4.602	1
21 $\bar{3}$ 2	12	.126	1.51	.3038				
30 $\bar{3}$ 0	3	1.00	3.00	.2887	31 4	1.324	4.587	1
21 $\bar{3}$ 3	12	.64	7.68	.2805	31 59	1.287	4.590	1
30 $\bar{3}$ 2	6	1.00	6.00	.2722	33 00	1.248	4.586	1
0003	1	.50	.50	.2722				
20 $\bar{2}$ 5	6	.64	3.84	.2607	34 33	1.195	4.582	0.7
10 $\bar{1}$ 6	6	.125	.75	.2596				
2240	3	1.00	3.00	.2500	36 00	1.148	4.591	0.4
3140	6	.25	1.50	.2402				
1126	6	.50	3.0	.2390	37 42	1.097	4.591	1
3141	12	.113	1.37	.2376				
20 $\bar{2}$ 6	6	.126	.76	.2304	39 4	1.061	4.603	0.5
3142	12	.126	1.51	.2304				
Mean ...							4.593	

* = Reflexion of β line.

The mean value of the side of the hexagonal prism, taken from nine exposures on various samples, was 4.593×10^{-8} cm.

The data do not afford a very precise direct determination of the axial ratio. The only line giving an independent measurement of the height of the elementary hexagonal prism is the second-order reflexion from the (0001) plane; the small angular deviation of this line gives a relatively low precision in the value of the planer spacing. Independent measurements of the side of the hexagon are given by four reflexions ($10\bar{1}0$), ($11\bar{2}0$), ($20\bar{2}0$) and $22\bar{4}0$). The mean value of the axial ratio, as determined from these reflexions in the nine exposures, was $1.633 \pm .008$.

Table III. gives the complete data on the line designated as (331) in Table II., showing how this fits the two nearest hexagonal spacings as compared with the cubic (331) spacing. The cubic (331) spacing lies nearly midway between the hexagonal ($21\bar{1}0$) and ($21\bar{3}1$) spacings; the reflexion from the ($21\bar{3}1$) plane would hardly be expected to appear on account of its low value of the product $N \times F$. In Table III. the edge of the elementary tetrahedron is computed from the position of the observed line, assuming it to be reflected from each of the three planes in turn, and these values are compared with the mean value of the tetrahedral edge for the given film. In every case the observed line fits the (331) spacing much more closely than either of the nearest hexagonal spacings.

The evidence appears quite conclusive that every sample of silver iodide studied contained the cubic form; in a few cases none but the cubic structure was evident; in some, one or two faint lines were present which belonged only to the hexagonal form; while in most of the samples the hexagonal form predominated. No systematic study was made of the conditions governing the production of one crystal form or the other; the first sample showing the cubic form was prepared by precipitation; the other cubic crystals were produced by fusion of the salt and quenching in cold water; as a rule, the predominantly hexagonal form was produced by every method tried, whether precipitation or the quenching or slow cooling of a fused sample.

The lattice constants of silver chloride and silver bromide were also re-determined. Silver chloride gave the lines of a face-centered cubic structure in which the reflexions from planes of all odd indices were of lower intensity than would be expected from such a structure composed of like atoms; this effect would be expected in a structure of the sodium chloride type where the two kinds of atoms differ considerably

in atomic number. The mean value of $d(100)$ from four exposures was 2.770×10^{-8} cm.

TABLE III.

Film No.	Observed Angular Deviation 2 θ .	Observed Spacing of Planes in Angstroms.	Mean Tetrahedral Edge or Hexagonal Side for each Film.	Tetrahedral Edge computed from observed line.	Differences.	Assumed Planes Indices of Form.
1	27° 36' 4"	1.486	4.587	4.542	-.045	21 $\bar{3}$ 0
				4.582	-.005	331
				4.632	+.045	21 $\bar{3}$ 1
2	27° 33' 6"	1.489	4.588	4.550	-.038	21 $\bar{3}$ 0
				4.589	+.001	331
				4.639	+.051	21 $\bar{3}$ 1
3	27° 36'	1.487	4.595	4.543	-.052	21 $\bar{3}$ 0
				4.583	-.012	331
				4.633	+.038	21 $\bar{3}$ 1
4	27° 29' 2"	1.493	4.597	4.562	-.035	21 $\bar{3}$ 0
				4.601	+.004	331
				4.651	+.054	21 $\bar{3}$ 1
5	27° 27' 2"	1.495	4.597	4.567	-.030	21 $\bar{3}$ 0
				4.607	+.010	331
				4.657	+.060	21 $\bar{3}$ 1
6	27° 28' 4"	1.494	4.593	4.524	-.069	21 $\bar{3}$ 0
				4.603	+.010	331
				4.654	+.061	21 $\bar{3}$ 1
7	27° 31' 4"	1.491	4.591	4.556	-.035	21 $\bar{3}$ 0
				4.595	+.004	331
				4.645	+.054	21 $\bar{3}$ 1
8	27° 30' 6"	1.492	4.593	4.558	-.035	21 $\bar{3}$ 0
				4.597	+.004	331
				4.648	+.055	21 $\bar{3}$ 1
9	27° 28' 2"	1.494	4.595	4.564	-.031	21 $\bar{3}$ 0
				4.604	+.009	331
				4.654	+.059	21 $\bar{3}$ 1
Mean ...			4.593			

Silver bromide gave the diffraction pattern of a simple cubic lattice. This pattern is accounted for by the sodium chloride type of structure where the two kinds of atoms are of sufficiently similar atomic numbers as to act as

similar diffracting centres. The mean value of d (100) from four films was 2.884×10^{-8} cm.

The deduction of the sodium chloride structure for both silver chloride and silver bromide follows simply from the published methods of analysis of powdered crystal diffraction patterns. The possibility that either of these simple compounds has any other structure seems so remote that it is considered superfluous to publish the data in detail.

Several samples of metallic silver of known high purity were also examined by the powder method; this substance gave photographs having unusually well-defined lines. The pattern was that of a face-centred cubic structure, as has been reported by other investigators*; the mean value of the side of the elementary cube from six exposures was 4.078×10^{-8} cm. Very good diffraction photographs were also obtained from the blackened silver of a developed photographic film.

The lattice constants of the structures studied are summarized in Table IV.

TABLE IV.			
Crystal.	Lattice Structure.	Side of Elementary Unit of Structure in Ångströms.	Distance apart of nearest Atomic Centres in Ångströms.
Silver chloride	Simple cubic, NaCl type.	5.540	2.770
Silver bromide	Simple cubic, NaCl type.	5.768	2.884
Silver iodide	Diamond cubic ZnS type.	6.493	2.812
Silver iodide	Hexagonal, ZnO type.	4.593 ($c/a=1.633$)	2.813
Metallic silver	Face-centred cubic.	4.078	2.884

In conclusion, it may be pointed out that while the X-ray powder method of crystal analysis has its limitations, as have other methods, it has also its advantages. The great majority of crystalline substances do not ordinarily occur in large crystals, and the powder method is the only method applicable to crystals as they exist in a finely divided state. The convenience with which it may be used to examine a large number of samples prepared in various ways has made it possible in the present case to obtain more complete information about the crystalline characteristics of silver iodide than has been obtained by other methods depending upon single large crystals.

Rochester, N.Y.,
May 8, 1923.

* L. Vegard, *Phil. Mag.*, xxxi. p. 83 (1916). L. W. McKeehan, *Phys. Rev.* xx. p. 424 (1922).

LIV. *Studies in the Electron Theory of Chemistry. On the changes in chemical properties produced by the substitution of one element or radicle by another, with applications to benzene substitutions.* By Sir J. J. THOMSON, O.M., F.R.S., Master of Trinity College, Cambridge*.

WHEN a monovalent atom or radicle—such as F, Cl, Br, I, OH, CH_3 , CN—is substituted for an atom of hydrogen the number of electrons is increased; these additional electrons, together with the corresponding positive charges, will change the electric field in and around the molecule. It is the object of this paper to investigate the nature of this change and the effect it might be expected to have on the chemical properties of the molecule.

I will begin with a case which I have already discussed to some extent in my lectures on “The Electron in Chemistry,” given at the Franklin Institute, Philadelphia (Journal of the Franklin Institute, June 1923), that of the replacement of hydrogen by halogens. As the halogen atom has seven electrons in the outer layer, while the hydrogen atom has only one, there will be six more disposal electrons after the halogen atom has been introduced, the negative charges on these will be balanced by the excess of six units of positive charge which the positive core of the halogen atom has over that of the hydrogen one.

The dispositions of the electrons before and after the substitution are represented in figs. 1 *a*, *b*. H, fig. 1 *a*, is the

Fig. 1 *b*.*b*Fig. 1 *a*.

H.

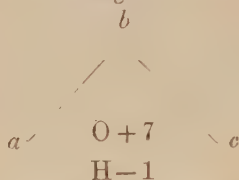
d.

positive core of the hydrogen atom, *d* the projection on the plane of the paper of the line joining the two electrons which bind it to the rest of the molecule. Cl, fig. 1 *b*, is the positive core of the chlorine atom, *a*, *b*, *c*, *d* the projections of the sides

* Communicated by the Author.

of the octet which surround this core, each side corresponds to two electrons. The difference in the electric field produced by substitution will be that due to the system represented in fig. 2, where again a, b, c represent the projections of three

Fig. 2.



sides of the octet, each side corresponding to two electrons, O represents the positive nucleus of the halogen atom with a charge 7; the negative charge -1 at H, where H is the position of the nucleus of the hydrogen atom which has been displaced, represents the effect of removing the positive part of the hydrogen atom. The four electrons at a and c together with the positive charge $+7$ at O are approximately equivalent to a charge $+3$ at O, and the whole system is equivalent to charges -1 at H, $+3$ at O and -2 at b . The -2 at b together with a charge $+2$ at O are equivalent to an electrostatic doublet whose moment is $2e \times Ob$, where e is the charge on an electron; the -1 at H and the $+1$ which is left over from O are equivalent to a doublet whose moment is $e \times OH$, the axis of this doublet is in the opposite direction to that of the previous one, the moment of the resultant doublet is equal to

$$e(2Ob - OH);$$

now

$$OH = Od - Hd = Ob - Hd,$$

hence the moment of the resultant doublet is equal to

$$e(Ob + Hd)$$

$$= es,$$

where s is the sum of the radii of the hydrogen and halogen atoms. The orientation of this doublet is the same as that of one with negative electricity on the halogen atom and positive on the one with which it is combined. Thus, for example, if we replace one of the hydrogen atoms in marsh gas by chlorine the molecule of CH_3Cl would have an electrostatic moment whose sign would be the same as that of an electric doublet with positive electricity on the carbon atom and negative on the chlorine one. The magnitude of the moment would be e times the sum of the radii of the

hydrogen and chlorine atoms, *i. e.*, it would not differ much from the electric moment of a molecule of HCl.

Let us now take the case of the replacement of H by OH. The fact that the water molecule has a considerable electrostatic moment shows that it cannot be represented by a symmetrical arrangement such as a cubical octet of electrons surrounding the positive core of an oxygen atom with the positive cores of two hydrogen atoms symmetrically placed outside. If one of the hydrogen atoms were to go inside the octet of electrons the water molecule could have a finite moment. We shall suppose, therefore, that the radicle OH consists of seven electrons arranged round the positive cores of atoms of hydrogen and oxygen. The problem is now practically the same as that of the chlorine atom and we see that the effect of replacement of H by OH will introduce a moment whose sign is the same as that of an electric doublet with negative electricity on (OH) and positive on the atom with which it is combined: the magnitude of the moment is es , where s is the sum of the radii of an atom of hydrogen and of a negatively charged OH radicle. This is also the moment of a water molecule approximately. Hence we see that the effect of replacing H by OH is to introduce into the molecule an electrostatic moment equal to that of a water molecule. Thus if we replace one of the hydrogens in CH_4 by OH, producing a molecule of methyl alcohol, the electrostatic moment of a molecule of methyl alcohol ought to be much the same as that of a molecule of water. Now the presence of electrostatic moments gives rise to abnormally large specific inductive capacities, and substances such as water and methyl alcohol, which have very large specific inductive capacities, owe them to the presence of electrostatic moment in their molecules, and the measure of the capacity is a measure of the moment. We have been led to the result that the moment of a molecule of water ought not to differ much from that of one of alcohol. Hence, if this result is true, the specific inductive capacities of water and methyl alcohol *estimated for the same number of molecules* ought not to be very different. This is in agreement with the results of experiments, for the specific inductive capacities in the liquid state of water H_2O , methyl alcohol CH_3OH , ethyl alcohol $\text{C}_2\text{H}_5\text{O}$, propyl alcohol $\text{CH}_3\text{CH}_2\text{CH}_2\text{OH}$ are in the proportion of 80:79:84:85. The specific inductive capacities are estimated for the same number of molecules. The value of the specific inductive capacity shows a tendency to rise as the complexity of the molecule increases, this is what we should expect as the intense electric field due to the

moment will give rise by induction on the rest of the molecule to moments of the same sign as the original moment, and thus the value of the moment of the whole molecule will be greater than that introduced by the substituent.

If we apply the same considerations to the substitutions of NH_2 for H, we find that it introduces a moment whose negative end is towards the NH_2 and positive end towards the atom with which it is combined and whose magnitude is es , where s is the sum of the radii of an atom of hydrogen and a negatively charged radicle NH_2 .

Another way of treating the problem is to notice that the electrical effect produced by a number of movable electrical charges when acted upon by an electric field is much the same as that of a conductor of electricity such as a metallic sphere filling the volume through which the charges are distributed. When such a collection of charges is acted upon by an electric field the charges will be displaced so that the force called into play by this displacement on any one of the charges is just sufficient to balance the force on that charge due to the external electric field. If we expose a metallic sphere to this field there will be a displacement of the electricity on the sphere, the negative moving in the opposite direction to the electric force, the positive in the same direction; the tangential force due to this displacement balances at any charge on the surface of the sphere the tangential force on the same charge due to the external electric field. Thus the effect of the displacement of a number of mobile charged bodies is much the same as that of the displacement of the electrification on a metallic sphere. An illustration of this is afforded by the Electron Theory of Specific Inductive Capacity, which shows that the electrostatic moment of a group of a considerable number of electrons with the corresponding positive charge is proportional to that which would be induced in a metallic sphere occupying the volume through which the charges are distributed.

Thus we may take as an approximation to the electrical effect produced by an atom or radicle with no intrinsic moment that which would be produced by a conducting sphere of the same radius; for the analogy to hold the radicle or atom must be able to receive a negative charge, so that the octet of electrons must not be complete.

We shall illustrate the use of this method by applying it to the case of the replacement of hydrogen by chlorine. Let us suppose that P is the electron in the parent substance which links it to the chlorine atom in one case and to the hydrogen atom in the other. What will be the effect of

bringing an uncharged metal sphere up to P? The sphere will receive the charge on the electron and become negatively charged. The electrical effect of this negatively charged sphere would to a first approximation be the same as if the negative charge were placed at C, the centre of the sphere. Thus the electrical effect of the introduction of the sphere is to move the electron from P to C. This is equivalent to leaving the electron where it was and introducing an electric doublet whose moment is $e \times PC$ and whose positive end is towards P and negative one towards C. Since the chlorine atom has only seven electrons in the outer layer it can receive another electron and will produce an effect similar to that of the sphere.

Now consider the effect of introducing an atom of hydrogen instead of one of chlorine. The hydrogen atom has an electrostatic moment of its own equal to er , where r is the radius of the atom, and it carries this or, at any rate, a large component of it into combination. The positive part of this electrostatic doublet is away from P while the negative end is towards it: thus the moment is of the opposite sign to that due to the introduction of the chlorine atom. Hence the change produced by the substitution of the chlorine atom for a hydrogen one is equivalent to the introduction of an electrostatic moment equal to $e(PC+r)$, i. e., e (sum of the radii of the chlorine and hydrogen atoms), the positive end of this moment is next the atom with which the chlorine combines, the negative end towards the chlorine; this is the same result as we got by the use of the other method.

We see from this result that whenever we introduce an atom or radicle which has no intrinsic moment and which can receive an additional electron, i. e., one which contains an uncompleted octet, the effect will be represented by an electrostatic doublet whose negative end is on the side of the radicle and the positive end on the side of the molecule with which the radicle combines.

Examples of atoms and radicles of this type are—



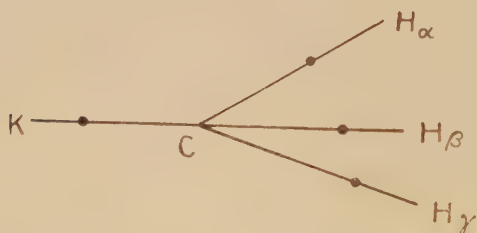
Each of these has seven disposable electrons.

The radicle CH_3 requires special consideration, for in some cases the substitution of this for hydrogen seems to produce a change in the moment, in other cases it does not. Thus in H.OH , $\text{CH}_3.\text{OH}$, $\text{CH}_2\text{CH}_2\text{OH}$, each molecule may be derived from the preceding by substituting CH_3 for H .

The specific inductive capacities per molecule of these substances are practically the same, so that the substitution of CH_3 for H has produced at most a very small change in the moment. On the other hand, when H in formic acid is replaced by CH_3 , as in acetic acid, a very large diminution in the specific inductive capacity is produced. Again, when one of the hydrogens in benzene is, as in toluene, replaced by CH_3 , the change in moment must be small as the specific inductive capacity of toluene is normal.

When an atom of hydrogen in a molecule of hydrogen with no moment is replaced by CH_3 a molecule of CH_4 , which has also no moment, is produced. Thus when CH_3 replaces an atom of hydrogen H_1 no moment is produced when H_1 is in combination with another atom of hydrogen. It might, however, happen that if H_1 was combined with something different from hydrogen a finite moment would be produced. For when H_1 is combined with K the configuration after the replacement of H is represented in fig. 3,

Fig. 3.



where K is the atom which was in combination with H, before the replacement, H_α , H_β , H_γ , the hydrogen atoms in CH_3 . The electrical moment will depend on the angles CH_α , CH_β , CH_γ make with each other; if these lines close up and get more nearly in a straight line, the moment due to this part of the system, which has the positive side towards C and the negative towards H_α , H_β , H_γ , will increase. The positions of CH_α , CH_β , CH_γ will depend upon the positive charge at K. The system CH_α consists of a positive ion and two electrons attached to C. The positive charge at K will make CH_α move as if it attracted it; if K is moved further away the lines CH_α , CH_β , CH_γ will make smaller angles with each other and the system will have a moment with the positive end towards C and the negative end to the right. If K were a more complex system than a hydrogen atom, say a hydrocarbon with a positive charge, the equivalent of

this positive charge might be further from the octet of electrons round C than it would if K were hydrogen, because the distance of hydrogen from the octet is equal to the distance of the electron in a hydrogen atom from the core, which is about the minimum distance of a positive charge from an electron; thus the replacement of H by CH₃ may introduce a moment, whose magnitude will depend upon the system with which CH₃ is in combination.

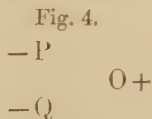
It must be remembered, too, that the measurement of the specific inductive capacity only gives us the resultant moment; which represents the action of the system at large distances, within the molecule itself large forces might be produced by distributions of electricity which have no finite moment.

$$\begin{array}{cccc} & B & C & D \\ & + & -2 & + \\ A & \frac{1}{1} & \text{---} & \frac{1}{1} \end{array}$$

Thus, for example, if there are positive unit charges at B and D and a negative charge -2 at C, the point midway between B and D, these constitute a system with no resultant moment, yet its effect at a point A, whose distance from B is comparable with BC, will be a considerable fraction of that due to a charge 1 at B and -1 at C, a system which has a finite moment. Thus in considering the effect produced by substitution on the electric field in the immediate neighbourhood of the substituted atom, the most important electrical effects are those which take place quite close to the atom.

Thus let P be the electron in the parent substance which binds the hydrogen atom before substitution and the substituted atom or radicle afterwards, to the parent molecule. Let us consider how the field due to P is modified when (1) it binds an atom of hydrogen, (2) when it binds an atom of a substituent.

When an atom of hydrogen is bound, an electron Q of this atom comes nearer to P than the positive hydrogen ion O, forming a system like fig. 4; to the left of P the



force due to the electron Q will overbalance that due to the ion O, so that the effect of the hydrogen will be of the same sign as that which would in the absence of the hydrogen be produced by an increase in the negative charge at P.

Now suppose that instead of combining with hydrogen the molecule combines with a substituent for hydrogen. If among the atoms that make up the substituent there is one that has not got a complete octet, P may join up with this; this, as we have seen, from the analogy with the metal sphere, has much the same effect as removing P to the centre of this atom: thus a combination with a substituent of this kind will produce a change in the electrical field of the same sign as that which would be produced by a diminution of the electrical charge on P, or what is equivalent, by the introduction of an electrical doublet with its positive side towards the parent system. For places close to P this change will determine the nature of the change in the electrical forces, even though in other parts of the substituent there may be distributions of electrons and positive charges which introduce moments of opposite sign to these, and which may reverse the resultant moment, without reversing the sign of the effect near P. The case of C'H_3 is one in point; here we have 7 electrons round the carbon atom, forming a system of the kind we have contemplated, when P completes the octet, the effect is to introduce a doublet with its positive side towards the parent system; the hydrogen atoms in C'H_3 may be regarded as introducing a doublet of opposite sign, but this doublet is further away from P than the other and so cannot neutralize its effect at P, though it might do so further away.

In this case the removal of hydrogen and the introduction of the substituent both produce effects of the same sign and are equivalent to the introduction of an electric doublet with its positive part towards the molecule with which the hydrogen was combined. This result will be true for all substituents which contain an uncompleted octet such as Cl, OH, CH_3 , NH_2 .

There may be substituents, however, of another type, where, as in the hydrogen atom, we have a detached electron and some distance from it a unit positive charge.

When this substituent enters the parent molecule, it, like the hydrogen atom, produces an electric field whose sign is the same as that which would be produced by an increase in the negative charge on P. If this effect is greater than the corresponding one for hydrogen, then the result of substitution will be of the same sign as that due to the introduction of a doublet whose negative end is towards the parent molecule. If, on the other hand, the effect of the substituent is less than that of hydrogen, substitution will produce an effect of the same sign as that due to chlorine.

Substituents with a detached electron and a positive ion will have a finite electrical moment, the greater this moment the greater will be the distance of the positive ion from the two electrons which couple it with the molecule with which it combines. The positive ion produces an electric field of the same sign as that which would be due to a diminution in the electric charge on P; it diminishes the effect of the sign we are considering, the further it is away the less will be this diminution and therefore the greater the negative effect.

We shall consider some examples of this type of substituent. Let us take first NO_2 , which has 17 electrons, sufficient to make two complete octets and leave one electron over, as in fig. 5. This radicle, represented by $\text{O}=\text{N}=\text{O}$,

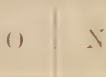


Fig. 5.



e

is a system of the type we are considering, with a positive NO_2 and a detached electron; the radicle in this form would be attached to the rest of the molecule by the nitrogen atom. If it were attached by the oxygen atom the constitution of the radicle would be represented by



$()$

where there is no detached electron but an incomplected octet round the atom of oxygen which is to be bound to the parent molecule. As this form contains an incomplete octet it will as a substituent produce the same type of electrical effect as OH , or Cl . This is the type of NO_2 which occurs in methyl nitrite, the other type is that found in nitromethane. The two types give electrical moments of opposite signs.

The most favourable arrangement of electrons for the production of electric effects of the second type, where the effect of substitution is of the same sign as that due to an increase in the negative charge on P, is evidently one where there is one electron over after saturating all the atoms. NO_2 is a case of this kind, COOH is another; here we have 17 electrons sufficient to give two complete octets and one over; CN has 9 electrons, these may be arranged in an octet surrounding the positive cores of both the carbon and nitrogen atoms, with an electron over. There are other arrangements of the electrons in the CN radicle which are not so favourable for the production of the second type of electrical effect. Thus the octet might only surround the nitrogen

Fig. 6.



atom as in fig. 6; with this arrangement the connexion would be made through the carbon atom. If the octet surrounded the carbon atom as in fig. 7, the connexion between

Fig. 7.



the radicle and the molecule with which it combines would be made through the nitrogen atom as in the isocyanides. In $\text{H}-\text{C}=\text{O}$ we have eleven electrons, eight of these may be used to form an octet round the oxygen, two to bind the hydrogen to the carbon, and one remains detached; so that we should expect this radicle to produce an effect of the second type.

Thus we have seen that the electrical effect of replacing an atom of hydrogen by another atom or radicle may be represented by the introduction of an electric doublet at the hydrogen atom. The sign of the doublet will depend upon the nature of the radicle.

- A. The *positive* end of the doublet will be toward the molecule with which the hydrogen is combined and the *negative* end away from it if the radicle is of Type I., which includes Cl , Br , I , OH , NH_2 , CH_3 .

All these radicles and atoms contain 7 electrons, which can thus form a system which wants but one electron to form a complete octet.

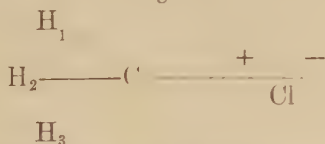
- B. The *negative* end of the doublet will be toward the molecule with which the hydrogen is combined and the positive away from it if the radicle is of Type II., which includes $\text{O}=\text{N}=\text{O}$, $\text{OH}-\text{C}=\text{O}$, $\text{H}-\text{C}=\text{O}$, CN .

In this type of radicle there is one electron over after providing for complete octets, thus there are 17 electrons in NO_2 and COOH which leaves one electron over after two octets have been completed.

Miss Hoffert, in a very interesting paper in the 'Journal of the Society of Chemical Industry,' has called attention to the fact that those radicles and atoms which when introduced into the benzene ring cause a second substitution to take place in the ortho or para positions, contain one electron less than is required to form complete octets, while those which give rise to substitution in the meta position contain one electron more than is required for complete octets.

We shall now try to interpret in terms of chemical properties the change of the electrical field due to substitution. To take an example, suppose one of the hydrogen atoms in CH_4 is replaced by an atom or radicle of Type I., say by chlorine. The difference in the electric fields of CH_4 and

Fig. 8.



CH_3Cl can be represented by an electric doublet at Cl whose positive end is toward C the centre of the carbon atom, and the negative end towards Cl (fig. 8). This doublet will produce an electric field which at H_1 , H_2 , H_3 , the positions of the three hydrogen atoms, tends to drive away positive electricity and to attract negative. If the molecule CH_3Cl were in an ionized medium, this field would make the negative ions congregate more intensely round H_1 , H_2 , H_3 , than they would have done if the fourth hydrogen atom had not been replaced by chlorine. Thus the field will concentrate the negative ions round the remaining hydrogen atoms and also repel

these atoms, and both effects will facilitate their replacement by other negative ions. Thus we see that where one carbon atom in a carbon compound has already been chlorinated it is more likely to be attacked still further by chlorine than a carbon atom none of whose hydrogen atoms have been replaced by chlorine. There are many illustrations of this effect. For example, when $\text{H}_3\text{C}-\text{CH}_2\text{Br}$ is brominated still further a considerable excess of $\text{H}_3\text{C}-\text{CHBr}_2$ over $\text{BrH}_2\text{C}-\text{CH}_2\text{Br}$ is produced; *i. e.*, the carbon atom which has already been brominated is brominated again in preference to the one not already attacked.

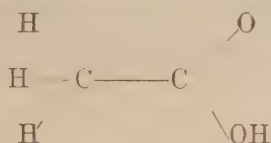
Again, it is a general rule in Organic Chemistry that "where an organic compound is submitted to oxidation the molecule is attacked at the part which already contains oxygen, that is, where oxidation has already begun" (Holleman's 'Organic Chemistry'). Since OH and O belong to type I, we see that the explanation we gave for the effect of chlorination applies also to this law.

Another illustration is that of vinyl chloride $\text{H}_3\text{C}-\text{CH}_2\text{Cl}$, this when exposed to chlorine in the light gives $\text{H}_3\text{C}-\text{CHCl}_2$.

Again, CH_3 is a radicle of type I, *i. e.*, its substitution for hydrogen produces an electric field which tends to attract negative ions; thus in propylene $\text{H}_3\text{C}.\text{CH}:\text{CH}_2$, which we may regard as derived from ethylene by substituting CH_3 for one of the hydrogens attached to C_1 , the CH_3 will make the central carbon more likely to attract halogen ions than C_2 where no substitution has taken place, consequently, when propylene is acted upon by hydriodic acid the main product is $\text{H}_3\text{C}.\text{CHI}.\text{CH}_3$. In $\text{H}_3\text{C}.\text{CBr}:\text{CH}_2$, the central carbon is exposed to the effect of Br as well as CH_3 , both belonging to type I, hence we should expect, as is the case, that when this compound is acted on by hydrogen bromide $\text{H}_3\text{C}.\text{CBr}_2.\text{CH}_3$ is produced. In the compound $\text{H}_3\text{C}.\text{CH}:\text{CHBr}$, the end carbon is under the influence of Br while the central one is under that of CH_3 , thus when hydrogen bromide is added, both $\text{H}_3\text{C}.\text{CBrHCH}_2\text{Br}$ and $\text{H}_3\text{C}.\text{CH}_2\text{CHBr}_2$ are formed.

Since the atoms and radicles of type I, produce, when they replace hydrogen, an electric field which tends to drive off the positive hydrogen atoms and thus produce free hydrogen ions, the entrance of these into a compound ought to increase its acidity. This is well marked in many cases, thus the replacement of two of the hydrogens in methyl alcohol by an atom of oxygen corresponding to the change to formic acid changes a weak base to a strong acid, presumably by facilitating the detachment of the hydrogen ion from the hydroxyl radicle. Again, while KOH is a strong base ClOH is an acid;

monochlor, dichlor and trichlor acetic acid are much stronger acids than acetic acid itself. The difference in strengths is so great that I do not think the whole of it can be ascribed to the direct effect of the kind we are considering, indeed the fact that acetic acid is a weaker acid than formic shows that other factors must be taken into consideration. Such a factor might be one of the following kind :—Acetic acid can decompose into CH_4 and CO_2 with complete separation of these constituents: if this is so, we might expect that at ordinary temperatures, when this separation is not effected, we might have in some of the molecules of acetic acid a grouping of the atoms and electrons corresponding to that of a molecular compound of CH_4 and CO_2 ; this need not be permanent but merely a phase passing back into the grouping represented by the usual formula for acetic acid, *i. e.*,



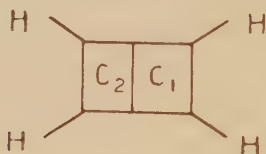
if we call this grouping phase II., the grouping corresponding to (CH_4CO_2) phase I., then the compound when in phase II. would be an acid, but would not be so when in phase I. Thus its strength as an acid would depend upon the proportion between the times it was in phases I. and II. respectively, or what is the same thing, on the proportion between the number of molecules which at any instant are in phases I. and II. If this view is correct then the strength of an acid cannot be calculated merely from the formula which represents its configuration when in its most acidic condition. We have to know whether the molecule spends the whole of its time in this condition, and if not, what are the duration and character of the other phases through which it passes. It may be that the introduction of chlorine into acetic acid may increase the duration of the more acidic condition as well as make that condition more intense than the corresponding one for acetic acid.

The Polarization of the Double Bond.

When two carbon atoms are connected as in ethylene by a double bond, the electrons are distributed in two octets round the carbon atoms, the octets having four electrons in common. As the potential energy will clearly be a minimum

when the distribution of electrons is symmetrical about the plane bisecting the line $C_1 C_2$ at right angles (fig. 9), this will be the stable distribution and there will not be any difference between the properties of the two carbon atoms. Suppose now, that one of the hydrogen atoms attached to C_1 is replaced by an atom of chlorine. The effect of this, as we have seen, is to introduce at this atom an electric doublet whose positive end is towards C_1 . The electrons between C_1 and C_2 in the octets will thereby be drawn closer to C_1 and away from C_2 , the density of the electrons on the C_1 side of the double bond will be greater than that of those on the C_2 side: the double bond will be polarized and the properties of the C_2 will differ from those of the C_1 carbon. If the displacements of the electrons were considerable the result would be that though the octet round C_1 would remain complete it could no longer be regarded as sharing four electrons with the system round C_2 ; thus C_2 would no longer be surrounded by

Fig. 9.



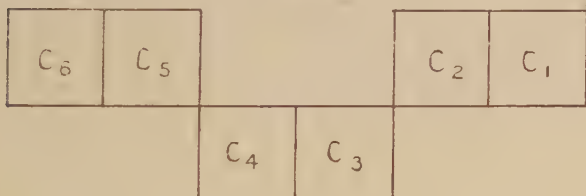
a complete octet, it would be unsaturated and could take up another electron and thus enter into combination with another atom, and the double bond would be converted into a single one. Thus on this view, *ceteris paribus*, addition compounds would be formed more freely with a compound like H_2CCHCl , than with one like H_2CCH_2 .

But even when the displacement of the electrons is not sufficient to loosen the double bond, the movement of electrons from C_2 towards C_1 will diminish the attraction which these electrons exert on the positive part of an atom of hydrogen attached to C_2 so that this hydrogen atom will be more easily detached than before the introduction of the chlorine. Again, the movement of the electrons away from C_2 will tend to increase the chance of molecular compounds being formed in its neighbourhood. In the undisturbed position of the electrons C_2 was coordinately saturated, it could not form either atomic or molecular compounds; with the movement of the electrons away from C_2 this saturation will be relaxed,

and the possibility of a molecule forming part of the system round C_2 increased. As the preliminary formation of "molecular compounds" is very often essential to chemical change, this effect will also increase the activity of C_2 .

If instead of two carbon atoms we have a series arranged as in fig. 10, then the movement of the electrons from C_2 towards C_1 will diminish the repulsion which these electrons exerted on those in C_3 , electrons will thus tend to crowd into C_3 from C_4 , thus the density of the electrons round C_3 will be increased while the density of those round C_4 will be diminished. Thus in a chain of carbon atoms of this kind the effect of the substitution of chlorine for hydrogen at one of them is to make the density of the electrons round successive carbon atoms alternately greater or less than the normal, *i. e.*, to make chemically inert and chemically active carbon atoms alternate with each other.

Fig. 10.



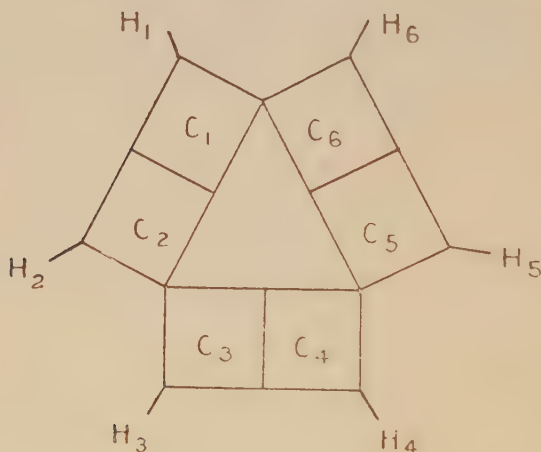
If instead of chlorine the substituent at C_1 had been one of type II, giving rise to an electrostatic moment with the *negative* end towards C_1 , the electrons would be displaced from C_1 towards C_2 ; this would increase the density of the electrons round C_2 and decrease its chemical activity, the electrons moving towards C_2 would exert an increased repulsion on those in C_3 , reducing the density round C_3 and thereby increasing the chemical activity of that atom.

Thus when the substituent is of type I, the active carbons are those which are 1, 3, 5, places from the atom where the substitution took place; when the substituent belongs to type II, the active atoms are 2, 4, 6, places away from the substituent.

Polarization of the double bond could be produced without substitution by the presence of polar molecules or charged ions.

An interesting example of this principle is that of benzene substitutions. Thus let fig. 11 represent the arrangement of the atoms in the benzene ring, and suppose H_1 the hydrogen attached to the carbon atom C_1 is replaced by an atom or radicle of type I. From what we have just seen the carbon atoms in the ortho and para positions will become active since these are respectively 1 and 3 places from the carbon where substitution took place; those in the meta position will be inert. If, however, the hydrogen at C_1 is replaced by an

Fig. 11.



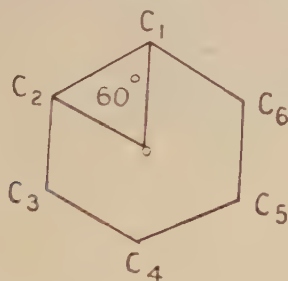
atom or radicle of type II., the carbons in the meta positions will be the active ones while those in the ortho and para positions will be inert. Now (see Holleman's 'Organic Chemistry,' English translation, p. 514) the substituents which direct a second substituent into the ortho and para positions are Cl , Br , I , OH , NH_2 , CH_3 , while those which direct a second substituent into the meta positions are NO_2 , $CO.OH$, CN , HSO_3 . It will be seen that this division is exactly the same as that arrived at from the consideration of the sign of the electric doublet which produces the same effect as the substitution of the atom or radicle for hydrogen.

The Polarity of the Substituted Benzenes.

Benzene itself is a non-polar substance and has a specific inductive capacity equal to the square of its refractive index,

the introduction of a substituent on our view introduces an electrical moment, *i.e.*, it makes the molecule polar, and should therefore endow the molecule with a high inductive capacity. The difference between the specific inductive capacities of the substituted benzene and benzene itself, estimated per molecule, is a measure of the moment of the doublet representing the effect of substitution. The substituted benzenes show, as a rule, very high specific inductive capacities, thus benzonitril has a specific inductive capacity of 26, nitrobenzol 33·4–37·4, benzol cyanide 16·7 (Walden, *Zeitschrift f. Phys. Chem.* lv. p. 232). There do not seem to be any measurements of the specific inductive capacity of bisubstituted benzenes; these would be of considerable interest. Let us consider first the case when both substituents are of the same kind and that I is the moment of the doublet for one substitution. Now

Fig. 12.



suppose that a second substitution takes place, the electrostatic moment of the molecule will depend upon whether the second substituent goes into the para, ortho, or meta position.

Neglecting the deflexion of the two doublets due to their action on each other we see from fig. 12 that :

1. If the second constituent goes into the para position the resultant moment is zero.
2. If it goes into the ortho position the resultant moment is

$$\{I^2 + I^2 + 2I^2 \cos 60^\circ\}^{1/2} = \sqrt{3}I.$$

3. If it goes into the meta position the resultant moment is

$$\{I^2 + I^2 + 2I^2 \cos 120^\circ\}^{1/2} = I.$$

Thus a para substitution destroys the moment and should therefore make the molecule non-polar and the dielectric capacity normal.

A meta substitution leaves the moment unchanged in magnitude.

An ortho substitution increases the moment and therefore increases the specific inductive capacity.

It would seem that determinations of the specific inductive capacity might be useful in determining whether the second substituent went into the para, ortho, or meta position.

If the second substituent is not the same as the first, thus if I' is the moment due to the second, the moment of the molecule if the second substituent goes into :

- (1) The para position is $I - I'$.
- (2) The ortho position is $(I^2 + I'^2 + II')^{1/2}$.
- (3) The meta position is $(I^2 + I'^2 - II')^{1/2}$.

If I and I' have the same sign, *i.e.*, if both substituents belong to the same type, the specific inductive capacity will be least for the para position and greatest for the ortho—that for the meta position will be between the values for the para and ortho.

If, however, the two substituents belong to different types I' will be of the opposite sign to I , and the specific inductive capacity will be *greatest* in the para position and least in the ortho.

LV. *On a Second Approximation to the Quantum Theory of the Simple Zeeman Effect and the Appearance of New Components.* By A. M. MOSHARRAFA, King's College, London*.

§ 1. *The Hypothetical Path of Equal Energy.*

IN a previous paper † a first approximation to the theory of the simple Zeeman effect was put forward, based on the extended form of the quantum restrictions, viz.

$$\int_0 (p_i - ea_i) dq_i = n_i h, \quad i = 1, 2, 3, \dots \quad (1)$$

where a is the magnetic vector potential and the integration extends from q_i =minimum to q_i =maximum and back again. It was found that the method of separation of the variables could be successfully applied in the presence of the field H , provided all terms of higher order than the first in H were

* Communicated by Prof. O. W. Richardson, F.R.S.

† Roy. Soc. Proc. A. vol. cii. p. 529 (1923). This will be referred to freely.

neglected. In this paper we shall show that the method can still be applied, without any restriction as to the degree of approximation, to a hypothetical motion which possesses the same energy as the actual motion.

Let Σ^* be one of the actual paths of the electron in the presence of the field. Thus Σ is completely defined by the following six equations in spherical polar coordinates† with the origin in the nucleus and Oz in the direction of H :

$$\left. \begin{aligned} d(m\dot{r})/dt - m\dot{\theta}^2 - m\dot{\psi}^2 \sin^2 \theta &= -eE/r + K_r, \quad (\alpha) \\ \frac{1}{r} d(mr^2\dot{\theta})/dt - m\dot{\psi}^2 \sin \theta \cos \theta &= K_\theta, \quad (\beta) \\ \frac{1}{r \sin \theta} d(mr^2 \sin^2 \theta \dot{\psi})/dt &= K_\psi, \quad (\gamma) \end{aligned} \right\} \quad (2)$$

$$\left. \begin{aligned} \int_0 p_r dr &= n_1 h, \quad (\alpha) \\ \int_0 p_\theta d\theta &= n_2 h, \quad (\beta) \\ \int_0 (p_\psi - m_0 \omega r^2 \sin^2 \theta) d\psi &= n_3 h, \quad (\gamma) \end{aligned} \right\} \quad (3)$$

where m is the mass of the electron [variable], m_0 is the value of m for zero velocity, $(-e)$ and E are the charges on the electron and nucleus respectively, ω is given by

$$\omega = eH/2m_0c, \quad (4)$$

and K is the so-called "Coriolis" force acting on the electron on account of its motion in the magnetic field, being equal per unit charge to the vector product of the velocity and the field. Thus

$$\left. \begin{aligned} K_r &= -eHr \sin^2 \theta \dot{\psi}/c, \quad (\alpha) \\ K_\theta &= -eHr \sin \theta \cos \theta \dot{\psi}/c, \quad (\beta) \\ K_\psi &= eH(\dot{r} \sin \theta + r \cos \theta \dot{\theta})/c. \quad (\gamma) \end{aligned} \right\} \quad (5)$$

Consider a hypothetical path Γ defined by the six equations obtained from (2) and (3) by putting $K_r = K_\theta = K_\psi = 0$ in the former but without altering the latter in any way. Σ can thus be conceived to be derived from Γ by the operation of

* Σ and Γ here used to denote the complete specific motions in the two respective cases.

† The proof is equally valid for any set of coordinates. We choose spherical polars in this section merely because they are adopted in the rest of the paper.

the coriolic forces alone *. Now the element of work done by the coriolic forces is equal to

$$(K_r v_r + K_\theta v_\theta + K_\psi v_\psi) dt,$$

where v is the velocity of the electron at the time considered. And, on using the values of v_r , v_θ , and v_ψ in terms of the coordinates, viz.

$$v_r = \dot{r}, \quad v_\theta = r\dot{\theta}, \quad v_\psi = r \sin \theta \dot{\psi},$$

this is seen from (5) to be identically equal to 0. In other words, the introduction of the coriolic forces alone cannot affect the energy of the electron, and therefore

$$W(\Sigma) = W(\Gamma) = W, \text{ say, } \dots \dots (6)$$

where $W(\Sigma)$ and $W(\Gamma)$ are the respective energies of the two paths. Hence we may calculate the value of W by considering the motion in Γ instead of in Σ .

§ 2. The Expression for W .

Any path Γ is a "relativity ellipse," the dimensions of which are defined by the modified quantum restrictions (3). We thus have for Γ , from the analysis given in § 2 of our previous paper, on putting $H=0$:

$$\left. \begin{aligned} p_r &= m\dot{r} = \sqrt{[A + 2B/r + C/r^2]}, & (\alpha) \\ p_\theta &= mr^2\dot{\theta} = \sqrt{[p^2 - F^2/\sin^2 \theta]}, & (\beta) \\ p_\psi &= mr^2 \sin^2 \theta \dot{\psi} = F, & (\gamma) \end{aligned} \right\} \quad (7)$$

where A , B , and C are given by

$$\left. \begin{aligned} A &= 2m_0 W (1 + W/2m_0 c^2), & (\alpha) \\ B &= eEm_0 (1 + W/m_0 c^2), & (\beta) \\ C &= -(p^2 - e^2 E^2/c^2), & (\gamma) \end{aligned} \right\} \quad (8)$$

and p and F are constants. From (3) and (7) we have

$$\left. \begin{aligned} \int_0^{\cdot} \sqrt{[A + 2B/r + C/r^2]} dr &= n_1 h, & (\alpha) \\ \int_0^{\cdot} \sqrt{[p^2 - F^2/\sin^2 \theta]} d\theta &= n_2 h, & (\beta) \\ \int_0^{2\pi} [F - m_0 \omega r^2 \sin^2 \theta] d\psi &= n_3 h, & (\gamma) \end{aligned} \right\} \quad (9)$$

* It must be clearly understood that this cannot be achieved by actually introducing the magnetic field, since the introduction of a magnetic field involves other forces besides K_ψ , viz. the induction forces, which do in fact alter the energy.

and the first two integrals yield as before

$$\left. \begin{aligned} 2\pi i[\sqrt{C+B}/\sqrt{A}] &= n_1 h, \quad . \quad . \quad . \quad (\alpha) \\ 2\pi(p-F) &= n_2 h, \quad . \quad . \quad . \quad (\beta) \end{aligned} \right\} \quad (10)$$

To evaluate the third integral we have to deal with

$$I = \omega m_0 \int_0^{2\pi} r^2 \sin^2 \theta d\psi, \quad . \quad . \quad . \quad (11)$$

or since

$$m = m_0 / \sqrt{(1-\beta^2)}, \quad . \quad . \quad . \quad (12)$$

we have from (7 γ), (11), and (12),

$$I = \omega F \int_0^T \sqrt{(1-\beta^2)} dt, \quad . \quad . \quad . \quad (13)$$

where T is the time from $\psi=0$ to $\psi=2\pi$. Let

$$T = T_0 + \delta_\omega T + \delta_\alpha T + \dots, \quad . \quad . \quad . \quad (14)$$

where $\delta_\omega T$ and $\delta_\alpha T$ are first-order terms in ω and α respectively, α being given by

$$\alpha = (2\pi)^2 e^2 E^2 / h^2 c^2, \quad . \quad . \quad . \quad (15)$$

and T_0 being the value of T calculated for $\omega=\alpha=0$.

We have as a first approximation to the value of I :

$$I = \omega F T_0 + \dots, \quad . \quad . \quad . \quad (16)$$

where

$$T_0 = (n_1 + n)^3 / 2N, \quad . \quad . \quad . \quad (17)$$

N being the Rydberg constant

$$N = (2\pi)^2 m_0 e^2 E^2 / 2h^3 \quad . \quad . \quad . \quad (18)$$

and

$$n = n_2 + n_3. \quad . \quad . \quad . \quad (19)$$

From (9 γ), (11), and (16), we have

$$2\pi F = n_3 h [1 + \omega T_0 / 2\pi + \dots]. \quad . \quad . \quad (10 \gamma)$$

Thus, as a first approximation, the motion in Γ is defined by exactly the same equations as in the ordinary Bohr-Sommerfeld atom, except that n_3 is now replaced by

$$n_3(1 + \omega T_0 / 2\pi).$$

Hence, using (17),

$$T_0 + \delta_\omega T = [n_1 + n_2 + n_3(1 + \omega T_0 / 2\pi)]^3 / 2N$$

to the first order,

so that $\delta_\omega T / T_0 = 3n_3 \omega T_0 / 2\pi(n + n_1). \quad . \quad . \quad . \quad (20)$

Now I can be put in the form

$$I = \omega F(1 + \delta_\omega T/T_0) \int_0^{T_0 + \epsilon_a T} \sqrt{1 - \beta^2} dt \quad (21)$$

to the second order, where the last integral is evaluated for $\omega = 0$. This evaluation is quite independent of a magnetic field, and merely relates to the Bohr-Sommerfeld atom. Quoting here the result given in the Appendix (*q. v.*) for this integral, and using the value for F given by (10 γ), we have

$$I = n_3 h \{ 1 + f_1(n) \cdot \omega T_0 / 2\pi - \alpha f_2(n) \} \omega T_0 / 2\pi, \quad (22)$$

where

$$\left. \begin{aligned} f_1(n) &= 1 + 3n_3 / (n + n_1), & (\alpha) \\ f_2(n) &= [1 + 5n_1 / 2n + n_1^2 / 2n^2] / (n_1 + n)^2, & (\beta) \end{aligned} \right\} \quad (23)$$

Equations (9 γ), (11), and (22) finally yield

$$2\pi F = n_3 h \{ 1 + \omega T_0 / 2\pi + f_1(n) (\omega T_0 / 2\pi)^2 - f_2(n) \cdot \alpha \omega T_0 / 2\pi + \dots \}. \quad (10 \gamma a)$$

Thus the equations defining Γ are identical, to the second order of small quantities, with those defining the normal atom if we write n_3' for n_3 , where

$$n_3 = n_3 \{ 1 + \omega T_0 / 2\pi + f_1(n) \cdot (\omega T_0 / 2\pi)^2 - f_2(n) \cdot \alpha \omega T_0 / 2\pi \}. \quad (24)$$

The change in energy can thus at once be calculated from the normal expression for the energy by making this substitution. The normal expression for the energy can be put in the form

$$W_{\text{norm.}} = -Nh \{ 1 + \alpha \phi_1(n_1/n) / (n_1 + n)^2 + \alpha^2 \phi_2(n_1/n) / (n_1 + n)^4 + \dots \} / (n_1 + n)^2, \quad (25)$$

where

$$\left. \begin{aligned} \phi_1(n_1/n) &= 1/4 + n_1/n, & (\alpha) \\ \phi_2(n_1/n) &= 1/8 + 3n_1/4n + 3n_1^2/2n^2 + n_1^3/4n^3; & (\beta) \end{aligned} \right\} \quad (26)$$

from which we calculate, using (23), (26 α), and (17) :

$$\left. \begin{aligned} \delta_\omega W &= n_3 h \omega / 2\pi, & (\alpha) \\ \delta_a W &= -Nh \alpha \phi_1(n_1/n) / (n_1 + n)^4, & (\beta) \\ \delta_{\omega^2} W &= (n_1 + n)^3 n_3 h \omega^2 [1 + 3n_3 / (2(n_1 + n))] / 2 \cdot (2\pi)^2 N, & (\gamma) \\ \delta_{a^2} W &= -Nh \alpha^2 \phi_2(n_1/n) / (n_1 + n)^6, & (\delta) \\ \delta_{\omega, a} W &= -n_3 \omega \alpha h / 4\pi (n + n_1)^2, & (\epsilon) \end{aligned} \right\} \quad (27)$$

§ 3. *Significance of the Results of § 2, and General Character of the Zeeman Decomposition.*

Of the five increments of energy given by (27) the first two merely give the simple Zeeman triplet and the first-order fine structure respectively, as already dealt with in the last paper. (27 δ) is the second-order term for the fine structure and leads to a change in wave-length of the order 10^{-5} Å, which is much too small to be detected. With regard to the other two terms, we have from (27)

$$\delta_{\omega, \alpha} W / \delta_{\omega^2} W = -2\pi\alpha N / \omega f_1(n)(n+n_1)^5, \quad . \quad . \quad (28)$$

and on substituting the values for ω , α , and N for hydrogen ($E=e$), viz.

$$\omega / 2\pi = 1.406 \times 10^6 \text{ H}, \quad . \quad . \quad . \quad . \quad (29)$$

$$\alpha = 5.5 \times 10^{-5}, \quad . \quad . \quad . \quad . \quad (30)$$

$$N = 3.290 \times 10^{15}, \quad . \quad . \quad . \quad . \quad (31)$$

we have, since $f_1(n) (=) 1$,

$$\delta_{\omega, \alpha} W / \delta_{\omega^2} W (=) 10^5 / \text{H}(n_1+n)^5, \quad . \quad . \quad . \quad (32)$$

where $(=)$ stands for equality of order of magnitude only.

Now the smallest value for H which will give a measurable second-order effect is of the order 10^6 Gauss; so that we have for a measurable effect:

$$| \delta_{\omega, \alpha} W / \delta_{\omega^2} W | < 1/10(n_1+n)^5.$$

Thus for the Balmer Series ($n_1+n=2$) the ratio is less than 10^{-2} , and it is still less for the enhanced series ($n_1+n>2$). It must, nevertheless, be noted that for fields higher than $\text{H}(=)10^8$ Gauss, although the above ratio is reduced to less than 10^{-4} , yet the $\delta_{\omega, \alpha} W$ term would lead to measurable effects. Such very high fields are, however, not likely to be attained at present. We thus see that the only second-order term that has any importance in (27) is the term in ω^2 , and the effect of the field may therefore still be described as a splitting of each of the fine structural components into a Zeeman multiplet. This multiplet is no longer a simple triplet, however, but may be described as a splitting of each of the components of the simple Zeeman triplet into a number of "sub-components." The number of these sub-components depends on (n_1+n) , i. e. on the value of the constant series term of the spectral "line" in question. Thus there are $(n+n_1+1)$ sub-components of the middle member of the triplet ($m_3-n_3=0$), $(n+n_1+1)$ of the "violet" member ($m_3-n_3=+1$), and

$(n+n_1)$ of the "red" member ($m_3-n_3=-1$), altogether $3(n+n_1)+2$ sub-components. One of these, belonging to the middle member of the triplet and corresponding to $m_3=n_3=0$, always occupies the position of the original line. It is also to be noted that, as in the case of the Stark effect*, this second-order deviation from symmetry increases as we approach the more violet end of a given series, *i. e.* as m_1+m increases. This is on account of the occurrence of $(m_1+m)^3$ in the expression for $\delta\nu$ [see equations (33) and (34) below]. Thus for the Balmer Series the effect would be more pronounced for H_β than for H_α , and so on.

§ 4. Application to the Balmer Series.

We choose H_γ as an example. We have from (27), on restricting ourselves to the second-order effect and dropping the suffix ω^2 for brevity,

$$\delta\nu = \omega^2(Z_m - Z_n)/2N \cdot (2\pi)^2, \quad . \quad . \quad . \quad (33)$$

where

$$\left. \begin{aligned} Z_m &= (m_1+m)^3 m_3 [1 + 3m_3/2(m_1+m)], \\ Z_n &= (n_1+n)^3 n_3 [1 + 3n_3/2(n_1+n)]. \end{aligned} \right\} \quad . \quad . \quad (34)$$

For H_γ , since $m_1+m=5$, $n_1+n=2$, (34) reduces to

$$\left. \begin{aligned} Z_m &= 125m_3(1 + 3m_3/10), \\ Z_n &= 8n_3(1 + 3n_3/4). \end{aligned} \right\} \quad . \quad . \quad . \quad (34a)$$

And from (33) we have for the increment of wave-length $\delta\lambda$

$$\delta\lambda = -\lambda^2 \omega^2 [Z_m - Z_n]/2Nc \cdot (2\pi)^2. \quad . \quad . \quad (35)$$

On putting $\lambda = 434 \times 10^{-4}$ and substituting for N and ω from (31) and (29) respectively for a hypothetical magnetic field :

$$H = 10^6 \text{ Gauss}, \quad . \quad . \quad . \quad (36)$$

we have

$$\delta\lambda' = -1.89 \times 10^{-3} [Z_m - Z_n], \quad . \quad . \quad (37)$$

where $\delta\lambda' = \delta\lambda \times 10^8$, *i. e.* where $\delta\lambda'$ is measured in Angström units.

The different possible values of Z'_m and Z_n are given in Table A, and the values of $(Z'_m - Z_n)$ corresponding to the three components of the simple Zeeman triplet are given in Table B, together with the values of $\delta\lambda'$ calculated from (37). Table B has been arranged so that the respective positions

* See A. M. Mosharrafa, Phil. Mag. vol. xlix, p. 373 (August 1922).

TABLE A.

	a.	b.	c.	d.	e.	f.	I.	II.	III.
$\eta_g =$	5	4	3	2	1	0	$\eta_g =$	2	1
$Z_m =$	1562.5	1100	712.5	400	162.5	0	$Z_m =$	10	14
									0

TABLE B.

	"Violet" Component, $m_g - n_g = +1.$			Middle Component, $\eta_g - n_g = 0.$			"Red" Component, $m_g - n_g = -1.$	
	I. c.	II. d.	III. e.	I. d.	II. e.	III. f.	I. c.	II. f.
$Z_m - Z_n$	672.5	386	162.5	360	148.5	0	122.5	-14
δN	-1.27	-.73	-.31	-.68	-.28	0	-.23	+ .03

of the sub-components are, in each of the three cases, the same as they would appear on a photographic plate with the usual convention. We note that all displacements are towards the violet, except in the case of one of the sub-components of the red component, which is very slightly displaced towards the red. The greatest value of $(-\delta\lambda')$ occurs for the violet component, and the least value for the red component: and this applies to all members of the Balmer series.

Summary.

- (1) A second approximation to the theory of the simple Zeeman effect is worked out, based on the extended form of the quantum restrictions already adopted in a previous paper.
- (2) It is shown that the method of separation of the variables can be successfully applied for higher approximations than the first to a hypothetical motion which possesses the same energy as the actual motion.
- (3) The analysis takes account of the refinement of Relativity, but it is shown that the second-order effect of this refinement is negligible compared with that of the field.
- (4) The theory predicts a modification in the simple Zeeman triplet, which may be described as a splitting of each of its three components into a number of "sub-components." The general character of these sub-components is discussed.
- (5) The results are worked out fully in the case of H_γ for a hypothetical field of 10^6 Gauss, where second-order displacements ranging from $+0.3$ A. to -1.27 A. are predicted.

APPENDIX (to § 2).

To find $\int_0^{T_\psi} \sqrt{(1-\beta^2)} dt$ for the Bohr-Sommerfeld atom, where T_ψ is the time from $\psi=0$ to $\psi=2\pi$:

Let (r, ϕ) be polar coordinates in the plane of motion of the electron, so that

$$\tan \phi = \tan \psi \cos \alpha, \quad . \quad . \quad . \quad . \quad . \quad (i.)$$

where α is the angle between the planes of ψ and ϕ , and the initial lines $\phi=0$, $\psi=0$ are both perpendicular to the line of intersection of these two planes. We see from (i.) that as ψ changes from 0 to 2π , ϕ changes

from 0 to 2π also, so that we have

$$T_{\downarrow} = T_{\phi}, \quad \dots \dots \dots (ii.)$$

where T_{ϕ} is the period for ϕ . Let T_r be the time from r =minimum to r =maximum and back again. We have by a well-known result to the first order in $1/c^2$:

$$T_{\phi} = T_r(1 - e^2 E^2 / 2p_0^2 c^2), \quad \dots \dots \dots (iii.)$$

or since

$$p_0 = nh/2\pi, \quad \dots \dots \dots (iv.)$$

we have from (ii.), (iii.), and (iv.)

$$T_{\psi} = T_r(1 - \alpha/2n^2), \quad \dots \dots \dots (v.)$$

where α is defined by equation (15) of the text. Thus to the first order in α

$$\int_0^{T_{\psi}} \sqrt{1 - \beta^2} dt = (1 - \alpha/2n^2) \int_0^{T_r} \sqrt{1 - \beta^2} dt. \quad \dots (vi.)$$

Now we see from (7 α) and (12) of the text that

$$\sqrt{1 - \beta^2} dt = m_0 dr_z / \sqrt{(A + 2B/r + C/r^2)};$$

so that

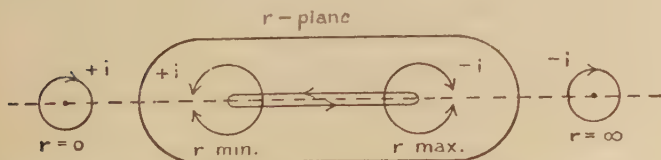
$$\int_0^{T_r} \sqrt{1 - \beta^2} dt = -m_0 J_r, \quad \dots \dots \dots (vii.)$$

where

$$J_r = \int_0 dr / \sqrt{(A + 2B/r + C/r^2)} \quad \dots (viii.)$$

and the negative sign is introduced on account of the negative nature of the integrand. J_r may now be evaluated by the usual method of contour integration in the complex plane. We have to find the residues of the integrand at $r=0$ and $r=\infty$. At $r=0$ it behaves as

$$\frac{1}{\sqrt{C}} \int_0^r r dr (1 + Ar^2 + 2Br)^{-1/2},$$



which is regular. So that putting $r=1/s$, we have

$$\left. \begin{aligned} J_r &= - \frac{1}{\sqrt{A}} \int_0^1 (1 - Bs/A + \dots) ds/s^2 \\ &= -2\pi i \times B/A \sqrt{A}, \end{aligned} \right\} \quad \dots (ix.)$$

where it is observed that the sense of rotation at $r=\infty$ is

negative. Also since $(-1/\sqrt{A})$ is seen from (ix.) to govern the sign of the integrand at $r=\infty$ it follows (see figure) that $(-1/\sqrt{A})$ must be negative and imaginary, and therefore \sqrt{A} must be taken as the negative (imaginary) root of A . On substituting for A and B in (ix.) from (8) of the text we have

$$J_r = -2\pi i e E m_0 [2m_0 W]^{-3/2} [1 + W/4m_0 c^2 + \dots],$$

which yields to the first order on substituting for W from (25),

$$J_r = -(n_1 + n)^3 h^3 [1 - \alpha \{ \frac{1}{4} + 3\phi_1(n_1/n) \} / 2(n_1 + n)^2] / (2\pi e E m_0)^2, \quad \dots \quad (\text{x.})$$

and from (vi.), (vii.), and (x.) we have

$$\int_0^{T_\psi} \sqrt{(1-\beta^2)} dt = T_0 [1 - \alpha f_2(n)], \quad \dots \quad (\text{xi.})$$

where T_0 has the same meaning as in the text and

$$\begin{aligned} f_2(n) &= \{ \frac{1}{4} + 3\phi_1(n_1/n) + (1 + n_1/n)^2 \} / 2(n_1 + n)^2 \\ &= [1 + 5n_1/2n + n_1^2/2n^2] / (n_1 + n)^2 \text{ from } (26 \text{ } \alpha). \end{aligned}$$

This is the result quoted in the text.

January 1923.

LVI. *Electrical Discharges in Geissler Tubes with Hot Cathodes.* By W. H. MCCURDY, M.A., 1851 Exhibition Scholar, Princeton University*.

IN a recent number of the 'Physical Review,' Duffendack† reported results obtained from work on low-voltage arcs, stimulated by the emission from a hot cathode, in diatomic gases. As his work dealt only with the arc characteristics, it was thought possible that additional light might be thrown on the process of ionization by a study of the discharge in Geissler tubes, if a hot filament were used as cathode to stimulate the discharge. This eliminated the uncertainty as to the source of the electrons which produced the ionization in the tube, and, at the same time, overcame the very high cathode fall of potential encountered in cold electrode tubes. With an apparatus provided with a hot cathode and a movable anode, it should be possible to study the successive stages in

* Communicated by Professor K. T. Compton.

† Phys. Rev. vol. xx, No. 6, p. 665.

the type of discharge as the type changes from the characteristic arc type at short distances to the characteristic Geissler tube type at greater distances. This may aid in identifying the causes of various features of the Geissler tube discharge.

The work here recorded was divided into three parts, which will be treated separately :—

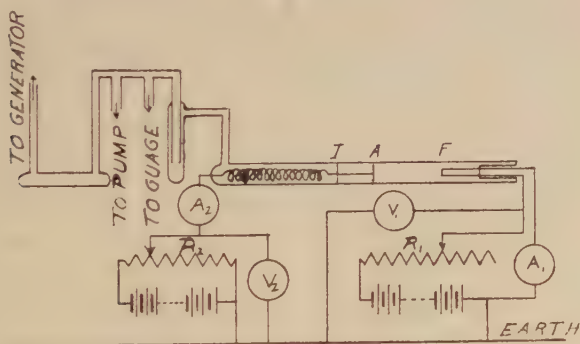
(1) Relation between current through the tube and potential applied to the tube; also observations on the appearance of the discharge under various conditions.

(2) Relations existing between the filament temperature pressure of the gas, and the least voltage (V_m) necessary to maintain the discharge in hydrogen.

(3) Similar observations in mercury vapour.

The apparatus used is shown in fig. 1. as are also the electrical connexions.

Fig. 1.



The filament (F) was a tungsten spiral of only a few turns, which served to concentrate the heat at the centre, thus making it possible to obtain a reasonably high electron emission without a large potential drop across the filament. This potential fall was never more than 3.75 volts; thus, assuming that the discharge was maintained to the centre of the filament, which seemed probable as it was the part of greatest electron emission, the correction was never more than 1.8 volt. Further, as the voltage across the tube was applied between the negative terminal of the filament and the anode (A), the correction due to potential drop was approximately balanced by that due to the initial velocities of emission of electrons from the filament. Consequently the voltages given in the following data are the actual voltmeter (V_m) readings. The anode (A) was either a nickel or an

aluminium disk with a piece of soft iron (I) attached to it, by means of which it was possible to place the anode at any desired position. The potential was supplied by a battery of accumulators and regulated by a rheostat (R_2), the current being measured by the milli-microammeter (A_2).

Two tubes of hard glass were used, one of diameter 4.0 cm. and the other 2.8 cm. Both were thoroughly baked out, and the filaments glowed until no appreciable amount of gas was given off.

The hydrogen used was obtained by the electrolysis of dilute sulphuric acid, dried and purified by phosphorus pentoxide and coconut charcoal in liquid air. The charcoal was so placed as to serve both as a purifying agent and as a reservoir to replace the hydrogen "cleaned up" by the discharge. The discharge was sustained before any readings were taken until the pressure, as measured on the McLeod gauge, no longer decreased.

PART I. — *Relation between current through the tube and potential applied to the tube; also observations on the appearance of the discharge under various conditions.*

The filament current was adjusted to the amount which gave the lowest value to the potential necessary to maintain the discharge at the distance between electrodes being used; then, with this current constant, the potential across the tube was gradually increased up to values of from 80 to 100 volts, and the current through the tube noted at suitable intervals. The potential was then decreased and current readings taken at intervals as when it was being increased. The whole process was then repeated at different distances and pressures.

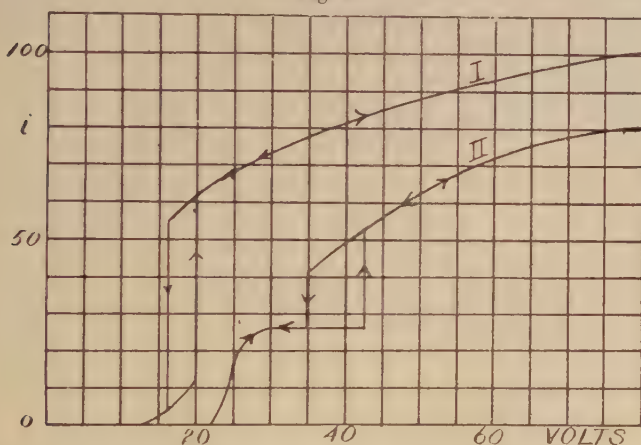
The relation between the current and voltage for two typical cases is shown in fig. 2. Curve I. shows the relation that was found to hold with the 4.0-cm. tube and at pressures about 0.4 mm. at distances less than about 1.2 cm. At lower pressures this sort of a relation would be found to hold at slightly greater distances. Under conditions given there was only one discontinuous change in the current, after which it gradually increased towards a maximum value. It will also be noted that the discharge was *maintained* at lower voltages than those necessary to start it, which has been explained by Duffendack* as due to the fact that the potential distribution is more favourable for maintaining the discharge if there is a region of positive space charge surrounding the cathode. Curve II. represents the type of relation that existed

* *Loc. cit.*

at distances greater than 1.2 cm. Here there were two distinctly marked discontinuities as the potential was increased, and sometimes, though not always, two as it was decreased. It will further be noticed from the figure that, for a portion of the region of voltage between the two discontinuities, the current remained constant as the voltage was increased. In some cases it was found to decrease with an increase in voltage. An explanation for this has not yet been found.

The two breaks in current at the greater distances were found to be associated with the appearance or disappearance

Fig. 2



of two distinct types of discharge, which were termed types A and B. This phenomenon was also found by MacLennan* in his work on low-voltage arcs in cadmium. Type A showed very feeble luminosity, and the current associated with it was much smaller than that which was found with type B. The striations which, in the discharge in cold electrode tubes, form the positive column, extended well in toward the cathode. An increase in potential caused them to approach the cathode at a constant distance of separation, new striations appearing at the anode as the first ones disappeared at the cathode.

Type B showed strong luminosity, and the current was much larger. The appearance of the discharge was the same as that in the cold electrode tubes, with a well-defined dark space but rather diffuse negative glow. In this case the striations approached the anode at a constant distance of

* Proc. Phys. Soc., Dec. 1918,

separation as the voltage increased, but no new striations appeared as the original ones disappeared at the anode.

The change in distribution of luminosity in the tube indicated that there must be a corresponding change in potential distribution between the electrodes. The two distributions possible which permit that the discharge may be maintained are a high cathode fall and the usual gradually increasing gradient in the region shortly in front of the negative dark space, or a cathode fall of only the ionizing potential of the gas at the cathode and a higher potential gradient in the dark space which may be shorter and a second region of ionization at the end of the dark space. The first distribution would cause intense ionization at the cathode, and thus a high space-charge is built up and the positive ions are drawn into the cathode at a relatively high velocity which would diminish the probability of recombination. Under such conditions it is possible that the proportion of the current carried by positive ions is comparable with the electron current; at any rate, the electron emission from the cathode must be increased by the building up of the high potential gradient at the cathode by the positive space charge. On the other hand, when the cathode fall is much smaller (about the ionizing potential of hydrogen) the ionization at the cathode is less, and consequently the positive space-charge is less. Also the positive ions produced in the second region (at the end of the dark space) have a very small chance of reaching the cathode before recombination, so contribute little or nothing to the current. Consequently, a smaller current is to be expected with such a distribution of potential.

The distance of separation of the striations was not affected by changes in either the filament current or the potential applied to the tube, which is in accordance with the equation for the distance between striations in cold electrode tubes

$d = \frac{2r^{1-m}}{p^m}$ *, where d is the distance between the striations, r the radius of the tube, and p the pressure in the tube, m having a value of about .5.

The spectra observed in both types appeared to be the same, differing only in intensity. The region of the positive column showed a strong band spectrum and weak Balmer lines, while the region near the cathode showed strong Balmer lines and very little trace of the band spectrum.

* Wehner, *Ann. der Physik*, xxxii. p. 49 (1910).

The position of the striations under different conditions was found to change as follows :—

Type B discharge :

(1) With filament current kept constant, they *approached* the anode as the potential applied to the tube was *increased*.

(2) With potential across the tube kept constant, they *approached* the anode as the filament current was *decreased*.

(3) With current through the tube kept constant, they *approached* the anode as the potential across the tube was *increased*.

Type A discharge :

With filament current kept constant, they *receded* from the anode as the potential across the tube was increased.

PART II.—*Relation between the pressure of the gas, the filament current, and the least voltage (V_m) necessary to maintain the discharge in hydrogen.*

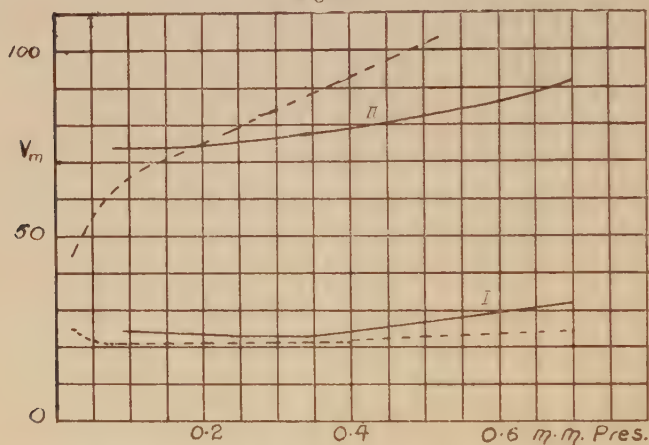
The apparatus used for this part of the investigation was the same as that shown for the first part.

The method employed was to determine the filament current at which the voltage necessary to maintain the discharge was a minimum, and to repeat this determination at various anode distances and gas pressures. This repetition was found necessary for the different distances and pressures on account of the variation of the behaviour of the maintaining voltage as the filament current was changed, when the anode was situated in the positive column. This was due to the high potential gradient in the vicinity of the striations, and, as was shown in the previous work, changes in the filament current cause a change in the position of the striations, hence a change in potential distribution.

The results of the work at various distances and pressures are indicated in the curves of fig. 3. Here Curve I. gives the variation of the least maintaining voltage V_m with pressure changes at an anode distance of 2.4 cm. in a tube 4.0 cm. diameter; curve II., the same with a 10-cm. distance, with a tube 4.0 cm. in diameter. The continuous curves here represent the voltage at which type B discharge disappeared, while the dotted lines give the disappearing potentials found for type A. It will be observed that at the larger distances the pressure at which V_m for type A increased was not reached. It was found, however, that at lower pressures it was very difficult to start the discharge, and it disappeared at

voltages higher than those shown. The fact that at higher pressures the voltage necessary to maintain type A discharge was higher than that necessary to maintain type B explains why it was not always possible to obtain the second discontinuity in the current in the previous part of the work, though in some cases the increase in potential across the tube due to the change in current through the resistance (R_2) was sufficient to make it possible to maintain type A

Fig. 3.



discharge after type B disappeared. Curve I. shows that the two types were scarcely distinguishable at the shorter distances and a region of pressures.

The results given in fig. 4 were obtained with a constant filament current, and give the relation between the least maintaining voltage V_m and the distance between electrodes—Curve I. when the pressure was such that the positive column was uniform with a tube 2.8 cm. in diameter, and curve II. when the positive column was striated with a tube 4.0 cm. in diameter.

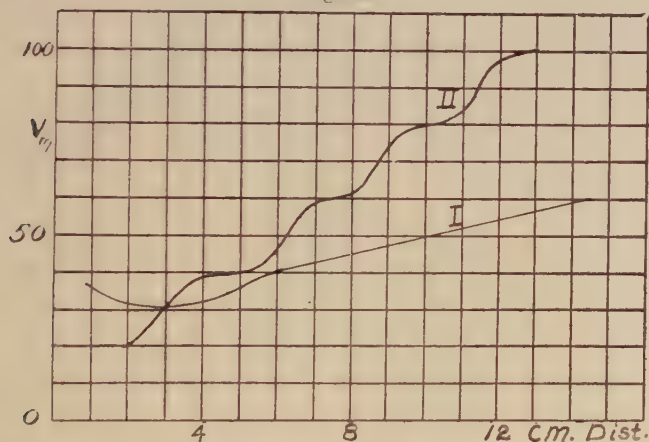
These results are not in accordance with those obtained by Gibson and Noyes*, who found that the least voltage at which it was possible to maintain the luminous discharge in hydrogen was a multiple of 30.9 volts. The present work shows maintaining voltages lower than those obtained by Gibson and Noyes, though the experimental conditions appear to have been similar to theirs. It is therefore possible that

* Journ. Amer. Chem. Soc., Oct. 1922.

they did not reach absolute minimum values of V_m in all cases.

A possible explanation of the results given here may be found on the assumption that the necessary condition for a discharge is that the electron must have sufficient energy to ionize at its first impact. If this condition is to be satisfied, and the potential distribution in Geissler tubes considered, it is evident that the voltage necessary to maintain the discharge must increase with the distance between the electrodes. Consider the case where the anode was situated in the positive column. The least voltage for any distance was found at gas pressures such that the positive column was uniform. Thus the least maintaining voltage V_m should be

Fig. 4.



expressible, for any position in the positive column, by an equation of the form $V_m = V_d + XV$, where V is the uniform potential gradient of the positive column, V_d the potential between the cathode and the head of the positive column, and X the distance of the anode from the head of the positive column. If, on the other hand, the distance between electrodes is such that the anode is situated in the Faraday dark space, when the discharge breaks no such simple expression for V_m could be found, for in that region the potential gradient is not uniform. The same would be expected to be true at pressure conditions such as to give a striated positive column, as in this case the potential gradient of the positive column is not uniform, but approximates more or less to a periodic value*. These relations seem to have held in results shown in fig. 4, where Curve I. represents the

* Thomson, Phil. Mag., Dec. 1921.

relation between distance and V_m when the positive column was uniform, while Curve II. represents the same when the positive column was striated. (The filament temperature was kept constant throughout the whole set of observations shown in fig. 4.) The potential difference between successive striations is seen to have been slightly more than the ionizing potential of hydrogen, the excess being attributed to the resistance of the gas.

PART III.—*Observations on V_m in mercury vapour.*

The only change in apparatus for this part of the work was the addition of a small side tube, in which the mercury was put to get the required pressure. This tube was immersed in a constant temperature bath, and the main tube enclosed in an electric furnace and kept at a temperature slightly higher than that of the mercury in the side tube. The tube was at all times left open to the evacuating system to remove impurities arising from the discharge, as were found by Yao in his work on low-voltage arcs in mercury. This procedure should not affect the pressure in the tube, as the pressure gradient should be taken up in the small tube communicating with the evacuating system.

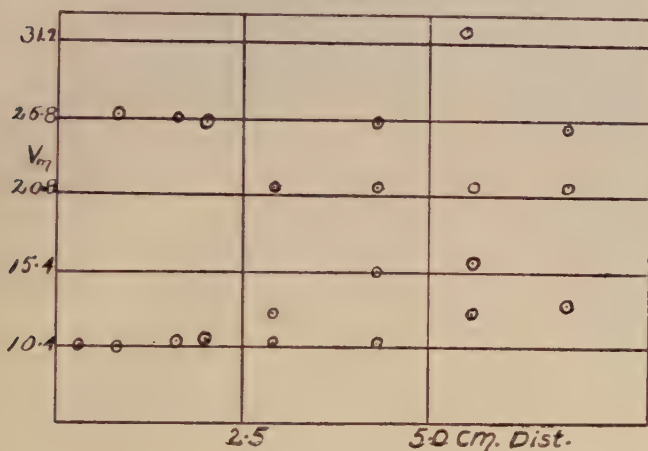
The results of this work so far have not been entirely satisfactory, which is due, probably, to slight variations in temperature of the tube during the course of a run. They appear to indicate, however, that the least maintaining voltage for the discharge in mercury may be expressed by equations of the form $V_m = nV_i + V_r$, or $V_m = nV_i$, where V_i is the ionizing potential of mercury 10.4 volts, and V_r the first radiating potential 4.9 volts, n being an integer. Gibson and Noyes* in their work found the second relation to hold, but did not find cases in which the first applied.

The results are shown in fig. 5, where the different voltages at which abrupt changes in the current occurred are plotted for different distances. Taking any distance given in the figure, it will be seen that there were several voltages at which the current changed abruptly, also that these voltages seem to obey quite well the relations stated above. At greater distances, however, it will be observed that the lowest point shown on the figure did not obey this relation so well. In the case of these points the current was very small and the luminosity in the tube correspondingly weak, so it was possible that this type of discharge might have been the same as has been called type A in hydrogen. At the pressure at which the results recorded were obtained, the

* *Loc. cit.*

discharge showed a striated positive column, but it was impossible to determine whether it was still striated when the final break occurred.

Fig. 5.



Summary.

(1) In Geissler tubes fitted with hot cathodes there were two discontinuous changes in the current as the voltage across the tube is increased, these changes being associated with the appearance of two types of luminous discharge. At short distances between the electrodes, however, one of these disappears, and the conditions of the low-voltage arc, stimulated by the emission from a hot cathode, appeared.

(2) The behaviour of the two types of discharge under various changes in conditions was not the same, although the spectra appeared to differ only in intensity.

(3) The least voltage at which it was possible to maintain a discharge was not found to bear any simple relation to the ionizing potential of hydrogen, a reason for which has been offered.

(4) The voltages at which discontinuous changes in the current with mercury vapour occurred were found to be multiples of the ionization potential or these multiples plus the first radiating potential.

In conclusion, the writer wishes to express his appreciation to Professor K. T. Compton, under whose supervision this work was done, for his unfailing interest and many valuable suggestions during the course of this investigation.

Palmer Physical Laboratory,
Princeton University.

LVII. *On the Physical Properties of Elements at High Temperatures.* By MEGH NAD SAHA *.

THE investigation of the physical properties of elements at high temperature is at present exciting a considerable amount of interest, on the theoretical as well as on the practical side. The present paper is the outcome of certain investigations undertaken by the author, which were withheld from publication because no positive result was obtained. But in view of the recent works, it appeared advisable to give publicity at least to certain points which appear to have been rather lightly passed over by recent workers.

Let us picture to ourselves a quantity of gas, elementary or compound, which is being raised to higher and higher temperatures. The physical changes occurring in the mass under such an increasing stimulus have been discussed in previous papers †. It has been shown that the gas will become luminous, will emit its characteristic lines—principal lines, sharp and diffuse lines, Bergmann lines—and ultimately will be ionized. The problem before us is: (1) to determine the statistical distribution of the atoms in the various quantum orbits, and from this to deduce the intensity of the different lines of the characteristic spectrum: (2) to determine the electrical and optical properties of such a mass of ionized gas.

The method which the present writer followed was purely thermodynamical. It consisted in the application of a form of the law of reaction-isochore, which was originally developed by Nernst for the study of the dissociation-equilibria of gaseous compounds from their physical properties, to the problem of ionization. The same method was followed in the extension of the method to mixtures of different elements by H. N. Russell ‡. But in this, as in other cases, thermodynamics lead us rather blindfolded to the goal, and do not enable us to see the details of the intervening stages.

A very powerful method has recently been developed by Messrs. Darwin and Fowler § in a number of important papers published in the *Phil. Mag.* and *Proc. of the Camb. Phil. Soc.* Probably with the aid of this method the problem is

* Communicated by the Author.

† M. N. Saha, *Proc. Roy. Soc. Lond.* May 1921. *Phil. Mag.* vol. xli. p. 267 *et seq.*, see particularly p. 274.

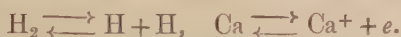
‡ Russell, 'The Astrophysical Journal,' vol. lv. p. 143. Milne, 'The Observatory,' vol. xlv. Sept. 1921.

§ Darwin & Fowler, *Phil. Mag.* vols. xlv. & xlv. *Proc. Camb. Phil. Soc.* vol. xxi. parts 3 & 4.

brought much nearer to solution, but it seems that there are a number of important points on which the authors have not laid sufficient stress. The first point to which I wish to call attention is that "no theory of dissociation-equilibrium can be said to be complete unless it takes account of the mutual interaction between matter (atoms) and radiant energy, because at high temperatures, exchange of energy takes place mainly by radiation, and only to a slight extent by collision."

Binding of an Electron with a Proton (H^+).

To make the above point clear, we shall consider the simplest case conceivable—namely, the binding of an electron with a proton to form an H-atom. This case can rightly be called the simplest, because, thanks to the Bohr theory, all the possible states of combination are known, and the dynamics can be handled with easy mathematics—advantages which are not present in such cases as the reactions



Let us first treat the dynamical part. An electron starts from infinity with velocity v , and passes past a stationary proton. What are the conditions that this will be captured by the proton? A little consideration will show that as long as the energy of the system remains conserved, the electron will describe an hyperbola with the proton as the inner focus, and thus, after wheeling round the proton, will pass off to infinity. In other words, it can never be captured by the proton and lodged in one of the stationary Bohr orbits (having the energy $-\frac{N^2h}{n^2}$) unless the system loses the energy

$$\frac{1}{2}mv^2 + \frac{N^2h}{n^2} \text{ presumably by radiation.}$$

From physical ground, it seems to be fairly well established that such a process actually takes place in nature in all cases of ionization, giving rise to a continuous spectrum beginning from the limit of the series lines. In the case of hydrogen, the continuous spectrum was first detected by Huggins during the observation of the eclipse spectra, and was confirmed by Evershed. The explanation cited above is due to Bohr. (See 'Atombau und Spektralanalyse,' p. 547, 3rd edition.)

But the dynamical interpretation of this process from the standpoint of quantum mechanics is far from satisfactory, as

has been pointed out by Nicholson* in a recent paper. Eddington† has thrown out the suggestion that during its orbital motion the electron loses energy by radiation just as an accelerated electron would do according to the classical theory. But here we are treading on rather dangerous ground, as the satisfactory working out of the suggestion means nothing less than the discovery of the linkage between the classical theory and the quantum theory.

In the case of hydrogen, the continuous spectrum has been observed at the limiting frequency of the Balmer series (quantum orbit 2, or 2_2), but this is owing to the fact that observations do not probably extend up to the limit of the Lyman series. In the case of the alkali elements, the continuous spectrum has been observed extending towards the short wave-length side from the limiting frequency of the principal series. These facts are very decisive in favour of the view that combination of an ionized atom with an electron is always accompanied by liberation of energy in the form of continuous waves of light.

The Statistical part ; deduction of the Law of Reaction-isochore for the Ionization of the H-atom.

This part has been worked out by Fowler, but before taking up his method of deduction, I shall give another deduction based on the older methods, because this may serve to bring out the details of the case in a more intelligible manner.

The problem which we are discussing is only a special case of the general problem of association of particles and dissociation of compound particles which was first treated from the standpoint of the kinetic theory by Boltzmann, Natanson, and J. J. Thomson about thirty years ago. A masterly discussion is given in Jeans's 'Dynamical Theory of Gases,' p. 213 *et seq.*, 3rd edition. This treatment is applicable, of course with some alteration, to the combination of protons and electrons.

Suppose we have a system consisting of $2\nu_1$ particles of type A, and ν_2 particles of type A_2 formed by the combination of two particles A. Let $\nu = 2(\nu_1 + \nu_2)$: i. e., ν is the total number of particles if there be no aggregation at all.

Then Jeans shows that an encounter between two particles of type A can never result in an association unless the quantity $\frac{1}{2}mv^2 + 2\psi$ (where 2ψ = mutual potential energy of the particles, v relative velocity of the two particles) assumes a negative value. According to Jeans, "this might be effected by collision with a third molecule [*it is not at all*

* Nicholson, Phil. Mag. vol. xlv. p. 193 (1922).

† Eddington, Monthly Notices R. A. S. vol. lxxxiii p. 43.

clear how]. or possibly, if $\frac{1}{2}mv^2 + 2\psi$ were small at the beginning of the encounter, sufficient energy might be dissipated by radiation for $\frac{1}{2}mv^2 + 2\psi$ to become negative before the termination of the encounter."

Jeans continues: "we may leave the consideration of this second possibility on one side for the present, with the remark that if this were the primary cause of aggregation, we should no longer be able to use the equations with which we have been working, since they rest upon the assumption of conservation of energy."

The simplest illustration of association is the binding of a proton (H^+) with an electron. As has been already shown, here it is not possible to leave on one side the action of radiation, for that will be tantamount to staging the play of Hamlet without Hamlet's part; for physical evidences decisively prove that radiation is emitted in all cases of the binding of an ionized atom with the electron. Similarly, absorption of radiation is essential for the splitting up of an atom M into M^+ and e .

In spite of rather uncertain knowledge regarding the rôle of radiant energy in these processes, Boltzmann deduced a formula on the assumption that potential energy exists between two molecules (here we should say between H^+ and e), when the centre of the second (e) lies within a sensitive region surrounding the first (H^+). With this assumption, Boltzmann obtains a formula (formula 503 of page 199, 3rd edition, Jeans's 'Dynamical Theory of Gases') which, with a slight change in notation, can be put in the form

$$\frac{x^2}{1-x^2} P = \frac{kT}{4\omega} e^{-\frac{U}{kT}}, \quad \dots \quad (A)$$

where ω = volume of the sensitive region.

Comparing this with the formula for reaction-isobar derived by me, viz.

$$\log \frac{x^2}{1-x^2} P = -\frac{U}{RT} + \frac{5}{2} \log T + \log \left\{ \frac{(2\pi m)^{3/2} k^{5/2}}{h^3} \right\}, \quad \dots \quad (B)$$

we find that

$$\omega = \frac{1}{4} \left(\frac{h^2}{2\pi m k T} \right)^{3/2}, \quad \dots \quad (C)$$

or r , the radius of the sensitive layer,

$$r = \left(\frac{3}{16\pi} \right)^{1/3} \left(\frac{h^2}{2\pi m k T} \right)^{1/2};$$

i. e., the radius of the sensitive layer varies as

$$\frac{2.95 \times 10^{-6}}{T^{1/2}} \text{ cm.}$$

Fowler's work on the Reaction-isobar of the Ionization of the H-atom.

We now turn to the very interesting and novel method of deriving the law of reaction-isochore by Messrs. Darwin and Fowler. Fowler deduced the law

$$\log \frac{x^2}{1-x^2} P = -\frac{U}{RT} + \frac{5}{2} \log T + \log \left\{ \frac{(2\pi m)^{3/2} k^{5/2}}{h^3} \right\} + B(T), \quad \dots \dots (D)$$

which differs from my formula in the term $B(T)$.

In the thermodynamical way of derivation of the reaction-isochore the roll of radiation is left obscure. The same remark may be applied to Fowler's method of deduction, as has been admitted by Fowler in the following passage (page 13, *Phil. Mag.*, Jan. 1923):—

"In conclusion, a possible objection may be raised to all the reasoning on which these results are based—namely, that it ignores radiation, whereas in fact a change of quantum state in the molecule probably seldom or never occurs without the emission or absorption of the appropriate radiation."

I would like to add to this passage: Likewise ionization of the H-atom, or association of the proton (H^+) and the electron, seldom or never occurs without the absorption or emission of the appropriate radiation.

Fowler continues: "It is, however, perfectly possible to include the temperature radiation in the statistical discussion, as has been shown elsewhere."

In the passage referred to above (*Proc. Camb. Phil. Soc.* vol. xxi. p. 263), Messrs. Darwin and Fowler, starting from the partition-function of a Planck line-vibrator, have given an interesting method of deduction of the laws of black-body radiation; but I find it difficult to agree with the view that this includes the temperature radiation in the statistical discussion. They have treated radiant energy as the energy of a single system, the aether, and neglected matter altogether, except through that somewhat shadowy medium, the Planck line-vibrator. But the problem before us is to find out the exact nature of exchanges between Bohr vibrators and radiant energy which has not been covered in the above treatment.

We now come to the consideration of the term $B(T)$ in Fowler's formula.

The term $B(T)$ represents the energy distribution amongst the Bohr vibrators, and is simply another form of the partition function for the internal energy of the Bohr atom. According

to Fowler this partition function $b(\vartheta)$ is given by

$$b(\vartheta) = \sum_{n=1}^{\infty} n(n+1) \vartheta^{\chi(1-\frac{1}{n^2})}$$

[equation 7.22, p. 20, Phil. Mag., Jan. 1923],

where

$$\vartheta = e^{-\frac{1}{kT}}, \quad \chi = Nh, \quad N = \text{Rydberg number.}$$

As Fowler himself points out, this is a divergent series, and cannot therefore be regarded as solution of the problem. But his suggestion, that the series ought to be cut down to a finite number of terms because the higher terms correspond to orbits with large radii, does not seem to lead out of the difficulty, as imagined by him. For whatever may be the origin of the higher Balmer lines, they are not unknown, nor do they require very special physical conditions for their development. For example, Mitchell could detect 35 lines of the Balmer series within the lower 2000 kms. of the solar chromosphere, and Wood has recorded 21 of them in his vacuum tubes. The difficulties of dealing with the higher orbits on the quantum conditions

$$\oint p \delta q = nh$$

also been emphasized by Nicholson.

To me, the divergence of Fowler's formula (7.22) appears to be a clear indication that Bohr's hypothesis regarding the weight factor of the higher quantum orbits, viz. $p_n = n(n+1)$, is wrong. In fact, any consideration * which tends to assign to the larger quantum orbits larger probability seems to be opposed to physical facts †.

Electrical and Optical Properties of Ionized Gases.

A mass of gas at ordinary temperatures, and not subjected to ultra-violet light, Röntgen light, or any other familiar ionizing agent, possesses no electrical conductivity, because there are no free carriers of electricity present. But if the gas be raised to a high temperature and partially ionized, it will acquire considerable conductivity.

This was pointed out by me in previous papers ‡, and the non-success of previous experiments, as those of J. J. Thomson

* For example, Planck, *Berl. Sitzungsberichte*, p. 407, 1915.

† M. N. Saha, *Phil. Mag.* vol. xli. p. 274.

‡ "On the Ionization of Gases by Heat," by M. N. Saha and P. Günther, *Journ. Dept. Sci. Calcutta University*, vol. iv. See also A. A. Noyes and H. A. Wilson, *Ast. Journ.* vol. lvi. p. 21.

and McLennan, on the electrical conductivity of mercury vapour were discussed in detail. It was shown that these investigators chose a substance which has too high an ionization-potential (10.45 volts), and hence at the temperature employed by them the mass of gas (mercury-vapour) remained practically unionized.

Cæsium is the element having the lowest ionization-potential, and hence I pointed out that this is the element with which success can be expected at temperatures available in the laboratory. Some preliminary experiments undertaken by me at Prof. Nernst's laboratory at Berlin confirmed these expectations. At 1250° C., Cs-vapour was found to have a specific resistance of only 50 ohms, which increased to about 100 ohms when the temperature was lowered to 1050° C. The current could be measured with a milliammeter with a voltage difference of 1 to 2 volts across the ionization-cell containing Cs-vapour, and obeyed Ohm's law throughout the range 1 to 6 volts. These figures are very rough, but they, taken along with the figures for Rb and K (which were found to have increasingly higher resistance), completely confirm the view that the ionization potential is the deciding factor in determining the electrical conductivity of heated vapours.

But great difficulty was encountered when I tried to calculate the conductivity from the Drude-Thomson theory. It was felt that if this theory were applicable to any case, it was the present one. But calculations have not answered to this expectation.

Suppose we have a mass of vapour, say of Cs, which is ionized by heat. Let n_1 denote the number of free electrons or Cs⁺-ions per unit volume, λ_1 and λ_2 the mean free paths, u_1 and u_2 the average velocities of the electrons and the positively-charged particles respectively. Then, according to the Drude-Thomson theory, the conductivity

$$\sigma = \frac{n_1 e^2}{6kT} (\lambda_1 u_1 + \lambda_2 u_2). \quad \dots \quad (E)$$

According to the kinetic theory of gases, if we have a mixture of gases of different kinds (1, 2, ..., r , s , ...), then the mean free path λ_r of any particular type r is given by the expression

$$\frac{1}{\pi \lambda_r} = \sum_{s=1} n_s A_{rs}^2 \sqrt{1 + \frac{m_r}{m_s}}. \quad \dots \quad (F)$$

[see Jeans, 'On the Dynamical Theory of Gases,' p. 268],

where $A_{rs} = A_r + A_s$; the sum of the radii of the "r" and "s" particles, n_s is the concentration of the "s" particle.

In the present case we have to deal with Cs, Cs^+ , and e^- , Cs-particles of course including different types distinguished by the quantum orbits (n_k). Let us neglect all the higher orbits and retain only the fundamental orbit (1_1), a step which will not be acceptable to many, but which is difficult to avoid or improve under the present state of our knowledge. Then

$$\frac{1}{\pi\lambda_1} = n \frac{A^2}{4}, \quad \frac{1}{\pi\lambda_2} = nA^2 \sqrt{2}, \quad \frac{1}{\pi\lambda} = nA^2 \sqrt{2}.$$

Assuming that the degree of ionization is small (i. e., n_1 is small compared with n , the concentration of Cs-atoms), A denotes the radius of Cs-atom, then $\lambda_1 = 4\sqrt{2}A$ (a well-known result) and

$$\lambda_2 = \lambda, \quad u_1 = \sqrt{\frac{3kT}{m}}, \quad u_2 = \sqrt{\frac{3kT}{M}}.$$

Since Cs^+ is $1836 \times A$ (atomic weight) times heavier than m , we see that u_2 is negligible compared with u_1 . This only means that the conductivity is mainly due to electrons.

We have now

$$\sigma = \frac{2\pi e^2}{\sqrt{3}mkT} \frac{1}{A^2} x, \quad \dots \quad (E')$$

where x = fraction ionized.

Now " x " can be calculated from the formula of reaction-isochores.

$$\text{We have} \quad \frac{x^2 P}{1-x^2} = \frac{(2\pi m)^{3/2} k^{5/2}}{h^3} T^{5/2} e^{-\frac{U}{RT}}. \quad \dots \quad (B')$$

$$\text{and} \quad P = n(1+x)kT,$$

$$\text{or} \quad \frac{x^2}{1-x} = \left(\frac{2\pi mkT}{h^2} \right)^{3/2} \frac{1}{n} e^{-\frac{U}{RT}} = \frac{B}{n}; \quad \dots \quad (B'')$$

therefore

$$x = \sqrt{\frac{B}{n}}, \quad \text{or} \quad \frac{B+n}{B+2n},$$

according as " n " is large, or "small" compared with " B ."

The second case will never arise, unless we have to deal with a case of very high temperature and very low pressure (e. g., in the giant stars).

Hence the conductivity

$$\sigma = \frac{(2\pi)^{3/2} (mkT)^{1/2}}{\sqrt{3}} e^2 \exp\left(-\frac{U}{2RT}\right) \frac{1}{\sqrt{n}} \dots (E'')$$

The only thing to notice about this complicated expression is that σ varies inversely as \sqrt{n} concentration.

This is an unexpected result, and is not corroborated by my experiments, for I found that the conductivity diminishes gradually as the vapour-content diminishes. *A priori*, it seems rather paradoxical that the conductivity will vary as $1/\sqrt{n}$.

Therefore, either we cannot calculate the percentage of ionization from the law of reaction-isobar at very low concentrations, or the Drude-Thomson theory of conduction which makes the conductivity proportional to the percentage of ionization, and not to the total number of ionized particles present, fails to give us a true picture of the phenomena.

The Mean Free Path of an Electron in a mass of Ionized Gas.

The cause of this failure is not far to seek. We have to calculate the "free life" of an electron in a mass containing normal atoms of Cs, atoms with higher quantum orbits, and Cs^+ -particles. The mean free path, as deduced in formula (F), is based upon the idea of elastic collisions, which is rather the opposite of what actually takes place. As has been explained in the previous sections, in representing the complicated reactions which occur when a free electron encounters a Cs^+ -atom, or a Cs-atom in normal or higher orbits, the idea of elastic collision is of no avail, the exchanges of energy through radiation must be taken into account.

The same considerations apply to the optical properties of ionized gases discussed by Prof. J. Q. Stewart in a letter to 'Nature,' Feb. 10, 1921, but the discussion is deferred to a future date.

[*Note*: Since the above paper was written, I have been made acquainted, through the courtesy of Messrs. Fowler and Darwin, with a paper by them "On the Intensities of Absorption Lines in Stellar Spectra, etc.," published in the M. N. R. A. S. vol. lxxxiii. p. 403. In this paper Fowler and Milne have given an interesting method of deducing the pressure in the reversing layer by applying a theory of

maximum intensities of subordinate lines which they have worked out. It must be admitted that the idea is pregnant with great possibilities, and would lead to important results if the correct partition function $b(\mathcal{S})$ can be discovered. But Fowler and Milne have used the function $b(\mathcal{S})$ mentioned above, which, being a divergent series, is rather unconvincing.—M. N. S.]

LVIII. *On the Colour of the Sea.* By K. R. RAMANATHAN, M.A., Assistant Lecturer in Physics, University College, Rangoon, Burma*.

1. Introduction.

IN a recent paper †, Prof. C. V. Raman has put forward the theory that the deep blue colour characteristic of the larger part of ocean waters is due to the molecular scattering of light in water, and supported it by calculations of the intensity and quality of the light returned from deep water. He has shown that pure, dust-free water scatters light in accordance with a formula originally deduced by Einstein for the critical opalescence of fluids, and that molecular scattering by itself without the aid of any extraneous agency is sufficient to account for the return of a part of the incident light. The following investigation was undertaken in order to test how far actual sea-water comes up to the ideal dust-free condition, and to find how the waters in seas showing different colours vary from one another.

2. Theoretical Discussion.

Preliminarily, it is useful to consider what intensity and colour we should expect from a *perfectly absorptionless* dust-free ocean of infinite depth. In such a case, the diminution of intensity of light in its passage through the medium would be wholly accounted for by molecular scattering. Since there is no transformation of the incident energy, it would be entirely thrown back, and the returned light would be of the same quality as the incident ‡. Since the scattering coefficient varies inversely as the fourth-power of the wave-length, the depth of the medium responsible for the return of a certain percentage of blue light would be smaller than that responsible for the return of the same

* Communicated by Prof. C. V. Raman, M.A., D.Sc.

† C. V. Raman, Proc. Roy. Soc. A, vol. ci. p. 64 (1922). See also 'Molecular Diffraction of Light,' Calcutta University Press, 1922, chapter v.

‡ *Vide* Schuster, 'Theory of Optics,' Second Edition, p. 271.

percentage of red light. Selective absorption, however, would modify the condition of affairs. The light of those wave-lengths for which the medium exercises a selective absorption would be gradually diminished in intensity as the light penetrates into the medium, and if the absorption is at all considerable, there would be very little of these radiations returned. Now, water is known to exercise a selective absorption in the red which gradually decreases as we proceed into the region of shorter wave-lengths. The most extensive measurements of absorption coefficients for water that we possess are those of Count Aufsess* between wave-lengths $658\mu\mu$ and $494\mu\mu$. Recently, W. H. Martin† has measured the absorption coefficients of water repeatedly distilled *in vacuo* for the mercury lines $578\mu\mu$, $546.1\mu\mu$, and $435.8\mu\mu$. As has been pointed out by Martin, there is an error in Aufsess's measurements, as he neglected to take into account the loss of light on reflexion at the glass surfaces at the ends of the absorption-tube. However, considering the length of tube which Aufsess employed (5.5 metres), the relative error involved is not large in the region of the red where the absorption is large. We shall therefore adopt Aufsess's values for the absorption coefficients in the red. In Table I. are shown the experimental values of the extinction coefficient γ , defined by $I = I_0 e^{-\gamma x}$, where I_0 is the intensity of a parallel beam of incident light, and I is the intensity after traversing a thickness x of water. In the fourth column are shown the values of the extinction coefficients, if the extinction were due *solely* to molecular scattering. These are calculated according to the formula

$$\alpha = \frac{8\pi^3}{27} \frac{RT\beta}{N\lambda^4} (\mu^2 - 1)^2 (\mu^2 + 2)^2 \dagger.$$

* Count Aufsess, *Ann. der Physik*, vol. xiii. (1904).

† W. H. Martin, *Journ. Phys. Chem.* xxvi. p. 471 (1922).

‡ *Vide* C. V. Raman, *loc. cit.* and 'Molecular Diffraction of Light,' chapter iv. p. 52.

This is derived on the assumption that the light scattered in a direction perpendicular to the incident beam is perfectly polarized. As a matter of fact, the transversely scattered light shows a defect in polarization. In addition to the polarized "Einstein scattering," there is an additional scattering due to the anisotropy of the molecules, which for the most part is unpolarized. If we take the latter also into account, the formula for the coefficient of extinction becomes

$$\alpha = \frac{2\pi^3}{9} \frac{RT\beta}{N\lambda^4} (\mu^2 - 1)^2 (\mu^2 + 2)^2 \left\{ \frac{4}{3} + \frac{r}{1-r} \right\},$$

where r is the ratio of the weak component to the strong in the transversely scattered light, and the values of the extinction coefficients come out to be 8.2×10^{-6} , 1.08×10^{-5} , 1.38×10^{-5} , 1.76×10^{-5} , and 5.0×10^{-5} for the wave-lengths given above.

TABLE I.

Wave-length.	Absorption coefficient.	Author.	Extinction coefficient due to scattering alone.
658.....	3.2×10^{-3}	Aufsess.	7.5×10^{-6}
612.....	2.33×10^{-3}	Aufsess.	9.9×10^{-6}
578.....	6.4×10^{-4}	Martin.	1.3×10^{-5}
546.1.....	3.4×10^{-4}	Martin.	1.6×10^{-5}
435.8.....	1.2×10^{-4}	Martin.	4.3×10^{-5}

In the red, yellow, and green, up to $546 \mu\mu$, practically the whole of the extinction is due to absorption, while in the blue and the violet, scattering takes away an appreciable part. The intensity of the incident radiation is reduced to one-half at a depth of approximately 2 metres for $658 \mu\mu$, 10 metres for $578 \mu\mu$, 20 metres for $546 \mu\mu$, and 60 metres for $435.8 \mu\mu$. Taking primary scattering alone into account and considering the directions of incidence and observation to be vertical, the total observed brightness due to an infinite depth of water can be easily shown to be $B/\gamma\lambda^4$ *, where the scattering coefficient in a transverse direction has the value

$$B = \frac{\pi^2}{18} \frac{RT\beta}{N\lambda^4} (\mu^2 - 1)^2 (\mu^2 + 2)^2.$$

We can now see why the returned light should be specially deficient in the red, yellow, and green. The increase in absorption goes hand in hand with the decrease in scattering, and the two together serve practically to eliminate the longer wave-lengths. The following Table gives the course of values of $B/\gamma\lambda^4$:—

λ in $\mu\mu$.	658.	612.	578.	546.	436.
$B/\gamma\lambda^4$	1.4×10^{-4}	2.5×10^{-4}	1.2×10^{-4}	2.8×10^{-5}	2.1×10^{-5}

In order to obtain the resultant colour of the sea, we have only to compound the effects of different wave-lengths in their proper proportions. The intensities for the different wave-lengths throughout the visible spectrum can be obtained

* C. V. Raman, *loc. cit.* If the anisotropic scattering is also taken into account this would become $B(1+r)/\gamma\lambda^4$.

by the above formula, and their colour effects expressed in terms of the spectrum colours $630.2 \mu\mu$, $538.1 \mu\mu$, and $456.9 \mu\mu$, using the values given by the late Lord Rayleigh in his paper on "The Colours of Thin Plates"*. The resultant colour is found to have the composition 1.56×10^{-3} red, 2.49×10^{-2} green, and 9.53×10^{-2} violet, and approaches the spectrum colour $475.0 \mu\mu$, being very near the indigo of the second order in the colours of thin plates. The inclusion of secondary scattering would reduce the effective depth of the sea from which the scattered light returns; it would also serve to further diminish the intensities of the red and yellow, for which the absorption is strong.

It is obvious that the presence of any dissolved matter giving rise to extra absorption in any particular region of the spectrum would cause a corresponding diminution of the intensity of the returning light in that region of the spectrum.

Let us now consider the effect of suspended matter. It would give rise to an additional scattering, and hence the depth to which the light would penetrate would get reduced. If the particles are small in comparison with the wave-length, the scattering would still be proportional to λ^{-4} . If present in small quantities, there would be little effect on the characters of the returned light, but if present in larger quantities, there would be less chance for the absorptive properties of the medium to have their full play, and as a consequence, the light would be more mixed with the longer wave-lengths, and the blue colour of the sea would tend to get less saturated. As the particles get larger in comparison with the wave-length, the scattering in the direction of primary propagation will be specially favoured, and also, instead of being proportional to, it would tend to be independent of the wave-length. Since the light of longer wave-lengths can return by other means than molecular scattering, their relative proportion in the light returned would increase more and more as the quantity of suspended matter increased, and the sea would get greenish blue, green, whitish green, and finally white. However, as we shall see, when the quantity of matter is not large, the light scattered against the direction of the incident light is but an insignificant fraction of that scattered in the direction of the incident light.

* Lord Rayleigh, 'Scientific Papers,' vol. ii. table i. p. 503.

III. *Examination of Light scattered by Sea-water.*

Samples of sea-water were collected in carefully cleaned stoppered bottles from the Bay of Bengal in two voyages between Calcutta and Rangoon from places where the sea exhibited different colours varying from deep indigo to green. The bottles were securely placed in a galvanized-iron wire cage tied to the end of a wire, and the cage was thrown into the sea from the lower deck of the ship near the bow. The bottles were rinsed out with the sea-water five or six times before each sample was finally collected. The colour of the sea at the time was also noted. In observing the proper colour of the sea, a nicol is helpful in abolishing sky-reflexion, as has been pointed out by Raman.

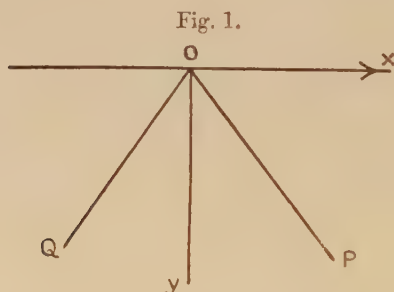
The scattering of light by the different specimens was examined by concentrating a beam of sunlight at the centre of each bottle in a dark room. The back surfaces of the bottles were painted black, in order to be better able to see the tracks. Table II. gives the details regarding the scattering in different specimens. The intensities of the transversely scattered light given in the last column are expressed in terms of that in dust-free distilled water.

TABLE II.

Specimen No.	Date and time of collection.	Approximate position of ship at time of collection.	Colour of Sea.	Appearance of transversely scattered light.	Intensity of transversely scattered light.
A	1.10.22. 10.30 A.M.	...	Indigo.	Indigo with visible particles.	1.68
B	4.11.22. 8 A.M.	Lat. 19° 40' N. Long. 90° E.	Greenish blue.	Blue—Few visible particles.	1.4
C	4.11.22. 11.15 A.M.	Lat. 19° 10' N. Long. 90° 30' E.	Deep blue.	Indigo—A few large particles.	1.5
D	4.11.22. 4 P.M.	Lat. 18° 30' N. Long. 91° E.	Indigo.	Indigo—A few large particles.	1.5
E	5.11.22. 7.30 A.M.	...	Greenish.	Blue with large thin flakes of something floating.	1.65
F	5.11.22. 11.40 A.M.	Lat. 15° 30' N. Long. 94° 15' E.	Green.	Bluish white—Motes visible.	1.6 Blue. 2.0 Red.

The colour of the transversely scattered light in specimens A, C, and D approached that of dust-free distilled water. The intensity of the transversely scattered light from A was compared with that from dust-free distilled water, by sending a concentrated beam of light through the two bottles in succession and making use of an Abney rotating disk-photometer for equalizing the intensities. Correction was made for the loss of light on reflexion at the glass surfaces. In the case of the other specimens, the comparisons were made by inserting perpendicularly in the path of the stronger beam a number of thin, selected microscope slides, so as to equalize the apparent brightnesses.

When the direction of observation was OP instead of O*y*, the suspended particles were much more in evidence

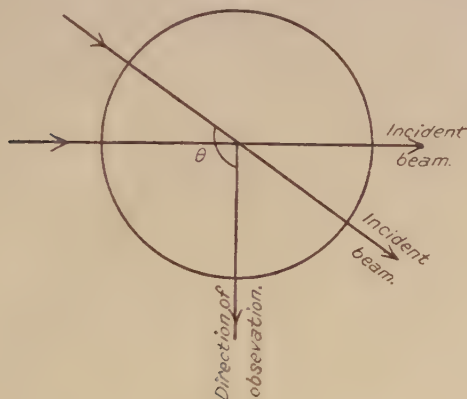


and the colour was more reddish. On the other hand, in the direction OQ, the particles were less conspicuous and the colour even more saturated than along O*y*. This is what we should expect if the particles are large in comparison with the wave-length. Since, in the case of the sea, we are primarily concerned with the light proceeding backward, we should consider the intensity of the scattered beam in a direction against that of the incident beam. Comparisons of the intensity of scattering in different directions were made by the method indicated below (fig. 2).

Two beams of sunlight were concentrated one above the other at the centre of the bottle by two lenses of the same focal length (nearly 100 cm. and achromatic) in directions making a definite angle with each other. The scattering was observed in a direction at right angles to one of the beams, and the apertures of the lenses were adjusted by suitable shutters so that the tracks appeared of equal intensity. The inverse ratio of the areas of the apertures

gives the ratio of the intensities scattered in the two directions. Since the depth of layer contributing to the luminosity is different in the two cases, being proportional to $\text{cosec } \theta$, where θ is the angle indicated in the figure, the

Fig. 2.



luminosity observed in the direction θ was multiplied by $\sin \theta$ in order to get the effect due to the same thickness of radiating column. Table III. gives the relative intensities of scattering in different directions in specimen A :—

TABLE III.

S_θ = Scattering in specimen in direction θ .

σ_θ = Scattering in dust-free distilled water in direction θ .

θ .	S_θ/S_{90° .	$S_\theta/\sigma_{90^\circ}$.	$\sigma_\theta/\sigma_{90^\circ}$.
30°	1.12	1.88	1.60
45°	0.91	1.53	1.40
60°	0.87	1.46	1.20
90°	1.00	1.68	1.00
120°	2.54	4.26	1.20
150°	5.5	9.2	1.60

The values in the fourth column are calculated on the assumption that the scattering by a pure, dust-free liquid in a direction θ is given by $\sigma \left(1 + \frac{1-r}{1+r} \cos^2 \theta \right)$, where σ is the scattering in a direction perpendicular to the incident beam. It will be seen that in the particular specimen of sea-water, when θ is greater than 90° , the scattering increases with

increasing values of θ at a much more rapid rate than in dust-free water, and that although the transverse scattering is 1.68 times that of dust-free water, the values of the scattering in directions 30° and 45° are not appreciably different from those of pure water. From the progress of values, we may expect that with smaller values of θ , the scattering will be practically the same as for dust-free water.

This result is of great importance in its bearing on the colour of the sea. Suspended matter, when present in small quantities, although it considerably increases the total scattering, contributes but little to the scattering against the direction of the incident light. The increase in the total scattering would reduce the transparency of the medium, but so long as the defect of transparency due to this cause is small compared with the absorption proper, the quality and intensity of the returned light would not be much affected by the presence of such matter.

Table IV. gives similar data for specimens B, C, and F. With a view to bringing out the difference in the distribution of scattered light for red and blue, comparisons were made after introducing ruby-red and deep-blue glasses respectively in the paths of the scattered beams.

TABLE IV.

θ .	S_θ/S_{90°					
	B.		C.		F.	
	Red.	Blue.	Red.	Blue.	Red.	Blue.
30°	1.01	1.22	1.06	1.13	0.88	1.03
45°	1.10	1.05	1.13	1.13	0.95	1.02
60°	0.90	1.00	0.97	0.97	0.83	0.95
90°	1.00	1.00	1.00	1.00	1.00	1.00
120°	1.65	1.52	1.55	1.60	2.09	1.63
135°	3.92	2.45	3.18	2.76	5.05	3.98
150°	9.0	6.0	8.3	6.3	16	9.4

It will be observed that in all cases the red gets more and more prominent as θ increases.

We shall now examine whether we can find in the varying amount of suspended matter a sufficient cause for the difference in the colour of the seas. For example, the specimen C was collected from a deep blue sea, while specimen B was from a sea which showed greenish blue,

and F from a place where the sea was green. Compared with C, the intensity of scattering in F, although nearly equal for the blue in a transverse direction, is greater by 30 per cent. in the red, and the asymmetry of scattering also is greater. Thus the total scattering of unit volume of specimen F is greater than that of C, and the colour is also much less blue. Both these causes would contribute to a less deep penetration of the light into the medium (relatively more so for longer wave-lengths), and thus the absorption would have less chance of playing its full role, so that the blue, indigo, and violet would be mixed up with a greater proportion of the longer wave-lengths. We should therefore expect the sea to be brighter and of a less saturated blue, but not the distinct green that it actually was. We have therefore to look for some other cause for the green colour. The point is even clearer if we compare the behaviour of B and C. B scatters actually less than C in a transverse direction (nearly 10 per cent. less); and although its track was not indigo like that of C, the asymmetry of scattering was of practically the same order of quantities, and yet the colour of the sea from which it was collected was *greenish blue*.

IV. *Fluorescence of Sea-Water.*

The reason for the difference was found on examining the transversely scattered light from a horizontal track for polarization by means of a double-image prism. When the double-image prism is so oriented as to transmit vertical and horizontal vibrations, the light corresponding to the horizontal vibrations does not actually vanish even in the case of dust-free distilled water*; but in this case the two beams are of practically the same colour, while in the case of specimens B and F the weaker component was found to be distinctly *greenish*. The contrast came out sharper when the two beams were equalized for brightness by means of a suitably oriented nicol placed behind the double-image prism, and a double thickness of blue glass was introduced in the path of the incident beam. The green was now much brighter than the blue and the colour contrast sharper. This was evidently a case of *fluorescence*.

To make quite sure, the following arrangement was adopted:—In the path of the incident beam were placed a double thickness of cobalt-blue glass with an absorption cell

* W. H. Martin, Journ. Phys. Chem. vol. xxiv. p. 478 (1920). C. V. Raman, 'Molecular Diffraction of Light,' chap. iv.

of a solution of potassium permanganate which cut off everything except the extreme blue and violet and a patch in the extreme red. The light was then passed through the sea-water, and the track therein was examined through a prism with its refracting edge horizontal. In addition to the blue and violet, the green was also conspicuously present. Yellow and red were present, but were very faint. Specimen F showed the effect best, B and E came next, and then C and D. The fluorescence was certainly present even in the last two specimens, though it was very weak.

Since the incident light did not contain any ultra-violet, the fluorescence should be excited by the blue and violet. This implies an extra absorption of the blue and the violet. A sea whose water shows the fluorescence would thus appear green, not only because there is a return of green light due to fluorescence, but also as there would be less of the blue and violet returning. As we have seen, that water looks most green which shows the most intense fluorescence, and the water gets more and more towards indigo as the fluorescent material gets less and less.

The transition from the indigo of the deep sea far from land to blue and green may thus be due either to the increase in the amount of suspended matter present, or to the presence of some fluorescent material (most probably organic) which not only causes a return of the green and longer wave-lengths, but also produces a greater absorption of the blue and the violet. The second cause is apparently the more important.

V. Summary.

The paper contains a discussion of Raman's theory of the colour of the sea with observations on the scattering of light by different specimens of sea-water from the Bay of Bengal.

(i.) It is shown that an ocean of pure dust-free water would, owing to the effects of molecular scattering and absorption, return light of an indigo-blue colour. The presence of *small* quantities of suspended matter would not appreciably affect the colour. With increasing quantities of suspended matter the colour would change to bluish, green, greenish white, and white.

(ii.) The transverse scattering from different specimens of sea-water has been compared with that of dust-free vacuum-distilled water. The water from the deep blue sea scatters light of nearly the same colour as dust-free water, and the intensity of the transversely scattered light is also of the same order.

(iii.) The intensity of scattering in different directions from different specimens of sea-water has been studied. The effect of dust is negligible so far as scattering against the direction of the incident light is concerned.

(iv.) The variation of the dust-content is found to be insufficient to explain the changes of the colour of the sea from place to place. An important reason for the colour changes has been traced to the presence of varying amounts of some fluorescent material present in the sea. It is pointed out that this fluorescence also implies a greater absorption in the blue and violet involving a diminution of intensity at this end of the spectrum in the light returned from the sea.

In conclusion, I would express my most sincere thanks to Professor C. V. Raman for his stimulating interest in the work.

Rangoon,
Feb. 10, 1923.

LIX. *The Motion of Electrons in Hydrogen under the action of Crossed Electric and Magnetic Fields.* By R. N. CHAUDHURI, M.Sc., Ph.D. (London) *.

[Published by permission of the Radio-Research Board.]

Introduction.

IN some previous work (by Richardson and Chaudhuri † ; and Chaudhuri ‡) on the motion of electrons in different gases, it was found that the initial current flowing from the cathode to the anode was diminished by applying a magnetic field perpendicular to the direction of the electric intensity : and the percentage of the residual current was directly proportional to the pressure (at least well up to 10^{-2} mm.). We drew the conclusion that the residual current was mostly due to the collision of electrons with gas molecules, and the mean free path of the electrons in these gases was found to agree fairly well with that deduced from the kinetic theory of gases. But in the case of hydrogen, the percentage of residual current was at first found to be NOT directly proportional to the pressure, nor did the

* Communicated by Prof. O. W. Richardson, F.R.S.

† Phil Mag. vol. xlv. p. 337 (1923).

‡ *Suprà*, p 461.

values at any particular pressure remain constant when larger initial currents were taken. In order to study this effect thoroughly in hydrogen the following investigation was undertaken.

Principle of the Method.

In the present case, the source of electrons was a hot tungsten filament, surrounded by a concentric cylindrical anode. If in a thermionic tube like this, an electric field of potential difference V is applied between the hot wire and the anode, and a magnetic field H acts parallel to the wire and so perpendicular to the direction of electric intensity, then, when H is greater than a certain critical value, the electrons will describe a path round the hot wire in such a way that the maximum distance r from the axis will be given by

$$H^2 = \frac{8V \log r/a}{e/m \cdot r^2 \cdot \log b/a} + \frac{8V_i}{e/m \cdot r^2} \quad \dots \quad (1)$$

where b , a are the radii of the cylinder and wire respectively, and V_i the average energy of the electrons at the point of emission.

Taking the values we had in our case, viz, $b=1.00$ cm., $a=0.005$ cm., and $V_i=1.5$ volts, V , the accelerating potential, $=4.5$ volts.

$$H^2 = \frac{37.8 \log r/0.005}{r^2} + \frac{67.5}{r^2} \quad \dots \quad (2)$$

Thus, if the magnetic field is gradually increased from 0, the current between the wire and the anode will remain constant up to a certain value of H , then it should fall suddenly to zero as the magnetic field is increased slightly. This will only be possible if all the electrons are coming out with zero or a constant velocity, and *when there is no gas present*. Thus in a perfect vacuum 14.1 units of magnetic field will stop all the current between cathode and anode if electrons are coming out with zero velocity, and 16.0 units if they are coming out with energy corresponding to 1.5 volts—so that if we use a larger magnetic field than this the electrons will have no chance of reaching the anode.

But if, however, there is some gas present, the magnetic field will not stop the current altogether, for a number

of electrons will reach the anode by collision with gas molecules during its passage. Or this residual current might be due to heavy ions formed by electrons combining with gas molecules, and the magnetic field being insufficient, the heavy ions will reach the anode. If the residual current is due to the collisions only, we should be able to get an estimate of the mean free path of an electron in this gas. If, however, the mean free path does not agree with that found otherwise, we can conclude that a certain fraction of the residual current is carried by heavy ions.

Description and Arrangement.

The description of the apparatus used in this experiment has been given in the previous paper (*loc. cit.*) page 342. The only change that has been made in this paper is that instead of the big electromagnet used there, we have a pair of Helmholtz coils which gives the desired magnetic field. The tube is placed half-way along the axis of the coils so that the magnetic field at the centre is uniform and exactly parallel to the length of the hot wire. The filament used here is of tungsten (3 cm. length and .01 cm. diameter), and the cylindrical anode of copper of 4.0 cm. length and 2.0 cm. diameter. They are inserted in the glass tube in such a way that the filament is axial to the anode, and both the ends of the wire are well within the cylinder. The magnetic field is measured by a fluxmeter and checked against the calculated value from the current passing through the coils. The temperature of the filament was found from the Richardson equation

$$i = AT^{\frac{1}{2}}e^{-b/T},$$

and also by measuring the resistance of the filament and comparing with Langmuir's data. Both these methods gave very nearly the same temperature.

Another point of difference in this paper was the use of a less sensitive galvanometer and a micro-ammeter, besides the sensitive one used previously. This was done in order to avoid any mistake that might arise in changing the resistance of the circuit by shunting the sensitive galvanometer for higher values of the initial saturation current. All these galvanometers are arranged in such a way that each could be put into the circuit as desired.

Experimental Results.

After joining the thermionic tube with the pump and P_2O_5 bulb, the coils were placed in such a way that the field was parallel to the hot wire. Care was taken to avoid as much as possible any greased taps in the apparatus, so that any vapour arising from them might not interfere with the results. The gas inside the tube was pumped out and the filament was heated very gradually to 2 amps., and all the time the pump was kept in action. In this way all the occluded gases from the filament were taken out. When the pressure inside the apparatus kept constant for three or four hours, the electrode was bombarded by connecting it and the filament with an induction coil, and the evolved gases were pumped out. When there is no more evolution of gas, the tube is in a proper working condition. Now, hydrogen is let in by heating the palladium tube: the whole tube is filled several times with hydrogen and pumped out again before any readings are taken in this gas. All this time, of course, the liquid air is kept in the trap LL, so that mercury, or grease or any other condensable vapour may not come into the apparatus. The spectrum of the gas was also examined, and when only the hydrogen lines were observed, the readings were taken.

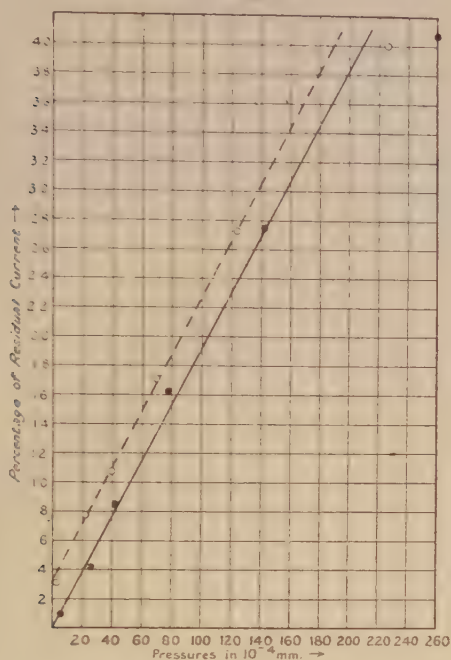
Effect of Condensable Vapour.

If no liquid air is kept in L, it is found that there is a residual current in the presence of the magnetic field (170), even at zero pressure, but as soon as liquid air is introduced, this current falls down, though the pressure inside the apparatus is not visibly decreased. This effect of condensable vapour has been noted in the previous paper. It is well shown in fig. 1 where the broken line is drawn through the observational points taken without the liquid-air trap and the full line through those taken with the liquid air in operation. In this case the two lines are parallel showing the effect of the presence of a constant excess pressure, not recorded by the McLeod gauge, of some vapour when the liquid-air trap is not working.

Effect due to altering the Temperature of the Filament.

It was noticed during some of these investigations that the percentage of the residual current at a given pressure under the same electric and magnetic fields did not keep

Fig. 1.



constant when the initial saturation current was increased by raising the temperature of the filament. This will be seen from the following:—

TABLE I.

Initial current in scale-divisions.	Percentage of Residual Current at pressures:—				
	40×10^{-4} mm.	80×10^{-4} mm.	120×10^{-4} mm.	160×10^{-4} mm.	180×10^{-4} mm.
3200	4.42	8.84	13.22	17.6	19.8
320	7.8	15.4	23.0	30.2	...

It will be seen from the above that the percentage of the residual current is larger when the saturation current is decreased, *i. e.* when the temperature of the filament is lower, all the other conditions in the experiment remaining the same.

It is of importance to know whether these lower values of the residual current at higher temperatures are due to the wire itself or to some change produced in the gas by the high temperature of the filament. If it were found that the residual current did not go back to its original high value at lower temperatures, after the filament had been once heated to a higher temperature, then we might conclude that the lower percentage of the residual current was caused by some change produced in the filament, such as emission of heavy particles at lower temperatures, which died off as the temperature was raised—this kind of phenomenon is known to exist in new wires. But in the case of hydrogen, it was found invariably that the higher percentage of the residual current repeated itself even after the filament had been heated very strongly. This will be seen from the following results.

TABLE II.

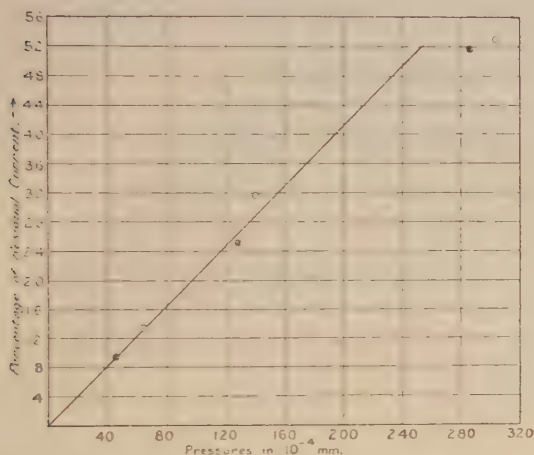
Before.			Temperature increased to give 100-150 times the initial current recorded here.	After.		
Pressure.	Initial current without magnetic field.	Percentage of residual current.		Pressure.	Initial current.	Percentage of residual current.
294×10^{-4}	340	53.0		286×10^{-4}	340	51.8
140 "	350	31.4		128 "	320	25.0
64 "	350	13.4		48 "	350	9.4
15.5 "	340	2.6		14 "	350	2.59

The readings on the left side of the above table were taken first, after which the filament temperature was raised to give a very high current, and then the readings on the right-hand side taken. These values are plotted in fig. 2, and it will be noticed that both the values of the percentage of the residual current under the action of the fields agree very well.

This shows, at least, that these higher values at lower temperatures are not due to the emission of heavy particles at lower temperatures of the wire, for the heavy emission is stopped completely when the filament is kept at a high temperature for a time. The probable cause of these lower values is that hydrogen is dissociated by the hot tungsten which occurs at about 1400°C ., *i. e.* at about the same temperature as when the emission from the hot wire begins to be perceptible. So, it is quite possible that when the filament

temperature is raised to give large initial saturation currents, more of the gas is dissociated, and the electrons are colliding with molecular as well as atomic hydrogen. And if the residual current is due to that carried by colliding electrons, then it should depend on the mean free path of the electrons

Fig. 2.



in the gas in the molecular or atomic state: the mean free path being larger when the gas is in the atomic state, we should expect the residual current to be smaller at higher temperatures of the wire. We shall return to the discussion of this later.

Variation of the Residual Current with the Temperature.

In order to get an idea about the exact amount of residual current at any particular temperature of the wire, the following results were obtained. The higher values of the residual current were recorded by the less sensitive galvanometer g , and the micro-ammeter. Temperatures were measured by the resistance data and compared with those obtained from the Richardson equation. Hydrogen was let in by heating the palladium tube, and the wire was kept hot; this was repeated several times till the tube was "seasoned" for the experiment. Then, finally, the gas was pumped out to a very low vacuum and fresh hydrogen was introduced before taking the readings. Liquid air was maintained during all these experiments.

TABLE III.

Accelerating potential = 4.5 volts.

(1) Average Temperature of the filament = 1730° K.

Pressure inside the tube.	Initial Current <i>without</i> magnetic field.	Residual Current <i>with</i> magnetic field.	Magnetic field.	Percentage of Residual Current.
334×10^{-4} mm.	120 G	57.5 G	174	47.9
162 "	125 "	31.0 "	170	29.8
67 "	131 "	14.0 "	172	10.7
33 "	126 "	6.0 "	172	4.7

(2) Average Temperature = 1750° K.

294×10^{-4} mm.	340 G	180 G	170	53.0
160 "	324 "	100 "	166	30.8
68 "	334 "	44 "	172	13.1
31 "	332 "	17 "	172	5.1

(3) Average Temperature = 1920° K.

388×10^{-4} mm.	220 g	72 g	168	32.7
330 "	230 "	64 "	172	27.8
158 "	235 "	34 "	170	14.5
67 "	225 "	12 "	172	5.3
29 "	225 "	5 "	170	2.2

(4) Average Temperature = 1970° K.

380×10^{-4} mm.	480 g	123 g	172	25.6
326 "	485 "	108 "	170	23.3
156 "	490 "	53 "	172	10.8
66 "	478 "	21 "	172	4.4
29 "	485 "	9.5 "	170	1.9

(5) Average Temperature = 2015° K.

372.5×10^{-4} mm.	10.5×10^{-6} amp.	218 g	170	18.7
322 "	10 "	182 "	170	16.4
152 "	10 "	87 "	170	7.8
65 "	10 "	37 "	172	3.2
27 "	10 "	15 "	170	1.3

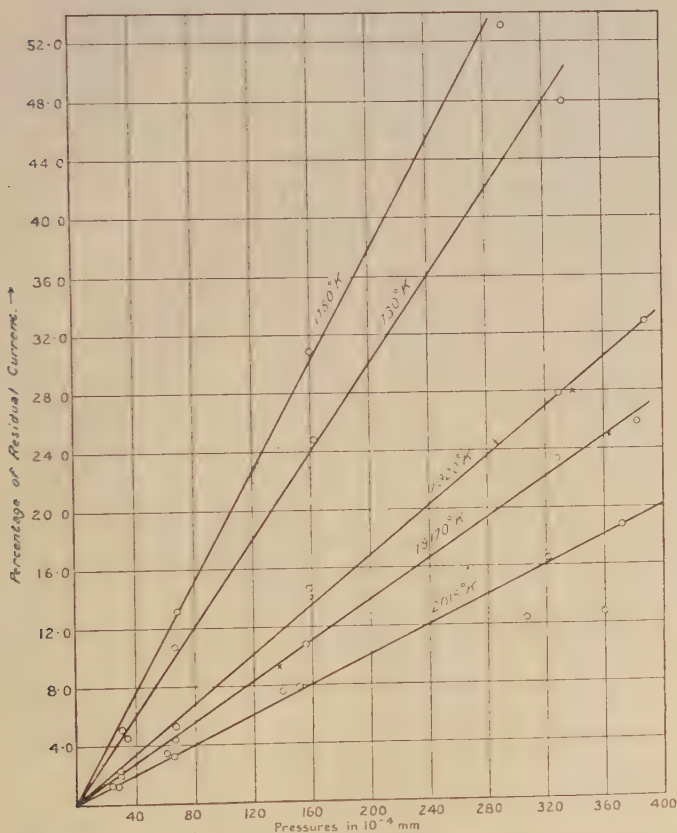
(6) Average Temperature = 2045° K.

360×10^{-4} mm.	20×10^{-6} amp.	280 g	168	12.7
306 "	20 "	275 "	170	12.4
140 "	21 "	180 "	170	7.6
60 "	20 "	77 "	174	3.5
24 "	20 "	30 "	158	1.3

All these points are plotted in fig. 3. It will be seen here that as the temperature of the filament is increased, the

percentage of the residual current decreases gradually to a limiting value. The points marked as **X** are obtained on repeating, after the filament has been raised to a higher temperature. In the above, the lower values of the residual current at temperature 1730° K. are probably due to some

Fig. 3.



error in reading the small deflexion. However, it will be seen here that the percentage of residual current under the action of fields at 1750° K. is 18.9, whereas under the same conditions at temperature 2015° K. it is only 5.1.

Discussion.

It was shown in a previous paper that such a large percentage of residual current under the magnetic field could be explained on the assumption that the electrons from the
Phil. Mag. Ser. 6. Vol. 46. No. 273. Sept. 1923. 20

hot wire find their way to the anode after a repeated number of collisions with the gas molecules. It might also be that a certain fraction of this residual current was due to the electrons combining with gas molecules and forming heavy ions. Anyhow, if the first supposition is true, we shall get an approximate value of the mean free path of an electron in this gas, from these data.

The path of an electron inside the thermionic tube, under the action of a magnetic field acting perpendicular to the electric intensity, can be found out from the equation (1), and the length of the path is approximately equal to that of a cardioid, of which the distance between the cusp and the middle point of the curve is equal to the maximum distance r of the path of the electron from the hot wire.

But the length of the cardioid

$$s = 2 \int_0^\pi a \{ (1 + \cos \theta)^2 + \sin^2 \theta \}^{\frac{1}{2}} d\theta = 2 \times 4a \left[\sin \frac{\theta}{2} \right]_0^\pi = 8 \cdot a \\ = 4 \times \text{maximum distance } r.$$

In our case, the magnetic field was about 170, and the applied potential between the filament and the anode was 4.5 volts. Besides we have to take into consideration the potential drop of 1 volt per cm. along the filament, due to which we shall have a total drop of 3 volts (because the filament is of length 3 cm.) Thus at the middle point of the filament we shall have a drop of 1.5 volts, which will thus give a total accelerating potential of 4.5 + 1.5 = 6.0 volts. Taking this latter value of V , we get from equation (2)

$$r = .085 \text{ cm.}$$

$$\therefore \text{length of the path } (s) = 4 \times .085 = .34 \text{ cm.}$$

Now, the fraction which collides in path x is $e^{-x/\lambda} \frac{dx}{\lambda}$, so that the fraction which collides in the total path s

$$\xi = \int_0^s e^{-x/\lambda} \frac{dx}{\lambda} \\ = 1 - e^{-s/\lambda},$$

$$\therefore \lambda = - \frac{s}{\log_e (1 - \xi)}.$$

In the above equation, we know s and ξ , and so we can find λ .

Thus, corresponding to the topmost part of the curve $\xi_1 = .189$ we get the mean free path of the electron at 10^{-2} mm. pressure

$$\lambda_1 = -\frac{s}{\log_e(1-\xi_1)} = -\frac{.34}{\log_e .811} = 1.63 \text{ cm.},$$

i. e., the mean free path λ_1 at 760 mm. and $0^\circ \text{ C.} = 2.15 \times 10^{-5}$ cm. Similarly, corresponding to the lowest curve, the mean free path at 10^{-2} mm.

$$\begin{aligned} \lambda_2 &= -\frac{s}{\log_e(1-\xi_2)} \\ &= \frac{.34}{\log_e .949} = 6.54 \text{ cm.}, \text{ where } \xi_2 = .051, \end{aligned}$$

i. e., m.f.p. at 760 mm. and 0° C. is 8.5×10^{-5} cm.

Thus the mean free path of an electron, obtained by this method, in hydrogen increases from 2.15×10^{-5} at about 1740° K to 8.5×10^{-5} cm., at 2015° K . Now, the mean free path of an electron in a gas in the atomic state is also about four times that in the molecular state (assuming the diameter of the molecule to be twice the diameter of the atom). What happens, therefore, in our case, is that the electrons are colliding with gas molecules when the temperature of the filament is low and with atoms when the temperature is high—the molecular hydrogen being dissociated into the atomic state by the hot filament. At temperatures between these two limits, the electrons are colliding with molecules as well as atoms.

The mean free paths obtained by this method as compared with those obtained in the kinetic theory on the assumption of the diameters of electrons and molecules and atoms, are

	Kinetic Theory.	This Method.
For molecules	6.3×10^{-5} cm. at 760 mm.	2.15×10^{-5} cm. at 760 mm.
„ atoms ...	25.2 „ „	8.5 „ „

The smaller values of the m.f.p. in hydrogen might be due to the fact that in our calculation above we have taken the whole of the residual current to be due to the electrons colliding with gas molecules and reaching the anode as electrons. If, however, a certain fraction of this residual

current be due to the heavy ions, then ξ will be smaller and λ will be bigger. Sir J. J. Thomson has found some evidence of the existence of heavy ions in hydrogen, so that it is quite possible that the whole of the residual current is not carried by electrons only. Besides, we have assumed that the temperature of the gas surrounding the hot wire is zero, but it actually varies from point to point along the radius of the anode.

Summary.

(1) It has been shown in this paper that the percentage of the residual current in hydrogen depends to a large extent on the temperature of the hot filament.

(2) The residual current comes back to its value at any particular temperature, even after the filament has been heated to give 100–150 times its initial saturation value.

(3) The residual current under the action of the crossed fields is proportional to the pressure up to at least 2×10^{-2} mm.

(4) The current is probably carried mainly by electrons colliding with gas molecules at the lower temperatures, and with dissociated atoms at the higher temperatures.

(5) The mean free paths of the electron in hydrogen in the molecular as well as in the atomic state have been estimated. These values are lower than those given by the kinetic theory of gases. No accurate determination of the m.f.p. is possible, however, until the fraction of the residual current carried by heavy ions is known.

In conclusion I must thank the Radio-Research Board for financial assistance in the carrying out of this investigation. I wish, also, to express my gratitude to Prof. Richardson, F.R.S., for his suggestions and advice during the course of the work.

Wheatstone Laboratory,
King's College, London.

LX. *Unit Curves of a Photographic Lens.* By ALICE EVERETT, M.A. (*From the National Physical Laboratory.*) *

A PREVIOUS note (Phil. Mag. vol. xlv. p. 450, 1923) described the unit curves of a solid sphere, which regarded as a lens is an uncorrected system. The figures accompanying the present note show unit curves for an axial section of a corrected photographic lens, a Tessar, for three different positions of an infinitely distant source.

Tessar (1907). $f_D = 100$. Aperture ratio = $f/4.5$.

	Radius.	Thickness.	
1	+ 26.3	3.7	1.61342
2	∞	4.0	1
3	- 58.1	1.7	1.57391
4	+ 23.9	5.3	1
5	-146.7	1.7	1.53
6	+ 22.3	4.6	1.61451
7	- 36.3		

To obtain these curves, three sets of parallel rays at inclinations 0° , 5° , and 20° to the axis, and apertures 0, $\frac{1}{3}$, $\frac{2}{3}$, full, were traced through the system in an axial plane, and on each ray the positions of the two pairs of unit points, primary and secondary, were found by putting the magnification equal to unity in Mr. T. Smith's formulæ connecting focal distance with magnification (Proc. Phys. Soc. vol. xxvii. p. 508 (1915) and vol. xxx. p. 232 (1918)). These positions were then transformed to rectangular coordinates, and plotted, taking the optic axis as axis of x , the first vertex of the lens as origin for the object space, and the last vertex as origin for the image space.

The incident ray is defined by its inclination ψ to the optic axis, and aperture, the aperture for the present purpose being measured by the length of the perpendicular on the ray from the vertex of the lens, and called "full" when this length is equal to the semi-diameter of the front lens.

The object and image unit curves are drawn separately to avoid overlapping. The paraxial unit points of the Tessar lie near the centre of the lens, only 1.0525 apart for a focal length 100, the first point being 8.7961 behind the first surface.

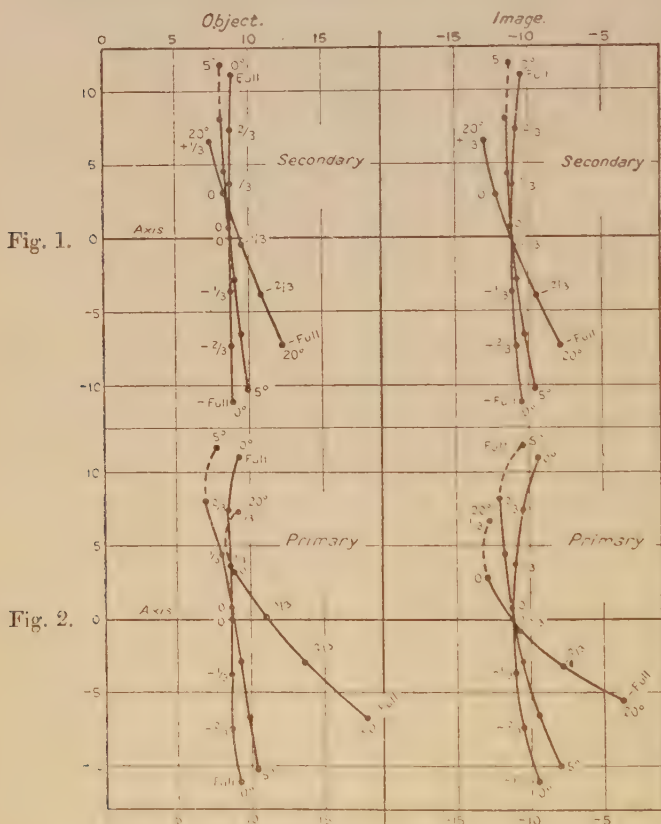
The secondary unit curves are shown in fig. 1, and the primary unit curves directly underneath them in fig. 2. Inspection shows that the following conclusions apply to both.

* Communicated by the Author.

Conclusions.

(1) The position of the unit curves changes with that of the source, *i. e.* with the inclination of the parallel pencil of chief rays.

(2) The curvature changes with the position of the source.



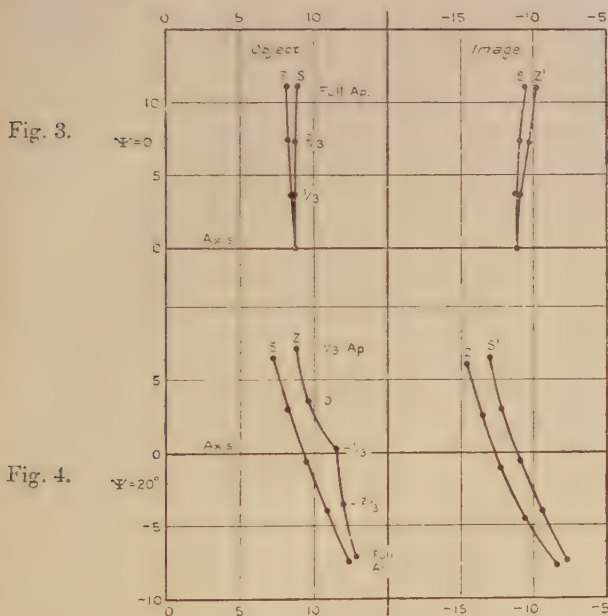
(3) The curvature changes also with the aperture or incident height; the curves are not circular, nor plane. Hence the object curves cannot coincide with the incident wave-front, which is plane.

(4) The unit curve in the image space, like the wave-front, is more convex to the source than the curve in the object space.

The primary unit curves exhibit greater variations in curvature than the secondary unit curves; moreover, while

the secondary curves are only slightly inclined to the wave-fronts, the primary curves for the higher inclinations show a very decided slant. The secondary curves are practically all convex to the source. The primary object curves are concave in parts, but on the other hand the primary image curves are more convex than the secondary image curves.

Each of the curves drawn is only a partial image (if image it can be called at all) of its conjugate. The image of each unit curve is astigmatic. Fig. 3 for $\psi = 0^\circ$, and fig. 4 for



$\psi = 20^\circ$ may serve to give an idea of the amount of astigmatism. S, S' are secondary unit curves, and the curves S', Z' on the right are the secondary and primary images of S on the left. Z' , of course, is not the same as the corresponding primary unit image curve. The curves S, Z on the left would be the secondary and primary images of S' for light travelling backwards.

Primary unit curves (not shown here) on the assumption of unit magnification perpendicular to the optic axis, instead of to the ray, have a still more marked slant than those drawn, and otherwise show greater departure from the secondary forms.

Unit curves of a Cooke lens (1894) have also been plotted and show much resemblance to those given here.

LXI. *Notices respecting New Books.*

The Air and its Ways. The Rede Lecture (1921) in the University of Cambridge, with other contributions to Meteorology for Schools and Colleges. By Sir NAPIER SHAW, Sc.D., F.R.S. (Pp. xx+237, with 28 plates and 100 figures.) (Cambridge: at the University Press, 1923. Price 30s. net.)

THIS volume contains a number of articles, papers, addresses, and miscellaneous contributions to meteorology by Sir Napier Shaw. They are concerned mainly with the physical explanation of the atmospheric circulation, though a few at the end are concerned with the application of meteorology to agriculture. The subjects dealt with are therefore of very general interest; and as the volume is written in the author's characteristic lucid style, it should offer a wide appeal not only to students and teachers, but also to the general reader. It is an easy matter to criticize the Meteorological Office on account of inaccuracy of weather forecasts, but an intelligent perusal of this book will bring home to the critic the complex processes concerned in the phenomena of atmospheric circulation. The volume contains a series of 24 plates, designed to represent the normal distribution of the meteorological elements over the globe. There are many figures in addition which help to make it easy to follow the arguments.

There are many readers who would be deterred from reading a text-book on meteorology to whom this series of essays which ramble from one subject to another, but which all illustrate the general physical principles at work, will appeal. Sir Napier Shaw is to be congratulated on a volume which would serve to stimulate interest in a subject which closely concerns us all.

The Analysis of Spectra. By W. M. HICKS. Pp. vi+326. Cambridge University Press. Price 35s.

PROFESSOR HICKS has seen the subject to which he has devoted so much time and energy grow from being the province of the few to one of the most widely studied branches of physics. Having had his work crowned by the award, in 1921, of the Adams Prize for an essay dealing with the Analysis of Spectra, he has now extended that essay into a treatise on the subject which is sure of the respectful attention of all spectroscopists.

The treatise has as its chief object the systematic presentation of the knowledge of the structure of line spectra which has been won by the study of the experimental data, without reference to or guidance from any special theory of the origin of spectra. Little use, for instance, is made of the quantum theory of spectra, not because any arguments are urged against it, but because the author's unlimited capacity for computation has enabled him to

reach empirical results whose validity he wishes to be judged simply by comparing them with the available measurements. This neglect of Bohr's theories sometimes leads to discussion which will appear pointless to the disciples of the quantum school; but this is inevitable where, to quote the author's words, "the data are studied in a purely objective manner, without any preconceived opinions based on theories as to the cause or manner of production."

Chapter I., which discusses standards, and the character and degree of accuracy of data, and Chapter V., on the effect of physical conditions, are altogether excellent. The latter contains a detailed discussion of the chief experimental results on the Zeeman effect, and emphasizes its value as an aid in the analysis of spectra: the Stark Effect and the investigations of Stark and his school on the Doppler Effect observable with positive rays are also discussed, and some space is devoted to radiation and ionization potentials, but here the neglect of recent theory is very noticeable. In Chapter II. the author deals with the types of series and their representation by formulae, and with those regularities which have been discovered in spectra where no series have been identified, and he follows this by discussing in detail the systems of series of the elements in each chemical group in turn. The monatomic gases, with the exception of helium (considered earlier), have a chapter to themselves towards the end of the book.

The data for the elements and their allocation into series, combinations, and groups are given in tabular form in the Appendix under a single heading, Table III. This, however, is actually a long set of tables extending over 75 pages. For the representation of the series the Hicks formula is, naturally, employed, and the values of the constants for the various series in Table III. are collected in Tables IV. and V. of the Appendix. If Professor Fowler's 'Report' had not appeared at about the same time as Professor Hicks's book, these tables would be of unique value.

Much of the 'Treatise' is based on the author's own extensive contributions to the subject, so that naturally considerable space is devoted to the special conceptions which he has introduced—the *oun*, displacements, links, and summation series. The necessity or utility of these conceptions, singly or collectively, is, it is true, contested by many spectroscopists. Discussion of such a debatable point is obviously out of place in a short notice like the present, for definite assertions as to the existence of the regularities expressed by these terms can clearly be made with safety only after an independent and exhaustive analysis by a spectroscopist with great experience in the handling of the experimental data. As regards the summation series, we will only venture to remark that, although many observed lines have been allocated to these series the tables show frequent irregularities of intensity and character, as well as some instances of the inclusion of arc, spark, and displaced lines in one and the same summation series.

Amongst such a mass of figures it is obviously unreasonable to expect a complete absence of errors. One mistake appears to be recurrent in the tables of the P series of the alkali metals, and in the S series of Zn, Al, and Tl. The values of m in the P tables of Na, K, Rb, and Cs must be reduced by unity throughout if the constants tabulated on page 316 are to apply. The values of m in the P terms in the combination tables of Na and Cs are in accord with the P formulæ constants, but not with the values of m in the P tables of these two elements. On the other hand, the values of m in the P terms in the combination tables of K and Rb agree with those in the P tables, but do not correspond with the P formulæ constants. This applies also to Na combination 13. There are errors of a similar nature in the Zn combinations and the sharp doublets of Al and Tl.

Readers acquainted with the abbreviated notation introduced by Paschen will perhaps experience a little inconvenience on first reading the present treatise. Professor Hicks represents the m th "term" or "sequent" by $P(m)$, $s(m)$, $d(m)$, $f(m)$ instead of by mP , mS , mD , mF . Again, the notation for doublets and triplets differs from that generally used. No doubt arguments can be advanced in favour of the retention of Rydberg's "index numbers," but it is a pity that some agreement cannot be reached among spectroscopists as regards the notation to be used. The unfamiliar appearance of the symbols to those accustomed to the notation of Professor Fowler and his school may prevent many from making the best use of Professor Hicks's extremely painstaking and praiseworthy treatise.

Collected Scientific Papers of John Aitken. Edited by CARGILL G. KNOTT. Pp. xxi+591. Cambridge University Press. 30s.

DR. AITKEN'S name is best known to physicists through his experiments on the condensation of water on dust particles, which follows on the slight supersaturation produced by a small expansion of moist air. The behaviour of dust particles as nuclei of condensation was actually observed by Coulier in 1875, before Aitken started his researches; but Aitken did not know of this, and built up his large and valuable body of research in this direction on original observations made by himself. His work on the part played by atmospheric dust in meteorological phenomena, his elegant dust counters, and the application of his methods to electronic measurements are too well known to need emphasis. The most important part of his other work is that dealing with the formation of dew, in the course of which he made the interesting discovery that the "dew drops" on the leaves of plants are exuded by the plant itself. He was keenly interested in all branches of meteorology, and wrote on the problem of the genesis and maintenance of cyclones, on hoar frost, ground ice, and other kindred subjects. The volume before us contains not all his

papers, but a full selection made by Dr. Cargill, who has prefixed to the collection a short account of the author's life. All the important papers are printed in full, and the volume, admirably produced by the Cambridge University Press, forms a fitting memorial of the modest and gifted investigator whose life-work it represents.

The Theory of Spectra and Atomic Constitution. By NIELS BOHR.
Pp. x+126. Cambridge University Press. Price 7s. 6d.

PROFESSOR BOHR's work is too well known to all readers of the *Philosophical Magazine* for this book to require commendation. It consists of three essays in which essential features of his theory of atomic structure are developed in simple language, with but little resort to mathematical symbols. The first essay dates from the end of 1913, and gives an account of his pioneer work on the spectrum of hydrogen, which first established the quantum theory of spectra: it is translated from a Danish address. The second essay, translated from the *Zeitschrift für Physik*, is based on an address delivered in 1920, in which consideration is devoted to the application of the theory to certain general features of series spectra, and, in the relatively simple case of hydrogen, to the Zeeman and Stark Effects and the fine structure of spectral lines. The famous Correspondence Principle receives a general explanation here. The third essay, based on a Danish address given towards the end of 1921, deals more particularly with the general theory of the structure of the atom, and the variation of atomic properties expressed in the periodic table. The essential feature of Bohr's newest developments, *i. e.* the variation of strength of binding of the electron last added as we proceed from lighter to heavier atoms, which leads in the long periods to the completion of inner groups after outer groups of electrons have been begun, is here expounded, and its important consequences emphasized. The nature of the evidence that can be derived from a study of the spectra is, of course, clearly indicated.

There is a certain amount of inevitable overlapping in the three essays, but this is rather to be welcomed than deplored, as it enables the reader to trace the development of the theory by the author from its inception to the start of the latest phase. The book is assured of the warm welcome it deserves as an authentic exposition of the work of one of the most original minds now active in the domain of physics.

A Theory of Natural Philosophy. By ROGER JOSEPH BOSCOVICH, S.J. Pp. xix+470. Open Court Publishing Company. Price £3 3s.

THIS handsome folio volume embodies the chief work of Father Boscovich, being a reprint of the *Theoria Philosophiæ Naturalis*, first published in 1758. The Latin text, now printed for the

sixth time, is given on the left-hand page, the opposite page being devoted to an English version by Mr. J. M. Child. As far as we know, this is the first time that the work has been translated into a modern tongue. It is prefaced by a short life of the author, written by Dr. Branislav Petroniević, and an explanatory introduction by the translator.

Boscovich's 'Natural Philosophy' is a work of considerable importance in the history of physical theory, and his atomic hypotheses—if they may be so called—are of particular interest to-day. He considers all matter to be made up of discrete points, "points that are perfectly simple, indivisible, of no extent and separated from one another," acting upon one another with a universal, if somewhat complicated, law of force. At very small distances two of Boscovich's points repel one another, and for very close approach the repulsive force tends to become infinite, so that two points can never be brought into coincidence. As the points are separated, the repulsion becomes an attraction, and as the separation is further increased, the force oscillates several times between repulsion and attraction, until finally, when the distance becomes large, the Newtonian law of attraction is approached more and more closely. The oscillations are invoked to explain evaporation, chemical generation of gases, including explosions, and are further utilized in the exposition of the corpuscular theory of light, of which Boscovich was an ardent supporter. The simple hypothesis of one reversal point between repulsion and attraction suffices to explain many of the properties of matter, such as cohesion and elasticity. The courageous attempt to explain all physical laws in terms of discrete centres of force entitles Boscovich to rank as one of the founders of our present atomic theories. Much of the book is very modern in spirit. The centres of force, all of one kind and governed by the same laws, remind us inevitably of electrons: the insistence on the penetrability of matter, illustrated by the analogy of an iron ball, moving with great velocity, making its way freely through a group of magnets, is an astonishing anticipation of Rutherford's work on the α particle. Too much stress must not, of course, be laid upon such general anticipations, but the average reader who takes up this book will probably be astonished by the power and directness of Boscovich's attack on the great problems of physics, and the scope of his method.

Although often called an Italian, notably in the biography in the *Encyclopædia Britannica*, Boscovich was of Slav descent, and prided himself on it. He was born at Ragusa, and on his father's side the family was of purely Serbian origin. The expenses of producing the present volume have been largely borne by the Government of the kingdom of Serbs, Croats, and Slovenes, an enlightened act in the interests of Slav science. We do not know why so large a format (15 × 11 inches, an awkward size for most bookshelves) has been chosen, especially as the original Venetian edition of 1763,

from which the text is taken, is a quarto of ordinary size. It is also strange that the original had to be borrowed from the Cambridge University library, which apparently involved some inconvenience, since the book is by no means very scarce, and can occasionally be purchased for less than the cost of the present edition, which will, however, be invaluable to those, and they are many, whose Latin is uncertain.

LXII. *Proceedings of Learned Societies.*

GEOLOGICAL SOCIETY.

[Continued from p. 224.]

March 14th, 1923.--Prof. A. C. Seward, Sc.D., F.R.S.,
President, in the Chair

THE following communications were read:—

1. 'The Geology of the Schists of the Schichallion District of Perthshire.' By Ernest Masson Anderson, M.A., B.Sc., F.R.S.E., F.G.S.

An examination of the area between Carn Mairg and Schichallion reveals the presence of the following succession:—Graphite-Schist: Pebbly Quartzite: Mica-Schist: Non-pebbly Quartzite: Schichallion Boulder-Bed. The Graphite-Schist is undoubtedly that which borders the Ben Lawers (Caenlochan or Calc-Sericite) Schist, and its position can therefore be fixed with regard to the undisputed part of the Perthshire Dalradian succession. It is inferred (*a*) that the Boulder-Bed is on the opposite side of the Quartzite from the Graphite-Schist, and the sequence which extends from the Ben Lawers Schist to the Ben Ledi Grits; and (*b*) that the Quartzite itself is heterogeneous, and must be regarded as a composite group.

Following the Boulder-Bed, and thus on the same side of the Quartzite, are a white limestone, a banded series of siliceous and micaceous rocks, a grey carbonaceous limestone, and a slightly carbonaceous mica-schist, which may be named the 'Grey Schist'. On approach to the white limestone the Boulder-Bed becomes highly calcareous. It seems likely that this conglomerate is a tillite, and the evidence suggests that it has been partly formed from the material of the limestone. If so, the latter is the older. There may thus be a chronological sequence, of which the oldest visible member is the Grey Schist, extending upwards to the Ben Ledi Grits in an adjoining part of Perthshire.

In the northern part of the Schichallion district the Dalradian Series is bordered by the Struan Flags. The latter probably underlie the former, while the boundary is a line of discordance. There is some evidence for the conclusion that the junction is not an unconformity, but either a normal fault which has been affected by strong horizontal movement, or else a folded thrust.

2. 'The Petrology of the Arnage District in Aberdeenshire: a Study of Assimilation.' By Herbert Harold Read, M.Sc., A.R.C.Sc., F.G.S.

This paper deals with the modification of magmas by the incorporation of material of sedimentary origin, a process to which the name contamination is given. In the Arnage mass in Aberdeenshire—one of the outcrops of what is probably an extensive gabbro-sheet—the sediments concerned in contamination are: (*a*) andalusite-schists and pebbly grits of the Fyvie Series; and (*b*) biotite-schists and subordinate hornblende-schists of the Ellon Series.

The contaminated rocks occur as a roof-zone, some hundreds of feet thick, overlying a sheet of norite rich in magnesia. The contaminated rocks are of four types:—

(1) Gabbro Type, occurring as small patches kneaded in among the other types.

(2) Arnage Type, consisting of various associations of quartz, cordierite, oligoclase-andesine, alkali-felspar, and biotite, with garnet, spinel, and tourmaline; the contaminators are argillaceous schists.

(3) Kinharrachie Type, a dioritic type produced by the contamination of the initial magma with hornblende-schist.

(4) Ardlethen Type, a granitic type transitional from the other types.

The first three types hold xenoliths, while the fourth is practically free from them. The xenoliths are rich in cordierite, spinel, sillimanite, and basic felspar, with some hypersthene.

On the assumption, for which there is some evidence, that the initial magma was normal gabbro, it is shown that the contamination-process depends on reciprocal reaction between initial magma and xenoliths, whereby the magma loses magnesia and lime and becomes richer in alumina and alkalis, the final results of the reciprocal reaction being the granitic Ardlethen type of contaminated rock and certain xenoliths extremely rich in magnesia and lime.

The operation of gravitative cleansing is examined: the modified xenoliths sink in the acidified magma of the contaminated zone; and they pass into the underlying sheet of initial gabbro, which becomes enriched in magnesia and lime, with the formation of the norite now seen beneath the contaminated zone.

The relations of the contamination-process to the assimilation hypothesis of magmatic differentiation are briefly discussed. Certain criticisms of the assimilation hypothesis can be met by the

principle of reciprocal reaction. The chemical variation in the contamination-process is exactly the same as that in igneous rocks as a whole, and it is considered that reciprocal reaction may play a part in magmatic differentiation, especially in the great gabbro-sheets.

March 28th, 1923.—Dr. Herbert H. Thomas, M.A.,
Vice-President, in the Chair.

The following communication was read :—

‘Further Researches on the Succession and Metamorphism in the Mona Complex.’ By Edward Greenly, D.Sc., F.G.S.

Since the publication of the Anglesey Geological Survey map and memoir, various aspects of this complex have been further investigated, and the following are some of the results.

The age of the Complex.—Fragments lately obtained from the Volcanic Series of Bangor show that the metamorphism of the Complex is older than that series.

The Gwna Beds.—Five new analyses of the quartzite are given; fresh evidence is adduced that the basic schists of the Eastern Aethwy Region are derived from the spilitic lavas; and two more occurrences of spilitic tuffs are described, the relations of which to adjacent jaspers and limestones indicate that the latter are not metasomatic products, but original sedimentary formations. A singular effect of anamorphism in its earliest stages is that quartz-epiclasts have been corroded and invaded by the carbonates of a calcareous grit.

The Fydlyn Beds.—A partial analysis is given of one of the rhyolitic tuffs. Fydlyn Beds have lately been identified at Mynachdy and two other places in the northern region. Their identification at Mynachdy throws great light on the succession, and, by indicating inversion, on the tectonics also.

The Penmynydd Zone.—Titaniferous varieties of the Bodwrog marble furnish evidence as to the conditions of development, under dynamic metamorphism, of rutile and of sphene. A small inlier of the Zone, lately discovered, with unusually clear passages from the Gwna mélange, throws light on the origin of the Penmynydd-Zone mica-schist and anamorphic processes.

The Ancient Floor.—More fragments of ancient crystalline schists have been found, one of them being in the Fydlyn Beds, a lower horizon than any that had hitherto yielded any such fragments.

The age of the Gneisses.—The discovery of the Fydlyn Beds at Mynachdy, of late dynamo-anamorphism in the adjacent

gneisses, and of a gneissose fragment in the Fydyln Beds, confirms the view that the gneissic structures are older than the deposition of the Bedded Succession.

The origin of the basic gneisses.—Banding is shown to have resulted from deformation of a differentiated basic magma at an advanced stage of consolidation. Three generations of pegmatite are distinguished, the earliest of which is subsequent to the consolidation of the banded gneiss. Yet foliated hornblende has developed in the gneiss in connexion with their segregation.

The relations of the basic and acid gneisses.—Granitoid banding has been found to be subsequent to granitoid permeation, so also has the appearance of the basic magma from which the hornblendic gneisses were developed. Thus, the micaeous gneisses must be regarded as the oldest known member of the Gneissoid Complex.

LXIII. *Intelligence and Miscellaneous Articles.*

THE THEORY OF THE ABNORMAL CATHODE FALL.

To the Editors of the Philosophical Magazine.

GENTLEMEN,—

WE hasten to assure Dr. Aston that we did not overlook any part of his important work. We did not mention his theory because, as he admits, it differs from ours in the only feature to which we attribute much importance. The whole object of our paper was to suggest that a theory of the abnormal fall is not impossible, in which it is supposed, in accordance with several lines of recent work, that the positive ions reach the cathode with nearly the full energy corresponding to the fall.

For the rest, we fully admit and indeed drew attention to the discrepancies which he notes. But we still believe that it may prove possible to remove these discrepancies when further knowledge is available concerning those factors which we mentioned explicitly as excluded from our preliminary theory.

Yours faithfully,

The Research Staff of the General Electric Co. Ltd.

July 19th, 1923.